Promotoren: Dr.ir. G. van Straten,
              hoogleraar meet-, regel- en systeemtechniek

              Dr.ir. H. Challa,
              hoogleraar tuinbouwplantenteelt,
              in het bijzonder de beschermde teelt

Co-promotor: Dr. J. Bontsema,
             universitair docent, vakgroep Agrotechniek en -fysica

GREENHOUSE CLIMATE MANAGEMENT: AN OPTIMAL CONTROL APPROACH

E.J. van Henten

GREENHOUSE CLIMATE MANAGEMENT: AN OPTIMAL CONTROL APPROACH

PROEFSCHRIFT

Stellingen

1. De onnauwkeurigheid van lange-termijn weersvoorspellingen is geen belemmering voor de toepassing van optimale besturingstheorie in de tuinbouwpraktijk.

Dit proefschrift

2. Door behalve de besturing van de gewasgroei ook de regeling van het kasklimaat te baseren op een economisch criterium, kan een nog efficiënter gebruik van energie en koolzuurgas worden gerealiseerd. Het feit dat dan niet langer gebruik wordt gemaakt van streefwaarden voor de klimaatgrootheden betekent een paradigma-verandering voor de tuinbouwpraktijk.

Dit proefschrift

3. De stelling: "Het is fundamenteel onjuist het momentane kasklimaat te optimaliseren op basis van (produktie) modellen die zijn verkregen uit lange-termijn proefnemingen", is niet juist.

Udink ten Cate, A.J., 1983. Modeling and (adaptive) control of greenhouse climates. Proefschrift, Landbouwuniversiteit Wageningen, stelling 3.

Dit proefschrift

4. Het experiment van Hand geeft niet voldoende grond voor de suggestie dat toediening van koolzuurgas bij sla pas vanaf het rozetstadium kosteneffectief is.

Hand, D., 1980. Winter CO_2 enrichment. The Grower, 94 (23): 17-20.

Hand, D., M. Hannah and G. Slack, 1986. The pollution penalty of CO_2 enrichment. The Grower, 105 (4): 17-22.

Dit proefschrift

5. Ten behoeve van economisch optimale besturing van het kasklimaat dient het ontwerp van kas en klimatiseringssysteem hand in hand te gaan met het ontwerp van de regeling.

6. Het grote aantal parameters dat de tuinder moet instellen bij de huidige generatie kasklimaatcomputers bevestigt dat het gebruikte besturingsalgoritme nog weinig geavanceerd is.

7. Het beschrijven van procesmodellen uitsluitend in de vorm van een computercode moet worden afgeraden.

8. Als de Landbouwuniversiteit "landbouw" uit haar naam verwijdert, dan zal zij haar unieke identiteit spoedig verliezen.

9. Geweldloze weerbaarheid wordt onvoldoende erkend als methode om gewelddadige conflicten te vermijden.

10. Women will never be truly independent until they have pockets in all their garments.

11. De rechtgeaarde radio-zendamateur is vrijgezel.

Stellingen behorende bij het proefschrift
'Greenhouse climate management: an optimal control approach',
E.J. van Henten, Wageningen, 20 december 1994.

Voor mijn schoonvader Koos Noorduyn,
die leefde voor de wetenschap,
en
voor het nieuwe leven
dat nog geen naam heeft.

DANKWOORD

Nu dit proefschrift gereed is gekomen wil ik iedereen bedanken die direct of indirect een bijdrage aan dit werk heeft geleverd.

Met name mijn promotoren Gerrit van Straten en Hugo Challa hebben dankzij vele discussies, commentaar en adviezen een belangrijke rol gespeeld bij de totstandkoming van dit proefschrift.

Met veel genoegen denk ik terug aan de vele middagen die ik samen met Jan Bontsema, mijn co-promotor, doorbracht discussiërend over systeem- en regeltheorie in het algemeen en kasklimaatregeling in het bijzonder. Jan, je brede kennis en de vele kritische vragen zijn een belangrijke stimulans geweest tijdens dit onderzoek en hebben bijgedragen aan de verdieping van mijn inzicht in de materie.

De directie van het Instituut voor Milieu- en Agritechniek (IMAG-DLO) wil ik bedanken voor de ruimte en middelen die mij voor dit onderzoek ter beschikking zijn gesteld.

Twee kasexperimenten met sla hebben mijn inzicht in de modellen die ik bij dit onderzoek heb gebruikt aanzienlijk vergroot. Het gewas is tijdens deze experimenten voortreffelijk verzorgd door Ferry Corver en zijn naaste medewerkers. Tevens gaat mijn dank uit naar Torsten Engelbrecht en Jan-Willem Scheijgrond voor hun hulp bij de gewaswaarnemingen, en naar Rein Bijkerk voor de verzorging van de data-acquisitie en de verwerking van de meetgegevens. Jan Selten, de systeembeheerder, heeft mij bij mijn zeer intensieve gebruik van de VAX regelmatig met raad en daad terzijde gestaan. Bedankt!

Mijn collega's bij het IMAG-DLO, met name Wim van Meurs en Theo Gieling, zorgden voor een fijne werksfeer en de broodnodige ontspanning tijdens koffie- en lunchpauzes.

Ik wil de leden van de sectie Meet- en Regel- en Systeemtechniek van de vakgroep Agrotechniek en -fysica bedanken voor de discussies over dit onderzoek en de ondersteuning die ze mij geboden hebben bij de afronding van dit proefschrift. Met name Paul van Espelo die de figuren en de omslag verzorgde.

Heel blij ben ik dat Gerard Bot, Bernard Bailey, Zaid Chalabi en Aad Termorshuizen het manuscript wilden lezen. Ik heb veel gehad aan hun waardevolle suggesties.

Leonore, mijn proefschrift is af! Ik zal het nooit meer doen.

Eldert Jan

CONTENTS

1. INTRODUCTION

Going back 2000 years in the literature, it can be discovered that the Romans already recognized the benefits of protecting crops from unfavourable outdoor climatic conditions by means of light transmitting shelters to facilitate the cultivation of exotic crops during winter and spring. Moreover, people seemed to be aware of the fact that crop productivity could be improved by actively modifying the climate in these shelters, *i.e.* by heating and humidification (Stanghellini, 1987). However, their limited qualitative knowledge of the processes involved in crop growth and production, as well as the poor technical status of the equipment available for climate conditioning, did not allow for any advanced climate control strategies.

Two millennia have passed and major advances in the field of science and technology have been achieved. Accurate sensors have become available, offering the opportunity of gaining insight into the relations between the crop and its environment. The present climate conditioning equipment allows for a wide range of modifications of the climatic factors relevant for crop growth, such as the temperature, humidity level, carbon dioxide concentration and radiation level in the greenhouse and the availability of water and nutrients in the root environment. Finally, developments in the field of analog and digital electronics have resulted in a high level of automation of greenhouse climate control. Today, greenhouse crop production has become a highly industrialized process.

Because the cost of operating modern, sophisticated greenhouses is high, optimal use of their potentials is required. For example, energy consumption amounts to approximately 15% of the total production costs and as such ranks amongst the three most important cost factors for a horticultural firm in the Netherlands. Therefore, any gain in energy efficiency may contribute significantly to an improvement in the economic result of greenhouse crop production. Moreover, improved production efficiency is in line with governmental policy aiming at efficient application of natural resources and reduction of emissions to the environment.

As an operator of the greenhouse crop production firm, it is one of the complex management tasks of the grower to run the available climate conditioning equipment such that the inputs like natural gas, carbon dioxide, electricity, water and nutrients, are applied efficiently in relation to the economic output. The grower's awareness of the need for economic efficient greenhouse climate conditioning was clearly illustrated during the energy crises in the early 70's and mid 80's. Besides investments in energy conservation

measures such as thermal screens, exhaust gas condensers and double glazing, lower set-points for the air temperature in the greenhouse and a reduction in ventilation, contributed to a reduction of the energy consumption in the horticultural sector (Bakker, 1991; Jansen, 1992). Still, in horticultural practice, climate control is essentially based on the realization of climate strategies originating from the grower's experience with plant growing and empirical horticultural research.

Greenhouse climate management can be made more efficient by explicitly balancing the benefits associated with the marketable product against the operating cost during the operation of the climate conditioning equipment. This is a typical example of an *optimal control* problem (see *e.g.* Pierre, 1969; Kirk, 1970; Bryson and Ho, 1975).

Optimal control theory emerged as a new field in academic research in the late 50's and early 60's when, using variational calculus (Pontryagin *et al.*, 1962) and dynamic programming techniques (Bellman, 1957), new insight into the construction and analysis of optimal control systems was gained. The literature survey in section 1.1 will reveal that the possible benefits of optimal greenhouse climate management were already discussed in the agricultural engineering society two decades ago. But, in terms of practical application, a drawback of optimal control theory is the requirement to have an appropriate model of the process to be controlled as well as sufficient computing power. This largely explains why progress in the field of modelling the dynamic responses of crop growth (Sweeney *et al.*, 1981; Goudriaan *et al.*, 1985; Goudriaan and Monteith, 1990) and greenhouse climate (Bot, 1983; Udink ten Cate, 1983) as well as a dramatic improvement of the price-performance ratio of digital computers during the last decade, renewed the interest in optimal greenhouse climate management (Challa *et al.*, 1988).

1.1. Optimal control of greenhouse climate: a literature survey

The following survey is restricted to greenhouse climate control research in which the process dynamics have, at least partially, been accounted for in the control system design. *Climate control procedures* or *operator rules* in which the dynamic nature of the process under control has not explicitly been accounted for, are not considered in this research.

A review of the literature reveals that optimal greenhouse climate management has been the subject of many philosophical thoughts throughout the last two decades. One of the first qualitative analyses on this subject dates back to 1978 when Udink

ten Cate, Van Dixhoorn and Bot considered greenhouse climate control and crop growth management from an integral point of view (Udink ten Cate *et al.*, 1978; Bot *et al.*, 1978). Their ideas were modified in particular details throughout the years (see *e.g.* Challa, 1985; Challa *et al.*, 1988; Challa and Van Straten, 1991, 1993; Tantau, 1991, 1993), but the fundamental concept remained the same. Within this concept, greenhouse climate management was established by defining a hierarchical set of sub-systems, where each sub-system is operated along guidelines defined at the higher levels.

The *main reason* for this hierarchical decomposition of greenhouse climate management is the inherent *complexity* of the process considered. The large number of process variables related to crop production and greenhouse climate as well as the complex interactions between the crop and the greenhouse climate inevitably demand a decomposition in sub-problems that are more tractable in control system design.

The *main premise* for the decomposition was the fact that in the crop production process considerable *differences in response times* exist. Compared with the fast dynamic response of the greenhouse climate, crop growth responds rather slowly to changes in the inputs. Also, the response time of the valves and servo motors is relatively short compared with the dynamic response of the greenhouse climate.

When a complex high dimensional system contains mutually interacting sub-processes with large differences in response times, it is standard engineering practice to make simplifications by neglecting time constants whose presence cause the system to be more complex than acceptable for practical design of optimally controlled systems (Kokotovic and Sanutti, 1968). Then, based on engineering experience, the process variables are classified as 'slow' and 'fast'. The only dynamics used in *short term* studies are determined by the 'fast' variables, disregarding the dynamics of the 'slow' process variables. In *long term* studies, only the dynamics determined by the slow state variables are considered and the dynamics of the 'fast' process variables are neglected. As illustrated by a hierarchical decomposition of greenhouse climate management into four levels (table 1.1), such a decomposition is certainly not limited to the coarse division of the system into two sub-processes, *i.e.* 'fast' and 'slow'. It can be extended to any desirable level of refinement as far as this is allowed by differences in the dynamic response times of the process variables considered.

The hierarchical decomposition of greenhouse climate management shows a great resemblance to the hierarchical schemes encountered in industrial process control (*e.g.* Richalet *et al.*, 1978). Inspired by the ideas of Richalet and co-workers, the 4-level hierarchical process control scheme presented in table 1.1 illustrates the basic

ideas about a hierarchical decomposition of greenhouse climate management.

Table 1.1.   A   hierarchical   decomposition   of   greenhouse   climate management (adapted from Richalet *et al.*, 1978).

Level	Control of	Time scale
3	production space and time	growing season/year
2	crop growth and production	hour/day/week
1	greenhouse climate	minute
0	actuators (*e.g.* valves)	second/minute

In greenhouse climate management, level 0 is concerned with the efficient operation of the valves of the heating system and carbon dioxide supply system as well as the servo motors of the ventilation windows. The settings for the valves and servo motors are determined at level 1 which is concerned with control of the greenhouse climate variables such as air temperature, carbon dioxide concentration and humidity. The required values, or set-points, of these climate variables are determined at level 2. The processes considered at level 0 and 1 have relatively short dynamic response times, *i.e.* of the order of minutes. Therefore, they are controlled on a minute by minute basis. In practice, level 0 and level 1 are commonly treated simultaneously in a cascade or master–slave control system concept in which the level 1 controller acts as the master on the slave controller at level 0.

At levels 0 and 1, climate control research has been mainly focused on air temperature control (O'Flaherty *et al.*, 1973; Udink ten Cate and Van de Vooren, 1978; Valentin and Van Zeeland, 1980; Udink ten Cate and Van Zeeland, 1981; Udink ten Cate, 1983; Tantau, 1985; Verwaayen *et al.*, 1985; Chotai *et al.*, 1991). The potentials of multi-variable control of the temperature and absolute humidity of the air was investigated by Van Henten (1989).

As in industrial process control (Richalet *et al.*, 1978), for a long time it has been assumed in greenhouse climate control that the economic benefits induced by levels 0 and 1 are negligible compared with the economic impact of process optimization at level 2. Consequently, at levels 0 and 1 economic criteria were not used and

control system design emphasized accurate realization and tracking of the set-point values for the greenhouse climate variables derived at level 2 as well as disturbance rejection. Quite recently, economic objectives have been introduced into the control of the greenhouse climate dynamics as well (Tchamitchan *et al.*, 1992; Tap *et al.*, 1992; Hwang, 1993). These authors emphasized economic optimal control of short term crop responses such as the crop photosynthesis rate.

Level 2 is concerned with the control of crop growth and production. Therefore, the dynamic response of the crop is explicitly accounted for in the control system design. At this level, climate variables such as the temperature, carbon dioxide concentration and humidity in the greenhouse are inputs which can be used to manipulate the crop production process. Consequently, control system design is aimed at the calculation of trajectories for these climate variables such that a specified crop production goal is achieved. These climate trajectories are to be used as set-point trajectories for greenhouse climate control at level 1.

The determination of optimal greenhouse climate trajectories has received considerable attention in agricultural engineering research. Beers (1983) and Lentz (1987) worked on climate optimization for radish; Lentz (1987), Critten (1991), Van Henten and Bontsema (1991) and Seginer *et al.* (1991[a]) considered lettuce; Seginer *et al.* (1986), Arnold (1988), Shina and Seginer (1989), Reinisch *et al.* (1989) and Seginer (1991[b]) focused on tomatoes; and cucumbers were considered in the climate optimization research of Schmidt *et al.* (1987), Lentz (1987) and Markert (1990).

Research mainly emphasized the optimization of carbon dioxide concentration and air temperature in the greenhouse because their effects on crop growth and production are quite well understood. In greenhouse climate optimization research, the humidity of the air has not been taken into account though it is known to affect crop production in a qualitative as well as a quantitative sense (Bakker, 1991).

Since process control at level 2 is considered to have a considerable impact on the overall economic performance of the crop production process, explicit economic performance criteria have been employed in control system design. A commonly used objective has been the economic efficiency expressed in terms of the difference between the revenue obtained when selling the harvested product at the auction and the operating costs of the greenhouse climate conditioning equipment (*e.g.* Seginer *et al.*, 1991; Arnold, 1988; Markert, 1990). Seginer (1989) and Van Henten and Bontsema (1991) used a slightly different design criterion by requiring the production of a crop with a pre-defined harvest weight at the lowest

possible cost.

Crop growth and development are known to respond rather slowly to changes in the environment and therefore optimal climate control strategies were derived on relatively large time scales. Shina and Seginer (1989) calculated hourly values for the greenhouse climate set-points. Van Henten and Bontsema (1991) used a time-scale of half a day to allow for different set-points during day and night, whereas Schmidt *et al.* (1987), Arnold (1988) and Markert (1990) used an interval of several days in their climate optimization research.

Finally, level 3 emphasizes the optimization of long term management objectives by means of scheduling crop production in space and time. As such it does not directly affect greenhouse climate management, but it supplies important boundary conditions for the optimization at level 2 in terms of *e.g.* the duration and economic objectives of a production cycle. In this way it constitutes an important interface between overall greenhouse crop production management and greenhouse climate control.

1.2. The objective of the present research

The main objective of the present research is to generate, analyse and evaluate the structure of a greenhouse climate control system which efficiently operates the climate conditioning equipment in relation to the economic return of the crop produced.

Unlike industrial process control, in agricultural engineering research, it has been recognized that to optimize the overall performance of greenhouse crop production, control of greenhouse climate dynamics should be based on economic arguments as well (Tchamitchan *et al.*, 1992; Tap *et al.*, 1992). However, from the literature it did not become clear how the performance criterion used at level 1 should be defined in relation to the performance criteria used at the higher levels. Moreover, the literature did not produce much evidence about the actual interaction between the different control levels. For instance, research on level 2 control suggests that the calculated climate set-points should be realized at level 1, whereas in research on economic optimal control at level 1, the realization of the set-points generated at level 2 was not considered (Tchamitchan *et al.*, 1992; Tap *et al.*, 1992). A discrepancy between both approaches seems to exist.

To achieve a unified framework for optimal control of all dynamic responses involved in the greenhouse crop production process, unlike the research reported in the literature, in the present approach the control problem is not *a priori* hierarchically decomposed. In this research, both greenhouse climate dynamics and

crop growth dynamics are considered in the control system design simultaneously. The singular perturbation method, which exploits the multiple time-scale properties of dynamic processes, will be used to investigate the simultaneous economic optimal control of the interacting fast greenhouse climate dynamics and the slow crop growth responses and to construct a new hierarchical decomposition of greenhouse climate management determined by the differences in response times in the crop production process.

In horticultural practice as well as in research, the humidity level in the greenhouse is considered to be an important climate variable determining crop growth and production both in a qualitative as well as a quantitative sense. However, until now, humidity control has not been considered in greenhouse climate optimization research. In the present research, the humidity level will be explicitly included in the control system design. Despite considerable progress in the field of humidity research (*e.g.* Stanghellini, 1987; Bakker, 1991), the relation between crop production and humidity is still poorly quantified. Therefore, humidity control will be accomplished by requiring the relative humidity level in the greenhouse to stay between a lower and an upper limit assuming that between these limits humidity does not affect crop production.

For application of optimal control in horticultural practice it is necessary to have a quantitative model of the response of the crop production process to control and external inputs, an accurate prediction of the weather and an assessment of the economic value of the crop at harvest time. In practice, modelling errors occur, long term weather forecasts are quite inaccurate and due to the free market mechanism involved in the price making process at the auctions, the economic value of the crop at harvest is hard to predict. These issues have not been given much attention in the literature on greenhouse climate management.

In this research validation experiments and sensitivity analysis will be used to analyse the behaviour of the process models in terms of control system design. A sensitivity analysis will be used to analyse the effect of modelling errors and external inputs on the performance of the optimal control system. A so-called sub-optimal control scheme with state feedback and feedforward of the external inputs will be developed to deal with the effects of model errors and errors in the prediction of the external inputs whilst maintaining near optimal performance. For state feedback control in greenhouse climate management, measurements of the state of the greenhouse climate as well as the crop are needed. Measurements of the greenhouse climate are readily available, but measurements of the crop are much more difficult to obtain, at least in a non-destructive way. In this thesis, a non-destructive method to measure the state of

the crop using image processing techniques is presented and evaluated. Finally, historical data of auction prices will be analysed to define a performance criterion for control system design and to gain insight into the predictability of auction prices.

In addition to use in an on-line environment, the calculated optimal control strategies can be used as a tool to analyse and evaluate the existing control strategies implemented by the grower. Although on-line implementation is not emphasized in this research, the control system will be designed and analysed in view of on-line application. Also the benefits of the optimal control approach to greenhouse climate management will be evaluated by comparing the controller performance with the performance of greenhouse climate control supervised by the grower.

1.3. Outline of this thesis

The structure of the thesis is largely based on the observation that, control system design involves a number of steps. A typical scenario adapted from Doyle *et al.* (1992) is as follows:

1. Formulate the control problem,
2. Model the system to be controlled,
3. Analyse the resulting model; determine its properties,
4. Simplify the model if necessary so that it is tractable,
5. Decide on the performance specifications,
6. Design the control system,
7. Analyse the control system; determine its properties,
8. Simulate the resulting controlled system,
9. Repeat from step 1 if necessary,
10. Choose hardware and software and implement the controller,
11. Tune the controller on-line if necessary,
12. Repeat from step 1 if necessary.

In chapter 2 the greenhouse climate control problem considered in this thesis is presented and assumptions about the particular greenhouse crop production process, used in this research as a vehicle for the illustration of the basic ideas, are outlined (Step 1). Chapter 3 is devoted to the description and analysis of dynamic models of the greenhouse crop production process used in the control system design. Methodology and results of validation experiments and a sensitivity analysis are presented (Steps 2 to 4). In chapter 4 the performance criterion is defined based on the analysis of historical data of the auction price of lettuce (Step 5).

In chapter 5, using variational calculus, the solution of the optimal control problem, stated in chapter 2, is derived in a formal way (Step 6). Additionally, methods are derived for the numerical solution and analysis of optimal control problems. First of all, it will be shown that the necessary conditions for optimality of a control strategy, derived in this chapter, have a meaningful and interesting economic interpretation which can be used to get a better understanding of the results obtained in later chapters. Secondly, a methodology is presented to assess the performance sensitivity of open-loop optimal control systems with respect to perturbations in the model parameters and external inputs. Thirdly, the multiple time-scale concept of singular perturbed systems will be introduced. It will be used to establish and analyse a hierarchical decomposition of greenhouse climate management based on differences in response times in the crop production process. Finally, the concept of a sub-optimal control scheme, including state feedback and feedforward of the external inputs, is presented. This control scheme will be used to deal with model errors and errors in weather forecasts. In chapter 6, the formal results of optimal control theory presented in chapter 5 are applied to the greenhouse climate control problem defined by the model equations presented in chapter 3 and the performance criterion presented in chapter 4 (Step 7). Equations describing the necessary conditions for optimality will be presented and analysed. In chapter 7, the greenhouse climate control system will be evaluated in simulations (Step 8). Amongst other things, results are presented of: (i) a comparison of optimal control with climate control supervised by the grower, (ii) a sensitivity analysis of the control system, (iii) the performance of the sub-optimal feedback–feedforward algorithm and (iv) the validation of a new hierarchical decomposition of the greenhouse climate management system. Since on-line implementation of the control algorithm is not particularly emphasized in this research, steps 9 to 12 are omitted. However, in chapter 8 the results obtained in the previous chapters are integrated. Based on the formal and simulation results obtained, the structure of an optimal greenhouse climate management system is presented and discussed with due consideration to future implementation in practice. Finally, chapter 9 contains concluding remarks and some suggestions for future research.

2. FORMULATION OF THE CONTROL PROBLEM

The crop production process is described by a dynamic model, represented in its general form by

(2.1) $\dot{x} = f(x,u,v,c,t)$, $x(t_b) = x_b$,

where $x = x(t) \in \mathbb{R}^n$ are the state variables (*i.e.* x is a n-dimensional state vector), $u = u(t) \in \mathbb{R}^m$ are the control inputs, $v = v(t) \in \mathbb{R}^p$ are the exogenous inputs, $c \in \mathbb{R}^q$ are the time invariant parameters and t denotes time. Both the initial state denoted by x_b, and the initial time, *i.e.* planting date, t_b are assumed to be fixed. The function $f: \mathbb{R}^{n+m+p+1} \to \mathbb{R}^n$ is generally a nonlinear function and $\dot{x}$ is the time derivative of x.

Though, from an economic point of view, lettuce is not counted as one of the important crops in Dutch horticultural practice, in this thesis, it will be used as a vehicle for the illustration of the methodology developed. It is a single harvest crop which, from the point of view of modelling and optimal control, is much easier to deal with than multiple harvest crops like tomatoes or cucumbers. However, most of the methodological results obtained can be applied to a multiple harvest crop as well.

In this research, crop dry weight is considered to be the major variable defining the state of the crop. The greenhouse climate is represented by the state variables: air temperature, carbon dioxide concentration and humidity. The energy input from the heating system, the ventilation rate through the windows and the carbon dioxide supply rate are the control inputs. External inputs are the outside climate conditions including the solar radiation, wind speed, temperature, carbon dioxide concentration and humidity. Dynamic models describing the evolution of the state variables are described and analysed in chapter 3.

In horticultural practice *physically realizable controls* have magnitude limitations. For instance, the amount of heating energy which can be supplied to the greenhouse is limited by the heating capacity of the boiler. Additionally, a negative energy supply is thought to be unrealistic, since the heating system is not intended to cool the greenhouse. These physical limitations need to be accounted for in the derivation of the optimal control strategies. They are represented in a straightforward way by the following simple bound constraints

(2.2) $u_{i,min}(t) \leq u_i(t) \leq u_{i,max}(t)$, $i = 1,...,m$,

where $u_{i,min}(t)$ and $u_{i,max}(t)$ are the lower and upper bound on the control inputs, respectively. Besides a constraint on the energy supply to the greenhouse, bound constraints will be imposed on the ventilation rate through the vents and the supply rate of carbon dioxide. The bounds will be defined in chapter 6.

Usually the process model represented by eqn. (2.1) does not constitute an exact and complete description of the process considered. For instance the effects of temperature and humidity on greenhouse crop production are not yet fully understood nor quantified. A climate control algorithm based on such a model may drive the state of the greenhouse climate into a condition known to be unfavourable for crop production. This will be prevented by constraining the greenhouse climate state variables to lie within a bounded region defined by

(2.3) $x_{i,min}(t) \leq x_i(t) \leq x_{i,max}(t)$, $i \in I_{xc}$,

where $x_{i,min}(t)$ and $x_{i,max}(t)$ are the lower and the upper bounds on the state variable, respectively and I_{xc} is the index set of the state variable constraints. In this research, state constraints will be imposed on the relative humidity level, the carbon dioxide concentration and the air temperature in the greenhouse. The bounds will be defined in chapter 6. It should be emphasized that in greenhouse climate management the origin of this type of constraints is rather artificial. Unlike control input constraints being a very clear mathematical representation of the limitations of the actuators, these state constraints express the effects of unfavourable conditions on the process behaviour which should have been explicitly accounted for in the process model of eqn. (2.1).

When economic optimal greenhouse climate control is considered, the fundamental question is: 'How to apply the control inputs to the greenhouse crop production process, taking into account predictions of the outdoor climate, the costs related to climate conditioning and the price obtained at the auction when selling the harvested product, such that the best net economic result, *i.e.* the largest difference between the gross economic return and the operating costs of the climate conditioning equipment, is obtained'.

In a formal way, the net economic revenue of the controlled process is described by

$$(2.4) \qquad J(u) = \Phi(x(t_f), c, t_f) - \int_{t_b}^{t_f} L(x, u, v, c, t)dt,$$

where Φ: $\mathbb{R}^{n+q+1} \rightarrow \mathbb{R}$ is the gross economic return of the produce sold, L: $\mathbb{R}^{n+m+p+q+1} \rightarrow \mathbb{R}$ is the operating costs of the climate conditioning equipment and t_f is the harvest date which is assumed to be fixed. The costs for heating, carbon dioxide supply and ventilation, represented by $L(x, u, v, c, t)$, will be defined in chapter 4. In that chapter also a relation between the harvest weight of lettuce and the auction price will be quantified using historical auction price data. This will yield a relation for the gross economic return $\Phi(x(t_f), c, t_f)$.

With the preliminaries presented above, the economic optimal control problem is then defined as finding the open-loop control strategy, $u^*(t)$, which maximizes the performance criterion $J(u)$, subject to the differential equation constraints (2.1) and the control and state constraints (2.2) and (2.3), given (a prediction of) the external inputs $v(t)$ throughout the whole growing period from the planting date, t_b, until the harvest date, t_f. In other words, given $v(t)$, $t \in [t_b, t_f]$, *the objective of the controller design* is to find

$$(2.5) \qquad u^*(t) = \arg \max_u J(u),$$

subject to eqns. (2.1), (2.2) and (2.3). In chapter 5 a formal solution of this control problem is derived and methods for the analysis of the control problem are presented. The resulting open-loop control strategies may supply valuable information about the efficient operation of the climate conditioning equipment. However, a poor performance can be expected when these control strategies are used in practice, since accurate long term weather predictions are impossible to obtain and modelling errors may occur. Therefore, in chapter 5, attention will be paid to a method based on feedback of the state and feedforward of the external inputs, to deal with modelling errors and errors in the weather forecast whilst minimizing the loss in economic performance.

3. DYNAMIC MODELS OF THE GREENHOUSE CROP PRODUCTION PROCESS

3.1. Introduction

To apply optimal control theory in horticultural practice it is necessary to have a dynamic model which describes the evolution of the state variables of the greenhouse crop production process as affected by the state of the process itself, as well as the control and the exogenous inputs. In fig. 3.1 a schematic diagram of the greenhouse crop production process considered in this research is depicted. The state of the production process is represented by variables related to the lettuce crop such as crop dry weight, as well as variables describing the indoor climate such as the air temperature, humidity and carbon dioxide concentration. Control inputs are the energy supply by the heating system which can be used to raise the air temperature, the aperture of the ventilation windows which will affect the air exchange between indoor and outdoor air and the carbon dioxide supply rate which is used to raise the carbon dioxide concentration in the greenhouse. Since the indoor climate is
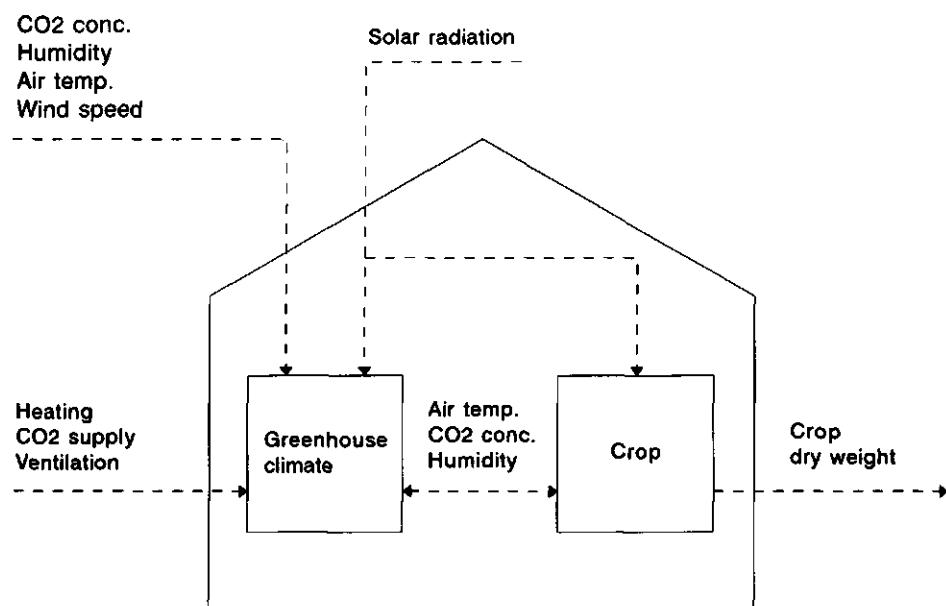
Fig. 3.1. A schematic diagram of the greenhouse crop production process.

poorly isolated from the outdoor climate, outdoor climate conditions or exogenous inputs such as solar irradiation, air temperature, wind speed, humidity and carbon dioxide concentration have a strong impact on the energy and mass balances of the greenhouse interior. Moreover, solar irradiation is a necessary condition for crop growth.

In the modelling literature, integrated descriptions of the greenhouse crop production process as outlined above are rarely found. Commonly, two sub-systems of the greenhouse crop production are considered in modelling research namely the greenhouse climate and the crop, and the dynamic response of these sub-systems is studied and described within the framework of two different scientific disciplines. Fig. 3.1 largely reflects this situation. The dynamic response of greenhouse climate variables such as air temperature, humidity and carbon dioxide concentration, to the energy input from the heating system, the aperture of the ventilation windows, outdoor wind speed, outdoor temperature etc., have been investigated and described within the framework of environmental physics (*e.g.* Bot, 1983; De Jong, 1991). Energy and mass transfer within the greenhouse were described in terms of fundamental transport phenomena like convection, conduction and radiation. The response of the crop to environmental factors like temperature and carbon dioxide concentration has been investigated within the framework of crop physiology and, for instance, the dry matter accumulation of a crop has been described in terms of fundamental physiological processes like crop photosynthesis, respiration and dry matter distribution (Penning de Vries *et al.*, 1974; Thornley and Hurd, 1974; Goudriaan and Van Laar, 1978; Farquhar *et al.*, 1980; Sweeney *et al.*, 1981).

Though for control system design an integrated description of the greenhouse climate and crop response is needed, first dynamic models of lettuce growth and greenhouse climate will be described, calibrated and validated separately in section 3.2. Later on, in section 3.4, the crop growth and greenhouse climate models will be integrated to yield an overall model of the greenhouse crop production process considered in this research.

In a simulation study by Tchamitchan *et al.* (1992), in which greenhouse climate optimization during the productive stage of a tomato crop was considered, it was found that additional heating of the greenhouse was not economically feasible. The authors suggested this was due to an incomplete model description of crop growth. The temperature dependent transformation of carbohydrates produced in crop photosynthesis to structural material was not included in their model and an extension of the model was proposed to obtain more realistic values for the air temperature. In line with this observation, in this thesis two models of lettuce growth will be

described. In the first model, the crop is represented by one state variable, total dry weight, while no carbohydrate buffer is considered. This model resembles the SUCROS-87 model (Spitters *et al.*, 1989). In the second model, the state of the crop is represented by two state variables, namely the structural dry weight and non-structural dry weight, *i.e.* the carbohydrate buffer (Sweeney *et al.*, 1981; Van Henten, 1994). In this model, a temperature dependent transformation of non-structural dry weight into structural dry weight is included. With these two models the effect of a carbohydrate buffer and the temperature dependent transformation of carbohydrates into structural material on optimal greenhouse climate control will be investigated in chapter 7.

The greenhouse climate is modelled with a highly aggregated model compared with for instance the model of Bot (1983). The model describes the dynamics of the air temperature, humidity and carbon dioxide concentration. In view of the objective of this research, *i.e.* the development of a methodology for optimal greenhouse climate control, application of a rather simple model of the greenhouse climate is considered justified.

To gain further insight into the structure of the model and the effects of small perturbations in the initial conditions, model parameters and inputs on the behaviour of the two state variable lettuce growth model, methodology and results of a sensitivity analysis are presented in section 3.3 (Van Henten and Van Straten, 1994).

After the dynamic models of lettuce growth and greenhouse climate have been individually described and analysed in sections 3.2 and 3.3, these models are integrated to give an overall model description of the greenhouse crop production process in section 3.4. Some simplifications in the models will be made and the resulting crop production models will be validated.

Finally, in section 3.5, the material presented in this chapter will be discussed in terms of the design of an optimal greenhouse climate control system.

3.2. Model description, calibration and validation

3.2.1. Materials and methods

To obtain data for the calibration and validation of dynamic models of the greenhouse crop production process, from 17 October 1991 until 16 December 1991 and from 21 January 1992 until 17 March 1992, a lettuce crop was grown in one compartment of an experimental greenhouse, located at the Institute of Agricultural Engineering

(IMAG-DLO) in Wageningen. The 4-span Venlo-type greenhouse was oriented East-West and had a span width of 3.2 m, gutters mounted at 3.7 m and a floor area of approximately 300 m^2. The roof consisted of single glass panes mounted at a slope of 26°. In the roof, a total of twenty half pane ventilation windows were installed on the lee and windward sides. These ventilation windows measured 0.8 by 2.0 m and had a maximum opening angle of 30°. A hot water heating system consisting of 4 pipes per span was mounted parallel to the gutters at a height of approximately 2.0 m. In the greenhouse a distribution network of one hose per span was used to supply carbon dioxide from a storage tank.

Lettuce plants (*Lactuca sativa L.*) were sown and raised at a nursery in peat blocks and then planted at a density of 18 plants per square metre of soil in a recirculating nutrient film technique (NFT) system consisting of 13 gutters per 2 spans. According to Dutch horticultural practice, during the autumn experiment, cultivar 'Berlo' was used. In the second experiment cultivar 'Norden' was employed. 'Norden' is frequently cultivated in winter and spring in The Netherlands.

Using an updated version of the IMAG computer control system implemented on a Digital PDP-11/73 (Van Meurs, 1980), the greenhouse climate was controlled according to the rules followed in normal horticultural practice. During the first few days of the cultivation period the day and night temperature set-point was 14 $^\circ$C. Then the night temperature was lowered to 10 $^\circ$C, whereas the day air temperature set-point was at least 14°C and increased dependent on the solar radiation level. During the day, carbon dioxide was supplied to a maximum concentration of 750 ppm depending on the amount of solar radiation and the opening of the ventilation windows. With a separate computer, the nutrient solution was controlled to have an EC of around 2.3 mS and a pH of around 6.

During the two experiments, measurements of the crop, the greenhouse climate, the actuators and the outdoor climate conditions were recorded. For the destructive crop measurements the greenhouse was divided into 4 blocks to account for the effect of temperature and radiation gradients in the greenhouse. Every 5 to 7 days throughout the growing season, from each block, five plants were randomly harvested and fresh and dry weights of both roots and shoots, as well as total leaf area, were determined for each plant. Dry weights were obtained after oven drying the plants at a temperature of 105 $^\circ$C for 24 hours.

With a data logging system connected to the greenhouse climate

computer, measurements of the indoor climate, outdoor climate and actuators of the climate control system were recorded at two minute intervals. The measurements of the indoor climate included single spot measurements of air temperature and humidity for which ventilated and radiation shielded dry and wet bulb thermometers were used. A spatial average value of the carbon dioxide concentration in the greenhouse was obtained from a mix of samples which were taken continuously at 6 places in the greenhouse. The carbon dioxide concentration was measured with a Siemens infrared absorption spectrometer. Solar radiation inside the greenhouse was measured at canopy level in the centre of each of the 4 blocks with Kipp solarimeters.

Recordings of the actuators of the climate control system included the mean value of the inlet and outlet temperature of the heating system, the valve position (open/closed) of the carbon dioxide supply system and the window aperture of both lee and windward side ventilation windows. At daily intervals, carbon dioxide supply was monitored with an accumulating flow meter as well. From the total amount of carbon dioxide supplied throughout the day and the valve position, the carbon dioxide supply rate was calculated.

Outside the greenhouse, solar radiation, air temperature, relative humidity and wind speed were measured with a Kipp solarimeter, ventilated and radiation shielded dry and wet bulb thermometers and a cup anemometer, respectively. The instruments were installed on a 10 m tower, located at a distance of approximately 25 m from the experimental greenhouse. The carbon dioxide concentration outside the greenhouse was not measured.

As will be shown later, most of the model parameters have been derived from the literature or were determined from physical properties. However, some of the parameters in the lettuce growth and greenhouse climate models were determined by means of model calibration. The lettuce growth models were manually calibrated using the data of the first growth experiment such that the data of the second experiment could be used for validation. The greenhouse climate model was calibrated using 5 days of measurement data obtained during the second experiment.

3.2.2. A one state variable lettuce growth model

3.2.2.1. Model equations

In this model of lettuce growth, the state of the lettuce crop is described by a single state variable, namely total crop dry weight

X_d [kg m^{-2}]. In line with the SUCROS-87 formulation of crop growth, the basis for calculating dry matter production, is the canopy net carbon dioxide assimilation rate (Spitters *et al.*, 1989). This gives rise to the following description of dry matter production

$$(3.1) \qquad \frac{dX_d}{dt} = c_\beta(c_\alpha\phi_{phot} - \phi_{resp}) \qquad\qquad \text{kg m}^{-2}\text{ s}^{-1},$$

where ϕ_{phot} [kg m^{-2} s^{-1}] is the gross carbon dioxide uptake due to canopy photosynthesis, ϕ_{resp} [kg m^{-2} s^{-1}] is the maintenance respiration rate expressed in terms of the amount of carbohydrates consumed, and c_α and c_β are parameters. The factor c_α converts assimilated carbon dioxide into sugar equivalents. The yield factor c_β accounts for the respiratory and synthesis losses during the conversion of carbohydrates to structural material and has a value between zero and one. These losses are dependent on the chemical composition of the dry matter formed (Penning de Vries *et al.*, 1974). Eqn. (3.1) asserts that the carbohydrates produced by carbon dioxide photosynthesis are partly consumed in maintenance respiration and the remaining carbohydrates are used for the production of structural material.

In accordance with Goudriaan and Van Laar (1978) and Goudriaan and Monteith (1990), gross canopy photosynthesis is described by the empirical relation

$$(3.2) \qquad \phi_{phot} = \phi_{phot,max}\left(1-e^{-c_k c_{lar,d}(1-c_\tau)X_d}\right) \qquad\qquad \text{kg m}^{-2}\text{ s}^{-1},$$

in which $\phi_{phot,max}$ [kg m^{-2} s^{-1}] is the gross carbon dioxide assimilation rate of the canopy having an effective canopy surface of 1 m^2 per square meter of soil at complete soil covering. The geometrical and optical properties of the canopy with respect to incident radiation before canopy closure are accounted for by the exponential relation $1-e^{-c_k c_{lar,d}(1-c_\tau)X_d}$ in which $c_{lar,d}(1-c_\tau)X_d$ represents the leaf area index, *i.e.* the amount of leaf area present per square meter of soil. The parameter $c_{lar,d}$ [m^2 kg^{-1}] is the shoot leaf area ratio, expressing the amount of leaf area per unit shoot dry weight. It is assumed to be constant in this model. The parameter

c_k is the extinction coefficient of the canopy. Finally, the parameter c_τ expresses the ratio of the root dry weight to the total crop dry weight. This parameter is also assumed to be constant in this model.

The response of canopy photosynthesis ($\phi_{phot,max}$) to the incident radiation and carbon dioxide concentration is described with a relation according to Acock *et al.* (1978). Their model has been extended to account for photorespiration and temperature effects on the light use efficiency as well as temperature effects on the carboxylation conductance in the leaf tissue:

$$(3.3) \quad \phi_{phot,max} = \frac{\varepsilon c_{par} c_{rad,rf} V_l \sigma_{co2}(X_c - \Gamma)}{\varepsilon c_{par} c_{rad,rf} V_l + \sigma_{co2}(X_c - \Gamma)} \quad \text{kg m}^{-2} \text{ s}^{-1},$$

in which ε [kg J^{-1}] is the light use efficiency, c_{par} expresses the ratio of photosynthetically active radiation to total solar radiation, $c_{rad,rf}$ is the transmission coefficient of the roof for solar radiation, V_l [W m^{-2}] is the solar radiation outside the greenhouse, σ_{co2} [m s^{-1}] is the canopy conductance for carbon dioxide transport into the leaves, X_c [kg m^{-3}] is the carbon dioxide concentration and Γ [kg m^{-3}] is the carbon dioxide compensation point which accounts for photorespiration at high light levels.

The carbon dioxide compensation point Γ is affected by the temperature X_t [$^\circ$C] according to the relation

$$(3.4) \quad \Gamma = c_\Gamma \, c_{Q10,\Gamma}^{(X_t - 20.)/10.} \quad \text{kg m}^{-3},$$

in which c_Γ [kg m^{-3}] is the carbon dioxide compensation point at 20 $^\circ$C. According to Goudriaan *et al.* (1985), the temperature effects on Γ are accounted for by the Q_{10} factor, $c_{Q10,\Gamma}$. For every temperature increase of 10 $^\circ$C, the carbon dioxide compensation point increases by a factor $c_{Q10,\Gamma}$.

At high light levels, the effect of photorespiration is only observable through the carbon dioxide compensation point. At low light levels, however, photorespiration has a pronounced effect on the light use efficiency. The effect of photorespiration on the light

use efficiency is accounted for by the relation

$$(3.5) \qquad \varepsilon = c_\varepsilon \frac{X_c - \Gamma}{X_c + 2\Gamma} \qquad\qquad\qquad \text{kg J}^{-1},$$

in which c_ε [kg J^{-1}] is the light use efficiency at very high carbon dioxide concentrations in the absence of photorespiration (Goudriaan *et al.*, 1985).

The canopy conductance σ_{co2} [m s^{-1}] for carbon dioxide transport from the ambient air to the chloroplast is determined by three series conductances. Two of them are of physical nature, namely the boundary layer conductance and stomatal conductance and one is of chemical nature, namely the carboxylation conductance (Goudriaan *et al.*, 1985). The canopy conductance is described by

$$(3.6) \qquad \frac{1}{\sigma_{co2}} = \frac{1}{c_{bnd}} + \frac{1}{c_{stm}} + \frac{1}{\sigma_{car}} \qquad\qquad \text{s m}^{-1},$$

where c_{bnd}, c_{stm} and σ_{car} [m s^{-1}] are the boundary layer conductance, the stomatal conductance and the carboxylation conductance, respectively. Because $\phi_{phot,max}$ is defined as the assimilation rate of an effective canopy surface of 1 m^2 per square meter of soil, leaf conductances may be used instead of canopy conductances. Generally, the boundary layer conductance of leaves depends on the wind speed of the surrounding air and the temperature difference between the leaves and the ambient air (Stanghellini, 1987). In this model, however, the boundary layer conductance is assumed to be constant. The stomatal resistance depends on the physiological state of the crop. In the literature, effects of temperature, carbon dioxide concentration, water vapour deficit and incident solar radiation on the stomatal conductance of tomato leaves have been reported (*e.g.* Stanghellini, 1987). These effects are not accounted for in this model and a constant stomatal resistance is assumed as well.

Complex biochemical models do exist which describe the temperature effects on the chemical reactions involved in the carboxylation process. In this research the carboxylation resistance is described by the following second order polynomial fitted to data from Goudriaan (1987):

$$(3.7) \qquad \sigma_{car} = c_{car,1} X_t^2 + c_{car,2} X_t + c_{car,3} \qquad\qquad \text{m s}^{-1},$$

with the parameters $c_{car,1}$ [m s^{-1} °C^{-2}], $c_{car,2}$ [m s^{-1} °C^{-1}] and $c_{car,3}$ [m s^{-1}]. The polynomial produces a quite accurate fit on the data for a temperature between 5 and 40 °C and has a maximum of 4.0×10^{-3} m s^{-1} at 17.5 °C and zero values around 5 and 40 °C. When the polynomial in eqn. (3.7) becomes zero, $1/\sigma_{car}$ will be infinite. This should be prevented during simulations with the model by limiting the air temperature to between 5 and 40 °C.

The maintenance respiration rate of the crop (ϕ_{resp}) is described by

$$(3.8) \qquad \phi_{resp} = (c_{resp,s}(1-c_\tau) + c_{resp,r}c_\tau) \, X_d \, c_{Q10,resp}^{(X_t-25.)/10.} \qquad \text{kg m}^{-2} \text{ s}^{-1},$$

where $c_{resp,s}$ and $c_{resp,r}$ [s^{-1}] are the maintenance respiration rates for the shoot and the root at 25 °C expressed in the mass of glucose consumed and $c_{Q10,resp}$ is the Q_{10}-factor for the maintenance respiration.

In chapter 4, where the performance criterion for optimal greenhouse climate control is defined in more detail, it will be shown that the value of a lettuce crop is determined by the fresh weight of the lettuce heads. Total head fresh weight is assumed to be proportionally related with the total amount of dry matter present:

$$(3.9) \qquad Y_{fw} = c_{fw}X_d(1-c_\tau) \qquad \text{kg m}^{-2},$$

where c_{fw} is the ratio of crop fresh weight to crop dry weight which is assumed to be constant in this model.

3.2.2.2. Parameterization and calibration

In table 3.1 the model parameters are listed. Most of them have been derived from the literature or from physical properties of the objects involved. The particular choice of some of the parameters is motivated as follows.

The parameter c_α, expressing the conversion of assimilated carbon dioxide into sugars (CH_2O), is taken to be the ratio of the

molecular   weights   of CH_2O and   carbon   dioxide (CO_2),   *i.e.*
$30/44 = 0.68$.

Table 3.1. Parameters of the one state variable lettuce growth model.

Parameter	Value	Dimension	Source
c_α	.68	–	physical constant
c_β	0.8	–	Sweeney *et al.* (1981)
c_{bnd}	0.004	$m\ s^{-1}$	Stanghellini (1993)
$c_{car,1}$	$-1.32{\times}10^{-5}$	$m\ s^{-1}\ {}^oC^{-2}$	estim. from Goudriaan (1987)
$c_{car,2}$	$5.94{\times}10^{-4}$	$m\ s^{-1}\ {}^oC^{-1}$	estim. from Goudriaan (1987)
$c_{car,3}$	$-2.64{\times}10^{-3}$	$m\ s^{-1}$	estim. from Goudriaan (1987)
c_ε	$17{\times}10^{-9}$	$kg\ J^{-1}$	Goudriaan *et al.* (1985)
c_{fw}	22.5	–	measurement
c_Γ	$7.32{\times}10^{-5}$	$kg\ m^{-3}$	Goudriaan *et al.* (1985)
c_k	0.9	–	Goudriaan and Monteith (1990)
$c_{lar,d}$	$62.5{\times}10^{-3}$	$m^2\ kg^{-1}$	calibration
c_{par}	0.5	–	Spitters *et al.* (1986)
$c_{Q10,\Gamma}$	2	–	Goudriaan *et al.* (1985)
$c_{Q10,resp}$	2	–	Van Keulen *et al.* (1982)
$c_{rad,rf}$	0.37 - 0.50	–	measurement
$c_{resp,s}$	$3.47{\times}10^{-7}$	s^{-1}	Van Keulen *et al.* (1982)
$c_{resp,r}$	$1.16{\times}10^{-7}$	s^{-1}	Van Keulen *et al.* (1982)
c_{stm}	0.007	$m\ s^{-1}$	Stanghellini (1993)
c_τ	0.07	–	measurement

The yield factor c_β was estimated by Sweeney *et al.* (1981) at 0.8, which compared with the value of 0.72 indicated by Van Keulen *et al.* (1982), seems relatively high. However, for lettuce specifically no other data for c_β were found in the literature.

According   to   Van   Keulen   *et   al.*   (1982)   the   maintenance

requirements for leaves and roots are set at 0.03 and 0.01 day^{-1}. Assuming that the shoot is essentially composed of leaves this results in the values 3.47×10^{-7} s^{-1} and 1.16×10^{-7} s^{-1} for $c_{resp,s}$ and $c_{resp,r}$ respectively. The canopy extinction c_k has a value of 0.9 and 0.3 for planophile and erectophile canopies respectively (Goudriaan and Monteith, 1990). Because lettuce is more a planophile than an erectophile crop, 0.9 seems to be most suitable. For the carbon dioxide compensation point Goudriaan *et al.* (1985) used c_Γ = 40 ppm, which is equivalent to 7.32×10^{-5} kg m^{-3} using a density of carbon dioxide of 1.83 kg m^{-3}.

From measurements of the solar radiation outside and inside the greenhouse at canopy level, the transmission coefficient of the greenhouse evaluated at canopy level was found to be 0.37 during the autumn experiment in late 1991 and 0.5 during the experiment in early 1992. The difference is largely explained by shading from fully grown tomato crops in neighbouring compartments during the first experiment. During the second experiment the neighbouring compartments were empty.

For lettuce grown in soil c_τ = 0.15 has been reported by Lorenz and Wiebe (1980) and Sweeney *et al.* (1981). This value was found to be rather high compared with 0.07 measured on lettuce plants grown in the NFT system during the first experiment in late 1991.

One parameter, the shoot leaf area ratio $c_{lar,d}$, has been determined by manual calibration using the measured data obtained during the first experiment. The resulting value closely accords with the value reported by Lorenz and Wiebe (1980).

3.2.2.3. Validation

Using half hour averages of the recorded greenhouse climate data, crop growth during both experiments was simulated. The data of the first experiment were used for model calibration as described in section 3.2.1. The data of the second experiment were used for an independent validation of the model. In fig. 3.2, the measured carbon dioxide concentration and air temperature in the greenhouse and solar radiation outside the greenhouse during the second experiment are shown. Simulated plant dry weight accumulation is presented in fig. 3.3 (p. 27) together with the weekly measurements and the dry matter production simulated with the two state variable lettuce growth model to be described in section 3.2.3. The vertical bars around the measurement points indicate the 95% confidence limits around the mean
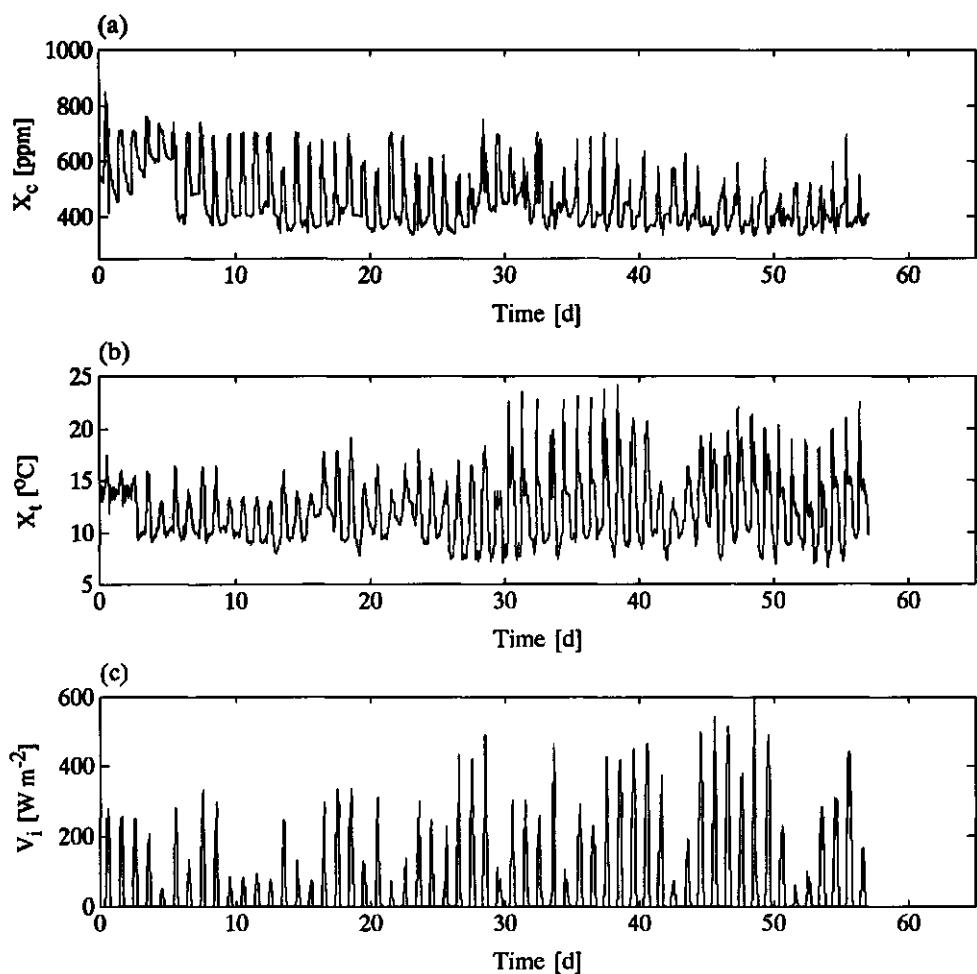
Fig. 3.2.   Half   hour   averages   of   the   measurements   of   the   carbon
            dioxide   concentration   (a)   and   temperature   (b)   in   the
            greenhouse and solar radiation outside the greenhouse (c).

value, based on the destructive measurements of all 20 plants at each
sample date.

        An   exact   criterion   of   success   of   the   validation   is   hard   to
define.   In   this   research   the   rather   intuitive   criterion   has   been
adopted that simulated growth should lie within the 95% confidence
limits of the measurements for most of the time. Preferably, but more
stringent,   the   model   should   be   able   to   follow   the   general   dynamic
trend in the mean of the measured plant dry weight. Fig. 3.3a shows
that   the   model   produces   a   good   fit   to   the   data   during   the   first
experiment   (calibration).   Also   during   the   second,   validation,

(a)

(b)
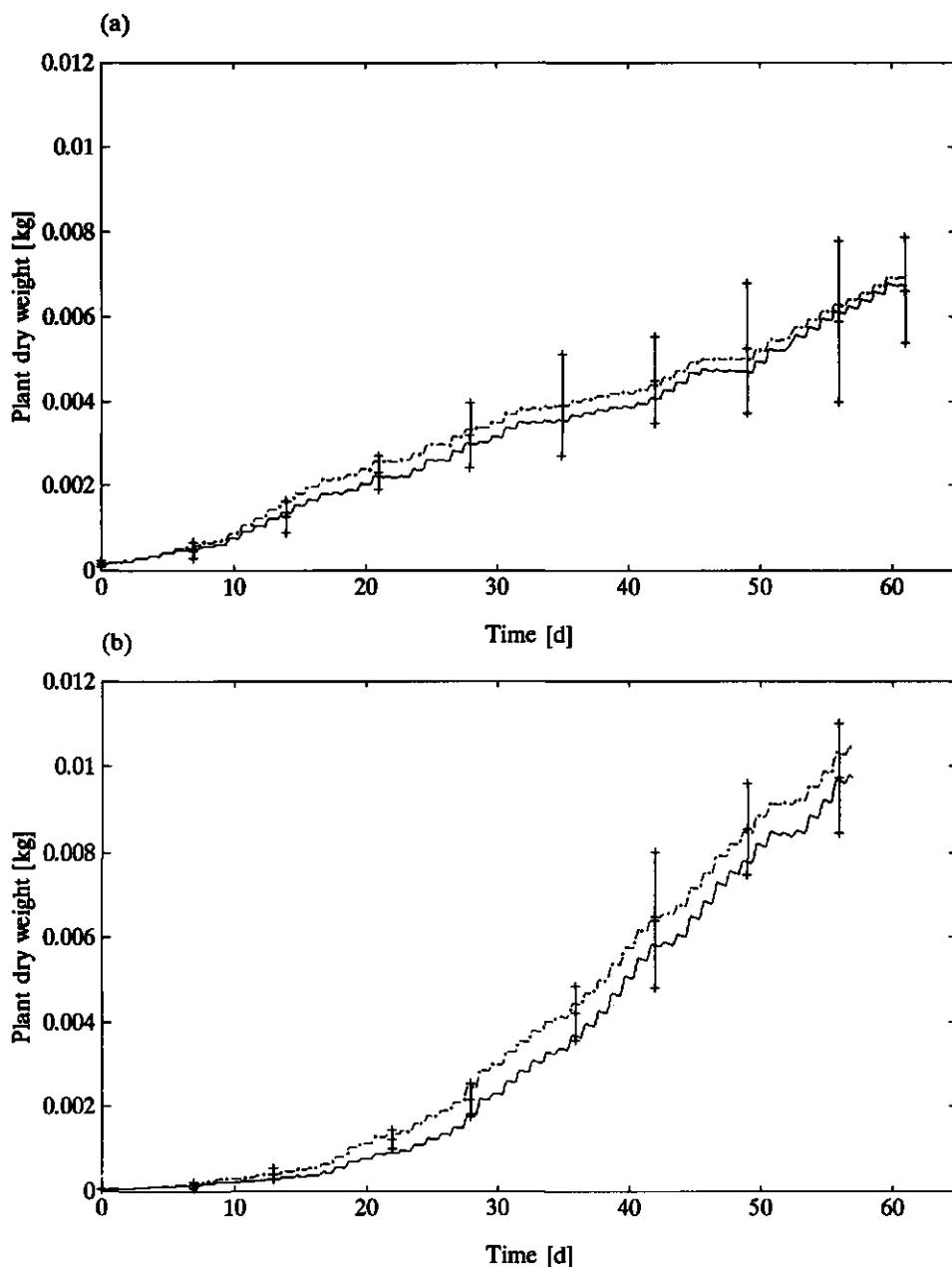
Fig. 3.3. Simulated and measured plant dry weight during experiment 1 (a) and experiment 2 (b); (-·) indicates the one state variable model and (—) indicates the two state variable model; the vertical bars express the 95% confidence limits around the mean value of the measurements.

experiment an accurate description of the mean measured dry matter accumulation is obtained (fig. 3.3b).

Fig. 3.3 reveals that the simulations of the dry matter content exhibit more dynamics than could be observed in the measurements using a measurement interval of 5 to 7 days. First of all, there is a diurnal trend consisting of a day time increment of dry weight due to canopy photosynthesis and a night time decrease caused by dry matter consumption in maintenance respiration. Secondly, there are variations in the simulated dry matter production with a duration of several days which will have been caused by day to day differences in the radiation conditions and the greenhouse climate (cf. fig. 3.2). To verify these faster responses, it would be necessary to sample crop dry weight more frequently. However, the measurements presented in fig. 3.3 show a large variability in the measured plant dry weight. This is partly due to an evident variability present in a crop grown under practical circumstances, and to a certain extent a consequence of errors in the measurements of plant dry weight. In view of this, crop variability and measurement errors will dominate the relatively small fast responses found in the simulations, so that it is arguable whether they can be validated under practical circumstances.

Between the two experiments a considerable difference in dry matter production can be observed; in the first experiment dry matter production was considerably smaller than in the second experiment. Since the indoor air temperature and carbon dioxide concentration were controlled in much the same way during both experiments, the observed difference in dry matter production must be largely due to the comparatively low solar radiation levels during the autumn experiment.

In horticultural practice cultivars 'Berlo' and 'Norden' are considered to have different growth responses which make them particularly suitable for cultivation in the autumn and winter, respectively. Van Holsteijn (1981) also reported different growth responses of distinct lettuce cultivars. These observations were partly explained by differences in morphology as expressed for instance by the leaf area ratio. In this study the leaf area ratio was calibrated on the measurement data obtained during the first experiment with cultivar 'Berlo' and produced an accurate simulation of the growth of cultivar 'Norden' throughout the second experiment. Though the arrangement of the two experiments does not allow for thorough evidence about a possible difference between the two cultivars, it seems that with a single value for the leaf area ratio the model is able to simulate crop growth of both cultivars equally well despite slight differences between the cultivars could be observed by visual inspection of the crop.

3.2.3. A two state variable lettuce growth model

3.2.3.1. Model equations

In this model representation of lettuce growth, the state of the crop is described by two state variables, namely the non-structural dry weight X_n and the structural dry weight X_s, such that total dry weight is equivalent to $X_n + X_s$ (Thornley and Hurd, 1974; Sweeney *et al.*, 1981). The non-structural dry weight consists, for instance, of glucose, sucrose and starch. The structural dry weight is the remaining component of the total dry weight and represents the weight of structural components like cell walls and cytoplasm.

   The model describes the dynamic behaviour of the state variables on a square meter soil basis with the differential equations

$$(3.10) \qquad \frac{dX_n}{dt} = c_\alpha \phi_{phot} - r_{gr}X_s - \phi_{resp} - \frac{1-c_\beta}{c_\beta} r_{gr}X_s \qquad \text{kg m}^{-2}\text{ s}^{-1},$$

$$(3.11) \qquad \frac{dX_s}{dt} = r_{gr}X_s \qquad \text{kg m}^{-2}\text{ s}^{-1},$$

where ϕ_{phot} [kg m^{-2} s^{-1}] is the gross carbon dioxide uptake due to canopy photosynthesis, r_{gr} [s^{-1}] is the specific growth rate, ϕ_{resp} [kg m^{-2} s^{-1}] is the maintenance respiration rate expressed in terms of the amount of carbohydrates used and c_α and c_β are parameters. The factor c_α converts assimilated carbon dioxide into sugar equivalents. The yield factor c_β accounts for the respiratory and synthesis losses during the conversion of carbohydrates to structural material and has a value between zero and one. These losses are dependent on the chemical composition of the dry matter formed (Penning de Vries *et al.*, 1974).

   The growth rate of the non-structural dry weight (eqn. (3.10)) is determined by the gross canopy photosynthesis rate (ϕ_{phot}), the rate with which non-structural material is used for growth of structural dry weight ($-r_{gr}X_s$), the maintenance respiration rate ϕ_{resp} which provides energy to maintain cells and their biostructure as well as ionic gradients, and synthesis and respiratory losses associated with growth (($1-c_\beta)/c_\beta r_{gr}X_s$). The growth rate of structural dry matter (eqn. (3.11)) depends on the rate at which the non-structural material is transformed into structural material.

In accordance with Goudriaan and Van Laar (1978) and Goudriaan and Monteith (1990) gross canopy photosynthesis is described by the empirical relation

$$(3.12) \qquad \phi_{phot} = \phi_{phot,max}\left(1 - e^{-c_k c_{lar,s}(1-c_\tau)X_s}\right) \qquad \text{kg m}^{-2}\text{ s}^{-1},$$

in which $\phi_{phot,max}$ [kg m^{-2} s^{-1}] is defined as the gross carbon dioxide assimilation rate of a canopy having an effective surface of 1 m^2 per square meter of soil at complete soil covering. The geometrical and optical properties of the canopy with respect to incident radiation before canopy closure are accounted for by the exponential relation $1 - e^{-c_k c_{lar,s}(1-c_\tau)X_s}$. The parameter $c_{lar,s}$ [m^2 kg^{-1}] is the shoot structural leaf area ratio, expressing the amount of leaf area per unit structural dry weight. It is assumed to be constant in this model. The parameter c_k is the extinction coefficient of the canopy and c_τ expresses the ratio of the root dry weight to the total crop dry weight. This parameter is also assumed to be constant in this model.

The response of canopy photosynthesis $(\phi_{phot,max})$ to the incident radiation and carbon dioxide concentration in the greenhouse air is described with a relation according to Acock *et al.* (1978) which has been extended to account for photorespiration and temperature effects on the light use efficiency as well as temperature effects on the carboxylation conductance in the leaf tissue

$$(3.13) \qquad \phi_{phot,max} = \frac{\varepsilon c_{par} c_{rad,rf} V_1 \sigma_{co2}(X_c - \Gamma)}{\varepsilon c_{par} c_{rad,rf} V_1 + \sigma_{co2}(X_c - \Gamma)} \qquad \text{kg m}^{-2}\text{ s}^{-1},$$

in which ε [kg J^{-1}] is the light use efficiency, c_{par} expresses the ratio of photosynthetically active radiation to total solar radiation, $c_{rad,rf}$ is the transmission coefficient of the roof for solar radiation, V_1 [W m^{-2}] is the solar radiation outside the greenhouse, σ_{co2} [m s^{-1}] is the canopy conductance for carbon dioxide transport into the leaves, X_c [kg m^{-3}] is the carbon dioxide

concentration and Γ [kg m^{-3}] is the carbon dioxide compensation point which accounts for photorespiration at high light levels.

The carbon dioxide compensation point Γ is affected by the temperature, X_t [$^{\circ}$C] , according to the relation

$$(3.14) \qquad \Gamma = c_\Gamma \, c_{Q10,\Gamma}^{(X_t-20.)/10.} \qquad\qquad \text{kg m}^{-3},$$

in which c_Γ [kg m^{-3}] is the carbon dioxide compensation point at 20 $^{\circ}$C and according to Goudriaan *et al.* (1985) the temperature effects on Γ are accounted for by the Q10 factor $c_{Q10,\Gamma}$.

At high light levels the effect of photorespiration is only observable through the carbon dioxide compensation point. At low light levels, however, photorespiration has a pronounced effect on the light use efficiency. The effect of photorespiration on the light use efficiency is accounted for by the relation

$$(3.15) \qquad \varepsilon = c_\varepsilon \, \frac{X_c - \Gamma}{X_c + 2\Gamma} \qquad\qquad \text{kg J}^{-1},$$

in which c_ε [kg J^{-1}] is the light use efficiency at very high carbon dioxide concentrations (Goudriaan *et al.*, 1985).

The canopy conductance σ_{co2} [m s^{-1}] for carbon dioxide transport from the ambient air to the chloroplast is determined by three series conductances:

$$(3.16) \qquad \frac{1}{\sigma_{co2}} = \frac{1}{c_{bnd}} + \frac{1}{c_{stm}} + \frac{1}{\sigma_{car}} \qquad\qquad \text{s m}^{-1},$$

where c_{bnd}, c_{stm} and σ_{car} [m s^{-1}] are the boundary layer conductance, the stomatal conductance and the carboxylation conductance, respectively. The boundary layer and stomatal conductance are assumed to be constant in this model. The carboxylation conductance is described with the polynomial

$$(3.17) \qquad \sigma_{car} = c_{car,1} X_t^2 + c_{car,2} X_t + c_{car,3} \qquad\qquad \text{m s}^{-1},$$

for a temperature between 5 and 40 °C, with the parameters $c_{car,1}$ [m s^{-1} °C^{-2}], $c_{car,2}$ [m s^{-1} °C^{-1}] and $c_{car,3}$ [m s^{-1}]. The carboxylation conductance has a maximum value of 4.0×10^{-3} m s^{-1} at 17.5 °C and zero values around 5 and 40 °C.

The maintenance respiration rate of the crop (ϕ_{resp}) is described by

$$(3.18) \quad \phi_{resp} = (c_{resp,s}(1-c_\tau) + c_{resp,r}c_\tau) \, X_s \, c_{Q10,resp}^{(X_t-25.)/10.}$$

$$\text{kg m}^{-2} \text{ s}^{-1},$$

where $c_{resp,s}$ [s^{-1}] and $c_{resp,r}$ [s^{-1}] are the maintenance respiration rates for the shoot and the root at 25 °C as expressed in the mass of glucose consumed and $c_{Q10,resp}$ is the Q_{10} factor of the maintenance respiration which has an analogous interpretation to $c_{Q10,\Gamma}$.

The growth rate coefficient r_{gr} [s^{-1}] describes the transformation of non-structural dry weight to structural dry weight. In accordance with Thornley and Hurd (1974) it is assumed that the specific rate of utilization of non-structural material for the construction of structural material depends on the ratio of non-structural dry weight to total dry weight, obeying a Michaelis-Menten type equation. Furthermore the transformation of non-structural material into structural material depends on the temperature (Sweeney et al., 1981). This results in the following expression for r_{gr}:

$$(3.19) \quad r_{gr} = c_{r,gr,max} \frac{X_n}{X_s+X_n} c_{Q10,gr}^{(X_t-20.)/10.} \qquad \text{s}^{-1},$$

where $c_{r,gr,max}$ [s^{-1}] is the saturation growth rate at 20 °C and $c_{Q10,gr}$ is the Q_{10} factor for growth.

With the model described so far the evolution of the non-structural dry weight and structural dry weight as affected by air temperature, carbon dioxide concentration and solar radiation can be simulated. However, with eqns. (3.10) and (3.11), it is also possible to describe other variables related to the state of the crop. For instance, total crop dry weight Y_d [kg m^{-2}] is related to both state variables according to the relation

(3.20) $Y_d = X_n + X_s$ kg m^{-2},

and total head fresh weight is given by:

(3.21) $Y_{fw} = c_{fw}(X_s + X_n)(1-c_\tau)$ kg m^{-2},

where c_{fw} is the ratio of crop fresh weight to crop dry weight.

3.2.3.2. Parameterization and calibration

The parameters of the two state variable lettuce growth model are listed in table 3.2. The majority of the parameters in the two state variable model have the same definition and the same value as in the one state variable model and the reasons for their choice are given in section 3.2.2.2.

Because no separate measurements of the non-structural and structural dry weights were available, the initial conditions of these state variables had to be determined from measurements of total dry weight at the planting date. Total crop dry weight amounted to 2.70×10^{-3} kg m^{-2} and 0.72×10^{-3} kg m^{-2} during the first and the second experiment, respectively. It was assumed by Sweeney *et al.* (1981) that at planting date the ratio of structural to total dry weight was 0.50. However, Goudriaan *et al.* (1985) state that the non-structural dry weight rarely exceeds 25% of the total dry weight. In the simulations an initial value of 0.75 for the ratio of structural dry weight to total dry weight was therefore used.

The shoot structural leaf area ratio, $c_{lar,s}$, was calibrated using the data of the first experiment resulting in a value of 75×10^{-3} m^{-2} kg^{-1}.

The remaining parameters have been derived from the literature to which reference is made in the table.

Table 3.2. Parameters of the two state variable lettuce growth model.

Parameter	Value	Dimension	Source
c_α	.68	–	physical constant
c_β	0.8	–	Sweeney *et al.* (1981)
c_{bnd}	0.004	m s^{-1}	Stanghellini (1993)
$c_{car,1}$	-1.32×10^{-5}	m s^{-1} °C^{-2}	estim. from Goudriaan (1987)
$c_{car,2}$	5.94×10^{-4}	m s^{-1} °C^{-1}	estim. from Goudriaan (1987)
$c_{car,3}$	-2.64×10^{-3}	m s^{-1}	estim. from Goudriaan (1987)
c_ε	17×10^{-9}	kg J^{-1}	Goudriaan *et al.* (1985)
c_{fw}	22.5	–	measurement
c_Γ	7.32×10^{-5}	kg m^{-3}	Goudriaan *et al.* (1985)
c_k	0.9	–	Goudriaan and Monteith (1990)
$c_{lar,s}$	75×10^{-3}	m^2 kg^{-1}	calibration
c_{par}	0.5	–	Spitters *et al.* (1986)
$c_{Q10,\Gamma}$	2	–	Goudriaan *et al.* (1985)
$c_{Q10,gr}$	1.6	–	Sweeney *et al.* (1981)
$c_{Q10,resp}$	2	–	Van Keulen *et al.* (1982)
$c_{rad,rf}$	0.37 – 0.50	–	measurement
$c_{r,gr,max}$	5×10^{-6}	s^{-1}	Van Holsteijn (1981)
$c_{resp,s}$	3.47×10^{-7}	s^{-1}	Van Keulen *et al.* (1982)
$c_{resp,r}$	1.16×10^{-7}	s^{-1}	Van Keulen *et al.* (1982)
c_{stm}	0.007	m s^{-1}	Stanghellini (1993)
c_τ	0.07	–	measurement

3.2.3.3 Validation

Using half hour averages of the recorded greenhouse climate data, crop growth during both experiments was simulated. The data of the first experiment were used for model calibration; the data of the second experiment were used for an independent simulation. The measurements of carbon dioxide concentration and air temperature in

the greenhouse and solar radiation outside the greenhouse during the second experiment are presented in fig. 3.2 (p. 26).

In fig. 3.3 (p. 27) crop dry weight simulations with the two state variable model are presented together with the weekly measurements during both experiments as well as the simulations with the one state variable lettuce growth model. The vertical bars around the measurement points indicate the 95% confidence limits. The model accurately describes the dry matter accumulation during the first (calibration) experiment. During the second (validation) experiment a slight underestimation in the dry matter accumulation can be observed. This may be due to an improper parameterization of the shoot structural leaf area ratio, $c_{lar,s}$. Still, the simulated dry matter production lies within the 95% confidence limits for most of the time.

A comparison of the response of the two growth models reveals that the one state variable model simulates a higher dry matter production throughout the growing period than the two state variable model. The difference in simulated dry weight originates from the earliest stages of growth and remains approximately constant during the remainder of the cultivation period. This observation may be explained as follows. In the one state variable model the leaf area is directly related to the amount of total dry weight present and any dry matter increment, however small, will have an immediate effect on the light interception by the canopy. This results in a positive feedback on the simulated dry matter accumulation. In the two state variable model, however, an increment in the non-structural dry matter does not directly affect the amount of leaf area and light interception. Since, in the two state variable model, the leaf area is related to the amount of structural material, an additional amount of non-structural material first needs to be transformed into structural material before it affects the leaf area and consequently dry matter production. This delay has a weakening effect on the positive feedback of leaf area expansion on the dry matter production.

As with the one state variable lettuce growth model, simulations with the two state variable model show more dynamics than could be observed by the destructive measurements using a measurement interval of 5 to 7 days. Though differences in simulated dry matter production between the two models do exist, the dynamics in the simulated crop growth strongly resemble each other.

3.2.4. A greenhouse climate model

3.2.4.1. Model equations

In this greenhouse climate model, the greenhouse interior is considered to be a perfectly stirred tank consisting essentially of one homogeneous component, the greenhouse air. The state of the greenhouse climate is represented by three state variables, namely indoor air temperature X_t [°C], carbon dioxide concentration X_c [kg m^{-3}] and absolute humidity X_h [kg m^{-3}]. For simplicity, construction elements of the greenhouse, the crop and the soil are not modelled as separate elements but their influence is implicitly accounted for in the model.

The dynamic changes in the greenhouse climate are determined by energy and mass flowes, originating from differences in energy and mass content between the inside and outside air or from control or exogenous energy and mass inputs. In this model, control inputs are the temperature of the heating system U_t [°C], the aperture of the lee and windward side ventilation windows, U_{ls} and U_{ws} [%] and the supply rate of carbon dioxide U_c [kg m^{-2} s^{-1}]. It is assumed that instantaneous changes in the temperature of the heating system can be achieved, though in practice dynamics will occur in the heating system. Exogenous inputs, or disturbances, are solar irradiation V_l [W m^{-2}], wind speed V_w [m s^{-1}], and the temperature V_t [°C], absolute humidity V_h [kg m^{-3}] and carbon dioxide concentration V_c [kg m^{-3}] outside the greenhouse.

The greenhouse climate model describes the dynamic behaviour of the state variables with the differential equations

$$(3.22) \qquad \frac{dX_t}{dt} = \frac{1}{c_{cap,q}}(Q_{pl,al} - Q_{al,ou} + Q_{rad}) \qquad \qquad °C\ s^{-1},$$

$$(3.23) \qquad \frac{dX_c}{dt} = \frac{1}{c_{cap,c}}(U_c - \phi_{c,al,pl} - \phi_{c,al,ou}) \qquad \qquad kg\ m^{-3}\ s^{-1},$$

$$(3.24) \qquad \frac{dX_h}{dt} = \frac{1}{c_{cap,h}}(\phi_{h,pl,al} - \phi_{h,al,ou}) \qquad \qquad kg\ m^{-3}\ s^{-1},$$

where $c_{cap,q}$ [J m^{-2} $^{\circ}$C^{-1}], $c_{cap,c}$ [m], $c_{cap,h}$ [m] are the heat and mass capacities of the greenhouse air respectively. In this model, the heat and mass transfer in the greenhouse are described per square metre soil.

The energy balance of the greenhouse air is affected by the energy supply from the heating system, $Q_{pl,al}$ [W m^{-2}], energy losses to the outside air due to transmission through the greenhouse cover and natural ventilation exchange through the windows, $Q_{al,ou}$ [W m^{-2}], and the heat load imposed on the greenhouse by the sun, Q_{rad} [W m^{-2}].

The carbon dioxide balance of the greenhouse air is determined by the carbon dioxide supply rate, U_c [kg m^{-2} s^{-1}], the net carbon dioxide uptake by the canopy, $\phi_{c,al,pl}$ [kg m^{-2} s^{-1}], and the ventilation exchange with the outside air, $\phi_{c,al,ou}$ [kg m^{-2} s^{-1}]. In the greenhouse considered, the soil was covered with plastic and therefore carbon dioxide emission from the soil due to respiration of plant roots and soil organisms is not considered in this model.

Finally, the humidity balance is affected by canopy transpiration, $\phi_{h,pl,al}$ [kg m^{-2} s^{-1}], and the ventilation exchange with the outside air, $\phi_{h,al,ou}$ [kg m^{-2} s^{-1}]. Condensation of water at the inner surface of the roof, although being significant during some parts of the day and night, is neglected in this model.

Other energy and mass transport phenomena, for instance at the greenhouse cover and the soil, are thought to be relatively unimportant in view of the objective of this research and are therefore neglected.

The individual energy and mass flows are modelled as follows. The convective energy transport from the heating pipes to the greenhouse is described by

$$(3.25) \qquad Q_{pl,al} = c_{pl,al}(U_t - X_t) \qquad\qquad \text{W m}^{-2},$$

where $c_{pl,al}$ [W m^{-2} $^{\circ}$C^{-1}] is the heat transfer coefficient expressed per square meter of soil. The heat load from the sun is governed by

$$(3.26) \qquad Q_{rad} = c_{rad}V_1 \qquad\qquad\qquad \text{W m}^{-2},$$

with the coefficient c_{rad} accounting for the transmission of the roof, the interception of the transmitted solar radiation by the structural components of the greenhouse and the conversion of the absorbed solar energy by the canopy into a sensible heat load on the greenhouse air.

The energy loss to the outside air is described by

$$(3.27) \qquad Q_{al,ou} = (\phi_{vent}c_{cap,q,v}+c_{al,ou})(X_t-V_t) \qquad\qquad W \ m^{-2},$$

where $c_{al,ou}$ [W m^{-2} $^{\circ}$C^{-1}] is the heat transfer coefficient for energy transport through the greenhouse cover and ϕ_{vent} [m s^{-1}] is the natural ventilation flux through the windows, both expressed per square meter of soil. $c_{cap,q,v}$ [J m^{-3} $^{\circ}$C^{-1}] is the heat capacity per volume unit of air.

The natural ventilation flux through the windows, ϕ_{vent}, is calculated from the wind speed and the aperture of the lee and windward side vents according to De Jong (1990). Using the measurement data of De Jong (1990, p.54) for the specific greenhouse considered in this research, curve fitting resulted in the following relation

$$(3.28) \qquad \phi_{vent} = c_{window}\left(\frac{c_{ls,1}U_{ls}}{1+c_{ls,2}U_{ls}}+c_{ws,1}+c_{ws,2}U_{ws}\right)V_w+c_{leak} \qquad\qquad m \ s^{-1},$$

where U_{ls} and U_{ws} [%] have values between 0 and 100%, $c_{ls,1}$, $c_{ls,2}$, $c_{ws,1}$ and $c_{ws,2}$ parameterize the ventilation function, c_{window} equals the amount of window aperture per square meter of soil and c_{leak} [m s^{-1}] is a leakage term. Since the contribution of ventilation induced by temperature differences between the inside and outside air is only significant at very low wind speeds, it is neglected in this model.

The net carbon dioxide uptake of the canopy due to photosynthesis, growth respiration and maintenance respiration is described by

$$(3.29) \qquad \phi_{c,al,pl} = \phi_{phot} - \frac{1}{c_{\alpha}}\phi_{resp} - \frac{1-c_{\beta}}{c_{\alpha}c_{\beta}}r_{gr}X_s \qquad\qquad kg \ m^{-2} \ s^{-1},$$

when crop growth is described by the two state variable lettuce growth model, and ϕ_{phot}, ϕ_{resp} and r_{gr} are defined as in section 3.2.3.1. The net carbon dioxide uptake is determined by the gross photosynthetic uptake, ϕ_{phot}, and the carbon dioxide production by growth respiration, $((1-c_\beta)/c_\alpha c_\beta)\, r_{gr}\, X_s$, and maintenance respiration, ϕ_{resp}/c_α. Since both growth and maintenance respiration are expressed in terms of the non-structural material used, the related carbon dioxide production is obtained by dividing the respiratory consumption of non-structural material by the conversion factor c_α. When the one state variable lettuce growth model is used to simulate crop growth, an equivalent relation derived from the model description in section 3.2.2.1, is employed.

The exchange of carbon dioxide and water vapour through the ventilation windows is described by

$$(3.30) \qquad \phi_{c,al,ou} = \phi_{vent}(X_c - V_c) \qquad\qquad \text{kg m}^{-2}\text{ s}^{-1},$$

and

$$(3.31) \qquad \phi_{h,al,ou} = \phi_{vent}(X_h - V_h) \qquad\qquad \text{kg m}^{-2}\text{ s}^{-1}.$$

Canopy transpiration acts as a source of water vapour to the greenhouse air. The driving force of this phenomenon is the difference in water vapour pressure between the ambient air and the sub-stomatal cavity, which is assumed to be saturated with respect to water vapour. The saturation pressure is determined by the canopy temperature which in this model is taken to be equivalent with the air temperature. Canopy transpiration is described by

$$(3.32) \qquad \phi_{h,pl,al} = (1 - e^{-c_{a,pl}X_s})c_{v,pl,al}\left(\frac{c_{v,0}c_{v,1}c_{H2O}}{c_R(X_t + c_{t,abs})}e^{\frac{c_{v,2}X_t}{X_t + c_{v,3}}} - X_h\right)$$

$$\text{kg m}^{-2}\text{ s}^{-1},$$

in which according to Goudriaan (1977) $\dfrac{c_{v,1}c_{H2O}}{c_R(X_t + c_{t,abs})}e^{\frac{c_{v,2}X_t}{X_t + c_{v,3}}}$ [kg m^{-3}] describes the saturation water vapour concentration of a unit amount

of air as a function of temperature, $c_{v,pl,al}$ [m s^{-1}] is the mass
transfer coefficient, c_R [J K^{-1} kmol^{-1}] is the gas constant,
c_{H2O} [kg kmol^{-1}] is the molecular mass of water, $c_{t,abs}$ [K] is the
absolute temperature and $c_{v,0}$ is a calibration parameter. In line
with the description of the canopy photosynthesis, apart from the
first factor on the right hand side, eqn. (3.32) describes the
transpiration of a canopy having an effective surface of 1 m^2 per
square meter soil after canopy closure. A reduction of the canopy
transpiration before canopy closure is expressed by the exponential
relation $(1-e^{-c_{a,pl}X_s})$.

As outlined in chapter 2, a secondary objective of the optimal
greenhouse climate control system is to maintain the relative
humidity between an upper and a lower bound. The relative humidity is
calculated from the absolute humidity with the equation

$$(3.33) \quad RH = 100X_h \left(\frac{c_{v,1}c_{H2O}}{c_R(X_t+c_{t,abs})} e^{\frac{c_{v,2}X_t}{X_t+c_{v,3}}} \right)^{-1} \quad \%.$$

3.2.4.2. Parameterization and calibration

The parameters of the greenhouse climate model are listed in table
3.3. As with the lettuce growth models, most of the parameters were
extracted from the literature or based on physical properties of the
greenhouse. As denoted in the table, some of the parameters were
manually calibrated. The model was calibrated using 5 days of
measurement data from the second experiment from 13 until 17
February. The parameters were manually adapted until the simulations
of the air temperature, carbon dioxide concentration, absolute and
relative humidity produced a fair fit to their measured values. Since
the model overestimated the absolute humidity in the greenhouse,
possibly due to neglecting condensation on the greenhouse cover, the
calibration parameter was introduced. The large value of $c_{cap,q}$
accounts for the fact that in the model the energy transfer to and
from the soil has not been included.

Table 3.3. Parameters of the greenhouse climate model.

Parameter	Value	Dimension	Source
$c_{al,ou}$	6	W m^{-2} ^{o}C^{-1}	calibration
$c_{a,pl}$	62.8	m^2 kg^{-1}	(see text)
$c_{cap,c}$	4.1	m	physical property
$c_{cap,h}$	4.1	m	physical property
$c_{cap,q}$	30000	J m^{-2} ^{o}C^{-1}	calibration
$c_{cap,q,p}$	1000	J kg^{-1} ^{o}C^{-1}	physical constant
$c_{cap,q,v}$	1290	J m^{-3} ^{o}C^{-1}	physical constant
c_{H2O}	18	kg kmol^{-1}	physical constant
$c_{ls,1}$	5.5×10^{-4}	–	estim. from De Jong (1990)
$c_{ls,2}$	1.56×10^{-2}	–	estim. from De Jong (1990)
$c_{pl,al}$	5	W m^{-2} ^{o}C^{-1}	calibration
c_R	8314	J K^{-1} kmol^{-1}	physical constant
c_{rad}	0.2	–	calibration
$c_{\rho,al}$	1.29	kg m^{-3}	physical constant
$c_{t,abs}$	273	K	physical constant
c_{leak}	0.75×10^{-4}	m s^{-1}	calibration
$c_{v,pl,al}$	3.6×10^{-3}	m s^{-1}	Stanghellini (1987)
$c_{v,0}$	0.85	–	calibration
$c_{v,1}$	611	J m^{-3}	Goudriaan (1977)
$c_{v,2}$	17.4	–	Goudriaan (1977)
$c_{v,3}$	239	^{o}C	Goudriaan (1977)
c_{window}	0.11	–	physical property
$c_{ws,1}$	2.46×10^{-4}	–	estim. from De Jong (1990)
$c_{ws,2}$	4.85×10^{-4}	–	estim. from De Jong (1990)

Other parameters were determined as follows. The heat capacity of a unit volume of air $c_{cap,q,v} = c_{\rho,al}\, c_{cap,q,p}$, with the density of the air $c_{\rho,al}$ = 1.29 kg m^{-3} and the heat capacity of the air at constant pressure $c_{cap,q,p}$ = 1000. J m^{-3} $^{\circ}$C^{-1}. The parameter c_{window} is calculated from the effective window aperture, being 1.60 m^{-2}, and the number of windows per square meter soil, 20/300 = 0.07 m^{-2}, resulting in c_{window} = 1.60×0.07 = 0.11. The parameter $c_{a,pl}$, which accounts for the effect of incomplete soil cover on canopy transpiration, was assumed to be equal to $c_k c_{lar,s}(1-c_\tau)$.

Since during the greenhouse experiments the carbon dioxide concentration outside the greenhouse was not measured, a constant value of 350 ppm, *i.e.* 6.41×10^{-4} kg m^{-3}, was used.

3.2.4.3. Validation

For the purpose of optimal greenhouse climate control, the greenhouse climate model is required to describe as accurately as possible the influence of the control and exogenous inputs on the evolution of the state variables representing the greenhouse climate throughout the growing period considered. To investigate the model's ability to describe the greenhouse climate during the different stages of crop growth, simulations were compared with measurements in three periods of 5 consecutive days in the beginning (27 – 31 January), the middle (13 – 17 February) and towards the end (1 – 5 March) of the second greenhouse experiment in 1992.

The data obtained in the period from 13 to 17 February 1992 were used for manual calibration of the model. The control inputs to the greenhouse, including the pipe temperature, aperture of the lee and windward side ventilators and carbon dioxide supply rate, measured in this period are presented in fig. 3.4. The external inputs to the greenhouse, including solar irradiation, outside temperature, wind speed and humidity are shown in fig. 3.5 (p. 44).

Assuming the state of the crop to be constant during the 5 day period and equal to the measured value obtained during the same period, the simulation results presented in fig. 3.6 (p. 45) were obtained.
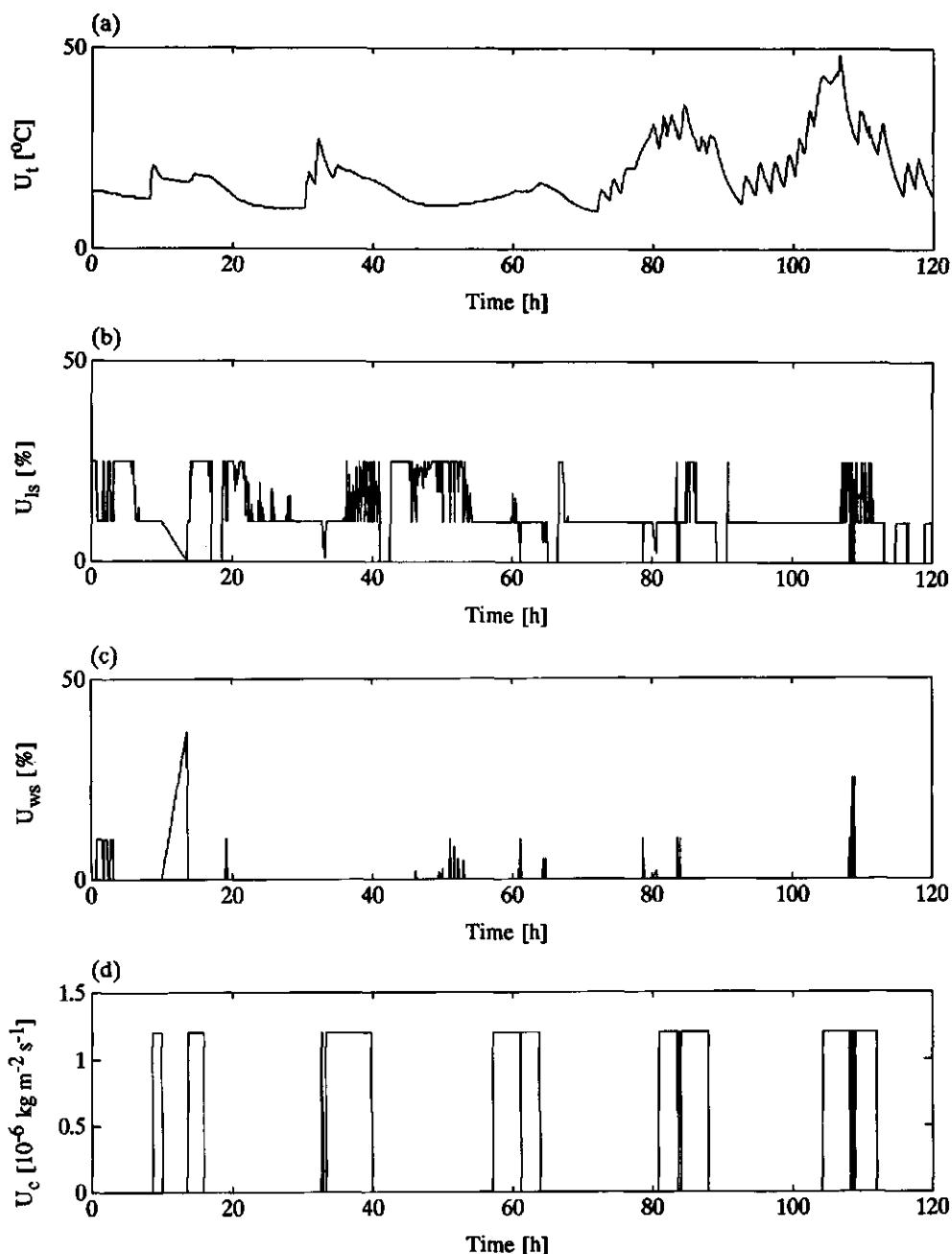
Fig. 3.4. Measurements of the control inputs from 13 to 17 February 1992: (a) pipe temperature, (b) aperture of the lee side ventilation windows, (c) aperture of the windward side ventilation windows, (d) carbon dioxide supply rate.
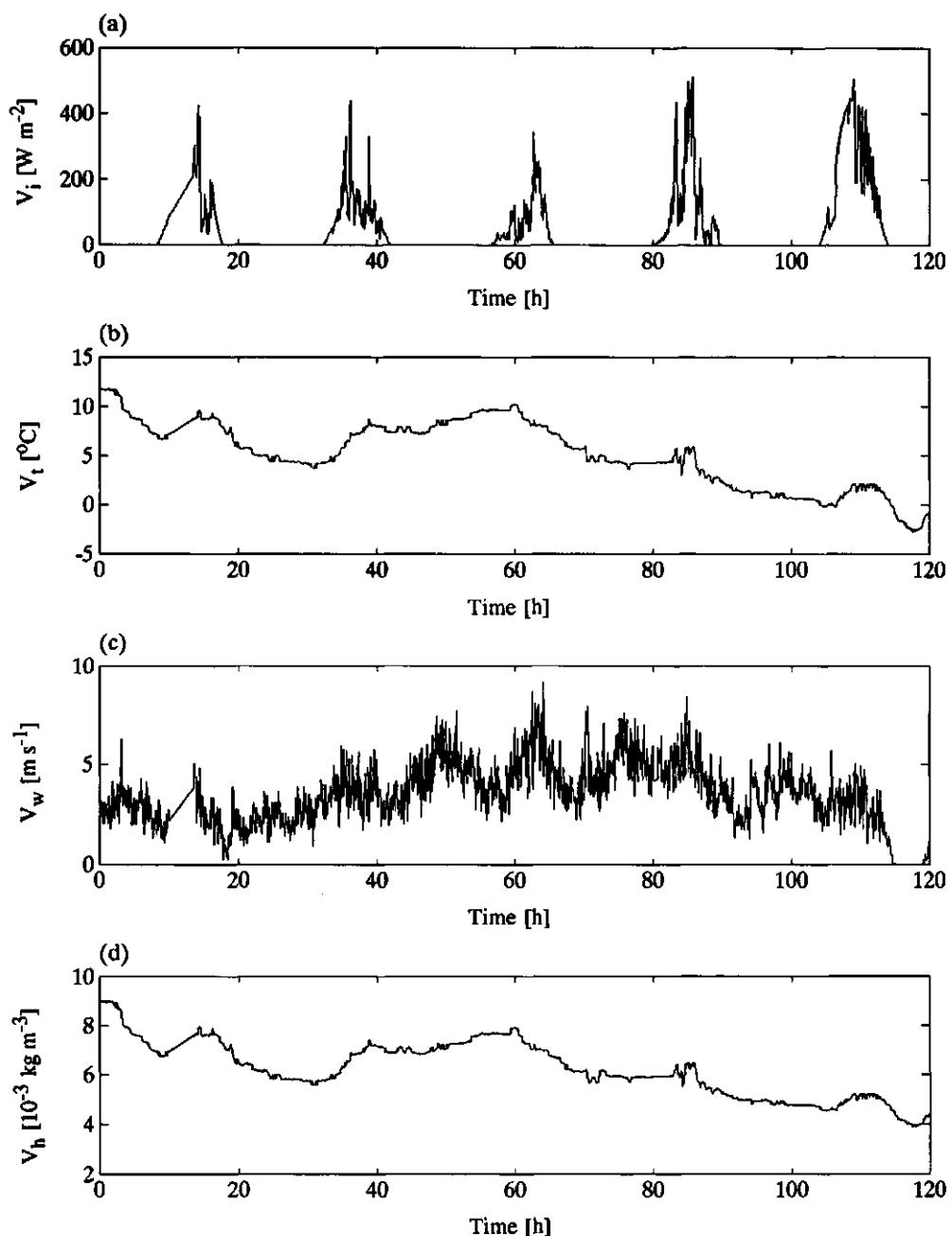
Fig. 3.5. Measurements of the outside climatic conditions from 13 to 17 February 1992: (a) solar radiation, (b) temperature, (c) wind speed, (d) absolute humidity.
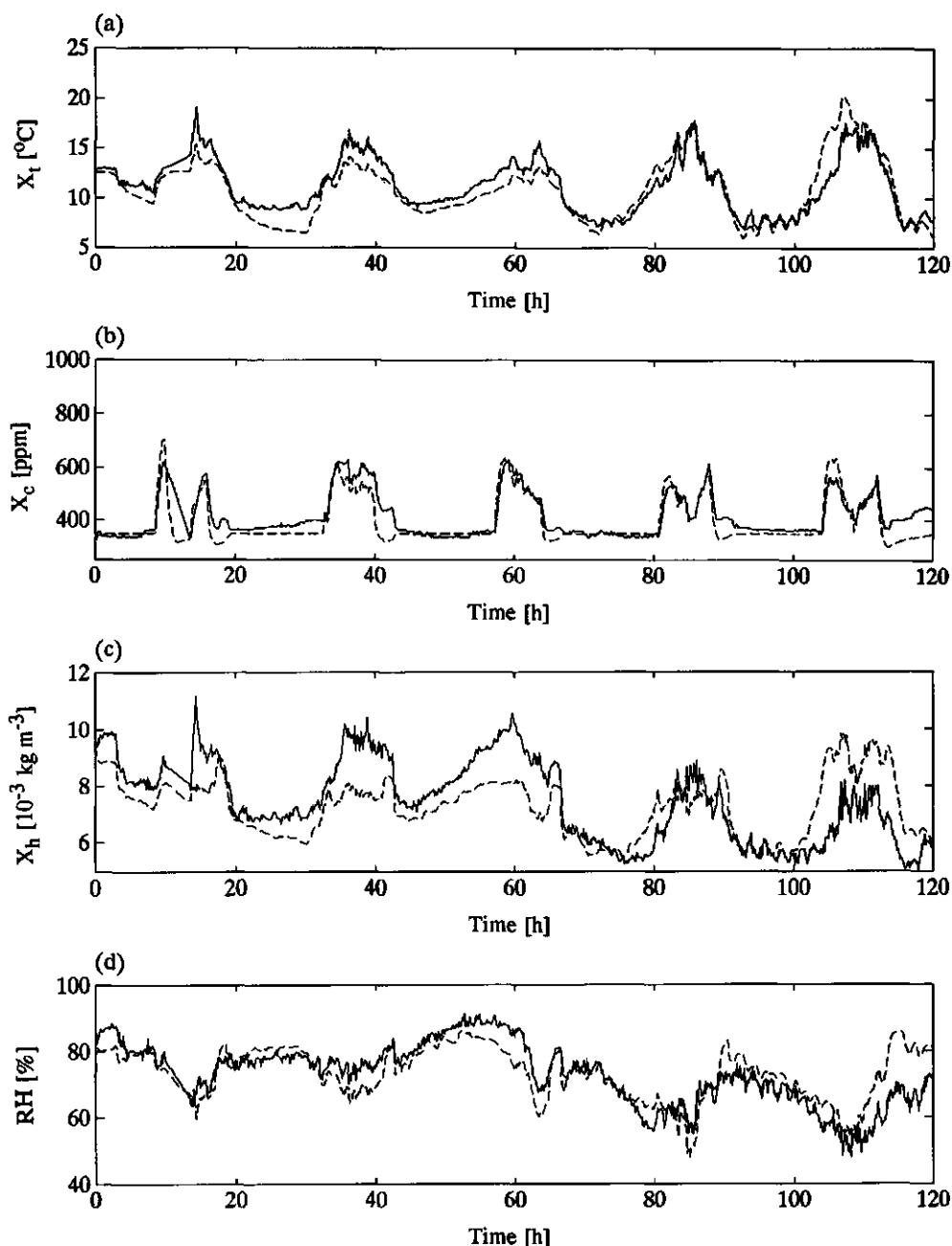
Fig. 3.6.   Measurements   (—)   and   simulations   (--)   of   the   air
temperature (a), carbon dioxide concentration (b), absolute
humidity (c) and relative humidity (d) in the greenhouse,
from 13 to 17 February 1992.
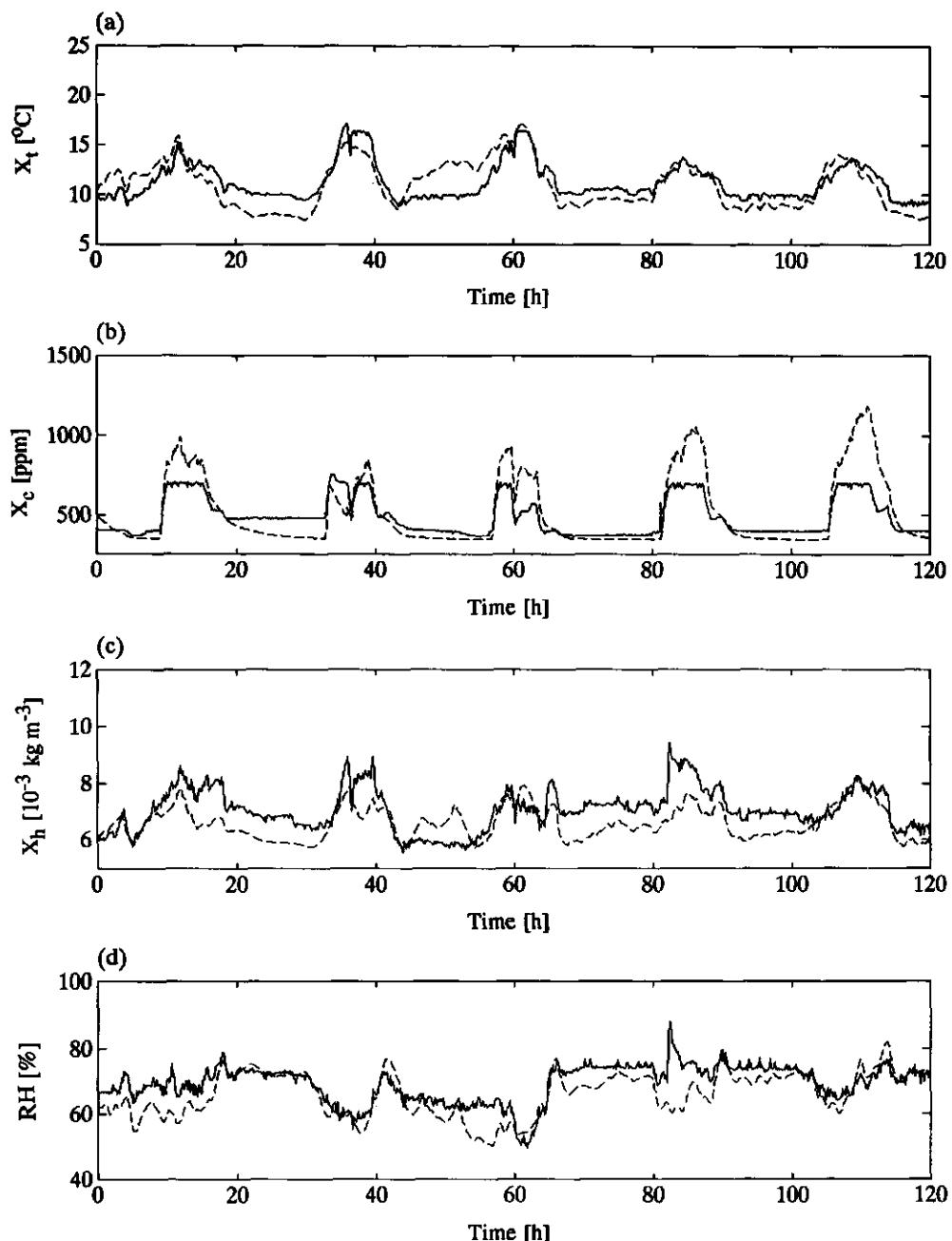
Fig. 3.7. Measurements (——) and simulations (--) of the air temperature (a), carbon dioxide concentration (b), absolute humidity (c) and relative humidity (d) in the greenhouse, from 27 to 31 January 1992.
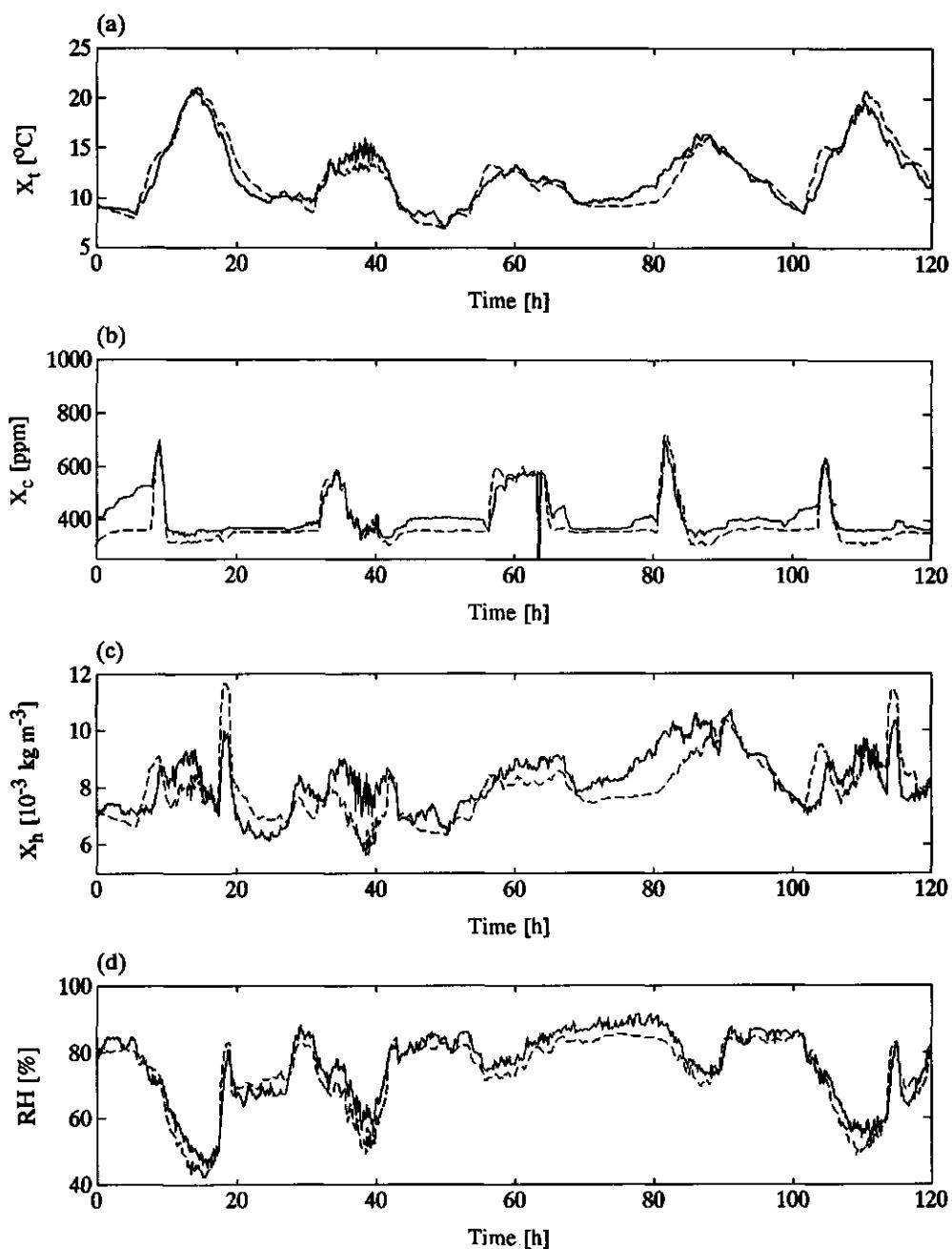
Fig. 3.8. Measurements (—) and simulations (--) of the air temperature (a), carbon dioxide concentration (b), absolute humidity (c) and relative humidity (d) in the greenhouse, from 1 to 5 March 1992.

The simulated carbon dioxide concentration and air temperature (figs. 3.6a and 3.6b) show a fair fit to the measured data. The simulated humidity follows the dynamic trends in the measurements, though sometimes significant under- and distinct overestimations do occur. Due to these simulation errors in the humidity, errors are also encountered in the simulated relative humidity, although besides some local over- and underestimation, it is quite accurately described by the model.

Fig. 3.7 (p. 46) and fig. 3.8 (p. 47) show the results of model validations using the measured data obtained from 27 to 31 January 1992 and from 1 March 1992 to 5 March 1992. In the first period, from 27 to 31 January 1992, the carbon dioxide concentration is overestimated during the day (fig. 3.7b). At that time, there was ample carbon dioxide supply, but the ventilation rate was very small. Because the plantlets had been planted very recently they were quite small and consequently their photosynthetic ability was almost negligible compared with the other carbon dioxide flows in the greenhouse. This may indicate that the greenhouse climate model is not very well able to describe the carbon dioxide balance at very low ventilation rates. The air temperature and humidity are simulated quite accurately by the model. The simulations of air temperature and humidity sometimes over and sometimes underestimate the measurements of the state variable. During the final five day period, 1 March 1993 - 5 March 1993, air temperature, carbon dioxide concentration, humidity and relative humidity are accurately described by the model.

Figs. 3.4 and 3.5 in conjunction with fig. 3.6 clearly illustrate the effect of the control and exogenous inputs on the state of the greenhouse climate. The control inputs allow for rapid modifications of the greenhouse conditions which is illustrated for instance by the influence of carbon dioxide supply and ventilation on the carbon dioxide concentration in the greenhouse, the effect of pipe temperature on the air temperature and the effect of ventilation rate on the humidity. Also the strong and fast impact of exogenous inputs, such as solar radiation and wind speed, on the air temperature are clearly visible in figs. 3.5 and 3.6.

3.3. Sensitivity analysis of a dynamic growth model of lettuce

3.3.1. Introduction

Simulations with a dynamic model like eqn. (2.1) are essentially determined by (a) the particular mathematical structure of the model equations, (b) the control and exogenous inputs u and v, (c) the initial conditions, $x(t_b)$, and (d) the model parameters, c. A

sensitivity analysis may reveal the impact of input variables, initial conditions and model parameters on the evolution of the state variables and is an often advocated tool to gain insight into the structure and behaviour of complex models (Frank, 1978; Janssen *et al.*, 1990). A sensitivity analysis is particularly useful in the early stages of model development, when it is used to indicate which parts of the model need particular attention in the design of specific modelling experiments. Also, once time series data are available, sensitivity analysis is useful in parameter estimation and model calibration, because sensitive parameters are easier to deduce from the data than insensitive parameters. However, insensitive parameters need not be known with large precision and can therefore be taken for granted. Alternatively, a sensitivity analysis may serve as a basis for model reduction. Finally, if the model is intended for use in control of the modelled process, a sensitivity analysis may reveal which parts of the process model are particularly sensitive to parameter variations and consequently may affect the performance of the optimal control system when applied in practice.

France and Thornley (1984) applied sensitivity analysis to assess the effects of model parameters and inputs on open field crops. As their interest was in the weight of the crop at harvest their sensitivity measure applied to only the final state of the crop at harvest time and did not consider the sensitivity during crop growth. With crops, however, the sensitivity coefficients are not expected to be constant in general. This means that parameters that do not seem to have an effect on the final state might be important during growth, and vice versa. This kind of information is particularly important in designing optimal control schemes.

Chalabi and Bailey (1991) have considered the time evolution of the sensitivity of the greenhouse micro-climate to parameter changes. In order to present the results in a concise way, they integrated the sensitivity measure for the state variables to one parameter over time, and over predefined ranges of the other parameters. The latter operation requires prior knowledge about the parameter ranges and is more akin to uncertainty analysis. By averaging over time, however, dynamic information may be lost.

The sensitivity analysis presented in this section emphasizes the time evolution of the model sensitivity. A first order approach is adopted which evaluates the sensitivity of the state trajectories to small parameter deviations around a nominal value by simultaneously solving the so-called sensitivity equations along with the dynamic model (Frank, 1978; Rinaldi *et al.*, 1979). This approach gives insight into the evolution of the sensitivity of the model over time and facilitates the association of certain characteristics of the system behaviour to particular parameters.

3.3.2. Methodology

The system is defined by the differential equation

(3.34) $\dot{x} = f(x,u,c), \quad x(t_b) = \beta,$

where $x = x(t) \in \mathbb{R}^n$ is the state vector, $c \in \mathbb{R}^q$ is the set of q time invariant system parameters, $\beta \in \mathbb{R}^n$ is the initial condition vector, t denotes time and $u = u(t) \in \mathbb{R}^m$ is the input vector described by

(3.35) $u = g(t,\gamma),$

where $\gamma \in \mathbb{R}^r$ parameterizes this input model. Substitution of eqn. (3.35) in (3.34) yields

(3.36) $\dot{x} = f(x,g(t,\gamma),c), \quad x(t_b) = \beta.$

For $\gamma = \gamma^0$, $c = c^0$ and $\beta = \beta^0$ being nominal parameter vectors in the physically feasible range, eqn. (3.36) is known to have an unique *nominal* solution, denoted by

(3.37) $x^0 = x(t,\gamma^0,c^0,\beta^0).$

The first order sensitivity analysis studies the effect of small variations in the parameters γ, c and β on the state trajectory as follows. Assuming the parameter vectors deviate from γ^0, c^0 and β^0 by $\Delta\gamma$, Δc and $\Delta\beta$, we obtain the *actual* solution of eqn. (3.36)

(3.38) $x = x(t,\gamma,c,\beta).$

Expansion of $x = x(t,\gamma,c,\beta)$ around the nominal parameter vectors γ^0, c^0 and β^0 in a Taylor-series and retaining only the first-order terms yields, for small variations in the parameters, a suitable approximation of the parameter induced state trajectory deviation $\Delta x(t,\gamma,c,\beta)$

(3.39) $\displaystyle \Delta x_i(t,\gamma,c,\beta) \cong \sum_{j=1}^{r} \frac{\partial x_i^0}{\partial \gamma_j^0} \Delta\gamma_j + \sum_{k=1}^{q} \frac{\partial x_i^0}{\partial c_k^0} \Delta c_k + \sum_{l=1}^{n} \frac{\partial x_i^0}{\partial \beta_l^0} \Delta\beta_l,$

for all x_1, $i = 1,...,n$, $\partial x_1^0/\partial.^0$ denotes the partial derivatives of x with respect to the independent variables, evaluated at their nominal values.

Let the state x of a continuous system be a continuous function of the parameter vectors γ, β and c, then the partial derivatives

$$(3.40) \qquad s_{ij}^\gamma(t) \equiv \frac{\partial x_1^0}{\partial \gamma_j^0}, \qquad i = 1,...,n; \qquad j = 1,...,r ,$$

$$(3.41) \qquad s_{1k}^c(t) \equiv \frac{\partial x_1^0}{\partial c_k^0}, \qquad i = 1,...,n; \qquad k = 1,...,q ,$$

$$(3.42) \qquad s_{1l}^\beta(t) \equiv \frac{\partial x_1^0}{\partial \beta_1^0}, \qquad i = 1,...,n; \qquad l = 1,...,n ,$$

express the sensitivity of the state trajectories for small variations in the parameters of the input model, the system parameters and the initial conditions, respectively. Note that the sensitivity is a function of time.

The evolution of the sensitivity in time is governed by a set of differential equations, the so-called sensitivity system, which is derived as follows. The solution presented in eqn. (3.37) can be written as

$$(3.43) \qquad x_1^0 = x_1(t,\gamma^0,c^0,\beta^0) = \beta_1^0 + \int_{t_b}^t f_1(x^0,g(\tau,\gamma^0),c^0) \, d\tau,$$

for $i = 1,...,n$. For ease of notation we introduce $f_1^0 = f_1(x^0,g(t,\gamma^0),c^0)$. Substitution of eqn. (3.43) in eqn. (3.41) yields

$$(3.44) \qquad s_{1j}^c = \frac{\partial}{\partial c_j^0} (\beta_1^0 + \int_{t_b}^t f_1^0 \, d\tau) =$$

$$\int_{t_b}^{t}\left[\sum_{k=1}^{n}\frac{\partial f_1^0}{\partial x_k^0}\frac{\partial x_k^0}{\partial c_j^0}+\frac{\partial f_1^0}{\partial c_j^0}\right]+\sum_{l=1,l\neq j}^{q}\left[\sum_{k=1}^{n}\frac{\partial f_1^0}{\partial x_k^0}\frac{\partial x_k^0}{\partial c_l^0}\frac{\partial c_l^0}{\partial c_j^0}+\frac{\partial f_1^0}{\partial c_l^0}\frac{\partial c_l^0}{\partial c_j^0}\right]d\tau,$$

for all x_i, $i = 1,...,n$ and c_j, $j = 1,...,q$. Applying eqn. (3.41) in eqn. (3.44) yields

$$(3.45)\qquad s_{1j}^C = \int_{t_b}^{t}\left[\sum_{k=1}^{n}\frac{\partial f_1^0}{\partial x_k^0}s_{kj}^C+\frac{\partial f_1^0}{\partial c_j^0}\right]$$

$$+\sum_{l=1,l\neq j}^{q}\left[\sum_{k=1}^{n}\frac{\partial f_1^0}{\partial x_k^0}s_{kl}^C\frac{\partial c_l^0}{\partial c_j^0}+s_{1l}^C\frac{\partial c_l^0}{\partial c_j^0}\right]d\tau.$$

The second term in eqn. (3.45) expresses the fact that the nominal values of some of the parameters in the model may depend on the nominal values of others. The reason behind this is that the nominal parameter values of many biological and physical models are usually deduced from fitting assumed functions of a number of parameters to observed data through the use of maximum likelihood or least squares techniques (*e.g.* photosynthesis relationships). The estimates of the parameters obtained through these techniques often yield highly correlated values, which implies that $\partial c_l^0/\partial c_j^0 \neq 0$ for some l and j. Since in this research the model equations and parameters have been derived from the literature from which no prior information on the correlation between parameters could be deduced, it is assumed that $\partial c_l^0/\partial c_j^0 = 0$ for all l and j. Because the second term on the right hand side disappears, eqn. (3.45) is then significantly simplified. Differentiating the remaining terms on both sides with respect to time yields

$$(3.46)\qquad \dot{s}_{1j}^C = \sum_{k=1}^{n}\frac{\partial f_1^0}{\partial x_k^0}s_{kj}^C+\frac{\partial f_1^0}{\partial c_j^0},$$

which describes the evolution of the systems sensitivity in time. For

all x_i, $i = 1,...,n$ and c_j, $j = 1,...,q$ combined, the sensitivity system is defined by

$$(3.47) \qquad \dot{S}^c = \frac{\partial f^0}{\partial x^0} S^c + \frac{\partial f^0}{\partial c^0}, \qquad S^c(t_b) = 0,$$

in which, for instance, S^c is the $n{\times}q$ dimensional sensitivity matrix

$$(3.48) \qquad S^c \equiv \begin{bmatrix} \dfrac{\partial x_1^0}{\partial c_1^0} & \cdot \ \cdot & \dfrac{\partial x_1^0}{\partial c_q^0} \\ \cdot & \cdot & \cdot \\ \cdot & \cdot & \cdot \\ \dfrac{\partial x_n^0}{\partial c_1^0} & \cdot \ \cdot & \dfrac{\partial x_n^0}{\partial c_q^0} \end{bmatrix},$$

and $\partial f^0/\partial x^0$ is the $n{\times}n$-dimensional Jacobian matrix, $\partial f^0/\partial c^0$ a $n{\times}q$ dimensional matrix, defined accordingly. Assuming independence of the parameters γ, in the same way the sensitivity system S^γ is derived

$$(3.49) \qquad \dot{S}^\gamma = \frac{\partial f^0}{\partial x^0} S^\gamma + \frac{\partial f^0}{\partial \gamma^0}, \qquad S^\gamma(t_b) = 0,$$

in which, for instance, S^γ is a $n{\times}r$ – dimensional matrices defined as

$$(3.50) \qquad S^\gamma \equiv \begin{bmatrix} \dfrac{\partial x_1^0}{\partial \gamma_1^0} & \cdot \ \cdot & \dfrac{\partial x_1^0}{\partial \gamma_r^0} \\ \cdot & \cdot & \cdot \\ \cdot & \cdot & \cdot \\ \dfrac{\partial x_n^0}{\partial \gamma_1^0} & \cdot \ \cdot & \dfrac{\partial x_n^0}{\partial \gamma_r^0} \end{bmatrix},$$

and $\partial f^0/\partial \gamma^0$ is defined accordingly. Finally, the systems sensitivity with respect to small variations in the initial conditions is described by

$$(3.51) \qquad \dot{S}^\beta = \frac{\partial f^0}{\partial x^0} S^\beta + \frac{\partial f^0}{\partial \beta^0},$$

with S^β a $n \times n$ matrix defined as

$$(3.52) \qquad S^\beta = \begin{bmatrix} \dfrac{\partial x_1^0}{\partial \beta_1^0} & & \dfrac{\partial x_1^0}{\partial \beta_n^0} \\ & \cdot & \cdot & \cdot \\ \cdot & & \cdot \\ \cdot & \cdot & \cdot \\ \dfrac{\partial x_n^0}{\partial \beta_1^0} & & \dfrac{\partial x_n^0}{\partial \beta_n^0} \end{bmatrix},$$

and $\partial f^0/\partial \beta^0$ is zero since f is not an explicit function of β. Taking the derivative of the initial state vector, $x(t_b) = \beta$, with respect to β_j supplies initial conditions, $S^\beta(t_b)$, in terms of the components

$$(3.53) \qquad s_{ij}^\beta(t_b) = \frac{\partial \beta_1^0}{\partial \beta_j^0} = 1, \quad i = j,$$

$$(3.54) \qquad s_{ij}^\beta(t_b) = \frac{\partial \beta_1^0}{\partial \beta_j^0} = 0, \quad i \neq j,$$

for $i = 1,...,n$ and $j = 1,...,n$. Independence of the initial conditions β is assumed.

Note that because first order approximations are used, the sensitivity systems are linear even if the original system of eqn. (3.36) is non-linear. Generally, due to the non-linearity of f, the sensitivity equations are non-linear. Therefore, a linear approximation of the sensitivity systems can be used only if the

model equations can be approximated by a linear equation. This is justified if infinitesimal variations in the parameters are considered.

Using the initial conditions given in eqns. (3.47), (3.49), (3.53) and (3.54), the sensitivity systems can be simulated parallel with the original system (3.34), once the partial derivatives in eqns. (3.47), (3.49) and (3.51) have been calculated. Both analytical derivatives and numerical approximations can be used in the derivation of the sensitivity systems (3.47), (3.49) and (3.51). Analytical derivatives offer some direct insight into the sensitivity of the state variables with respect to certain parameters. However, depending on the complexity of the system equations, analytical calculation of the partial derivatives can be quite cumbersome. In contrast, a numerical approximation is easily calculated in general terms by using central differences. In the case of the Jacobian, this reads

$$
(3.55) \qquad \frac{\partial f_i(x^0, g(t, \gamma^0), c^0)}{\partial x_j} \cong
$$

$$
\frac{f_i(x_j^0 + \Delta x_j, g(t, \gamma^0), c^0) - f_i(x_j^0 - \Delta x_j, g(t, \gamma^0), c^0))}{2\Delta x_j},
$$

for $i = 1,...,n$ and $j = 1,...,n$. The other partial derivatives are calculated analogously. This numerical approximation yields an order $(\Delta x_j)^2$ truncation error in the derivatives (Gill *et al.*, 1981). Holtzman (1992) suggests that the differences Δx_j can best be chosen in agreement with the expected stochastic variability in the independent variables. In this example, this information was not available, so it was decided to calculate the partial derivatives numerically with a variation of 1% in the independent variables.

In this research, the sensitivity eqns. (3.47), (3.49) and (3.51) were implemented in simulation software based on FORTRAN in which a fourth order Runge-Kutta algorithm described by Press *et al.* (1986) was used for numerical integration of the model equations and the sensitivity equations.

The interpretation of the simulated sensitivity trajectories is straightforward. If at time t the state trajectory is very sensitive to small variations in the parameters, then the sensitivity function S will take large positive or negative values and vice versa. In this way the first-order sensitivity analysis offers the opportunity to relate a parameter to the behaviour of the state variables in a

certain phase of the evolution of the system.

In order to compare the impact of perturbations in the different parameters on the system trajectories, it is often more convenient to express the sensitivity as the fractional change in the state trajectory as a result of a fractional change in the parameter value: a relative sensitivity measure. The relative sensitivity vectors, denoted by $\bar{s}^\gamma$, $\bar{s}^c$ and $\bar{s}^\beta$ are defined in terms of their components by

$$(3.56) \qquad \bar{s}^c_{ik} = s^c_{ik} \frac{c^0_k}{x^0_i}, \qquad \bar{s}^\beta_{il} = s^\beta_{il} \frac{\beta^0_l}{x^0_i}, \qquad \bar{s}^\gamma_{ij} = s^\gamma_{ij} \frac{\gamma^0_j}{x^0_i}.$$

Insight in the relative importance of the parameters γ, c and β is established by evaluating the simulated sensitivity trajectories graphically. Since this is a rather laborious task when a large number of state variables and parameters are involved, a first classification of the systems sensitivity can be obtained by considering the integrated sensitivity measures

$$(3.57) \qquad \hat{s}^c_{ik} = \int_{t_b}^{t_f} |\bar{s}^c_{ik}| \ dt, \qquad \hat{s}^\beta_{il} = \int_{t_b}^{t_f} |\bar{s}^\beta_{il}| \ dt, \qquad \hat{s}^\gamma_{ij} = \int_{t_b}^{t_f} |\bar{s}^\gamma_{ij}| \ dt.$$

If $|\bar{s}|$ is small throughout the interval $t \in [t_b, t_f]$, the integrated sensitivity measure will be small and vice-versa. Once a first classification of the parameters is obtained, the evolution of the sensitivity can be evaluated on the interval $t \in [t_b, t_f]$ for the parameters of interest.

3.3.3. Results

In the present sensitivity analysis of the two state variable model of lettuce growth, presented in section 3.2.3.1, the photosynthetically active radiation (PAR) level in the greenhouse, air temperature, X_t, and carbon dioxide concentration, X_c, are considered as inputs to the model. The photosynthetically active radiation level in the greenhouse is represented by the term $c_{par}c_{rad,rf}V_1$ in eqn. (3.13). By replacing V_1 by PAR, the parameters c_{par} and $c_{rad,rf}$ will not be considered in the sensitivity analysis. However, their impact on lettuce growth will be discussed later.

The dependence of lettuce growth on the PAR level, X_t and X_c, implies that these inputs will also affect the sensitivity functions S, defined in eqns. (3.47), (3.49) and (3.51), associated with this model. Because we are dealing with a non-linear dynamic model (eqns. (3.10) to (3.21)), a rigorous sensitivity analysis requires a wide range of input amplitudes and frequencies to be supplied to the model. With the PC-Matlab (Anonymous, 1989) program, uniform white noise data $\omega(t) \in [-1,1]$ were generated. These time series were transformed using the linear mapping

$$(3.58) \qquad u(t) = \alpha_1 + \alpha_2\omega(t),$$

into time sequences for temperature, PAR and carbon dioxide concentration. In this input model α_1 and α_2 represent the average of the input data and the amplitude of the variations around this average value, respectively. These parameters were chosen such that the temperature was allowed to vary with a maximum amplitude $\alpha_2 = 11.25$ $^{\circ}$C around a mean value $\alpha_1 = 18.75$ $^{\circ}$C. The PAR data had an average value and a maximum amplitude of $\alpha_1 = \alpha_2 = 125$ W m^{-2} and the CO_2 concentration varied around $\alpha_1 = 1.464 \times 10^{-3}$ kg m^{-3} with a maximum amplitude $\alpha_2 = 1.281 \times 10^{-3}$ kg m^{-3}. Data were generated which covered a period of 40 days with a time increment of 1/48 day. Fig. 3.9, which shows a small portion of the generated sequences, illustrates the randomness of the data. The sequences of temperature, carbon dioxide concentration and photosynthetically active radiation were mutually uncorrelated.
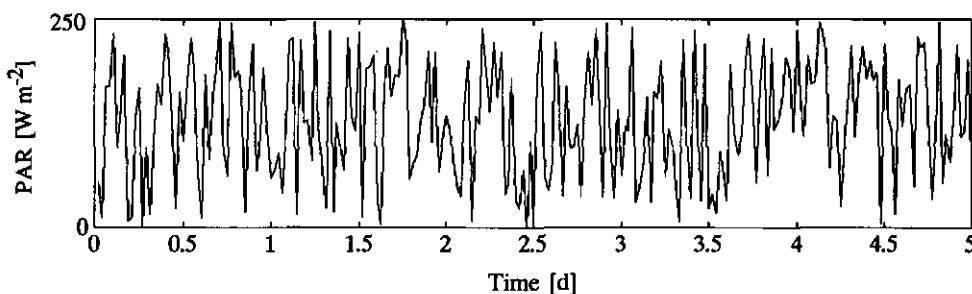
Fig. 3.9. A portion of the generated data of the photosynthetically active radiation level in the greenhouse.

Simulated growth of non-structural dry weight, X_n, and structural dry weight, X_s, using the model parameters listed in table 3.2 in section 3.2.3.2, and initial conditions $X_n(t_b) = 1.0 \times 10^{-3}$ kg m^{-2} and $X_s(t_b) = 2.5 \times 10^{-3}$ kg m^{-2}, is presented in fig. 3.10. Initially the photosynthetic production of carbohydrates dominates growth conversion, growth related losses and maintenance respiration, and so X_n exhibits a pronounced increase. Then, growth and maintenance become increasingly important and the amount of non-structural material starts to decrease until a steady-state is reached. The accumulation of structural material is modelled as an irreversible process (see eqn. (3.11)). Structural dry matter grows monotonically throughout the whole growing period considered. Also, it can be seen that rapid variations in the input data are effectively filtered out by the crop model.
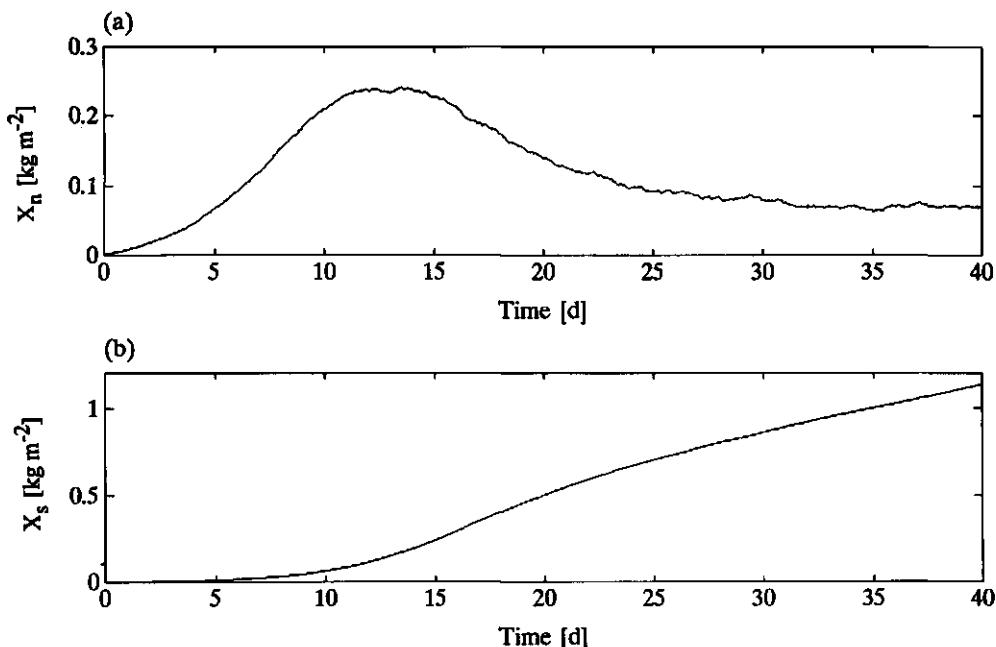
Fig. 3.10.   Growth trajectories of non-structural dry weight (a) and structural dry weight (b), simulated with white noise data.
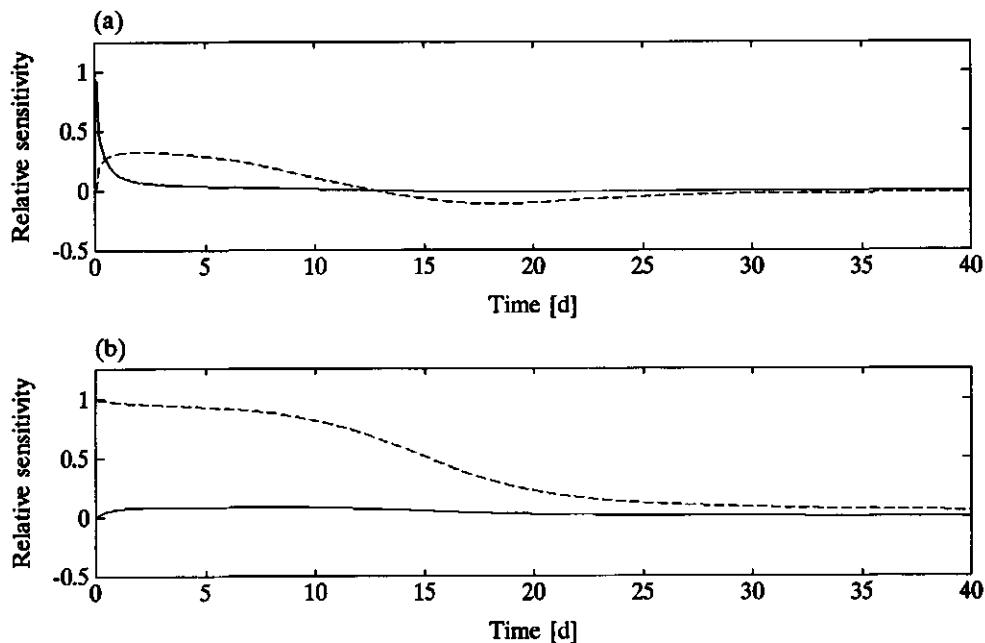
Fig. 3.11. Relative sensitivity of non-structural dry weight (a) and structural dry weight (b), to a variation in the initial conditions of non-structural dry weight (—) and structural dry weight (--), evaluated with white noise input data.

A variation in the initial structural dry weight has a pronounced effect on the evolution of both state variables during the first half of the growing period (fig. 3.11). The effect of a variation in the initial value of the non-structural dry weight is smaller in magnitude as is demonstrated in fig. 3.11. During the early stages of growth, dry matter production mainly depends on the ability of the crop to intercept light. The leaf area of the crop and consequently, the canopy photosynthesis rate, is related to the amount of structural material present (eqn. (3.12)). Therefore, a small increase in the initial dry weight will have a significant effect on the production of dry matter at that stage. The increased growth rate results in an earlier closure of the canopy and an early increase of the maintenance respiration rate which partly outweighs the benefits of rapid growth during the early stages of growth. This explains why the relative sensitivity to changes in the initial conditions gradually diminishes towards the end of the growing period. A perturbation in the initial condition of the structural dry weight

still has a small but distinct effect on the amount of dry matter harvested, as was expected.

Evaluation of the integrated sensitivity measures (cf. eqn. (3.57)) related to variations in the model parameters, revealed that, in this model, crop growth is mainly determined by only a few parameters. The integrated sensitivity measures presented in table 3.4 have been normalized based on the largest observed integrated sensitivity measure.

Table 3.4. The normalized integrated relative sensitivity measure of the non-structural dry weight, X_n, and the structural dry weight, X_s, evaluated with white noise input data.

	c_β	c_{bnd}	$c_{car,1}$	$c_{car,2}$	$c_{car,3}$	c_ε	c_Γ
X_n	0.451	0.151	0.229	0.558	0.150	0.446	0.086
X_s	0.787	0.225	0.340	0.826	0.220	0.664	0.128

	c_k	$c_{lar,s}$	$c_{Q10,\Gamma}$	$c_{Q10,gr}$	$c_{Q10,resp}$	$c_{resp,r}$	$c_{resp,s}$
X_n	0.194	0.194	0.006	0.025	0.113	0.006	0.257
X_s	0.257	0.257	0.007	0.028	0.077	0.005	0.176

	$c_{r,gr,max}$	c_{stm}	c_τ
X_n	1.000	0.046	0.027
X_s	1.000	0.070	0.018

The most sensitive parameters are the maximum growth rate, $c_{r,gr,max}$, the yield factor, c_β, the light use efficiency, c_ε, and, $c_{car,2}$, which determines the linear response of the carboxylation conductance to temperature. The parameters $c_{Q10,gr}$, c_τ, $c_{Q10,\Gamma}$ and c_{stm} have a very small influence on the simulated dry matter production.
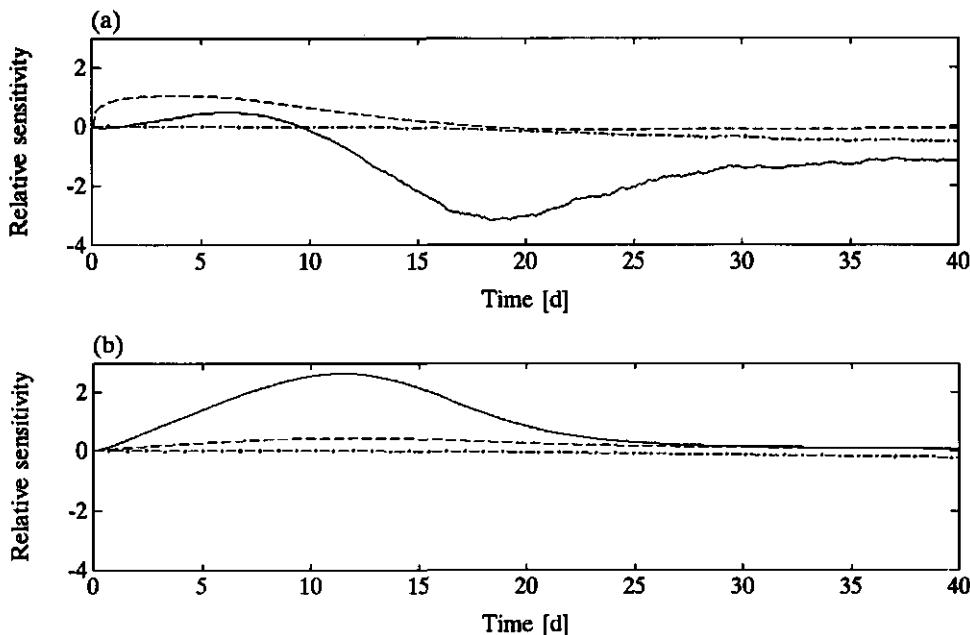
Fig. 3.12. Relative sensitivity of non-structural dry weight (a) and structural dry weight (b), to a variation of the maximum growth rate coefficient $c_{r,gr,max}$ (—), extinction coefficient c_k (--) and maintenance respiration coefficient $c_{resp,s}$ (-·), evaluated with white noise input data.

Some of the parameters only affect crop growth during a short period of time (see fig. 3.12). For instance the extinction coefficient, c_k, as well as the leaf area ratio, $c_{lar,s}$, have a most distinct effect on growth before closure of the canopy. However, the benefits of an enhanced growth rate during the early stages of growth are partly offset by an early increase of the maintenance respiration. Thus, the effect on the amount of dry matter harvested is less pronounced.

The maintenance respiration of the shoot, $c_{resp,s}$, is related to the amount of structural dry matter present (cf. eqn. (3.18)) and imposes a load on the available non-structural material for growth (eqn. (3.10)). An increased maintenance respiration, therefore, will have a negative effect on the evolution of total crop dry weight. This is clearly demonstrated in fig. 3.12.

Enhanced growth, for instance generated by a small increment in

the parameter $c_{r,gr,max}$, first contributes to the development of more leaf area. Consequently, the canopy intercepts more light which stimulates the photosynthetic production of carbohydrates and results in an increment of the amount of available non-structural dry material. This is illustrated by the first part of the sensitivity trajectory shown in fig. 3.12a. However, the contribution made by enhanced carbohydrate production to non-structural matter is soon outweighed by increasing growth related losses and maintenance respiration consuming some of the available non-structural material such that finally there is less non-structural material left. It is shown in fig. 3.12b that the effect of a small variation in the growth parameter $c_{r,gr,max}$ on the evolution of structural material is not long lasting, and consequently does not affect the harvested structural dry weight significantly.

As illustrated in fig. 3.10, crop growth does not respond to a great extent to fast fluctuations in the input data and so it was expected that the model would be most sensitive to a variation in the average values of the input data represented by parameter α_1 in eqn. (3.58), rather than by the amplitudes (α_2). This was confirmed by the results of the sensitivity analysis as is demonstrated in fig. 3.13.
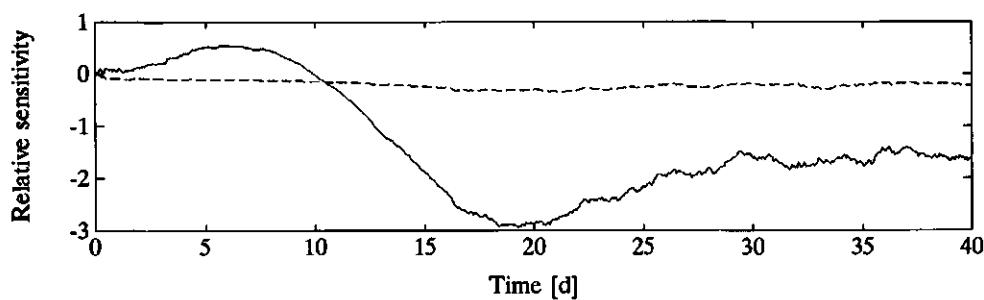
Fig. 3.13. Relative sensitivity of non-structural dry weight to a bias in the average (—) and the amplitude (--) of the white noise temperature data.

For the non-structural dry weight, the sensitivity to the average value and amplitude of the temperature data are shown. A comparison of fig. 3.13 with fig. 3.12a reveals that the sensitivity trajectory related with the temperature evolves more or less the same as the sensitivity trajectory related to the maximum growth rate coefficient, $c_{r,gr,max}$. This is an indication of the fact that, although the temperature has an effect on the photosynthesis and maintenance respiration rate, it mainly affects the transformation of

non-structural material to structural material.

During the first half of the growing period, the evolution of non-structural dry weight is much more sensitive to variations in photosynthetically active radiation than the structural dry weight. This is shown in fig. 3.14. This difference in sensitivity follows directly from the fact that, in this model representation, growth of structural dry matter, contrary to growth of non-structural dry matter, is not directly affected by the radiation level (eqns. (3.11) and (3.19)). The same argument holds for the carbon dioxide concentration. Consequently, the sensitivity trajectories for structural dry matter are mainly determined by perturbations in the growth of non-structural dry matter.
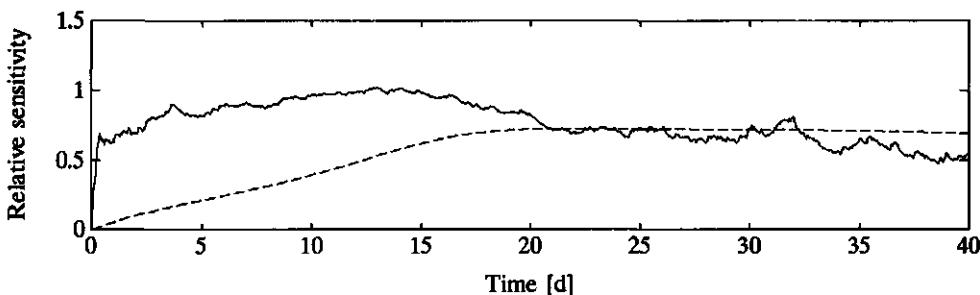
Fig. 3.14.   Relative sensitivity of non-structural dry weight (—) and structural dry weight (--), to a variation in the average PAR level.

Overall crop growth is slightly more affected by the PAR level in the greenhouse than by the carbon dioxide concentration. The difference, however, is small. Except for this small fractional difference, the evolution of the sensitivity trajectories for both model inputs is the same. This is due to the structure of eqn. (3.13) describing the gross photosynthesis rate. When comparing the effects of PAR and temperature on the evolution of non-structural dry matter, shown in fig. 3.13 and fig. 3.14, respectively, it is clear that the temperature plays a dominant role in the accumulation of non-structural dry matter during the second half of the growing period.

The sensitivity of the system under normal operating conditions may deviate from the sensitivity observed in the analysis with white noise input data. In horticultural practice, a strong correlation exists between the temperature and carbon dioxide concentration in the greenhouse and the solar radiation, respectively. Solar radiation has a strong impact on the energy balance of the greenhouse. Moreover, the greenhouse climate control schemes employed in practice

emphasize the adaptation of the indoor climate to the solar radiation level and other outdoor climate variables.

To evaluate the influence of the particular choice of input data on the results of the sensitivity analysis, an analysis was performed using time series data of the temperature, carbon dioxide concentration and solar radiation obtained during the validation experiment early 1992. Also in this sensitivity analysis the photosynthetically active radiation in the greenhouse was used as input in stead of the solar radiation level outside the greenhouse.

Fig. 3.15 presents the relative sensitivity to changes in the initial conditions of the non-structural and structural dry weight. The sensitivity trajectories obtained when using realistic input data differed from the ones obtained in the simulation with white noise input data. However, when fig. 3.15 is compared with fig. 3.11, a similarity of the trends in the sensitivity trajectories can be observed.
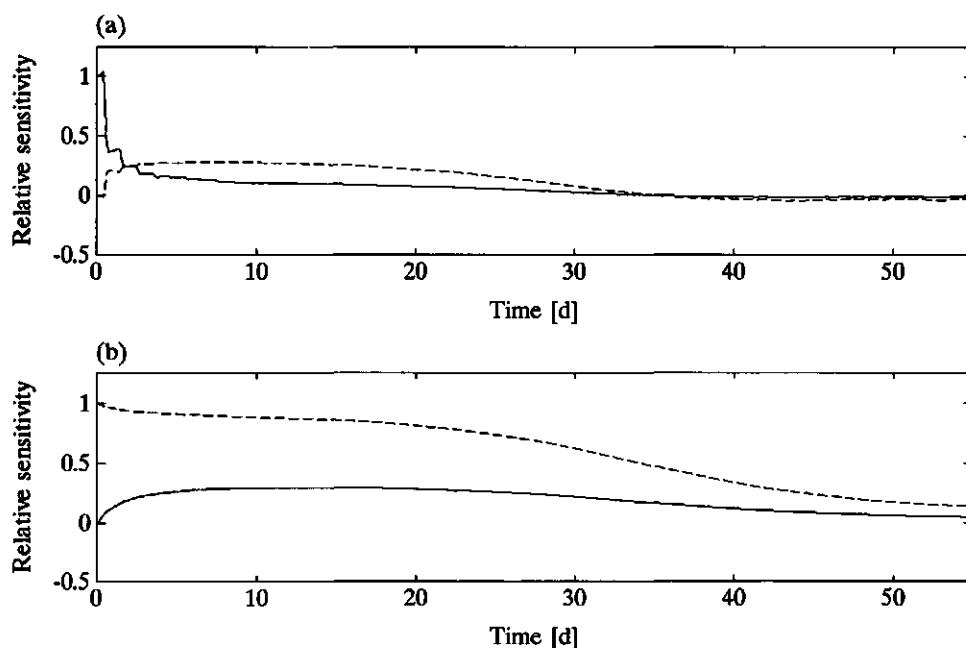

Fig. 3.15.   Relative sensitivity of non-structural dry weight (a) and structural dry weight (b), to a variation in the initial conditions of non-structural dry weight (—) and structural dry weight (--), evaluated with the measured input data.

Since a diurnal variation was not present in the white noise input data and especially in the photosynthetically active radiation level, simulation with the realistic input data resulted in a reduced growth rate and the sensitivity for changes in the initial conditions propagated during a longer period of time. The effect on the harvest weight was more pronounced than in the case when white noise input data was used. However, it seems to be dependent of the harvest date since it can be observed that the sensitivity diminishes gradually towards the end of the growing period.

To assess the relative importance of the different parameters, the sensitivity of the states to small changes in the model parameters was evaluated. The integrated sensitivity measures are listed in table 3.5.

Table 3.5. The normalized integrated relative sensitivity measure of the non-structural dry weight, X_n, and the structural dry weight, X_s, evaluated with the measured input data.

	c_β	c_{bnd}	$c_{car,1}$	$c_{car,2}$	$c_{car,3}$	c_ε	c_Γ
X_n	0.895	0.107	0.120	0.384	0.124	0.936	0.156
X_s	0.914	0.143	0.160	0.480	0.143	1.000	0.194

	c_k	$c_{lar,s}$	$c_{Q10,\Gamma}$	$c_{Q10,gr}$	$c_{Q10,resp}$	$c_{resp,r}$	$c_{resp,s}$
X_n	0.583	0.583	0.097	0.893	0.269	0.005	0.180
X_s	0.825	0.825	0.100	0.469	0.145	0.003	0.106

	$c_{r,gr,max}$	c_{stm}	c_τ
X_n	1.000	0.033	0.047
X_s	0.711	0.044	0.057

Again, the simulated non-structural and structural material are found to be most sensitive to the maximum growth rate coefficient, $c_{r,gr,max}$, the yield factor, c_β, the light use efficiency, c_ε, and

$c_{car,2}$. However, now, the extinction coefficient, c_k, and the leaf area ratio, $c_{lar,s}$, and the Q_{10}-factor for growth, $c_{Q10,gr}$, also have a strong influence on the simulated dry weight.

Though with a few exceptions, the relative importance of the parameters was not much altered by the particular choice of data set used for the sensitivity analysis. The evolution of the sensitivity trajectories was in some cases rather different from the ones obtained by simulation with white noise data.
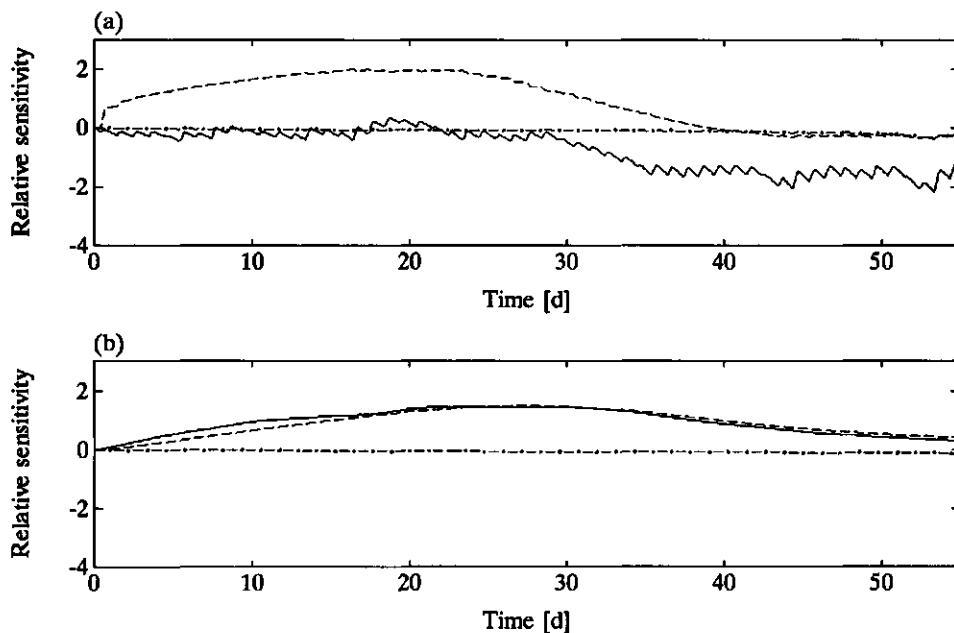

Fig. 3.16.   Relative sensitivity of non-structural dry weight (a) and structural dry weight (b), to a variation of the maximum growth rate coefficient $c_{r,gr,max}$ (—), extinction coefficient c_k (--) and maintenance respiration coefficient $c_{resp,s}$ (-·), evaluated with the measured input data.

In fig. 3.16 the relative sensitivity of the non-structural and structural dry weight to small changes in the maximum growth rate coefficient, $c_{r,gr,max}$, the extinction coefficient, c_k, and the maintenance respiration coefficient, $c_{resp,s}$ are presented.

Compared with the results obtained when using white noise data

in the simulations, both state variables are more sensitive to changes in the extinction coefficient, c_k, and less sensitive to small changes in the growth rate coefficient, $c_{r,gr,max}$. With the low radiation levels encountered in The Netherlands during winter time, the production of photosynthates governed for instance by the extinction coefficient, c_k, is limiting crop growth instead of the transformation of carbohydrates to structural material governed by the maximum growth rate coefficient $c_{r,gr,max}$.

Because under realistic input data, dry matter production is smaller compared with simulations with white noise inputs, the maintenance respiration coefficient $c_{resp,s}$ has a less distinct effect on crop growth (compare figs. 3.12 and 3.16).

Finally, using the measured input data, the relative importance of the model inputs was evaluated. The sensitivity of the system for small perturbations in the inputs was determined by multiplying the inputs with an artificial parameter having a nominal value of 1 and evaluating the system's sensitivity for small variations of these parameters around their nominal value in the usual way.

In fig. 3.17 the relative sensitivity of the non-structural dry weight and the structural dry weight for small changes in air temperature, carbon dioxide concentration and PAR is presented. Note the remarkable similarity of the effect of air temperature on both state variables and the influence of the maximum growth rate coefficient, $c_{r,gr,max}$, (fig. 3.16), indicating that also under realistic input conditions, temperature has the strongest impact on the transformation of non-structural material to structural material. On average, temperature has a positive effect on the accumulation of structural dry matter and a negative effect on the accumulation of non-structural material. Both effects are largely explained by the fact that a higher temperature stimulates the transformation of non-structural material to structural material. Moreover, a higher temperature will result in higher maintenance losses, which will put a negative load on the available non-structural material towards the end of the growing period.

The carbon dioxide concentration and the radiation level have a positive effect on the accumulation of both non-structural and structural material as was expected.

In economic optimal greenhouse climate control, the revenues of the crop production are determined by the amount of dry matter harvested without making a distinction between non-structural and structural dry matter (see chapter 4 for more details). Economic optimal greenhouse climate control is based on a trade-off between the revenues of increased dry matter production and the costs of greenhouse climate conditioning to establish the increased dry matter
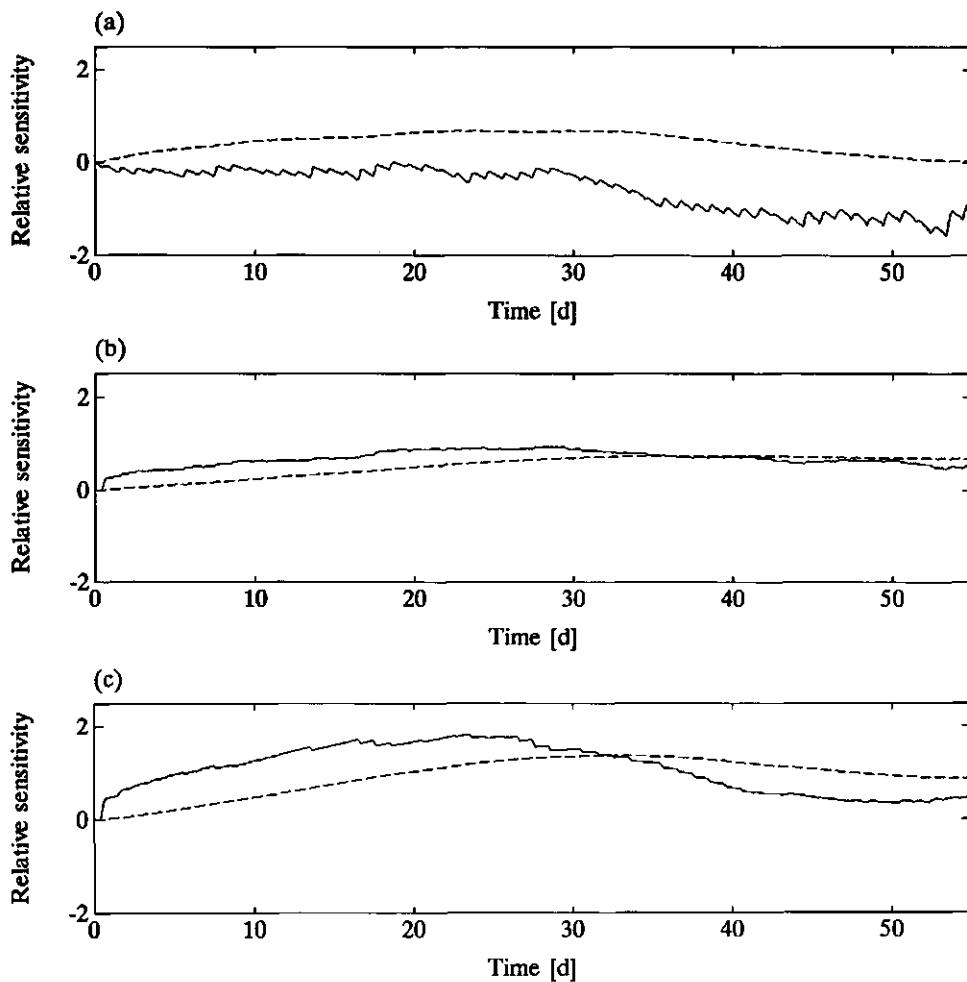
Fig. 3.17. Relative sensitivity of non-structural dry weight (—) and structural dry weight (--), to a variation of air temperature (a), carbon dioxide concentration (b) and PAR (c) in the greenhouse, evaluated with measured input data.

production. Therefore, the relative impact of the greenhouse climate variables on dry matter production is of great interest since optimal control will try to establish dry matter production by means of modifying the climate variable having the strongest impact on crop growth at the lowest expense. The relative impact of the inputs on total dry matter production is shown in fig. 3.18. Apart from solar radiation which has a strong influence on crop growth but is not

considered to be a controllable greenhouse climate variable in this research, the carbon dioxide concentration clearly has the strongest impact on dry matter production. The temperature has a comparably small positive impact on dry matter during the early stages of growth, but the effect of the temperature turns negative towards the end of the growing period when increased maintenance respiration puts a significant negative load on the amount of non-structural material available for growth (see fig. 3.16a).
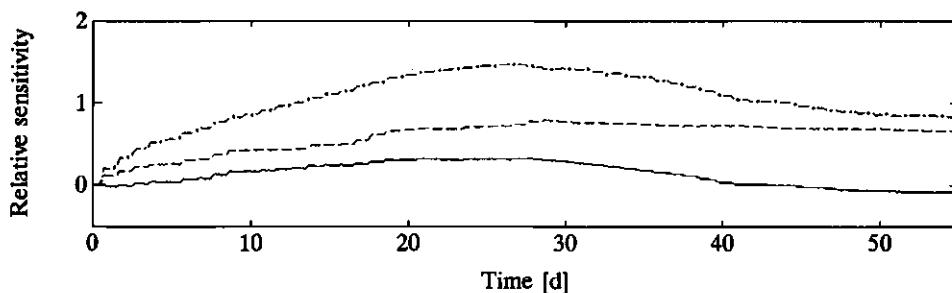
Fig. 3.18. Relative sensitivity of total crop dry weight to a variation of temperature (—), carbon dioxide concentration (--) and PAR (-·) in the greenhouse, evaluated with measured input data.

3.3.4. Discussion

The aim of section 3.3 was to develop a methodology to assess the sensitivity of a dynamic model to variations in the model parameters, the initial conditions and the inputs. Unlike methods which evaluate the model sensitivity at the end of a simulation interval (France and Thornley, 1984) or integrate the sensitivity measure over time (Chalabi and Bailey, 1991), the first order sensitivity analysis, presented in this section, explores the evolution of the sensitivity in time and offers, in this way, the opportunity to associate certain characteristics of the system behaviour to particular parameters, initial conditions or inputs.

The example of first order sensitivity analysis applied to a dynamic lettuce growth model revealed, first of all, that variations in the initial conditions of the state variables have a pronounced effect on the evolution of both state variables. However, the harvest weight is much less affected. This implies that measurement errors in the determination of the initial plant weight are not of major concern when the aim is to predict the harvest weight. If the model

is to be used for predicting growth throughout the growing period, however, the accurate determination of the average as well as variability in the initial conditions should be taken much more seriously.

The results show that just a few parameters determine crop growth in this model representation. Among the important parameters are the yield factor c_β, the maximum growth rate coefficient, $c_{r,gr,max}$, the light use efficiency, c_ε, the extinction coefficient, c_k, and the leaf area, $c_{lar,s}$. Determination of the relative importance of the model parameters is of crucial importance in model calibration studies where large numbers of parameters are involved. Also, the results of the sensitivity analsysis can serve as basis for reduction of non-linear dynamic models.

It was found that some parameters, such as the extinction coefficient c_k, the structural leaf area ratio, $c_{lar,s}$, and the maintenance requirements of the shoot, $c_{resp,s}$, have a pronounced effect on the evolution of the state variables during a limited time span. This clearly illustrates that the first order sensitivity analysis offers insight into the relationship between certain parameters and characteristic behaviour of the process. Moreover, the information can be used in the determination of a suitable experimental arrangement for model calibration. The fluctuations in the sensitivity functions can be used to determine the measurement frequency that is needed for accurate calibration of the model. Since the sensitivity trajectories related to the structural dry weight did not exhibit large short-term fluctuations, a measurement interval of 1 or 2 days would be sufficient. However, some of the sensitivity trajectories related to the non-structural dry weight show a diurnal trend indicating that this state variable responds a bit faster to changes in the environmental conditions than the structural dry weight. The variations in the sensitivity trajectory suggest a measurement frequency of several times a day.

In the sensitivity analysis, the photosynthetically active radiation (PAR) level inside the greenhouse was considered to be one of the model inputs. In practice, the PAR level in the greenhouse is determined by the solar radiation level outside the greenhouse, V_1, the transmission coefficient of the greenhouse cover for solar radiation, $c_{rad,rf}$, and the fraction PAR in the solar radiation, c_{par}. Due to the structure of the model, in a sensitivity analysis, the same relative sensitivity would be found for c_{par} and $c_{rad,rf}$ as for the light use efficiency c_ε (see eqn. (3.13). Consequently, from table 3.4 it follows that, under low radiation conditions commonly

encountered in The Netherlands, c_{par} and $c_{rad,rf}$ will have a strong influence on lettuce growth and their accurate parameterization is required.

In the simulation example, white noise data of the input variables were used in the sensitivity analysis of the lettuce growth model. However, this data set is not a realistic representation of the outdoor climate in which a strong periodicity and correlation are known to be present. It could be observed in the derivation of the first order sensitivity measure that its evolution is affected by the inputs of the model. For a rigorous sensitivity analysis of a non-linear dynamic model, the input data should contain a wide range of uncorrelated input amplitudes and frequencies to excite the model completely. In horticultural practice, data are correlated and contain a limited number of frequency and amplitude variations. The methodology can be applied to these type of inputs without any modifications. In the particular example considered in this section it was observed that the sensitivity trajectories obtained in simulations with white noise data are different from the results obtained with realistic data. However, it was found that the relative importance of the parameters was not affected by the choice of the input data.

Nominal parameter values for the lettuce growth model were known from different information sources and proved to give a fair fit to actual observations as was shown in section 3.2.3. Thus, the potential disadvantage of the results being conditional on the actual choice of the nominal parameters is largely immaterial in this case. However, in case a correct parameterization of the model is not available, the model sensitivity should be investigated over the whole parameter space or a sub-space originating from physical or physiological insight into the process mechanisms involved.

3.4. Model simplification and integration

In the previous sections dynamic models describing lettuce growth and greenhouse climate have been presented and analysed individually. In this section these models will be integrated to yield a dynamic model of the total greenhouse crop production process conforming to eqn. (2.1). First some model simplifications will be addressed which facilitate the manipulation of the equations in the control system design and improve the insight into the results obtained.

In the lettuce growth models the following simplifications are made. Since the sensitivity analysis of the two state variable lettuce growth model revealed that simulated crop growth is rather insensitive to small changes in the parameter $c_{Q10,\Gamma}$, the temperature

effect on the carbon dioxide compensation point will be neglected and the carbon dioxide compensation point has been calculated to have a value of 5.2×10^{-5} kg m^{-3} at 15.0 $^{\circ}$C.

The leaf conductance to carbon dioxide transport described by eqn. (3.6) has been approximated by the temperature dependent polynomial:

$$\sigma_{co2} = -5.11 \times 10^{-6} X_t^2 + 2.30 \times 10^{-4} X_t - 6.29 \times 10^{-4} \qquad \text{m s}^{-1}.$$

To accomplish a further simplification of the equations, the effect of the carbon dioxide concentration on the light use efficiency was neglected. For a carbon dioxide concentration of 450 ppm, the light use efficiency ε was calculated from eqn. (3.5) to have a value of 14.2×10^{-9} kg J^{-1}.

With respect to the greenhouse climate, the following changes were made to the model. The aperture of the lee and windward side ventilation windows, U_{ls} and U_{ws}, have been replaced by the ventilation flux, U_v, as the control variable determining the air exchange between inside and outside air. In horticultural practice, the grower distinguishes between the lee and windward side of the greenhouse when using the ventilation windows. Usually, the lee side ventilation windows are opened at first and when large ventilation fluxes are required, the windward side ventilation windows are also opened. Since in the model description of the greenhouse climate both ventilation windows essentially have the same effect on the greenhouse climate, there is no criterion which can be used to distinguish between these two windows in the derivation of the optimal control strategies. Therefore, in the control system design the ventilation flux, U_v, will be used as the control variable. From the ventilation rate the window aperture can be calculated again by rewriting eqn. (3.28).

The temperature of the heating system, U_t, has been replaced by the energy input from the heating system denoted by U_q, as the control variable determining the energy input to the greenhouse.

Application of the previously described simplifications and aggregation of the parameters yields the following two descriptions of the crop production process.

Integration of the one state variable lettuce growth model and the greenhouse climate model results in the following four state variable dynamic model

$$(3.59) \quad \frac{dX_d}{dt} = c_{\alpha\beta}\left(1-e^{-c_{pl,d}X_d}\right)\frac{c_1V_1(-c_{co2,1}X_t^2+c_{co2,2}X_t-c_{co2,3})(X_c-c_\Gamma)}{c_1V_1+(-c_{co2,1}X_t^2+c_{co2,2}X_t-c_{co2,3})(X_c-c_\Gamma)}$$

$$- c_{resp,1}X_d2^{(0.1X_t-2.5)} \qquad\qquad \text{kg m}^{-2}\text{ s}^{-1},$$

$$(3.60) \quad \frac{dX_c}{dt} = \frac{1}{c_{cap,c}}\left(-\left(1-e^{-c_{pl,d}X_d}\right)\frac{c_1V_1(-c_{co2,1}X_t^2+c_{co2,2}X_t-c_{co2,3})(X_c-c_\Gamma)}{c_1V_1+(-c_{co2,1}X_t^2+c_{co2,2}X_t-c_{co2,3})(X_c-c_\Gamma)}\right.$$

$$\left. + c_{resp,2}X_d2^{(0.1X_t-2.5)} + U_c - (U_v+c_{leak})(X_c-V_c)\right) \qquad \text{kg m}^{-3}\text{ s}^{-1},$$

$$(3.61) \quad \frac{dX_t}{dt} = \frac{1}{c_{cap,q}}\left[U_q-(c_{cap,q,v}U_v+c_{al,ou})(X_t-V_t)+c_{rad}V_1\right] \qquad \text{°C s}^{-1},$$

$$(3.62) \quad \frac{dX_h}{dt} = \frac{1}{c_{cap,h}}\left(\left(1-e^{-c_{pl,d}X_d}\right)c_{v,pl,al}\left(\frac{c_{v,5}}{c_R(X_t+c_{t,abs})}e^{\frac{c_{v,2}X_t}{X_t+c_{v,3}}}-X_h\right)\right.$$

$$\left. - (U_v+c_{leak})(X_h-V_h)\right) \qquad\qquad \text{kg m}^{-3}\text{ s}^{-1},$$

in which X_d [kg m^{-2}], X_c [kg m^{-3}], X_t [°C] and X_h [kg m^{-3}] are the crop dry weight, carbon dioxide concentration, air temperature and absolute humidity, U_v [m s^{-1}] is the ventilation flux through the windows, U_q [W m^{-2}] the energy input by the heating system, U_c [kg m^{-2} s^{-1}] the carbon dioxide supply rate, V_1 [W m^{-2}] the solar radiation, V_t [°C] the outdoor temperature, V_c [kg m^{-3}] the outdoor carbon dioxide concentration, and V_h [kg m^{-3}] the outdoor absolute humidity. The parameters are listed in table 3.6. Some of the parameters in this model are aggregations of parameters used in the model descriptions presented in chapter 3.2. They are explicitly defined in the table. Others directly stem from the original

model descriptions which is referred to for more detail.

Table 3.6. Parameters of the crop production models.

$c_{\alpha\beta} = c_\alpha\, c_\beta = 0.544$	–
$c_{pl,d} = c_k\,(1-c_\tau)\,c_{lar,d} = 53.$	$m^2\ kg^{-1}$
$c_l = c_{par}\,c_{rad,rf}\ 14.2\times10^{-9} = 3.55\times10^{-9}$	$kg\ J^{-1}$
$c_{co2,1} = 5.11\times10^{-6}$	$m\ s^{-1}\ {}^\circ C^{-2}$
$c_{co2,2} = 2.30\times10^{-4}$	$m\ s^{-1}\ {}^\circ C^{-1}$
$c_{co2,3} = 6.29\times10^{-4}$	$m\ s^{-1}$
$c_\Gamma = 5.2\times10^{-5}$	$kg\ m^{-3}$
$c_{resp,1} = c_\beta(c_{resp,s}\,(1-c_\tau)+c_{resp,r}c_\tau) = 2.65\times10^{-7}$	s^{-1}
$c_{resp,2} = (c_{resp,s}(1-c_\tau)+c_{resp,r}c_\tau)/c_\alpha = 4.87\times10^{-7}$	s^{-1}
$c_{al,ou} = 6 + c_{cap,q,v}c_{leak} = 6.1$	$W\ m^{-2}\ {}^\circ C^{-1}$
$c_{v,5} = c_{v,0}\,c_{H20}\,c_{v,1} = 9348.$	$J\ kg\ m^{-3}\ kmol^{-1}$
$c_{pl,s} = c_k\,(1-c_\tau)\,c_{lar,s} = 62.8$	$m^2\ kg^{-1}$
$c_{gr} = c_{r,gr,max}/c_\beta = 6.25\times10^{-6}$	s^{-1}
$c_{resp,3} = (c_{resp,s}\,(1-c_\tau) + c_{resp,r}\,c_\tau) = 3.3\times10^{-7}$	s^{-1}
$c_{resp,4} = c_{r,gr,max}(1-c_\beta)/c_\beta c_\alpha = 1.8\times10^{-6}$	s^{-1}

Integration of the two state variable model of lettuce growth and the greenhouse climate model yields a five state variable model of the lettuce crop production process. Its dynamics are described on a square meter of soil basis with the differential equations

$$
(3.63)\qquad \frac{dX_n}{dt} = c_\alpha\left(1-e^{-c_{pl,s}X_s}\right)\frac{c_lV_l(-c_{co2,1}X_t^2+c_{co2,2}X_t-c_{co2,3})(X_c-c_\Gamma)}{c_lV_l+(-c_{co2,1}X_t^2+c_{co2,2}X_t-c_{co2,3})(X_c-c_\Gamma)}
$$

$$- \frac{c_{gr}X_nX_s}{X_s+X_n}1.6^{(0.1X_t-2.)} - c_{resp,3}X_s2^{(0.1X_t-2.5)} \qquad \text{kg m}^{-2}\text{ s}^{-1},$$

(3.64) $$\frac{dX_s}{dt} = \frac{c_{r,gr,max}X_nX_s}{X_s+X_n}1.6^{(0.1X_t-2.)} \qquad \text{kg m}^{-2}\text{ s}^{-1},$$

(3.65) $$\frac{dX_c}{dt} = \frac{1}{c_{cap,c}}\left(-\left(1-e^{-c_{pl,s}X_s}\right)\frac{c_1V_1(-c_{co2,1}X_t^2+c_{co2,2}X_t-c_{co2,3})(X_c-c_\Gamma)}{c_1V_1+(-c_{co2,1}X_t^2+c_{co2,2}X_t-c_{co2,3})(X_c-c_\Gamma)}\right.$$

$$+ c_{resp,2}X_s2^{(0.1X_t-2.5)} + \frac{c_{resp,4}X_nX_s}{X_s+X_n}1.6^{(0.1X_t-2.)}$$

$$\left. + U_c - (U_v+c_{leak})(X_c-V_c)\right] \qquad \text{kg m}^{-3}\text{ s}^{-1},$$

(3.66) $$\frac{dX_t}{dt} = \frac{1}{c_{cap,q}}\left[U_q-(c_{cap,q,v}U_v+c_{al,ou})(X_t-V_t)+c_{rad}V_1\right] \qquad °\text{C s}^{-1},$$

(3.67) $$\frac{dX_h}{dt} = \frac{1}{c_{cap,h}}\left(\left(1-e^{-c_{pl,s}X_s}\right)c_{v,pl,al}\left(\frac{c_{v,5}}{c_R(X_t+c_{t,abs})}e^{\frac{c_{v,2}X_t}{X_t+c_{v,3}}}-X_h\right)\right.$$

$$\left. - (U_v+c_{leak})(X_h-V_h)\right] \qquad \text{kg m}^{-3}\text{ s}^{-1}.$$

in which X_n [kg m^{-2}] is the non-structural dry weight and X_s [kg m^{-2}] is the structural dry weight. The parameters are listed in table 3.6.

From the amount of energy supplied by the heating system the pipe temperature can be calculated, still assuming immediate realisation as follows:

(3.68) $$U_t = \frac{1}{c_{pl,al}} U_q + X_t \qquad °\text{C}.$$

Assuming that first the lee side ventilation windows are opened and

then the windward side windows, using eqn. (3.28), the aperture of the ventilation windows is calculated by

$$(3.69a) \quad U_{ls} = \frac{U_v}{V_w \, c_{window} \, c_{ls,1} - U_v \, c_{ls,2}} \qquad \%.$$

If $U_{ls} > 100.$, then $U_{ls} = 100.$ and U_{ws} is calculated from

$$(3.69b) \quad U_{ws} = \frac{U_v}{c_{window} \, V_w \, c_{ws,2}} - \frac{c_{window} \, c_{ls,1}}{(1+c_{ls,2})c_{ws,2}} - \frac{c_{ws,1}}{c_{ws,2}} \qquad \%.$$

The relative humidity in the greenhouse air is calculated with eqn. (3.33).

Using the two minute measurements of the control and exogenous inputs obtained during the second greenhouse experiment, simulations with the two crop production models were performed. Simulated crop growth is presented in fig. 3.19 together with the destructive measurements. It can be seen that overall a fairly accurate description of dry matter production is obtained, though the four state variable model tends to overestimate dry matter production during the first part of the growing season. The simulated greenhouse climate did not show significant differences from the results presented in section 3.2.4.
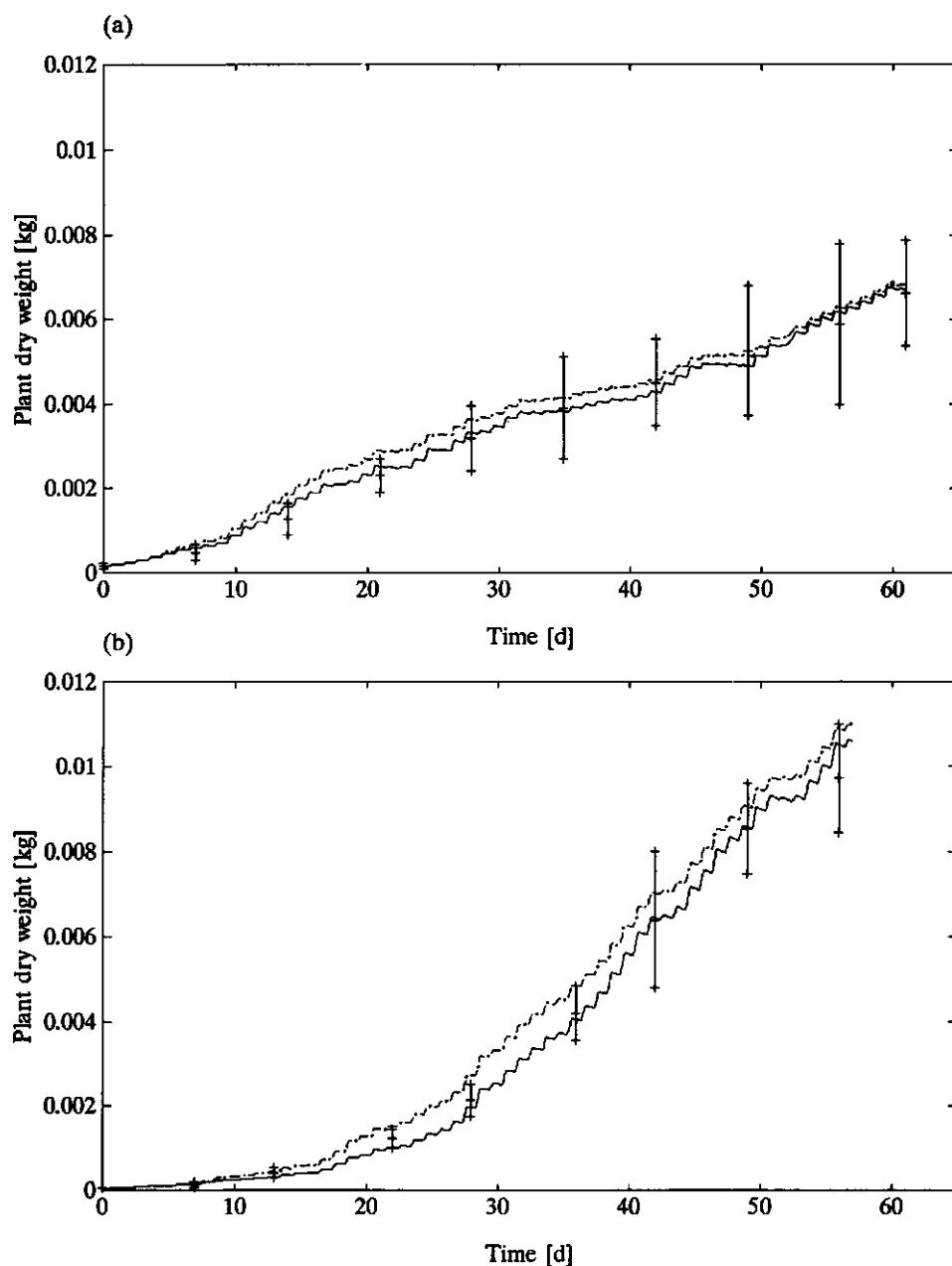
Fig. 3.19. Simulated and measured plant dry weight during experiment 1 (a) and experiment 2 (b); (—) indicates the five state model, (−·) indicates the four state model; the vertical bars indicate the 95% confidence limits around the mean value of the measurements.

second experiment, allows for a comparison of optimal control strategies with the greenhouse climate control implemented by the grower. This comparison may reveal the advantages and/or shortcomings of optimal greenhouse climate control.

The sensitivity analysis of the two state variable lettuce growth model produced some valuable information which may become useful during the analysis and evaluation of the optimal greenhouse climate control system. First of all it was found that only a few parameters in this model description determine the dry matter production of the lettuce crop. Since in the optimal control system to be developed in the subsequent chapters, crop dry weight determines the economic revenues of the crop production process (see also chapter 4 for the definition of the performance criterion), the control strategies also are expected to be sensitive to the parameters which most strongly affect dry matter production. Secondly, the sensitivity analysis revealed that the carbon dioxide concentration in the greenhouse has a stronger positive effect on dry matter production than air temperature. Though the temperature has a positive effect on canopy photosynthesis until a maximum is reached, it also has a counteracting effect on dry matter accumulation through its influence on respiration. Therefore increasing the carbon dioxide concentration in the greenhouse is a much more effective tool to enhance crop production, than increasing the air temperature.

4. DEFINITION OF THE PERFORMANCE CRITERION

4.1. Introduction

In chapter 2 the objective of the control system design was formulated as the derivation of climate control strategies which maximize the economic return of a lettuce crop throughout the whole growing period considered. The economic return was defined by

$$(4.1) \qquad J(u) = \Phi(x(t_f),c,t_f) - \int_{t_b}^{t_f} L(x,u,v,c,t)dt \qquad \text{ct m}^{-2},$$

in which $\Phi(x(t_f),c,t_f)$ is the income due to selling the harvested product at the auction, $L(x,u,v,c,t)$ is the momentary operating cost of the climate conditioning equipment, t_b is the planting date and t_f is the harvest date. In this chapter $\Phi(x(t_f),c,t_f)$ and $L(x,u,v,c,t)$ will be defined for the lettuce production process considered in this research.

4.2 The value of a lettuce crop

Since in this thesis the state of the crop is represented by its dry matter content (eqns. (3.1) and (3.10), (3.11)) and head fresh weight is related to crop dry weight (eqns. (3.9) and (3.21)), in this section, the relation between the harvest fresh weight and the value of the lettuce crop is investigated. The majority of lettuce produced in the Netherlands is sold at auctions in grades based not only on the fresh weight but also on the quality of the product. Despite the fact that quality aspects largely affect the value of the crop, quantitative relations between the greenhouse climate and crop quality, needed to derive optimal greenhouse climate control strategies, are much less developed than for instance the quantitative relation between greenhouse climate and for instance dry matter production. Therefore, crop quality will not be considered in this research.

If a uniform crop is produced and all lettuce heads grown on a square meter of soil are actually sold, the gross economic return is represented by

(4.2) $\Phi(Y_{fwh}(t_f),t_f) = c_{pl} \; pph(Y_{fwh}(t_f),t_f)$ ct m^{-2},

where c_{pl} [head m^{-2}]   is   the   plant   density, $pph(Y_{fwh}(t_f),t_f)$ [ct head^{-1}] is the price per head and Y_{fwh} [g head^{-1}] is the fresh weight of a lettuce head which is determined by $1000Y_{fw}/c_{pl}$, with Y_{fw} [kg m^{-2}] the head fresh weight per square meter of soil (eqns. (3.9) and (3.21)).

The accurate prediction of the auction price of lettuce is rather complicated. The price-making process at the auction is governed by a free market mechanism in which the amount of supply by the growers and demand by the consumers play an important role. Although product flows like domestic production and consumption, export and import, which essentially determine the supply and demand, are quite distinct, the actual volumes involved are hard to predict. Work on the mechanistic description of the auction price of white cabbage in relation with these product flows has been reported for instance by Janecke (1989).

In this research a different approach was adopted. Historical data of the auction price of lettuce were analysed by means of regression and time series analyses to obtain a quantitative relation between the value of a lettuce head, the harvest date and the weight of the lettuce head at harvest time.

From the Central Bureau of Fruit and Vegetable Auctions (CBT), historical data of the auction price of lettuce dating from 1985 to 1989 were collected. The data consisted of the auction price averaged over a week and over all Dutch auctions, of lettuce belonging to quality class I, subdivided in the weight grades 13-14, 15-16, 17-18, 19-20, 21-22, 23-24, 25-27, 28-30, 31-33, 34-36, 37-40, 41-44, 45-49, 50-59 kg fresh weight per 100 lettuces. The data included only lettuce produced in greenhouses.

In general, the production of a heavier crop will require more time and effort and will result in higher production expenses. Then, presumably, the production of a heavier crop is only justified if the related increase in production cost is compensated by an increase of the auction price obtained for the harvested crop. This suggests a positive correlation between the harvest weight of the crop and its value.

For every week contained in the data set from 1985 to 1989, the data were analysed for a linear relation between the value of a lettuce head and its fresh weight

(4.3) $pph(Y_{fwh}(t),t) = \alpha + \beta Y_{fwh}(t) + e$ ct head^{-1},

where α [ct head^{-1}] and β [ct g^{-1}] are the intercept and the additional price per unit head weight, respectively, and e is the residual error. The resulting parameter values are shown in figs. 4.1a and 4.1b, respectively. Parameter α was found to have values in
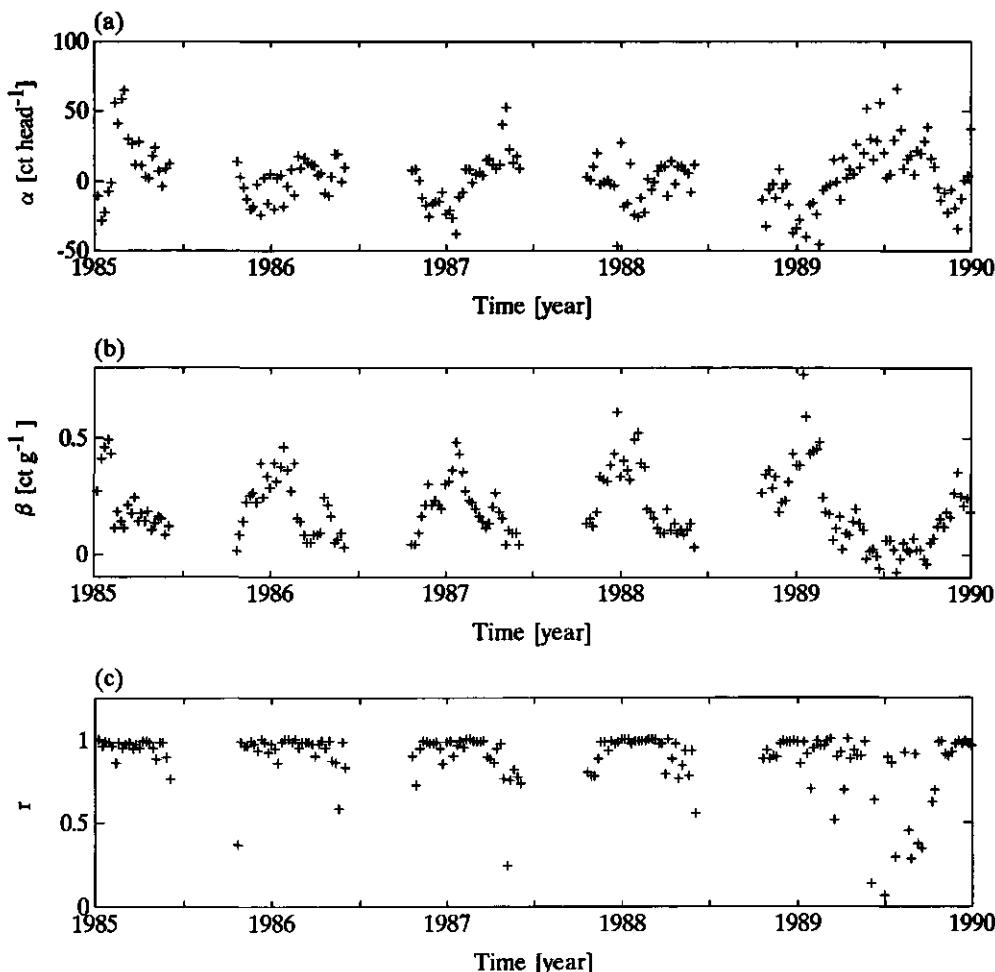
Fig. 4.1. The estimates of the parameters α (a) and β (b) and the correlation coefficient (c) of the linear relation between harvest fresh weight and auction price of lettuce, for auction price data from week 1 in 1985 to week 52 in 1989.

the range of -50 to $+70$ ct head^{-1} and β ranged from -0.1 to $+0.8$ ct g^{-1}.

The generally positive correlation between the lettuce weight and the auction price confirmed the afore-mentioned hypothesis. Additionally, the distinct trends of the parameter values in time show the seasonal effects commonly observed in the price of horticultural products. Usually, the value of the lettuce crop is high in winter and shows a declining trend during the spring to attain a minimum in summer.

As can be seen in fig. 4.1c, a strong correlation between the linear model and data was obtained; the majority of the data sets analysed had a correlation of 0.8 and higher. As a representative example of the large number of data sets having a high correlation, fig. 4.2a shows the data of the first week of 1988. Some exceptions, however, did occur as demonstrated in fig. 4.2b, in which poorly correlated data during week 26 of 1989 are shown. Fig. 4.1c reveals that a poor correlation between the harvest weight of the crop and its value coincides with the summer season. At that time the market
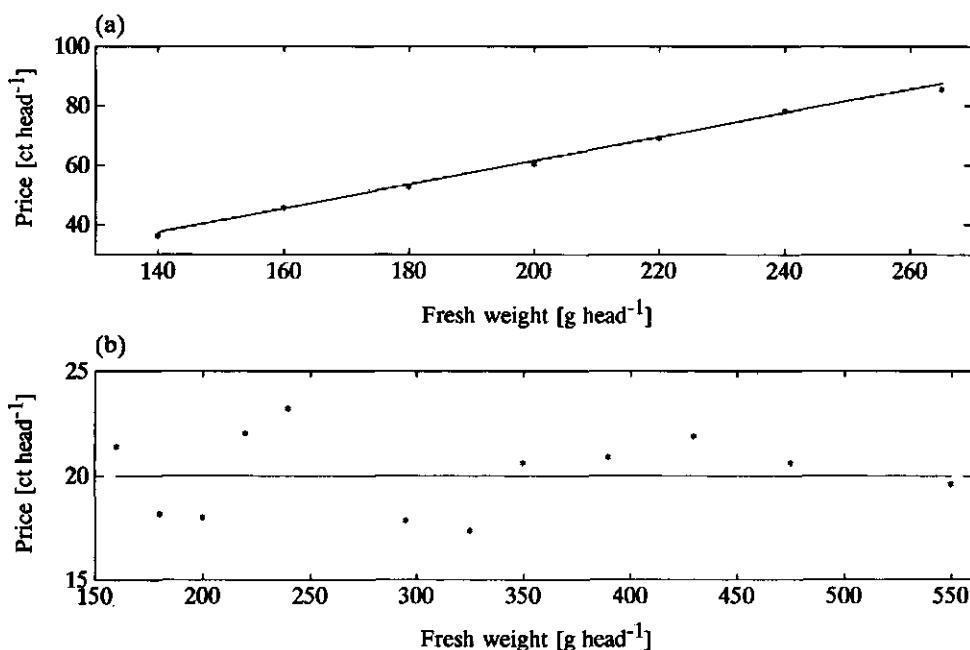
Fig. 4.2. The auction price of lettuce as a function of the fresh weight in week 1 of 1988 (a) and in week 26 of 1989 (b).

is saturated with lettuces produced in the open air and the value of
the crop is low, irrespective of its harvest weight.

It suffices for the present research to conclude that the value
of a lettuce head can be described as a linear function of the fresh
weight of the lettuce. The seasonal effects on the auction price are
reflected by seasonal trends in the values of the parameters in this
linear relation. The data shown in fig. 4.1 supply sufficient insight
in the parameter values to make the results of optimizations and
sensitivity analysis, presented in chapter 7, relevant with respect
to horticultural practice. However, the following remarks should be
kept in mind.

As a matter of principle, optimal control strategies are
calculated for a whole growing period in advance, so accurate
prediction of the economic revenue from the crop is of obvious
importance. Though the prediction of auction prices has not been
considered in this thesis, some insight into the predictability of
the auction prices can be given. Despite the fact that there is a
considerable variance in their values at a certain time of the year,
annual trends can clearly be observed in the parameter estimates of α
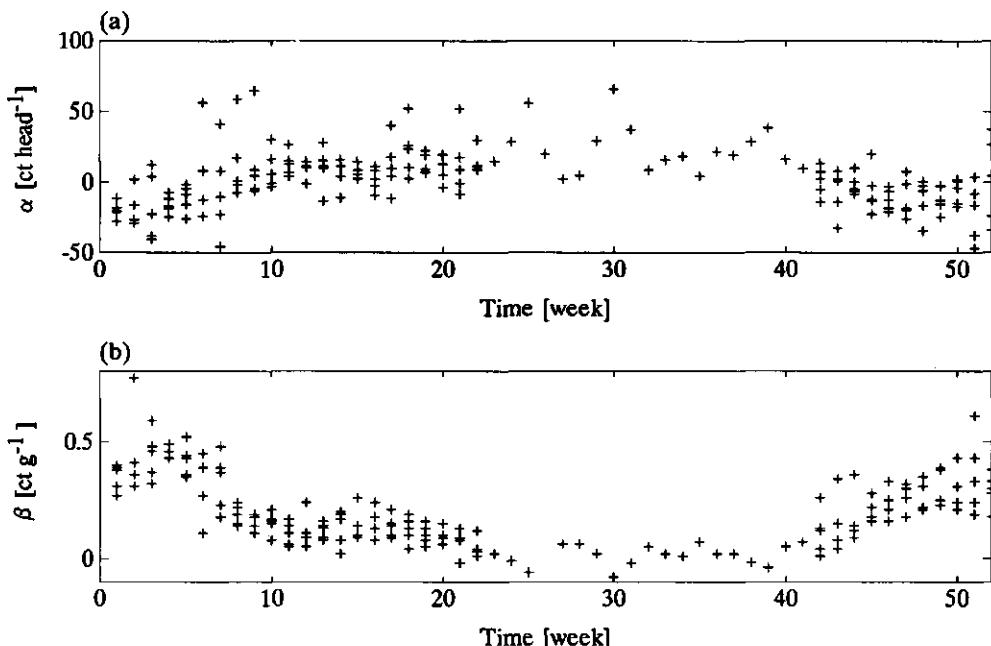
Fig. 4.3. Combined data from 1985 to 1989 of the parameter estimates
of α (a) and β (b).

and β, presented in fig. 4.1. This becomes even more apparent when all the data from 1985 to 1989 are combined, as in fig. 4.3. Time series analyses of these estimates revealed a high auto-correlation in the estimates of both α and β. For the data set of 1989 the auto-correlation in the estimates of α and β is shown in fig. 4.4. The high auto-correlation found in the estimates of both parameters offers an opportunity for predicting the price of lettuce, with for instance, an auto-regressive model.
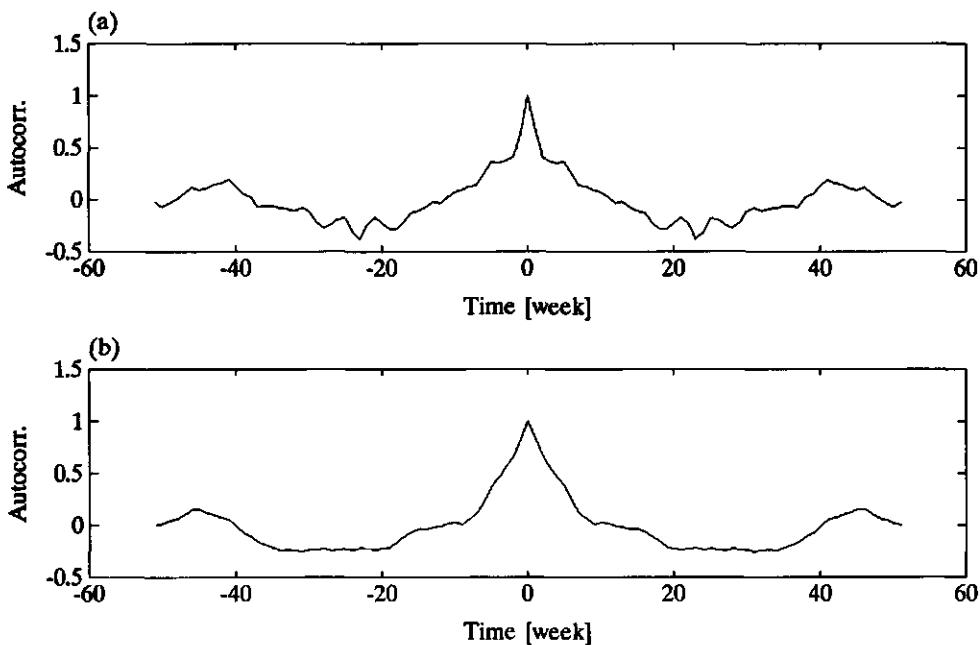
Fig. 4.4.   Auto-correlation of the parameter estimates of α (a) and β (b) in 1989.

The positive and negative values of α indicate benefits or losses when lettuce with a harvest weight of 0 g is sold. This interpretation is fallacious, contradicts reality and stresses the fact that the quantitative relation describing the economic return of lettuce production should only be used within the range of data for which it has been parameterized.

The small values of β during the summer indicate that there does not seem to be much sense in trying to produce a heavy crop. In case the economic return of the crop is low, the control algorithm will be more sensitive to changes in the operating costs and will try to

minimize them. In horticultural practice the production of lettuces in greenhouses in summer is regarded to be difficult due to the high temperature and not very profitable due to the large amount of lettuce produced in the open air. In summer factors related to the quality of the product instead of the harvest weight, may be of more importance in the determination of the auction price. This issue, however, is not covered in this thesis.

The linear price model describes a continuous relation between the harvest weight and the auction price and thus suggests that every increase in harvest weight, however small, will result in a higher price at the auction. Since in Dutch horticultural practice lettuce are sold in discontinuous weight classes, this observation is not completely in line with reality.

4.3. The operating costs of the climate conditioning equipment

In this research three control inputs to the greenhouse crop production process are considered, namely the energy supply by the heating system, supply of pure carbon dioxide and the ventilation exchange with the outside air. Costs related to changing the aperture of the ventilation windows due to *e.g.* the electricity consumption by the motors are neglected. Then the operational cost of the climate conditioning equipment is essentially determined by the amount of natural gas used for heating and the amount of pure carbon dioxide supplied to the greenhouse:

$$(4.4) \qquad L(U_q, U_{co2}) = c_q U_q + c_{co2} U_c \qquad\qquad \text{ct m}^{-2}\text{ s}^{-1},$$

in which c_q [ct J^{-1}] and c_{co2} [ct kg^{-1}] are parameters representing the unit prices of heating energy and pure carbon dioxide respectively, U_q [W m^{-2}] is the amount of heating energy applied to the greenhouse and U_c [kg m^{-2}] is the amount of carbon dioxide supplied. The contribution of the electrical equipment used in greenhouse climate conditioning, such as pumps and valves, to the operating costs is ignored. Furthermore, it is assumed that other production factors, such as the nutrient and water supply, screening and those not directly related to greenhouse climate control, such as labour, pest and disease control, do not affect the control strategies. Consequently they are not included in the performance criterion.

5. METHODS FOR SOLVING AND ANALYSING OPTIMAL CONTROL PROBLEMS

5.1. Introduction

In this chapter methods for solving and analysing the economic optimal greenhouse climate control problem are presented. For completeness, in section 5.2 the optimal control problem, as defined in chapter 2, will be restated. Using variational arguments, in section 5.3, necessary conditions for the existence of an optimizing control strategy will be derived. The resulting equations will be used to generate numerical solutions of the optimal control problems considered in this thesis. First, an unconstrained optimal control problem will be considered. Secondly, extensions will be derived to account for constraints on the control inputs and the states. Some extra attention will be paid to bang-singular-bang type optimal control strategies, since due to the linear appearance of the control inputs in the system description as well as in the performance criterion (see chapters 3 and 4) this type of control behaviour is expected to appear in greenhouse climate management.

    The variational approach to solve optimal control problems offers a richness of methods for the analysis of optimal control problems. For instance, in section 5.4, it will be shown that the necessary conditions for optimality, derived in section 5.3, have a meaningful and interesting economic interpretation. In section 5.5, using variational arguments, a first order approach to evaluate the performance sensitivity of open-loop optimal control systems with respect to perturbations in the model parameters and external inputs, is derived. Finally, in section 5.6, the two time-scale concept of singular perturbed systems will be introduced. As was illustrated in chapter 3, in the greenhouse crop production process, sub-processes with significant differences in dynamic response times are involved. It could be observed that crop growth responds rather slowly to external inputs, compared with the relatively fast response of the greenhouse climate. Using the singular perturbation method, these differences in response times will be exploited to decompose the economic optimal greenhouse climate control problem into a sub-problem in which the slow (crop growth) dynamics are considered and a sub-problem in which the relatively fast (greenhouse climate) dynamics are accounted for. This issue, first addressed in greenhouse climate control by Van Henten and Bontsema (1992, 1994), will be elaborated upon in section 5.6 where the formal results of this decomposition will be presented.

    Generally, the necessary conditions for optimality of an optimizing control strategy contain a non-linear two-point boundary-

value problem which can not be solved analytically to obtain an optimal control law, or an optimal open-loop control. In such cases iterative schemes are used to generate a numerical solution. In section 5.7, such a numerical scheme is described.

In section 5.8 the concept of a sub-optimal control algorithm is described. This sub-optimal control algorithm contains a state feedback loop to deal with errors in the process model and a feedforward loop in which unmodelled disturbances are dealt with while maintaining near optimal performance.

5.2. Statement of the problem

Consider a dynamic system of which the evolution in time is described by a set of ordinary differential equations

$$(5.1) \qquad \dot{x} = f(x,u,v,c,t), \quad x(t_b) = x_b,$$

with the state vector $x = x(t) \in \mathbb{R}^n$, the control vector $u = u(t) \in \mathbb{R}^m$, the exogenous input vector $v = v(t) \in \mathbb{R}^p$, the time invariant parameters $c \in \mathbb{R}^q$ and t denoting time. The continuously differentiable function $f: \mathbb{R}^{n+m+p+q+1} \longrightarrow \mathbb{R}^n$, may be linear or non-linear. The initial time t_b and initial state $x(t_b)$ are assumed to be fixed and therefore not subject to optimization.

As defined in chapters 2 and 4, with this system a *Bolza* type performance criterion $J(u)$ is related, which is given by

$$(5.2) \qquad J(u) = \Phi(x(t_f),c,t_f) - \int_{t_b}^{t_f} L(x,u,v,c,t)dt,$$

where $\Phi: \mathbb{R}^{n+q+1} \longrightarrow \mathbb{R}$ and $L: \mathbb{R}^{n+m+p+q+1} \longrightarrow \mathbb{R}$ are differentiable a sufficient number of times with respect to their arguments. In this research, the final time t_f is considered to be fixed and therefore will not be subject to optimization.

The control inputs are constrained by

$$(5.3) \qquad u_{i,min}(t) \leq u_i(t) \leq u_{i,max}(t), \quad i = 1,...,m ,$$

and the following inequality constraints are imposed on the states

(5.4) $x_{1,\min}(t) \leq x_1(t) \leq x_{1,\max}(t), \quad i \in I_{xc}$,

with I_{xc} the index set containing the constrained states. State and control vectors $x(t)$ and $u(t)$ that satisfy the constraints (5.3) and (5.4) are called admissible.

With these preliminaries the control problem is to find

(5.5) $u^*(t) = \arg \max_u J(u)$,

given (a prediction of) $v(t)$ for $t \in [t_b, t_f]$, subject to the differential equation constraints (5.1) and the control and path constraints (5.3) and (5.4). In other words, the objective is to find the admissible input trajectory $u^*(t)$ on the time interval $t \in [t_b, t_f]$ such that the process given by eqn. (5.1) is driven along an admissible trajectory $x^*(t)$ in such a way that the performance criterion J is maximized. Then, $u^*(t)$ and $x^*(t)$ are referred to as optimal control and state trajectories.

Since, the model parameters, c, and the exogenous inputs, $v(t)$, do not affect the derivation of the necessary conditions for the existence of an optimal control strategy $u^*(t)$, for simplicity they will be omitted from the notation in sections 5.3 and 5.4. In fact, the dependence of the system and performance criterion on the exogenous inputs is adequately represented by the dependence of the functions f and L on time t. For sure, the model parameters and exogenous inputs will have a considerable influence on the calculated optimal control and state trajectories. Therefore, they will reappear in the notation when their effect on the performance and evolution of the optimal control and state trajectories is explicitly considered.

5.3. Necessary conditions for optimality

The maximization of the performance criterion $J(u)$ is subject to three types of constraints, namely differential equation constraints, control constraints and path constraints, as defined in eqns. (5.1), (5.3) and (5.4) respectively. Since each of these constraints is treated differently in the derivation of the optimizing control strategies, $u^*(t)$, they will be considered separately in the following sections. First, in section 5.3.1, necessary conditions will be derived for the existence of $u^*(t)$ maximizing $J(u)$ subject to the differential equation constraints. Secondly, the control

constraints will be dealt with in section 5.3.2 and finally the effect of path constraints on the solution of the optimal control problem will be demonstrated in section 5.3.3.

5.3.1. Differential equation constraints

In this section the derivation of necessary and sufficient conditions for the existence of u^* maximizing the performance criterion J, subject to the differential equation constraints (5.1) is considered. Basically, the derivation given below can be found in any textbook on optimal control; see *e.g.* Pierre (1969), Kirk (1970), Bryson and Ho (1975), Sage and White (1977) or Lewis (1986). It is repeated here in some detail since it will act as a basis for *e.g.* economic interpretation and sensitivity analysis of optimal control problems, presented in the subsequent sections.

A functional $J(u)$ has a *relative maximum* at $u^*(t)$ if there is an $\varepsilon > 0$ such that for all functions u which satisfy $\|u-u^*\| < \varepsilon$ the increment of J is non-positive, *i.e.*

$$(5.6) \qquad \Delta J = J(u) - J(u^*) \leq 0.$$

If eqn. (5.6) is satisfied for arbitrarily large ε, then $J(u^*)$ is a *global maximum*. Although this definition supplies information about the behaviour of a functional J around a maximum, still we have to find the extremum by defining *necessary* and *sufficient* conditions for its existence.

The fundamental theorem of the calculus of variations states that if u^* is an extremal, it is *necessary* that the first variation of J vanishes in u^*; that is

$$(5.7a) \qquad \delta J(u^*,\delta u) = \left.\frac{\partial J}{\partial u}\right|_{u^*} \delta u = 0,$$

for all admissible δu (Kirk, 1970). For an extremal to be a *local maximum* it is sufficient that the second variation is less than zero at u^*; *i.e.*

$$(5.7b) \qquad \delta^2 J(u^*,\delta u) < 0.$$

Expressions for the variations $\delta J(u^*,\delta u)$ and $\delta^2 J(u^*,\delta u)$ are obtained

by a Taylor series expansion of J about u^*. For small variations around u^*, $u = u^* + \delta u$, the increment of J is defined as

$$(5.8) \qquad \Delta J(u^*, \delta u) \equiv J(u^* + \delta u) - J(u^*) = \delta J(u^*, \delta u) + \delta^2 J(u^*, \delta u) + O(\|\delta u\|^3),$$

in which $O(\|\delta u\|^3)$ denote the third order terms. If δu is sufficiently small, the second order and higher terms vanish and the variation $\delta J(u^*, \delta u)$ is taken to be the first order approximation of the increment $\Delta J(u^*, \delta u)$. To obtain the first order approximation of the increment in J, the performance criterion, eqn. (5.2), is rewritten as

$$(5.9) \qquad J(u) = \int_{t_b}^{t_f} \left\{ \left[\frac{\partial \Phi}{\partial x}(x,t) \right]^T \dot{x} + \frac{\partial \Phi}{\partial t}(x,t) - L(x,u,t) \right\} dt + \Phi(x(t_b), t_b),$$

in which superscript T denotes transpose. Using the Lagrange multiplier $\lambda(t)$ the performance criterion is augmented to deal with the differential equation constraint (5.1):

$$(5.10) \qquad J_a(u) = \int_{t_b}^{t_f} \left\{ \left[\frac{\partial \Phi}{\partial x}(x,t) \right]^T \dot{x} + \frac{\partial \Phi}{\partial t}(x,t) - L(x,u,t) + \lambda^T \left[f(x,u,t) - \dot{x} \right] \right\} dt$$
$$+ \Phi(x(t_b), t_b).$$

Then, by introducing

$$(5.11) \qquad L_a(x, \dot{x}, \lambda, u, t) = \left[\frac{\partial \Phi}{\partial x}(x,t) \right]^T \dot{x} + \frac{\partial \Phi}{\partial t}(x,t) - L(x,u,t) + \lambda^T \left[f(x,u,t) - \dot{x} \right],$$

equation (5.10) is condensed to

$$(5.12) \qquad J_a(u) = \int_{t_b}^{t_f} L_a(x, \dot{x}, \lambda, u, t) dt + \Phi(x(t_b), t_b).$$

Using $x = x^* + \delta x$, $\dot{x} = \dot{x}^* + \delta \dot{x}$, $u = u^* + \delta u$ and $\lambda = \lambda^* + \delta \lambda$, an increment in

J_a is defined as

$$(5.13) \quad \Delta J_a(u^*,\delta u) = \int_{t_b}^{t_f} L_a(x^*+\delta x, \dot{x}^*+\delta\dot{x}, \lambda^*+\delta\lambda, u^*+\delta u, t)dt$$

$$- \int_{t_b}^{t_f} L_a(x^*, \dot{x}^*, \lambda^*, u^*, t)dt + \Phi(x^*(t_b)+\delta x(t_b), t_b) - \Phi(x^*(t_b), t_b).$$

Since in this research the initial state, $x(t_b)$, is assumed to be fixed, the terms in eqn. (5.13) related to $x(t_b)$ actually disappear. However, in the following equations $\delta x(t_b)$ will be explicitly accounted for since it will yield a result (eqn. (5.17)) which will serve as a basis for economic interpretation and sensitivity analysis of optimal control problems in sections 5.4 and 5.5, respectively.

Taylor series expansion of the integrand in eqn. (5.13) about $x^*(t)$, $\dot{x}^*(t)$, $u^*(t)$ and $\lambda^*(t)$ yields

$$(5.14) \quad \Delta J_a(u^*,\delta u) = \int_{t_b}^{t_f} \left\{ \left[\frac{\partial L_a}{\partial x}(x^*, \dot{x}^*, \lambda^*, u^*, t) \right]^T \delta x \right.$$

$$+ \left[\frac{\partial L_a}{\partial \dot{x}}(x^*, \dot{x}^*, \lambda^*, u^*, t) \right]^T \delta\dot{x} + \left[\frac{\partial L_a}{\partial u}(x^*, \dot{x}^*, \lambda^*, u^*, t) \right]^T \delta u$$

$$+ \left. \left[\frac{\partial L_a}{\partial \lambda}(x^*, \dot{x}^*, \lambda^*, u^*, t) \right]^T \delta\lambda \right\} dt + \left[\frac{\partial \Phi}{\partial x}(x^*(t_b), t_b) \right]^T \delta x(t_b)$$

$$+ O(\delta u^2),$$

in which $O(\delta u^2)$ denotes the second order terms. Partial integration of the terms containing $\delta\dot{x}$ and collecting terms gives

$$(5.15) \quad \Delta J_a(u^*,\delta u) = \int_{t_b}^{t_f} \left\{ \left[\frac{\partial L_a}{\partial x}(x^*, \dot{x}^*, \lambda^*, u^*, t) \right. \right.$$

$$\left. \left. - \frac{d}{dt}\left[\frac{\partial L_a}{\partial \dot{x}}(x^*, \dot{x}^*, \lambda^*, u^*, t) \right] \right]^T \delta x + \left[\frac{\partial L_a}{\partial u}(x^*, \dot{x}^*, \lambda^*, u^*, t) \right]^T \delta u \right.$$

$$+ \left[\frac{\partial L_a}{\partial \lambda}(x^*,\dot{x}^*,\lambda^*,u^*,t)\right]^T \delta\lambda \Bigg\} dt + \left[\frac{\partial L_a}{\partial \dot{x}}(x^*,\dot{x}^*,\lambda^*,u^*,t_f)\right]^T \delta x(t_f)$$

$$- \left[\frac{\partial L_a}{\partial \dot{x}}(x^*,\dot{x}^*,\lambda^*,u^*,t_b)\right]^T \delta x(t_b) + \left[\frac{\partial \Phi}{\partial x}(x^*(t_b),t_b)\right]^T \delta x(t_b)$$

$$+ O(\delta u^2).$$

Using eqn. (5.11), the arguments of the variations in eqn. (5.15) can be written explicitly in terms of x^*, u^*, $\dot{x}^*$, λ^*. Then, in line with eqn. (5.8), the following relation for the increment ΔJ is obtained

$$(5.16) \qquad \Delta J_a(u^*,\delta u) = \delta J_a(u^*,\delta u) + O(\delta u^2)$$

with

$$(5.17) \qquad \delta J_a(u^*,\delta u) = \int_{t_b}^{t_f} \Bigg\{ \left[\left[-\frac{\partial L}{\partial x}(x^*,u^*,t) + \left[\frac{\partial f}{\partial x}(x^*,u^*,t)\right]^T \lambda^* + \dot{\lambda}^*\right] \delta x \right.$$

$$+ \left[-\frac{\partial L}{\partial u}(x^*,u^*,t) + \frac{\partial f}{\partial u}(x^*,u^*,t)\right]^T \delta u + \left[f(x^*,u^*,t) - \dot{x}^*\right]^T \delta\lambda \Bigg\} dt$$

$$+ \left[\frac{\partial \Phi}{\partial x}(x^*(t_f),t_f) - \lambda^*(t_f)\right]^T \delta x(t_f) + \lambda^*(t_f)\delta x(t_f).$$

According to the Lagrange theory, the constrained maximum of J is attained at the unconstrained maximum of J_a. This is achieved when $\delta J_a(u^*,\delta u) = 0$ for all independent variations in its arguments. Since $x(t_b)$ is fixed, $\lambda^*(t_b)\delta x(t_b)$ is eliminated from eqn. (5.17) at this stage. The necessary conditions for optimality are obtained through the requirement that all the coefficients of the independent variations δx, δu and $\delta\lambda$ be zero for $t \in [t_b, t_f]$. Using, for convenience, the Hamiltonian defined by

$$(5.18) \qquad \mathcal{H}(x^*,u^*,\lambda^*,t) \equiv -L(x^*,u^*,t) + \lambda^{*T}f(x^*,u^*,t),$$

these necessary conditions are given by:

$$(5.19a) \quad \dot{x}^* = \frac{\partial \mathcal{H}}{\partial \lambda}(x^*,\lambda^*,u^*,t),$$

$$(5.19b) \quad -\dot{\lambda}^* = \frac{\partial \mathcal{H}}{\partial x}(x^*,\lambda^*,u^*,t),$$

$$(5.19c) \quad \frac{\partial \mathcal{H}}{\partial u}(x^*,\lambda^*,u^*,t) = 0,$$

and initial and final boundary conditions

$$(5.19d) \quad x^*(t_b) = x_b,$$

$$(5.19e) \quad \lambda^*(t_f) = \frac{\partial \Phi}{\partial x}(x^*(t_f),t_f).$$

It should be noted that eqns. (5.19a) to (5.19e) constitute necessary conditions for optimality; these conditions are not, in general, sufficient. A sufficient condition is obtained by taking the second order terms of the Taylor series expansion of $\Delta J(u^*,\delta u)$, *i.e.*

$$(5.20) \quad \delta^2 J(u,\delta u) = \frac{1}{2}\left[\delta x^T \frac{\partial^2 \Phi}{\partial x^2} \delta x\right]\Big|_{t_b}^{t_f} + \frac{1}{2}\int_{t_b}^{t_f}\left[\delta x^T \ \delta u^T\right]\begin{bmatrix} \dfrac{\partial^2 \mathcal{H}}{\partial x^2} & \dfrac{\partial^2 \mathcal{H}}{\partial u \partial x} \\ \left[\dfrac{\partial^2 \mathcal{H}}{\partial u \partial x}\right]^T & \dfrac{\partial^2 \mathcal{H}}{\partial u^2} \end{bmatrix}\begin{bmatrix}\delta x \\ \delta u\end{bmatrix}dt$$

where $\partial^2\Phi/\partial x^2$ and $\partial^2\mathcal{H}/\partial x^2$ are $n{\times}n$ dimensional matrices, $\partial^2\mathcal{H}/\partial u\partial x$ is a $n{\times}m$ dimensional matrix and $\partial^2\mathcal{H}/\partial u^2$ is a $m{\times}m$ dimensional matrix. For an extremum to be a maximum it is required that $\delta^2 J(u,\delta u) < 0$. This will be the case if the $(n+m){\times}(n+m)$ dimensional square matrix in the integrand and $\partial^2\Phi/\partial x^2$ are non-positive definite around u^* and x^* (Sage and White, 1977).

Inspection of the necessary conditions summarized in eqns. (5.19a) to (5.19e), shows that the solution of the optimal control problem contains a two point boundary value problem. At the initial time, t_b, conditions are imposed on the state variables, *i.e.* $x^*(t_b) = x_b$. At the final time, t_f, conditions are imposed on the

costates by the requirement that $\lambda^*(t_f) = \partial\Phi(x^*(t_f),t_f)/\partial x$. In general, two point boundary value problems are difficult to solve, since both the initial and final boundary conditions need to be satisfied and usually an iterative numerical scheme is required for its solution. Section 5.7 contains a description of such a numerical scheme.

5.3.2. Control constraints

5.3.2.1. The maximum principle of Pontryagin

When the control vector u is required to stay in a closed and bounded region, *i.e.*

$$(5.21) \qquad u_{i,min}(t) \le u_i(t) \le u_{i,max}(t), \quad i = 1,...,m \ ,$$

the necessary conditions derived in section 5.3.1 are slightly modified according to the *Maximum Principle of Pontryagin* (Pontryagin *et al.*, 1962).

By definition, the control u^* causes the functional J to have a relative maximum if the increment $\Delta J_a(u^*,\delta u) \le 0$ for all admissible controls sufficiently close to u^*, with $\Delta J_a(u^*,\delta u)$ defined in eqns. (5.16) and (5.17). Since the control u is bounded, not every variation around u^*, *i.e.* $u = u^*+\delta u$, is allowed. An arbitrary variation δu can be taken, only if the extremal control is within the boundary defined by eqn. (5.21) for all $t \in [t_b,t_f]$. Then, as before, the necessary condition for optimality of u^* is

$$(5.22a) \quad \delta J_a(u^*,\delta u) = 0$$

and the control constraints do not affect the solution of the control problem. If, however, an extremal control lies on a boundary during a sub-interval $[t_1,t_2]$ of the optimization interval $[t_b,t_f]$, then not all the control variations δu are admissible, since a violation of the constraint may occur. In that case, the necessary condition

$$(5.22b) \quad \delta J_a(u^*,\delta u) \le 0$$

must be satisfied (Kirk, 1970). This results in the following modification of the necessary conditions.

If the state and costate satisfy eqns. (5.19a) and (5.19b) and the associated boundary conditions, the variation δJ_a reduces to

$$(5.23) \qquad \delta J_a(u^*,\delta u) = \int_{t_b}^{t_f} \left[\frac{\partial \mathcal{H}}{\partial u}(x^*,u^*,\lambda^*,t)\right]^T \delta u \ dt \ + \ O(\delta u^2).$$

The integrand in eqn. (5.23) is a first order approximation to the change in $\mathcal{H}$ caused by a change in u, *i.e.*

$$(5.24) \qquad \left[\frac{\partial \mathcal{H}}{\partial u}(x^*,u^*,\lambda^*,t)\right]^T \delta u = \mathcal{H}(x^*,u^*+\delta u,\lambda^*,t) - \mathcal{H}(x^*,u^*,\lambda^*,t).$$

For a control u^* to satisfy the necessary condition of eqn. (5.22b) it is required that

$$(5.25) \qquad \delta J_a(u^*,\delta u) = \int_{t_b}^{t_f} \left\{\mathcal{H}(x^*,u^*+\delta u,\lambda^*,t)-\mathcal{H}(x^*,u^*,\lambda^*,t)\right\}dt \ \leq \ 0$$

for all admissible δu, such that $\|\delta u\| \leq \varepsilon$, which is equivalent to

$$(5.26) \qquad \mathcal{H}(x^*,u^*+\delta u,\lambda^*,t) \leq \mathcal{H}(x^*,u^*,\lambda^*,t)$$

for all admissible δu and for all $t \in [t_b,t_f]$. This can be demonstrated as follows. Take

$$(5.27) \qquad \begin{aligned} u(t) &= u^*(t), \quad t \notin [t_1,t_2], \\ u(t) &= u^*(t)+\delta u(t), \ t \in [t_1,t_2], \end{aligned}$$

where $[t_1,t_2]$ is an arbitrary small, non-zero sub-interval of $[t_b,t_f]$. Suppose that for an admissible control variation, δu, the inequality constraint (5.26) is not satisfied. Then

$$(5.28) \qquad \mathcal{H}(x^*,u,\lambda^*,t) > \mathcal{H}(x^*,u^*,\lambda^*,t)$$

in the interval $[t_1,t_2]$ and consequently

$$(5.29) \quad \int_{t_b}^{t_f} \left\{ \mathcal{H}(x^*,u,\lambda^*,t) - \mathcal{H}(x^*,u^*,\lambda^*,t) \right\} dt =$$

$$\int_{t_1}^{t_2} \left\{ \mathcal{H}(x^*,u,\lambda^*,t) - \mathcal{H}(x^*,u^*,\lambda^*,t) \right\} dt > 0.$$

Because the interval $[t_1,t_2]$ can be anywhere in the interval $[t_b,t_f]$, it is clear that if

$$(5.30) \quad \mathcal{H}(x^*,u,\lambda^*,t) > \mathcal{H}(x^*,u^*,\lambda^*,t)$$

for any $t \in [t_b,t_f]$, it is always possible to construct an admissible control which results in $\Delta J > 0$, thus contradicting the optimality of the control $u^*(t)$.

Summarizing, for all $t \in [t_b,t_f]$ and all controls $u(t)$ satisfying the constraints (5.21) the necessary conditions for optimality are given by

$$(5.31a) \quad \dot{x}^* = \frac{\partial \mathcal{H}}{\partial \lambda}(x^*,\lambda^*,u^*,t),$$

$$(5.31b) \quad -\dot{\lambda}^* = \frac{\partial \mathcal{H}}{\partial x}(x^*,\lambda^*,u^*,t),$$

$$(5.31c) \quad \mathcal{H}(x^*,u,\lambda^*,t) \leq \mathcal{H}(x^*,u^*,\lambda^*,t),$$

and initial and final boundary conditions

$$(5.31d) \quad x^*(t_b) = x_b,$$

$$(5.31e) \quad \lambda^*(t_f) = \frac{\partial \Phi}{\partial x}(x^*(t_f),t_f).$$

Eqn. (5.31c) is known as the *Maximum Principle of Pontryagin.* Although the Maximum Principle is derived for bounded controls, it can also be applied to problems with unbounded controls by viewing the unbounded control region as having arbitrarily large bounds, thus ensuring that the optimal control will not be constrained by the boundaries.

Again it should be noted that eqns. (5.31a) to (5.31e)

constitute a set of necessary conditions for optimality; these conditions are not, in general, sufficient.

5.3.2.2. Bang-singular-bang control

Chapters 3 and 4 revealed that both the dynamic model of the greenhouse crop production process as well as the performance criterion used in this research, are linear in the control inputs u. In such a case the optimizing control has a special structure. This is best illustrated for a one dimensional example, as follows.

   If a system is linear in the control, for instance

(5.32) $\dot{x} = f(x,t) + c_1 u$

and the performance criterion J is also linear in the control, *i.e.* for example

$$(5.33) \qquad J(u) = \Phi(x(t_f),t_f) - \int_{t_b}^{t_f} \left\{ l(x,t) + c_2 u \right\} dt,$$

then the Hamiltonian is linear in the control u. In line with the Maximum Principle presented in section 5.3.2.1, a necessary condition for optimality is

(5.34) $(-c_2 + \lambda^* c_1)u < (c_2 + \lambda^* c_1)u^*.$

With the *switching function* $s(t)$ defined as

$$(5.35) \qquad s(t) = \frac{\partial \mathcal{H}}{\partial u} = -c_2 + \lambda^* c_1,$$

this leads to the following *Bang-Singular-Bang* control

$$(5.36) \qquad u^*(t) = \begin{cases} u_{max} & \text{if } s(t) > 0, \quad t \leq t_1, \\ u_{sing} & \text{if } s(t) = 0, \quad t_1 \leq t \leq t_2, \\ u_{min} & \text{if } s(t) < 0, \quad t \geq t_2. \end{cases}$$

On a singular interval $[t_1,t_2]$, the maximum principle does not

provide the optimal control $u^*(t)$. However, if $s(t) = 0$ for $t \in [t_1, t_2]$ then $ds(t)/dt$ as well as the higher order derivatives are zero and $u^*(t)$ can be found from the requirement that

(5.37) $$\frac{d^k s(t)}{dt^k} = 0, \quad k = 1, 2, ..., \; \forall t \in [t_1, t_2],$$

(Kirk, 1970; Bryson and Ho, 1975). That is to say, the switching function $s(t)$ is repeatedly differentiated with respect to time until the control u explicitly appears. Application of this notion to the specific example defined by eqns. (5.32) and (5.33), yields the following result. Differentiating (5.35) with respect to time yields

(5.38) $$\frac{ds(t)}{dt} = c_1 \frac{d\lambda^*}{dt} = c_1 \left(\frac{\partial l}{\partial x} - \lambda^* \frac{\partial f}{\partial x} \right) = 0,$$

with the derivatives evaluated along the optimal trajectories. Again differentiating (5.38) with respect to time results in

(5.39) $$\frac{d}{dt} \frac{ds(t)}{dt} = c_1 \frac{d}{dt} \left(\frac{\partial l}{\partial x} - \lambda^* \frac{\partial f}{\partial x} \right)$$

$$= c_1 \left(\frac{\partial^2 l}{\partial t \partial x} + \frac{\partial^2 l}{\partial x^2} \dot{x}^* - \dot{\lambda}^* \frac{\partial f}{\partial x} - \lambda^* \frac{\partial^2 f}{\partial t \partial x} - \lambda^* \frac{\partial^2 f}{\partial x^2} \dot{x}^* \right) = 0.$$

Rewriting (5.39) using (5.32) we obtain

(5.40) $$u^*_{\text{sing}}(t) = \frac{-\dfrac{\partial^2 l}{\partial t \partial x} + \dot{\lambda}^* \dfrac{\partial f}{\partial x} + \lambda^* \dfrac{\partial^2 f}{\partial t \partial x}}{c_1 \left(\dfrac{\partial^2 l}{\partial x^2} - \lambda^* \dfrac{\partial^2 f}{\partial x^2} \right)} - \frac{f(x,t)}{c_1}.$$

The control law (5.40) maintains the stationarity condition $s(t) = 0$ if $s(t) = 0$ and $ds(t)/dt = 0$ at the beginning and at the end of the

singular arc. In this example, the implication of this control law is that a singular arc is not possible at all points of the $2n$ dimensional state, costate space. It is restricted to a hyper-surface of dimension $2n$-1, called a singular surface. This singular surface originates from the requirement that $s(t) = 0$ and $ds(t)/dt = 0$ for $t \in [t_1, t_2]$, thus limiting the evolution of the costate λ.

A generalization to multivariable systems with more than one input can be found in Kirk (1970) and Bryson and Ho (1975).

Although eqn. (5.40) is a rather straightforward expression for the optimal control during a singular interval, its application is generally more complicated because it requires prior information about the start and termination of the singular interval expressed by t_1 and t_2, respectively. They are usually not easily determined, especially if multiple singularities occur in the optimization interval. Additionally, in this research the optimal control of a system with exogenous inputs v is considered, which yields another complicating factor. Because f is a function of the exogenous input v which in turn is a function of time, besides a prediction of $v(t)$, a prediction of the time derivative of $v(t)$ is required for the actual calculation of the singular control using eqn. (5.40). Therefore, in this research a singular control law like eqn. (5.40) is not used and a numerical search procedure is employed to approximate the optimizing control trajectory. Since the numerical accuracy of the digital computer used for the calculations is limited, the optimizing control trajectory may take values $u_{min}(t) < u(t) < u_{max}(t)$ with $s(t) \neq 0$ but very small, thus contradicting the requirements listed in eqn. (5.36). Here, it is assumed that if $|s(t)| < \varepsilon$ for some small positive ε, the necessary conditions for optimality are satisfied up to the numerical accuracy.

5.3.3. Path constraints

In this paragraph the effect of simple bound path constraints of the form

(5.41) $x_{i,min}(t) \leq x_i(t) \leq x_{i,max}(t), \quad i \in I_{xc},$

with I_{xc} the index set of the constrained states, on the solution of the optimal control problem is demonstrated. State variable constraints like (5.41) define a connected region of allowable states in the space of possible states. This region may be a function of time.

In this research a *penalty-function* method is employed to deal

with path constraints of the form (5.41). The *penalty-function* method is based on the premise that if the performance criterion is severely penalized when the constraint is not satisfied and the performance criterion is not penalized when the same constraint is satisfied, then the optimal solution will be forced to satisfy the state constraints. For this purpose a function

$$p_i = p(x_i(t), x_{i,min}(t), x_{i,max}(t))$$

is adopted which has the following properties

(5.42a) $p_i \cong 0$ for $x_{i,min}(t) \leq x_i(t) \leq x_{i,max}(t)$

and

(5.42b) $p_i \gg 0$ for $x_i(t) < x_{i,min}(t)$ or $x_i(t) > x_{i,max}(t)$.

The performance criterion is augmented with n_{xc} penalty functions

$$(5.43) \quad J(u) = - \int_{t_b}^{t_f} \left\{ L(x,u,v,t) + \sum_{i=1}^{n_{xc}} p(x_i(t), x_{i,min}(t), x_{i,max}(t)) \right\} dt$$
$$+ \Phi(x(t_f), t_f),$$

where n_{xc} equals the number of state constraints and the transformation of the constrained optimal control problem into an unconstrained problem is established.

The addition of penalty functions, however, changes the interpretation of the performance criterion J. Although, the value of the penalty function may be interpreted as an assessment of a risk related to violating the constraint, in general, the penalty function used to force the solution of the optimal control problem to satisfy the constraints imposed on the states, will not have an economic interpretation. Consequently, the economic interpretation of J seems lost. Still, if the constraints are satisfied by the optimal solution, $p_i \cong 0$, this results in a value of J representing the economic revenues due to the control. Moreover, the economic interpretation of $\Phi(x(t_f), t_f)$ and $L(x,u,v,t)$ is preserved and their values associated with the constrained optimum can be computed.

To the resulting unconstrained problem the necessary conditions (5.19a) to (5.19e) do apply, with the Hamiltonian given by

$$(5.44) \quad \mathcal{H} = -L(x,u,t) - \sum_{i=1}^{n_{xc}} p(x_i(t), x_{i,\min}(t), x_{i,\max}(t)) + \lambda^T f(x,u,t).$$

The penalty function should be twice differentiable with respect to its arguments. The following function proposed by Pierre (1969) meets this requirement:

$$(5.45) \quad p(x_i(t), x_{i,\min}(t), x_{i,\max}(t)) = \alpha \left[\frac{2x_i(t) - x_{i,\min}(t) - x_{i,\max}(t)}{x_{i,\max}(t) - x_{i,\min}(t)} \right]^{2k},$$

where k is a positive integer and α is a scaling factor. For various values of k, in fig. 5.1 curves of p are shown with x ranging from 0 to 1 , $x_{\min} = 0.1$ and $x_{\max} = 0.9$.
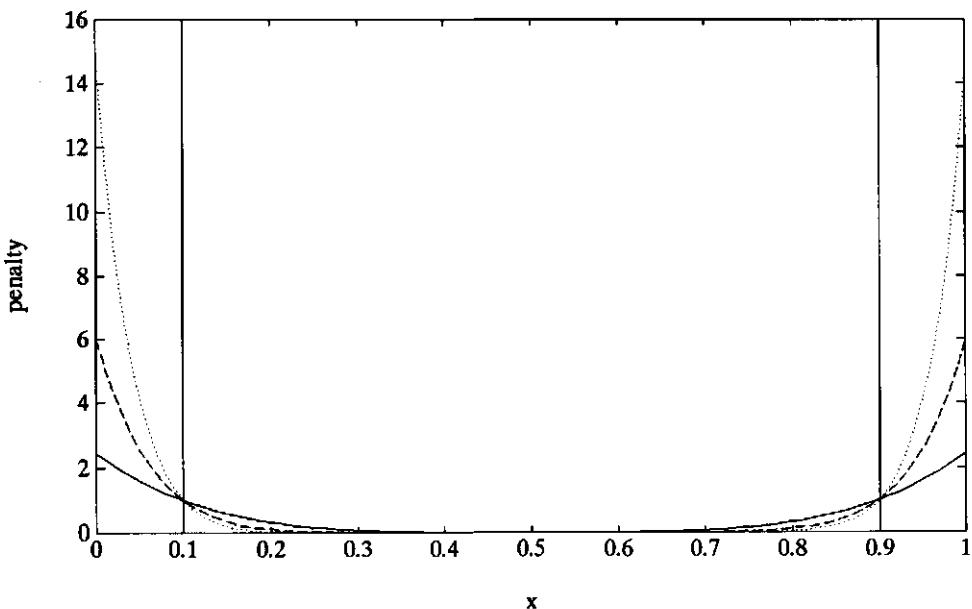

Fig. 5.1.   The penalty function for $x_{\min} = 0.1$, $x_{\max} = 0.9$ and $k = 4$ (—), $k = 8$ (--) and $k = 12$ (...).

Generally, numerical solution of the optimal control will start with small values of k. Once, a solution is found, k is increased and the calculations are repeated for more accuracy. As k tends to infinity the solution of the unconstrained problem approaches the original constrained one. However, then the dynamics of the costate variables will exhibit discontinuities around the state variable constraints, which renders the numerical solution of the optimal control problem impractical. Normally, values for k much smaller than infinity will already yield an appropriate result. Then small violations of the state constraints may occur. These are due to the fact that the penalty will only cause an effect once $p_1 \gg L(x,u,v,t)$. This emphasizes a suitable choice of the scaling factor α.

The path constraint (5.41) can be generalized to include control and exogenous inputs as well, *i.e.*

$$(5.46) \qquad h_{min}(t) \le h(x(t),u(t),v(t),t) \le h_{min}(t).$$

In greenhouse climate management, this type of constraint can be encountered when for example, crop transpiration is required to be restricted to pre-specified ranges. Then, the penalty function approach is also applicable and the penalty function

$$p = p(h(x(t),u(t),v(t),t),h_{min}(t),h_{max}(t))$$

takes the form

$$(5.47) \qquad p = \alpha \left[\frac{2h(x(t),u(t),v(t),t)-h_{min}(t)-h_{max}(t)}{h_{min}(t)-h_{max}(t)} \right]^{2k}.$$

Besides the penalty function method, in the literature two other methods can be found to deal with state variable inequality constraints of the form (5.45), namely the *direct method* and the *slack-variable method*.

In the *direct method*, necessary conditions of optimality are obtained by *directly* adjoining the state variable constraints to the cost functional (Kirk, 1970; Jacobson *et al.*, 1971; Kreindler, 1982). The major advantage of this approach over the penalty function method is that in the solution of the control problem, constraint violations do not occur. It is found, however, that on a constrained arc, the costate differential equations are different from those along the unconstrained arcs, and at junction points of the constrained and unconstrained arcs, the costates suffer discontinuities. From a

numerical point of view these properties are not very convenient if it is not known *a priori* when as well as how many discontinuities will occur. However, if this information is available, the *direct method* is very powerful as was shown for some examples by Jacobson *et al.* (1971), Kreindler (1982) and Maurer and Wiegand (1992).

       Discontinuities in the costate differential equations are not encountered in the *slack-variable method* (see *e.g.* Jacobson and Lele, 1969; Pierre, 1969). In the *slack-variable* method, originally suggested by Valentine in 1937, the inequality constraint is converted into an equality constraint using a quadratic slack variable. The major advantage of this approach is that no violations of the constraints will occur. From the computational point of view, however, a disadvantage of this approach is that the original control problem is transformed into a problem of higher dimension. Additionally the number of state variable constraints should not exceed the number of control variables, unless some of these variables are dependent upon each other.

5.4. Economic interpretation of optimal control problems

Optimal control problems have an interesting and meaningful economical interpretation (see *e.g.* Dorfman, 1969; Kamien and Schwartz, 1981). In this section, it will be shown first that the costate can be interpreted as the marginal value with respect to the control input of the associated state variable at any time in the interval $[t_b, t_f]$. Then, secondly, by virtue of this result, an interpretation of the Hamiltonian and the necessary conditions of optimality (eqns. (5.19a) to (5.19e)) will be given from an economic point of view.

       Given a predefined trajectory of the exogenous inputs $v(t)$, $t \in [t_b, t_f]$, the solution of the optimal control problem yields an optimal value of the performance criterion J^*, and optimal trajectories for the state, costate and control variables, $x^*(t)$, $\lambda^*(t)$, $u^*(t)$, respectively. Once the necessary conditions for optimality (5.19a) to (5.19e) are satisfied, the variation $\delta J_a(u^*, \delta u)$ derived from eqn. (5.17) without omitting $\delta x(t_b)$, reduces to

(5.48) $\delta J_a(u^*, \delta u) = \lambda^*(t_b) \delta x(t_b)$.

Dividing both sides of eqn. (5.48) by $\delta x(t_b)$ and letting $\delta x(t_b)$ approach zero results in

(5.49) $\displaystyle \lim_{\delta x(t_b) \to 0} \frac{\delta J_a}{\delta x(t_b)} = \frac{\partial J_a}{\partial x}\bigg|_{t=t_b} = \lambda^*(t_b).$

The left hand side of equation (5.49) is by definition the derivative of J_a with respect to x at time $t = t_b$. Provided that the limit exists, the costate vector $\lambda(t_b)$ represents the marginal value of the state vector x at time t_b.

This result can be extended for all $t \in [t_b, t_f]$. The performance criterion is additive, *i.e.* for any $t_1 \in [t_b, t_f]$

(5.50) $\displaystyle J(u) = \Phi(x(t_f), t_f) - \int_{t_b}^{t_1} L(x, u, t)dt - \int_{t_1}^{t_f} L(x, u, t)dt.$

Bellman's principle of optimality states that 'An optimal policy has the property that whatever the initial state and initial decision are, the remaining decisions must constitute an optimal control policy with regard to the state resulting from the first decision' (Kirk, 1970).

In view of this theorem, the following result is obtained. Suppose the optimal solution of the control problem defined in eqns. (5.1) to (5.5), $x^*(t)$, and $u^*(t)$, is used for a period $t_b \leq t \leq t_1$ with $t_1 \in [t_b, t_f]$, and from t_1 on an optimal control $\tilde{u}^*(t)$ and state $\tilde{x}^*(t)$ are calculated for $t_1 \leq t \leq t_f$ maximizing the performance criterion

(5.51) $\displaystyle \tilde{J}(u) = \Phi(\tilde{x}(t_f), t_f) - \int_{t_1}^{t_f} L(\tilde{x}, \tilde{u}, t)dt$

subject to

(5.52) $\displaystyle \frac{d\tilde{x}}{dt} = f(\tilde{x}, \tilde{u}, t), \quad \tilde{x}(t_1) = x^*(t_1).$

Then, because of Bellman's principle of optimality, the solution will

be $\tilde{u}^*(t) = u^*(t)$ and $\tilde{x}^*(t) = x^*(t)$ for $t \in [t_1,t_f]$; that is to say it is exactly the same as the solution of the original problem. If $\tilde{u}^*(t) \neq u^*(t)$ and $\tilde{x}^*(t) \neq x^*(t)$, it would contradict the optimality of $u^*(t)$ and $x^*(t)$ for all $t \in [t_0,t_f]$.

By virtue of this result, the same approach as was used to develop the result of eqn. (5.49) may be applied to the optimal control problem defined by (5.51) and (5.52), *i.e.*

$$(5.53) \qquad \lim_{\delta x(t_1) \to 0} \frac{\delta J_a}{\delta x(t_1)} = \frac{\partial J_a}{\partial x}\bigg|_{t=t_1} = \tilde{\lambda}^*(t_1)$$

for all $t_1 \in [t_0,t_f]$. Since t_1 may be chosen arbitrarily in the interval $[t_0,t_f]$, $\lambda^*(t)$ represents the marginal value of the state variables at any time t within this time interval.

The interpretation of $\lambda^*(t)$ at the end of the time interval t_f can be checked easily. At t_f the marginal value of the state $\lambda^*(t_f)$ is the marginal contribution of the state to the income term $\Phi(x(t_f),t_f)$, *i.e.*

$$(5.54) \qquad \lambda^*(t_f) = \frac{\partial \Phi}{\partial x}(x^*(t_f),t_f),$$

which follows directly from the boundary conditions derived in section 5.3.1. Obviously, if there is no income term, then $\lambda^*(t_f) = 0$.

With this result in mind, the Hamiltonian and the necessary conditions (5.19b) and (5.19c) have the following economic interpretation (Dorfman, 1969; Kamien and Schwartz, 1981). The Hamiltonian

$$\mathcal{H}(x^*,u^*,\lambda^*,t) = -L(x^*,u^*,\lambda^*,t) + \lambda^T f(x^*,u^*,\lambda^*,t),$$

is an expression for the momentary net return of the process, since $-L(x^*,u^*,\lambda^*,t)$ is the operating cost of the control system and $\lambda^T f(x^*,u^*,\lambda^*,t)$ expresses the contribution of the process to the final economic return valued at its marginal value λ.

The stationarity condition (5.19c), *i.e.*

(5.55) $-\dfrac{\partial L}{\partial u}(x^*,u^*,t) + \left[\dfrac{\partial f}{\partial u}(x^*,u^*,t)\right]^{\mathrm{T}}\lambda^* = 0,$

states that at every moment $t \in [t_b,t_f]$, the control input u should be chosen such that its marginal contribution to the immediate costs, $\partial L(x^*,u^*,t)/\partial u$, just equals the marginal contribution to the long-term economic return, which is measured by the marginal value of the state, λ^*, multiplied by the marginal effect of the current control input on the accumulation of the state, $\partial f(x^*,u^*,t)/\partial u$.

The costate equation (5.19b), *i.e.*

(5.56) $-\dot{\lambda}^* = -\dfrac{\partial L}{\partial x}(x^*,u^*,t) + \left[\dfrac{\partial f}{\partial x}(x^*,u^*,t)\right]^{\mathrm{T}}\lambda^*,$

describes the rate at which the marginal value of a unit state is changing at any time. This equation asserts that when the optimal trajectories of the control, the state and the costate are followed, a unit change in the marginal value of a state variable equals the difference between the marginal contribution of that state variable to enhance the long-term revenue, $[\partial f(x^*,u^*,t)/\partial x]^{\mathrm{T}}\lambda^*$, and its marginal contribution to the momentary operating costs, $\partial L(x^*,u^*,t)/\partial x$. Consequently, stationarity of the marginal of the state, *i.e.* $\dot{\lambda}^* = 0$, indicates a balance between the marginal contribution of the state to the running cost and the long-term revenue. Rapid changes of λ^* suggest that the marginal contribution of the state to the running cost and the long-term revenue are largely unbalanced. Because the marginal value of the state affects the actual control policy through eqn. (5.55), large changes of the marginal value indicate that changes in the control, *i.e.* investment, may be required.

5.5. Performance sensitivity of open-loop optimal control systems

Sensitivity considerations are among the fundamental aspects of the synthesis and analysis of optimal control systems. As illustrated in the previous sections, optimal control systems are based on a model description of the dynamic process to be controlled and are designed in such a way that a performance criterion is optimized with respect to the control action applied to the system. In practice, the structure as well as the parameter values of the model rarely coincide exactly with the real process. Since the control system is

designed to be optimal with particular regard to the nominal structure and parameter values of the model used, it can be expected that the control system is sensitive to modelling errors which may reduce the performance of an optimal control system in practice.

In this section a method is presented to evaluate the *performance sensitivity* of open-loop optimal control systems with respect to changes in the model parameters and initial conditions. One way to assess performance sensitivity is to substitute one by one the original values of the model parameters by slightly perturbed values and to compute the new optimal control and corresponding value of the performance criterion. This, however, is a rather time consuming procedure. In this paragraph a first order approach to the sensitivity analysis of open-loop optimal control problems is presented (Courtin and Rootenberg, 1971; Evers, 1979, 1980). Using variational arguments, the methodology requires a single calculation of the open-loop optimal control and corresponding state and costate trajectories which are then used to calculate a first order approximation of the performance sensitivity, thus saving a considerable amount of computation time.

Consider the system

$$(5.57) \qquad \dot{x} = f(x,u,c,t), \qquad x(t_b) = x_b$$

and the performance criterion

$$(5.58) \qquad J(u) = \Phi(x(t_f),t_f) - \int_{t_b}^{t_f} L(x,u,c,t)dt,$$

with the time invariant parameters $c \in \mathbb{R}^q$ and the effect of the exogenous inputs $v(t)$ being represented by the dependence of the functions f and L on time t. The controls and states are constrained by inequality constraints given in eqns. (5.3) and (5.4), respectively.

In the sensitivity analysis, the first variation of the performance criterion J, due to small variations in the initial conditions and the model parameters around their nominal value, is used as a measure for the performance sensitivity of the open-loop optimal control problem. Evers (1980) showed that if the variations of the initial conditions and parameters satisfy $\|\delta x(t_b)\| < \varepsilon_1$ and $\|\delta c\| < \varepsilon_2$, with ε_1 and ε_2 small positive numbers, then

$$\int_{t_b}^{t_f} \|\tilde{u}^*(t) - u^*(t)\| dt = O(\varepsilon), \quad \text{with} \quad \varepsilon = \max(\varepsilon_1, \varepsilon_2).$$ Here, $\tilde{u}^*(t)$ denotes

the optimal control of the perturbed problem. Then, $\tilde{u}^*(t)$ is a so-called *near optimal control* which assures that the performance sensitivity with respect to initial conditions and parameters can be assessed by evaluating the first order variation of the performance criterion due to variations in the initial conditions and parameters.

With u^* and x^* optimal control and state trajectories associated with the nominal initial conditions $x^0(t_b)$ and model parameters c^0, the first order variation in the performance J is given by

(5.59) $\quad \Delta J(x^0(t_b) + \delta x(t_b), u^* + \delta u, c^0 + \delta c) =$

$\quad J(x^0(t_b) + \delta x(t_b), u^* + \delta u, c^0 + \delta c) - J(x^0(t_b), u^*, c^0) =$

$\quad \delta J(x^0(t_b) + \delta x(t_b), u^* + \delta u, c^0 + \delta c) + O(\varepsilon^2),$

in which $\delta J = \delta J(x^0(t_b) + \delta x(t_b), u^* + \delta u, c^0 + \delta c)$ is defined as

(5.60) $\quad \delta J = \Phi(x^*(t_f) + \delta x(t_f), t_f) - \int_{t_b}^{t_f} L(x^* + \delta x, u^* + \delta u, c^0 + \delta c, t) dt$

$\quad - \Phi(x^*(t_f), t_f) + \int_{t_b}^{t_f} L(x^*, u^*, c^0, t) dt =$

$\quad \sum_{i=1}^{n} \frac{\partial \Phi}{\partial x_i}(x^*(t_f)) \delta x(t_f) - \int_{t_b}^{t_f} \Big\{ L(x^* + \delta x, u^* + \delta u, c^0 + \delta c, t)$

$\quad + L(x^* + \delta x, u^*, c^0 + \delta c, t) - \sum_{i=1}^{n} \frac{\partial L}{\partial x_i}(x^*, u^*, c^0, t) \delta x_i$

$\quad - \sum_{k=1}^{q} \frac{\partial L}{\partial c_k}(x^*, u^*, c^0, t) \delta c_k \Big\} dt + O(\varepsilon^2).$

Using the Hamiltonian, $\quad \mathcal{H}^* = -L(x^*,u^*,c^0,t) + \sum\limits_{i=1}^{n} \lambda_i^* f_i(x^*,u^*,c^0,t),\quad$ the necessary conditions for optimality require that

$$(5.61)\qquad \dot\lambda_i^* = -\frac{\partial \mathcal{H}^*}{\partial x_i} = \frac{\partial L}{\partial x_i}(x^*,u^*,c^0,t) - \sum\limits_{j=1}^{n}\lambda_j^*\frac{\partial f_j}{\partial x_i}(x^*,u^*,c^0,t),$$

which can be used to eliminate the term $\sum\limits_{i=1}^{n}\dfrac{\partial L}{\partial x_i}(x^*,u^*,c^0,t)\delta x_i$ from eqn. (5.60).

$$(5.62)\qquad (d/dt)\left[\sum\limits_{i=1}^{n}\lambda_i^*\delta x_i\right] = \sum\limits_{i=1}^{n}\left[(d/dt)(\lambda_i^*\delta x_i)\right] = \sum\limits_{i=1}^{n}\dot\lambda_i^*\delta x_i + \sum\limits_{i=1}^{n}\lambda_i^*\delta\dot x_i =$$

$$\sum\limits_{i=1}^{n}\frac{\partial L}{\partial x_i}(x^*,u^*,c^0,t)\delta x_i - \sum\limits_{i=1}^{n}\sum\limits_{j=1}^{n}\lambda_j^*\frac{\partial f_j}{\partial x_i}(x^*,u^*,c^0,t)\delta x_i + \sum\limits_{i=1}^{n}\lambda_i^*\delta\dot x_i$$

up to second order terms, and so by re-arranging, eqn. (5.62) becomes

$$(5.63)\qquad \sum\limits_{i=1}^{n}\frac{\partial L}{\partial x_i}(x^*,u^*,c^0,t)\delta x_i =$$

$$(d/dt)\left[\sum\limits_{i=1}^{n}\lambda_i^*\delta x_i\right] + \sum\limits_{i=1}^{n}\sum\limits_{j=1}^{n}\lambda_j^*\frac{\partial f_j}{\partial x_i}(x^*,u^*,c^0,t)\delta x_i - \sum\limits_{i=1}^{n}\lambda_i^*\delta\dot x_i,$$

with

$$(5.64)\qquad \delta\dot x_i = \delta f_i = f_i(x^*+\delta x,u^*+\delta u,c^0+\delta c,t) - f_i(x^*,u^*,c^0,t) =$$

$$f_i(x^*+\delta x,u^*+\delta u,c^0+\delta c,t) - f_i(x^*+\delta x,u^*,c^0+\delta c,t)$$

$$+ \sum_{j=1}^{n} \frac{\partial f_1}{\partial x_j}(x^*,u^*,c^0,t)\delta x_j + \sum_{k=1}^{q} \frac{\partial f_1}{\partial c_k}(x^*,u^*,c^0,t)\delta c_k.$$

Substituting (5.63) and (5.64) in (5.60) yields

$$(5.65) \quad \delta J = \sum_{l=1}^{n} \lambda_1^*(t_b)\delta x_1(t_b) + \int_{t_b}^{t_f} \Big\{ \mathcal{H}(x^*+\delta x, u^*+\delta u, c^0+\delta c, t)$$

$$- \mathcal{H}(x^*+\delta x, u^*, c^0+\delta c, t) + \sum_{k=1}^{q} \frac{\partial \mathcal{H}}{\partial c_k}(x^*,u^*,c^0,t)\delta c_k \Big\} dt + O(\varepsilon^2).$$

Eq. (5.65) can be rewritten as

$$(5.66) \quad \delta J = \sum_{l=1}^{n} \lambda_1^*(t_b)\delta x_1(t_b) + \int_{t_b}^{t_f} \Big\{ \mathcal{H}(x^*,u^*+\delta u, c^0,t) - \mathcal{H}(x^*,u^*,c^0,t)$$

$$+ \sum_{k=1}^{q} \frac{\partial \mathcal{H}}{\partial c_k}(x^*,u^*,c^0,t)\delta c_k \Big\} dt + \int_{t_b}^{t_f} \sum_{l=1}^{n} \Big\{ \frac{\partial \mathcal{H}}{\partial x_1}(x^*,u^*+\delta u, c^0+\delta c, t)$$

$$- \frac{\partial \mathcal{H}}{\partial x_1}(x^*,u^*,c^0+\delta c,t) \Big\} \delta x_1 dt + \int_{t_b}^{t_f} \sum_{k=1}^{q} \Big\{ \frac{\partial \mathcal{H}}{\partial c_k}(x^*,u^*+\delta u, c^0,t)$$

$$- \frac{\partial \mathcal{H}}{\partial c_k}(x^*,u^*,c^0,t) \Big\} \delta c_k dt + O(\varepsilon^2).$$

Evers (1980) proved that the last two terms in eqn. (5.66) are of order ε^2. So, the first order sensitivity measure for small changes in the initial conditions, the control and the model parameters is given by

$$(5.67) \quad \delta J = \sum_{i=1}^{n} \lambda_i^*(t_b)\delta x_i(t_b) + \int_{t_b}^{t_f}\left\{\mathcal{H}(x^*,u^*+\delta u,c,t) - \mathcal{H}(x^*,u^*,c^0,t)\right.$$

$$\left. + \sum_{k=1}^{q} \frac{\partial\mathcal{H}}{\partial c_k}(x^*,u^*,c^0,t)\delta c_k\right\}dt.$$

Then, evaluated at the nominal values of the individual initial conditions and model parameters and the optimal value of the individual control inputs, the performance sensitivity is defined as

$$(5.68) \quad \lim_{\delta x_i(t_b) \to 0} \frac{\delta J}{\delta x_i(t_b)} = \frac{\partial J}{\partial x_i(t_b)}\Big|_{t=t_b} = \lambda_i^*(t_b),$$

$$(5.69) \quad \lim_{\delta c_k \to 0} \frac{\delta J}{\delta c_k} = \frac{\partial J}{\partial c_k} = \int_{t_b}^{t_f}\frac{\partial\mathcal{H}}{\partial c_k}(x^*,u^*,c^0,t)dt,$$

and

$$(5.70) \quad \lim_{\delta u \to 0} \frac{\delta J}{\delta u} = \frac{\partial J}{\partial u} = \int_{t_b}^{t_f}\left\{\mathcal{H}(x^*,u^*+\delta u,c^0,t) - \mathcal{H}(x^*,u^*,c^0,t)\right\}dt.$$

In order to compare the impact of perturbations in the different model parameters and the initial conditions of the different state variables on the system performance criterion, it is more convenient to express the sensitivity as the fractional change in the performance criterion as a result of a fractional change in the parameter value, *i.e.* a relative sensitivity criterion. For every state variable and model parameter the relative sensitivity measures are defined as

$$(5.71) \quad \frac{\partial J^*}{\partial x(t_b)}\frac{x_i^0(t_b)}{J^*}, \ i = 1,\dots,n \ \text{and} \ \frac{\partial J^*}{\partial c}\frac{c_j^0}{J^*}, \ j = 1,\dots,q \ ,$$

respectively.

5.6. Optimal control of singularly perturbed systems

The solution of economic optimal greenhouse climate control problems over a whole growing period accounting for both dynamics in the greenhouse climate as well as crop growth is numerically very involved. This is partly due to the large scale of the problem, *i.e.* the number of state variables used to describe the process. The solution of the optimal control problem requires the solution of two sets of non-linear differential equations (see section 5.2): one set describing the evolution of the state and one set describing the evolution of the costate in time. More important however is the fact that, in optimal greenhouse climate control, interactions of fast and slow phenomena occur. As already pointed out in chapter 3, crop growth is rather slow compared with the fast dynamic response of the greenhouse climate. The solution of a two-point boundary value problem containing both fast and slow dynamic phenomena, a so-called stiff problem, usually requires a considerable amount of computation time. Moreover, the resulting control system may exhibit excessive sensitivity with respect to the fast system dynamics which may render the control system unuseable for actual implementation in practice (Kokotovic *et al.*, 1986).

   If the system contains state variables with large differences in response times, simplifications are usually made by neglecting some time constants whose presence causes the model order to be higher than acceptable for practical design of optimal controlled systems (Kokotovic and Sanutti, 1968). The underlying assumption of this simplification is that during the fast transients the slow variables remain constant and that by the time their changes become noticeable, the fast transients have already reached their quasi-steady-states. Based on this quasi-steady-state assumption and engineering experience, the state variables are classified as 'slow' states x and 'fast' states z and the full scale model is described by

(5.72a) $\quad \dot{x} = f(x,z,u,v,t), \quad x(t_b) = x_b$,

(5.72b) $\quad \dot{z} = G(x,z,u,v,t), \quad z(t_b) = z_b$,

where $x = x(t) \in \mathbb{R}^{nx}$, $z = z(t) \in \mathbb{R}^{nz}$, $u = u(t) \in \mathbb{R}^m$ and $v = v(t) \in \mathbb{R}^p$ and t denotes time. Note that the n-dimensional state space used in the previous sections is divided into two sub-spaces, the nx-dimensional space containing the slow state variables x and the nz-dimensional space containing the fast state variables z. Then the only states used in short term studies are z, disregarding (5.72a) and considering the states x as constant parameters. In long term studies the only states used are x and the differential equations for

z are reduced to algebraic equations by formally setting $\dot{z} = 0$. The quasi-steady-state model is thus

(5.73a) $\dot{\bar{x}} = f(\bar{x},\bar{z},\bar{u},v,t)$, $\bar{x}(t_b) = \bar{x}_b$,

(5.73b) $0 = G(\bar{x},\bar{z},\bar{u},v,t)$.

     This method has been used in many control engineering applications (Kokotovic *et al.*, 1980) including greenhouse climate control. For instance the control studies of Schmidt *et al.* (1987), Seginer (1989) and Van Henten and Bontsema (1991) emphasized economically optimal control of the slow crop growth dynamics, and the greenhouse climate dynamics were commonly neglected.
     This quasi-steady-state approach, however, suffers from some drawbacks. First of all, the requirement that $\bar{z}$ is constant, as implied by $d\bar{z}/dt = 0$, is violated by (5.73b) which defines $\bar{z}$ as a time-varying quantity. Secondly, the initial conditions for z have to be dropped in (5.73b), since there is no freedom to satisfy them. Thirdly, if the inputs u and v are slow compared with the dynamic response of the 'fast' state variables, as was assumed by *e.g.* Schmidt *et al.* (1987), Seginer (1989) and Van Henten and Bontsema (1991), who considered only slow diurnal variations in the exogenous inputs, eqn. (5.73b) will give a sufficiently accurate description since the slow inputs will allow the fast state variables z to settle in the quasi-steady-state described by eqn. (5.73b). However, serious errors may occur when the inputs u and v exhibit fast fluctuations compared with the dynamic response of the state variables z. In greenhouse climate control this situation exists. For instance the solar radiation, which strongly influences the indoor climate, exhibits rapid fluctuations throughout the day. Then eqn. (5.73b) will fail to give a good approximation of z because it implies an instantaneous convergence of z to a quasi-steady-state $\bar{z}$, whereas in reality, due to the process dynamics, the system requires time to settle in the quasi-steady-state. Finally, if the quasi-steady-state approach fails to provide a good approximation to the actual solution $x(t)$ and $z(t)$, there is no provision for improving the approximation (Kokotovic *et al.*, 1980).
     By modifying the quasi-steady-state assumption into the multi-time-scale property of *singular perturbed systems*, a separation of slow and fast modes can be obtained without the drawbacks of the quasi-steady-state approach. Besides alleviating the stiffness problem, the singular perturbation approach offers the opportunity to improve the lower order models to any desired level of accuracy.
     In the singular perturbation approach, differences in the dynamics between the slow and the fast sub-processes are expressed by a time scaling parameter ε, such that the full model is described by

(5.74a) $\dot{x} = f(x,z,u,v,t)$, $x(t_b) = x_b$,

(5.74b) $\varepsilon\dot{z} = g(x,z,u,v,t)$, $z(t_b) = z_b$.

In linear systems ε can be related to small physical parameters, such as masses, and time constants. However, in most cases, including non-linear systems, the identification of the time scaling parameter is not straightforward and will usually involve considerable effort. Shinar (1983) suggested that the parameter ε can be obtained by a rescaling transformation such that on average $f(x,z,u,v,t)/g(x,z,u,v,t) \cong 1$ and therefore using eqn. (5.72b) gives $\varepsilon \cong g(x,z,u,v,t)/G(x,z,u,v,t)$. Alternatively, circumventing the complexity of the rescaling transformation, the time derivative of the fast variable z can be multiplied by an artificially created perturbation parameter, which nominally has the value 1.

Once ε has been suitably defined, the full system (5.74) is approximated by two time-scale asymptotic expansions of x and z:

$$(5.75) \qquad x(t,\varepsilon) \cong \sum_{j=0}^{\infty} [\bar{x}_j(t)+\hat{x}_j((t-t_b)/\varepsilon)]\varepsilon^j,$$

$$z(t,\varepsilon) \cong \sum_{j=0}^{\infty} [\bar{z}_j(t)+\hat{z}_j((t-t_b)/\varepsilon)]\varepsilon^j.$$

The slow response, denoted by $\bar{x}$ and $\bar{z}$, is commonly referred to as the outer solution of the system (5.74) and is described on the t time-scale. The fast response, denoted by $\hat{x}$ and $\hat{z}$, is called the boundary layer solution or correction and is described on the *stretched time-scale* $\tau = (t-t_b)/\varepsilon$.

As a matter of fact t and τ are expressions for the same time. However, we may look at t as a macroscopic time-scale adapted to the slow system dynamics and τ as a microscopic time-scale adapted to the fast system dynamics. For example, crop growth does not show large dynamic changes within several minutes or even hours, whereas the greenhouse climate dynamics may exhibit changes on a time-scale of minutes or even seconds. Expressing crop growth on the time-scale of days and the greenhouse climate on the time-scale of seconds would suggest $\varepsilon = 1/86400$.

Explicit relations for the slow system response, $\bar{x}_j(t)$ and $\bar{z}_j(t)$, and fast system response, $\hat{x}_j((t-t_b)/\varepsilon)$ and $\hat{z}_j((t-t_b)/\varepsilon)$, are required to establish the desired approximation. The zero-th order responses are derived as follows.

Zero-th order slow response

The zero-*th* order 'slow' responses ($\bar{x}_0(t)$ and $\bar{z}_0(t)$) are obtained through a parameter *perturbation*, called *singular*, by setting $\varepsilon = 0$. The dimension of the state space of (5.74a) and (5.74b) reduces from $nx+nz$ to nx because the differential equation (5.74b) degenerates into the algebraic equation

(5.76) $0 = g(\bar{x}_0, \bar{z}_0, u, v, t)$.

It is assumed for the moment that (5.76) has one distinct real solution $\bar{z}_0(t)$ which is expressed in terms of $\bar{x}_0$, u, v and t as

(5.77) $\bar{z}_0(t) = h(\bar{x}_0, u, v, t)$.

This ensures that a well-defined nx-dimensional reduced model will correspond to the solution (5.77). In chapter 6, it will be shown that eqn. (5.77) may have more than one solution. In the particular example considered there, analytic manipulation of eqn. (5.77) yields two solutions one of which is clearly not valid within the context of the problem considered and is therefore easily eliminated. However, if eqn. (5.77) is solved numerically, the uniqueness or validity of the solution is usually not guaranteed.
        Substituting of eqn. (5.77) in (5.74a) yields the reduced model

(5.78) $\dfrac{d\bar{x}_0}{dt} = f(\bar{x}_0, h(\bar{x}_0, u, v, t), u, v, t), \quad \bar{x}_0(t_b) = x_b$.

This model strongly resembles the quasi-steady-state model (5.73). However, $\varepsilon = 0$ does not imply $\dot{z} = 0$. As a matter of fact, $\dot{z}$ can take any value. This means that if we observe the system at the time-scale of the slow state variables x, dynamic transients in the fast state variables z are not noticeable, but z reaches a quasi-steady-state infinitely fast.

Zero-th order fast response

The zero-th order 'fast' transients can be seen as the difference between the zero-th order slow response and the response of the full system (5.74), *i.e.*

(5.79) $\hat{x}_0(t/\varepsilon) = x(t) - \bar{x}_0(t), \quad \hat{z}_0(t/\varepsilon) = z(t) - \bar{z}_0(t)$.

The fast transients are described on the 'stretched' time-scale $\tau = (t-t_b)/\varepsilon$. Taking the derivatives of (5.79) with respect to t and τ yields

(5.80) $\qquad \dfrac{d\hat{x}_0(\tau)}{d\tau} \dfrac{d\tau}{dt} = \dfrac{dx(t)}{dt} - \dfrac{d\bar{x}_0(t)}{dt}, \qquad \dfrac{d\hat{z}_0(\tau)}{d\tau} \dfrac{d\tau}{dt} = \dfrac{dz(t)}{dt} - \dfrac{d\bar{z}_0(t)}{dt}.$

Note that $d\tau/dt = 1/\varepsilon$. Rewriting eqn. (5.80) using (5.74), and (5.76) to (5.78), yields

(5.81a) $\qquad \dfrac{d\hat{x}_0(\tau)}{d\tau} = \varepsilon[f(\bar{x}_0+\hat{x}_0,\bar{z}_0+\hat{z}_0,u,v,t_b) - f(\bar{x}_0,\bar{z}_0,u,v,t_b)].$

As $\varepsilon \rightarrow 0$, it is found that $d\hat{x}_0(\tau)/d\tau = 0$. Since $\hat{x}_0(\tau) = 0$, at $\tau = 0$, $\hat{x}_0(\tau)$ will be zero for all τ. The fast response of the fast state variable z is described by

$$\frac{d\hat{z}_0(\tau)}{d\tau} = g(\bar{x}_0+\hat{x}_0,\bar{z}_0+\hat{z}_0,u,v,t) - \varepsilon\frac{d}{dt}h(\bar{x}_0,\bar{u},\bar{v},t),$$

with $\hat{z}_0(0) = z(t_b)-\bar{z}_0(t_b)$. Substitution of $t = t_b+\varepsilon\tau$ and setting $\varepsilon = 0$ yields

(5.81b) $\qquad \dfrac{d\hat{z}_0(\tau)}{d\tau} = g(\bar{x}_0(t_b),\bar{z}_0(t_b)+\hat{z}_0(\tau),u(t_b),v(t_b),t_b),$

with $\hat{z}_0(0) = z(t_b)-\bar{z}_n(t_b)$. The power series (5.75) are asymptotically convergent if the equilibrium $\hat{z}(\tau) = 0$ is asymptotically stable (Hoppensteadt, 1971). Essentially, this holds if

(5.82) $\qquad \text{Re } \lambda \left(\dfrac{\partial g}{\partial z}\right) < 0,$

evaluated along $\bar{x}_0$ and $\bar{z}_0$, where Re λ denotes the real part of the eigenvalues of the system matrix $\partial g/\partial z$. This assures that,

(5.83) $\qquad \lim_{\tau \rightarrow \infty} \hat{z}(\tau) = 0,$

which means that as $\tau \to \infty$, $z(t) \to \bar{z}_0(t)$. In optimal greenhouse climate control the state variables z are related to the greenhouse climate. Because the description of the greenhouse climate dynamics is non-linear, $\partial g / \partial z$ will be time varying and the stability requirement is not easily verified. However, intuitively, instabilities in the greenhouse climate process are not expected.

   The foregoing analysis, although being limited to the zero-th order terms, shows some important facts. First of all, it illustrates that in the power series approximation of $x(t,\varepsilon)$ and $z(t,\varepsilon)$, the fast transients are completely decoupled from the slow transients. The slow transients $\bar{x}_j(t)$ and $\bar{z}_j(t)$ are calculated first and then the fast transients $\hat{x}_j(\tau)$ and $\hat{z}_j(\tau)$ are superimposed on the slow transients. Secondly, to first order approximation, the slow sub-system x is not affected by fast transients in z, since $\hat{x}(\tau) = 0$ for all τ. Thirdly, if the zero-th order approximations fail to give an accurate description of the full system, higher order corrections can be applied to attain the desired level of accuracy. Generalizations of these power series up to infinite order have been presented for instance by Freedman and Granoff (1976). Finally, if the system is driven by constant or slowly varying exogenous inputs v, the fast transient $\hat{z}_0(\tau)$, will converge rapidly to $\bar{z}_0$ due to the stability requirement (5.82) and consequently these transients are limited to a *boundary layer* around the initial time t_b. However, if the system is driven by rapidly fluctuating exogenous inputs, $\bar{z}_0$ will not be an accurate approximation of the fast sub-system beyond the initial time boundary layer, and fast transients have to be accounted for throughout the whole time interval t_b to t_f. For that purpose eqn. (5.81b) is not suitable. We may see this as follows. If the system is affected by rapidly varying inputs $u(t)$ and/or $v(t)$ and $\hat{z}_0(0) = 0$, then $\hat{z}_0(\tau) = 0$ for all τ, since $g(\bar{x}_0,\bar{z}_0,u,v,t) = 0$ as a result of the zero-th order slow solution. This suggests that $\bar{z}_0$ is an accurate approximation of z, which, however, is clearly not true, since the quasi-steady-state description $\bar{z}_0$ will follow the rapid fluctuations in $u(t)$ and $v(t)$ that would have been filtered out by z and consequently large differences between $\bar{z}_0$ and z will occur. It is concluded that beyond the initial boundary layer, the previously outlined decomposition is not succesfull in case the system is driven by high frequency inputs and a modification of this decomposition is required.

   This modification proceeds as follows. The fast phenomena are

induced by the term $\varepsilon\dfrac{d}{dt}h(\bar{x}_0,\bar{u},\bar{v},t) = \dfrac{d\bar{z}_0}{dt}\dfrac{dt}{d\tau}$ which expresses the changes of the zero-th order slow solution of z on the τ time-scale. In line with this observation, rewriting the equation for the zero-th order fast response of z yields

$$\frac{d\bar{z}_0(t)}{dt}\frac{dt}{d\tau} + \frac{d\hat{z}_0(\tau)}{d\tau} = g(\bar{x}_0+\hat{x}_0,\bar{z}_0+\hat{z}_0,u,v,t),$$

which by virtue of eqn. (5.79) and the fact that $\hat{x}_0 = 0$ yields the zero-th order approximation of z, z_0 ,described by

$$(5.84) \qquad \frac{dz_0(\tau)}{d\tau} = g(\bar{x}_0,z_0,u,v,\varepsilon\tau), \qquad z_0(0) = z_b.$$

with $\tau = t/\varepsilon$. Eqn. (5.84) states that up to first order, during simulation of the fast system dynamics, the zero-th order slow solution $\bar{x}_0$ is used as a slow (reference) input and the dynamics in x are not explicitly taken into accounted. Eqn. (5.84) has the favourable characteristic that it directly describes the approximate dynamics of the fast state variable z instead of the dynamics of the difference $\hat{z}_0$ with the zero-th order outer solution. If $\bar{x}_0$ and z_0 fail to provide an accurate description of x and z, higher order corrections are required.

The advantage of the previously shown two time-scale decomposition is the fact that, since the slow state does not respond to fast changes in the inputs, averaged values of the inputs and relatively large integration time steps can be used during numerical solution of the slow differential equations without a significant loss of accuracy. Using the resulting slow state trajectory as a reference trajectory, a second simulation with an integration time step adapted to the fast responses will yield a description of the fast system's states. More important however is the fact, that the previously shown decomposition allows for a decomposition of the optimal control problem into a sub-problem which deals with the slow system dynamics and a sub-problem which deals with the fast system dynamics.

5.6.1. Optimal control of singularly perturbed systems: slow exogenous inputs

In this section the effect of the two time-scale properties of singularly perturbed systems on the solution of the optimal control problem will be analysed. For the moment it is assumed that the system is affected by constant or slowly varying exogenous inputs v. In section 5.6.2, optimal control of singularly perturbed systems affected by rapidly fluctuating inputs will be dealt with.

The following singularly perturbed system is considered

$$(5.85a) \quad \dot{x} = f(x,z,u,v,t), \quad x(t_b) = x_b,$$
$$(5.85b) \quad \varepsilon\dot{z} = g(x,z,u,v,t), \quad z(t_b) = z_b.$$

With this system the performance criterion

$$(5.86) \quad J(u,\varepsilon) = \Phi(x(t_f),t_f) - \int_{t_b}^{t_f} L(x,z,u,v,t)dt$$

is related and the optimal control problem is defined as to find

$$(5.87) \quad u^* = \arg\max_{u} J(u,\varepsilon).$$

With the Hamiltonian defined by

$$(5.88) \quad \mathcal{H} = -L(x,z,u,v,t) + \lambda^T f(x,z,u,v,t) + \eta^T g(x,z,u,v,t),$$

derivation of the necessary conditions of optimality in line with what has been shown in section 5.3, gives rise to the following system of equations

$$(5.89a) \quad \dot{x}^* = \frac{\partial\mathcal{H}}{\partial\lambda}(x^*,z^*,\lambda^*,\eta^*,u^*,v,t), \quad x^*(t_b) = x_b,$$

$$(5.89b) \quad \varepsilon\dot{z}^* = \frac{\partial\mathcal{H}}{\partial\eta}(x^*,z^*,\lambda^*,\eta^*,u^*,v,t), \quad z^*(t_b) = z_b,$$

$$(5.90a) \quad -\dot{\lambda}^* = \frac{\partial\mathcal{H}}{\partial x}(x^*,z^*,\lambda^*,\eta^*,u^*,v,t), \quad \lambda^*(t_f) = \frac{\partial\Phi}{\partial x}(x^*(t_f),t_f),$$

(5.90b) $-\varepsilon\dot{\eta}^* = \dfrac{\partial \mathcal{H}}{\partial z}(x^*,z^*,\lambda^*,\eta^*,u^*,v,t), \quad \eta^*(t_f) = 0,$

and according to the maximum principle of Pontryagin

(5.91) $\mathcal{H}(x^*,\lambda^*,z^*,\eta^*,u,v,t) \le \mathcal{H}(x^*,\lambda^*,z^*,\eta^*,u^*,v,t).$

According to Freedman and Granoff (1976) and Freedman and Kaplan (1976) the states, costates and controls can be approximated by the two time-scale asymptotic expansions

(5.92a) $x(t,\varepsilon) \cong \displaystyle\sum_{j=0}^{\infty} [\bar{x}_j(t)+\hat{x}_j^L((t-t_b)/\varepsilon)+\hat{x}_j^R((t_f-t)/\varepsilon)]\varepsilon^j,$

(5.92b) $z(t,\varepsilon) \cong \displaystyle\sum_{j=0}^{\infty} [\bar{z}_j(t)+\hat{z}_j^L((t-t_b)/\varepsilon)+\hat{z}_j^R((t_f-t)/\varepsilon)]\varepsilon^j,$

(5.93a) $\lambda(t,\varepsilon) \cong \displaystyle\sum_{j=0}^{\infty} [\bar{\lambda}_j(t)+\hat{\lambda}_j^L((t-t_b)/\varepsilon)+\hat{\lambda}_j^R((t_f-t)/\varepsilon)]\varepsilon^j,$

(5.93b) $\eta(t,\varepsilon) \cong \displaystyle\sum_{j=0}^{\infty} [\bar{\eta}_j(t)+\hat{\eta}_j^L((t-t_b)/\varepsilon)+\hat{\eta}_j^R((t_f-t)/\varepsilon)]\varepsilon^j,$

(5.94) $u(t,\varepsilon) \cong \displaystyle\sum_{j=0}^{\infty} [\bar{u}_j(t)+\hat{u}_j^L((t-t_b)/\varepsilon)+\hat{u}_j^R((t_f-t)/\varepsilon)]\varepsilon^j.$

Also the performance criterion is approximated by a power series expansion, which has the form (Belokopytov and Dmitriev, 1986; Bensoussan, 1986)

(5.95) $J(u,\varepsilon) \cong \displaystyle\sum_{j=0}^{\infty} [\bar{J}_j(\bar{u}_j)+\hat{J}_j^L(\hat{u}_j^L)+\hat{J}_j^R(\hat{u}_j^R)]\varepsilon^j.$

Again $^-$ indicates the slow transients, whereas $\hat{}$ denotes the fast transients and superscript L and R refer to the boundary layer transients near the initial time t_b and the final time t_f,

respectively.

Since the inputs are assumed to be constant or slowly varying, the fast states z will rapidly converge to their quasi-steady-state described by the outer solution. Consequently, the fast transients in z and η will be concentrated around the initial time t_b and final time t_f to account for discrepancies between the outer solution and the initial and final boundary conditions on z and η.

Up to first order, $i.e.$ for $j = 0$, the state, costate and control trajectories are approximated by

$$x(t) \cong \bar{x}_0(t) + \hat{x}_0^L((t-t_b)/\varepsilon) + \hat{x}_0^R((t_f-t)/\varepsilon),$$

$$z(t) \cong \bar{z}_0(t) + \hat{z}_0^L((t-t_b)/\varepsilon) + \hat{z}_0^R((t_f-t)/\varepsilon),$$

$$\lambda(t) \cong \bar{\lambda}_0(t) + \hat{\lambda}_0^L((t-t_b)/\varepsilon) + \hat{\lambda}_0^R((t_f-t)/\varepsilon),$$

$$\eta(t) \cong \bar{\eta}_0(t) + \hat{\eta}_0^L((t-t_b)/\varepsilon) + \hat{\eta}_0^R((t_f-t)/\varepsilon) \text{ and}$$

$$u(t) \cong \bar{u}_0(t) + \hat{u}_0^L((t-t_b)/\varepsilon) + \hat{u}_0^R((t_f-t)/\varepsilon).$$

The control problems related to the zero-th order slow response and the zero-th order initial and final time fast response of the system (5.85) are derived as follows.

Zero-th order slow response

The zero-th order slow response denoted by $\bar{x}_0(t)$ and $\bar{z}_0(t)$ is obtained by setting $\varepsilon = 0$ in eqn. (5.85b) and solving the reduced order optimal control problem

(5.96a) $\dfrac{d\bar{x}_0(t)}{dt} = f(\bar{x}_0, \bar{z}_0, \bar{u}_0, v, t), \quad \bar{x}_0(t_b) = x_b,$

(5.96b) $0 = g(\bar{x}_0, \bar{z}_0, \bar{u}_0, v, t),$

(5.97) $\bar{J}_0(\bar{u}_0) = \Phi(\bar{x}_0(t_f), t_f) - \displaystyle\int_{t_b}^{t_f} L(\bar{x}_0, \bar{z}_0, \bar{u}_0, v, t)dt,$

(5.98) $\bar{u}_0^*(t) = \arg \max_{\bar{u}_0} \bar{J}_0(\bar{u}_0).$

For the zero-th order slow response, necessary conditions of optimality can be obtained in two ways. First of all, optimality

conditions like eqns. (5.89) to (5.91) can be derived which are then simplified by setting $\varepsilon = 0$. This will result in the so-called *reduced optimality conditions*. Secondly, by neglecting ε in the system (5.85b), optimality conditions for the *reduced system* (5.96) can be derived. Kokotovic *et al.* (1986) showed that for the singularly perturbed optimal control system in the standard form (cf. eqns. (5.85a) and (5.85b)), the *reduced optimality conditions* and the optimality conditions for the *reduced system* are equivalent, and concluded that the *reduced problem* (5.96) to (5.98) is formally correct.

Boundary layer corrections at the initial time t_b and final time t_f are needed to account for the simplifications made by neglecting the dynamics of z. In the initial boundary layer the transformation $\tau = (t-t_b)/\varepsilon$ is used, which gives rise to the following control problem.

Zero-th order fast response around initial time

Through the time transformation $\tau = (t-t_b)/\varepsilon$, the fast response around t_b is accounted for in the control problem described by Belokopytov and Dmitriev (1986) and Bensoussan (1988) as

(5.99) $$\frac{d\hat{z}_0^L(\tau)}{d\tau} = g(\bar{x}_0^*(t_b),\bar{z}_0^*(t_b)+\hat{z}_0^L(\tau),\bar{u}_0^*(t_b)+\hat{u}_0^L(\tau),v(t_b),t_b),$$
$$\hat{z}_0(0) = z(t_b)-\bar{z}_0(t_b),$$

(5.100) $$\hat{J}_0^L(\hat{u}_0^L) =$$
$$\int_0^\infty \Bigg\{ \mathcal{H}(\bar{x}_0^*(t_b),\bar{\lambda}_0^*(t_b),\bar{z}_0^*(t_b)+\hat{z}_0^L(\tau),\bar{\eta}_0^*(t_b),\bar{u}_0^*(t_b)+\hat{u}_0^L(\tau),v(t_b),t_b)$$
$$- \mathcal{H}(\bar{x}_0^*(t_b),\bar{\lambda}_0^*(t_b),\bar{z}_0^*(t_b),\bar{\eta}_0^*(t_b),\bar{u}_0^*(t_b),v(t_b),t_b)\Bigg\}d\tau,$$

(5.101) $$\hat{u}_0^{L^*}(\tau) = \arg \max_{\hat{u}_0^L} \hat{J}_0^L(\hat{u}_0^L).$$

In the zero-th order initial time fast response, the transients in the slow states and costates, $\hat{x}_0(\tau)$ and $\hat{\lambda}_0(\tau)$, are neglected.

Zero-th order fast response around final time

Through the time-scale transformation $\sigma = (t_f - t)/\varepsilon$, the fast response around t_f is accounted for in the control problem described by Belokopytov and Dmitriev (1986) and Bensoussan (1988) as

$$(5.102) \qquad -\frac{d\hat{z}_0^R(\sigma)}{d\tau} = g(\bar{x}_0^*(t_f),\bar{z}_0^*(t_f)+\hat{z}_0^R(\sigma),\bar{u}_0^*(t_f)+\hat{u}_0^R(\sigma),v(t_f),t_f),$$

$$(5.103) \qquad \hat{J}_0^R(\hat{u}_0^R) =$$

$$\int_0^\infty \left\{ \mathcal{H}(\bar{x}_0^*(t_f),\bar{\lambda}_0^*(t_f),\bar{z}_0^*(t_f)+\hat{z}_0^R(\sigma),\bar{\eta}_0^*(t_f),\bar{u}_0^*(t_f)+\hat{u}_0^R(\sigma),v(t_f),t_f) \right.$$

$$\left. - \mathcal{H}(\bar{x}_0^*(t_f),\bar{\lambda}_0^*(t_f),\bar{z}_0^*(t_f),\bar{\eta}_0^*(t_f),\bar{u}_0^*(t_f),v(t_f),t_f) \right\} d\tau,$$

$$(5.104) \qquad \hat{u}_0^{R*}(\tau) = \arg \max_{\hat{u}_0^R} \hat{J}_0^R(\hat{u}_0^R).$$

In the zero-th order final time fast response, the transients in the slow states and costates, $\hat{x}_0(\sigma)$ and $\hat{\lambda}_0(\sigma)$, are neglected.

As was stated earlier, if the zero-th order approximations do not suffice to give the desired accuracy of control, higher order corrections can be applied.

For unconstrained optimal control problems, Freedman and Kaplan (1976) and Freedman and Granoff (1976) investigated the convergence properties of the power series (5.92) to (5.94), whereas convergence results for the power series of J were established by Belokopytov and Dmitriev (1986) and Bensoussan (1988). These results do not directly apply to control problems in which the state and control variables are bounded. Then the convergence of the power series (5.92) to (5.95) is not guaranteed, since the boundary layers may have a finite instead of an infinite duration. Although from a formal point of view the convergence properties of the power series may be seriously affected, it is assumed for the moment that this does not cause serious problems when greenhouse climate control is considered.

With respect to application of the foregoing results in optimal greenhouse climate control and the results reported so far in this field, the following observations can be made. If the dimension of the control vector u equals the dimension of the state vector z and

there exists a *unique* solution of the reduced order eqn. (5.96b) then $\bar{u}_0$ can be expressed as a function of $\bar{x}_0$, $\bar{z}_0$, v and t:

(5.105) $\bar{u}_0(t) = h'(\bar{x}_0, \bar{z}_0, v, t),$

and the zero-th order slow control problem can be rewritten as

(5.106) $\dfrac{d\bar{x}_0(t)}{dt} = f(\bar{x}_0, \bar{z}_0, h'(\bar{x}_0, \bar{z}_0, v, t), v, t),\quad \bar{x}_0(t_b) = x_b,$

(5.107) $\bar{J}_0(\bar{z}_0) = \Phi(\bar{x}_0(t_f), t_f) - \displaystyle\int_{t_b}^{t_f} L(\bar{x}_0, \bar{z}_0, h'(\bar{x}_0, \bar{z}_0, v, t), v, t)dt,$

(5.108) $\bar{z}_0^*(t) = \arg \max_{\bar{z}_0} \bar{J}_0(\bar{z}_0).$

Since in the greenhouse climate control problem z refers to greenhouse climate variables like air temperature and carbon dioxide concentration, the preceding transformation changes the problem of finding optimal trajectories for the control inputs into a problem of finding optimal trajectories for the greenhouse climate or so-called *optimal set-point trajectories for the greenhouse climate.* It was this optimal control problem, formulated in eqns. (5.105) to (5.108), which was explicitly or implicitly used by for instance Seginer *et al.* (1991), Chalabi (1991) and Van Henten and Bontsema (1991). Because their investigations emphasized the derivation of economically optimal greenhouse climate trajectories, information about the control trajectories was felt to be redundant though the relation between greenhouse climate and control trajectories was still uniquely defined by eqn. (5.105). There is however a disadvantage related to this approach. Since the dynamic models of greenhouse climate may include more state variables than control variables, an unambiguous relation between control variables and greenhouse climate related state variables conforming to eqn. (5.105) may not exist. An unique relation between control and state variables may not exist either, when the number of control variables exceeds the number of state variables. This was encountered by Seginer *et al.* (1991) who considered one greenhouse climate variable, *i.e.* air temperature, and two control variables, namely energy supply by the heating system and ventilation rate through the windows. Since different settings of the heat supply and ventilation result in the

same air temperature, the plausible assumption was made that ventilation and heating are mutually exclusive, and thus an unique relation between these control variables and the air temperature was obtained. If, however, the problem has been formulated as in eqns. (5.96) to (5.98), such an artificial solution would not be needed since for reasons of energy conservation, heating would not be administered to the greenhouse together with ventilation.

Seginer et $al.$ (1991), Chalabi (1992) and Van Henten and Bontsema (1991) considered only slow, $i.e.$ diurnal, trends in the exogenous inputs such as solar radiation and outside air temperature. The boundary layer corrections around t_b and t_f, formally needed to account for discrepancies between the outer solution and the initial and final boundary conditions on z and η, were neglected by the previous authors. This is acceptable since (i) they have a short duration compared to the overall duration of the growing/optimization period; the greenhouse climate is settled within hours, which is relatively short compared to a cultivation period of at least several months, (ii) they do not have a significant effect on crop growth and development, (iii) the boundary layer transients do not include large investments in energy so the outer solution without boundary layer corrections will give a sufficiently accurate approximation of J, and (iv) in horticultural practice the greenhouse climate is not accurately controlled during planting and harvesting which coincides with these boundary layer phenomena.

In horticultural practice, however, the exogenous inputs v exhibit fast variations, the outer solution may not be a sufficiently accurate representation of the real process, because large differences between $\bar{z}_0$ and z may occur. Then, the resulting control trajectories can not be used for the control of the greenhouse crop production process and the greenhouse climate dynamics need to be explicitly taken into account. Still, assuming slowly varying inputs v, the previously presented computational scheme is a powerful tool to investigate economic optimal control of the slow crop growth process, the results of which may provide new insight into, and rules for the operation of, the crop production process.

5.6.2. Optimal control of singularly perturbed systems: fast exogenous inputs

In this section optimal control of singularly perturbed systems influenced by rapidly fluctuating exogenous inputs is studied. Unlike the case for optimal controlled systems with slow driving inputs, $\bar{z}_0$ and $\bar{\eta}_0$ are not valid approximations of z and η as $\varepsilon \rightarrow 0$ if the

system is excited with driving inputs having high frequency characteristics. Boundary layer corrections need to be applied, not only to deal with errors in the initial and final conditions, but also to account for the effects of the fast driving inputs on the dynamics of the fast sub-system throughout the whole optimization interval.

Besides examples in the field of stochastic control (*e.g.* Kokotovic *et al.* (1986)), optimal control of singularly perturbed systems with inputs exhibiting high frequency characteristics is rarely encountered in the literature. No references were found on the control of singularly perturbed non-linear systems excited by inputs having deterministic high frequency properties and non-quadratic performance criteria. In this section it will be shown that, in line with standard singular perturbation theory, the control problem with deterministic fast varying exogenous inputs can be decomposed into sub-problems related to the slow and the fast dynamics respectively.

The following system is considered

(5.109a) $\quad \dot{x} = f(x,z,u,v,t), \quad x(t_b) = x_b,$

(5.109b) $\quad \varepsilon\dot{z} = g(x,z,u,v,t), \quad z(t_b) = z_b,$

with the state and control variables required to lie within a bounded sub-space of the state and control space. With this system the performance criterion

$$(5.110) \quad J(u,\varepsilon) = \Phi(x(t_f),t_f) - \int_{t_b}^{t_f} L(x,z,u,v,t)dt$$

is related and the optimal control problem is defined as to find

$$(5.111) \quad u^* = \arg\max_u J(u),$$

subject to the state and control constraints. With the Hamiltonian defined by

$$(5.112) \quad \mathcal{H} = -L(x,z,u,v,t) + \lambda^T f(x,z,u,v,t) + \eta^T g(x,z,u,v,t),$$

necessary conditions for this singularly perturbed system are

$$(5.113a) \quad \dot{x}^* = \frac{\partial \mathcal{H}}{\partial \lambda}(x^*,\lambda^*,z^*,\eta^*,u^*,v,t), \quad x^*(t_b) = x_b,$$

$$(5.113b) \quad \varepsilon \dot{z}^* = \frac{\partial \mathcal{H}}{\partial \eta}(x^*,\lambda^*,z^*,\eta^*,u^*,v,t), \quad z^*(t_b) = z_b,$$

$$(5.114a) \quad -\dot{\lambda}^* = \frac{\partial \mathcal{H}}{\partial x}(x^*,\lambda^*,z^*,\eta^*,u^*,v,t), \quad \lambda^*(t_f) = \frac{\partial \Phi}{\partial x}(x^*(t_f),t_f),$$

$$(5.114b) \quad -\varepsilon \dot{\eta}^* = \frac{\partial \mathcal{H}}{\partial z}(x^*,\lambda^*,z^*,\eta^*,u^*,v,t), \quad \eta^*(t_f) = 0,$$

and according to the Maximum Principle of Pontryagin

$$(5.115) \quad \mathcal{H}(x^*,\lambda^*,z^*,\eta^*,u,v,t) \leq \mathcal{H}(x^*,\lambda^*,z^*,\eta^*,u^*,v,t).$$

Unlike the standard singular perturbation solution shown in section 5.6.1, when the system is disturbed by rapidly fluctuating exogenous inputs, the fast transients are not limited to the boundary layer around the initial time and final time, respectively. They occur throughout the whole interval $[t_b,t_f]$ (Kokotovic *et al.*, 1986). Therefore, with $^-$ indicating the slow transients, and $^\wedge$ denoting the fast transients the states, costates and controls are approximated by two time–scale asymptotic expansions

$$(5.116) \quad x(t,\varepsilon) \cong \sum_{j=0}^{\infty} [\bar{x}_j(t) + \hat{x}_j(t/\varepsilon)]\varepsilon^j, \quad z(t,\varepsilon) \cong \sum_{j=0}^{\infty} [\bar{z}_j(t) + \hat{z}_j(t/\varepsilon)]\varepsilon^j,$$

$$(5.117) \quad \lambda(t,\varepsilon) \cong \sum_{j=0}^{\infty} [\bar{\lambda}_j(t) + \hat{\lambda}_j(t/\varepsilon)]\varepsilon^j, \quad \eta(t,\varepsilon) \cong \sum_{j=0}^{\infty} [\bar{\eta}_j(t) + \hat{\eta}_j(t/\varepsilon)]\varepsilon^j,$$

$$(5.118) \quad u(t,\varepsilon) \cong \sum_{j=0}^{\infty} [\bar{u}_j(t) + \hat{u}_j(t/\varepsilon)]\varepsilon^j.$$

The performance criterion is also approximated by a power series expansion of the form

$$(5.119) \quad J(u,\varepsilon) \cong \sum_{j=0}^{\infty} [\bar{J}_j(\bar{u}_j) + \hat{J}_j(\hat{u}_j)]\varepsilon^j.$$

Explicit relations for the slow and fast system response are required

to establish the desired approximation. The zero-th order terms are derived as follows. To a first order approximation, the variables in the Hamiltonian are approximated by

$x(t) = \bar{x}_0(t) + \hat{x}_0(t/\varepsilon)$, $z(t) = \bar{z}_0(t) + \hat{z}_0(t/\varepsilon)$, $\lambda(t) = \bar{\lambda}_0(t) + \hat{\lambda}_0(t/\varepsilon)$,

$\eta(t) = \bar{\eta}_0(t) + \hat{\eta}_0(t/\varepsilon)$, $u(t) = \bar{u}_0(t) + \hat{u}_0(t/\varepsilon)$ and the Hamiltonian is approximated by

(5.120) $\mathcal{H}(x,z,\lambda,\eta,u,v,t) \cong \mathcal{H}(\bar{x}_0 + \hat{x}_0, \bar{z}_0 + \hat{z}_0, \bar{\lambda}_0 + \hat{\lambda}_0, \bar{\eta}_0 + \hat{\eta}_0, \bar{u}_0 + \hat{u}_0, v, t)$.

Then the time derivative of x is described by

(5.121) $\dfrac{d}{dt}(\bar{x}_0^* + \hat{x}_0^*) = \dfrac{\partial \mathcal{H}}{\partial \lambda}(\bar{x}_0^* + \hat{x}_0^*, \bar{z}_0^* + \hat{z}_0^*, \bar{\lambda}_0^* + \hat{\lambda}_0^*, \bar{\eta}_0^* + \hat{\eta}_0^*, \bar{u}_0^* + \hat{u}_0^*, v, t)$,

which can be rewritten as

(5.122) $\dfrac{d}{dt}(\bar{x}_0^* + \hat{x}_0^*) = \dfrac{\partial \mathcal{H}}{\partial \lambda}(\bar{x}_0^*, \bar{z}_0^*, \bar{\lambda}_0^*, \bar{\eta}_0^*, \bar{u}_0^*, v, t)$

$+ \dfrac{\partial \mathcal{H}}{\partial \lambda}(\bar{x}_0^* + \hat{x}_0^*, \bar{z}_0^* + \hat{z}_0^*, \bar{\lambda}_0^* + \hat{\lambda}_0^*, \bar{\eta}_0^* + \hat{\eta}_0^*, \bar{u}_0^* + \hat{u}_0^*, v, t)$

$- \dfrac{\partial \mathcal{H}}{\partial \lambda}(\bar{x}_0^*, \bar{z}_0^*, \bar{\lambda}_0^*, \bar{\eta}_0^*, \bar{u}_0^*, v, t)$.

According to the theory (*e.g.* Kokotovic *et al.*, 1986), the zero-th order slow response is governed by

(5.123) $\dfrac{d\bar{x}_0^*(t)}{dt} = \dfrac{\partial \mathcal{H}}{\partial \lambda}(\bar{x}_0^*, \bar{z}_0^*, \bar{\lambda}_0^*, \bar{\eta}_0^*, \bar{u}_0^*, v, t)$, $\bar{x}_0^*(t_b) = x_b$,

With $\hat{\mathcal{H}}(\bar{x}_0^*, \hat{x}_0^*, \bar{z}_0^*, \hat{z}_0^*, \bar{\lambda}_0^*, \hat{\lambda}_0^*, \bar{\eta}_0^*, \hat{\eta}_0^*, \bar{u}_0^*, \hat{u}_0^*, v, t) \equiv$

$\mathcal{H}(\bar{x}_0^* + \hat{x}_0^*, \bar{z}_0^* + \hat{z}_0^*, \bar{\lambda}_0^* + \hat{\lambda}_0^*, \bar{\eta}_0^* + \hat{\eta}_0^*, \bar{u}_0^* + \hat{u}_0^*, v, t) - \mathcal{H}(\bar{x}_0^*, \bar{z}_0^*, \bar{\lambda}_0^*, \bar{\eta}_0^*, \bar{u}_0^*, v, t)$, the zero-th order fast response is described by

(5.124) $\dfrac{d\hat{x}_0^*(\tau)}{dt} = \dfrac{\partial \hat{\mathcal{H}}}{\partial \lambda}(\bar{x}_0^*, \hat{x}_0^*, \bar{z}_0^*, \hat{z}_0^*, \bar{\lambda}_0^*, \hat{\lambda}_0^*, \bar{\eta}_0^*, \hat{\eta}_0^*, \bar{u}_0^*, \hat{u}_0^*, v, t)$, $\hat{x}_0^*(t_b) = 0$.

Applying the same procedure to eqns. (5.113b), (5.114a) and (5.114b) results in the following differential equations for $\bar{z}_0^*$, $\hat{z}_0^*$, $\bar{\lambda}_0^*$, $\hat{\lambda}_0^*$,

$\overline{\eta}_0^*$, $\hat{\eta}_0^*$ and necessary conditions for $\overline{u}_0^*$ and $\hat{u}_0^*$.

Zero-th order slow response

The zero-th order slow responses $(\overline{x}_0^*(t)$, $\overline{z}_0^*(t))$ are governed by the equations

$$(5.125a) \quad \frac{d\overline{x}_0^*(t)}{dt} = \frac{\partial \mathcal{H}}{\partial \lambda}(\overline{x}_0^*,\overline{z}_0^*,\overline{\lambda}_0^*,\overline{\eta}_0^*,\overline{u}_0^*,v,t) = f(\overline{x}_0^*,\overline{z}_0^*,\overline{u}_0^*,v,t),$$

with $\overline{x}_0^*(t_b) = x_b$ and

$$(5.125b) \quad \varepsilon\frac{d\overline{z}_0^*(t)}{dt} = \frac{\partial \mathcal{H}}{\partial \eta}(\overline{x}_0^*,\overline{z}_0^*,\overline{\lambda}_0^*,\overline{\eta}_0^*,\overline{u}_0^*,v,t) = g(\overline{x}_0^*,\overline{z}_0^*,\overline{u}_0^*,v,t).$$

Since in the zero-th order approximation first order terms in ε are neglected, (5.125b) reduces to

$$(5.126) \quad 0 = g(\overline{x}_0^*,\overline{z}_0^*,\overline{u}_0^*,v,t),$$

$$(5.127a) \quad -\frac{d\overline{\lambda}_0^*(t)}{dt} = \frac{\partial \mathcal{H}}{\partial x}(\overline{x}_0^*,\overline{z}_0^*,\overline{\lambda}_0^*,\overline{\eta}_0^*,\overline{u}_0^*,v,t), \quad \overline{\lambda}_0^*(t_f) = \frac{\partial \Phi}{\partial x}(x_0^*(t_f),t_f),$$

$$(5.127b) \quad -\varepsilon\frac{d\overline{\eta}_0^*(t)}{dt} = \frac{\partial \mathcal{H}}{\partial z}(\overline{x}_0^*,\overline{z}_0^*,\overline{\lambda}_0^*,\overline{\eta}_0^*,\overline{u}_0^*,v,t),$$

which also reduces to

$$(5.128) \quad 0 = \frac{\partial \mathcal{H}}{\partial z}(\overline{x}_0^*,\overline{z}_0^*,\overline{\lambda}_0^*,\overline{\eta}_0^*,\overline{u}_0^*,v,t),$$

as $\varepsilon \rightarrow 0$. Due to Pontryagin's maximum principle

$$(5.129) \quad \mathcal{H}(\overline{x}_0^*,\overline{z}_0^*,\overline{\lambda}_0^*,\overline{\eta}_0^*,\overline{u},v,t) \leq \mathcal{H}(\overline{x}_0^*,\overline{z}_0^*,\overline{\lambda}_0^*,\overline{\eta}_0^*,\overline{u}_0^*,v,t).$$

As a matter of fact, and in line with standard singular perturbation theory, these equations are related to the control problem

(5.130a) $\dfrac{d\bar{x}_0(t)}{dt} = f(\bar{x}_0,\bar{z}_0,\bar{u}_0,\nu,t), \qquad \bar{x}_0(t_b) = x_b,$

(5.130b) $0 = g(\bar{x}_0,\bar{z}_0,\bar{u}_0,\nu,t),$

(5.131) $\bar{J}_0(\bar{u}_0) = \Phi(\bar{x}_0(t_f),t_f) - \displaystyle\int_{t_b}^{t_f} L(\bar{x}_0,\bar{z}_0,\bar{u}_0,\nu,t)dt,$

(5.132) $\bar{u}_0^*(t) = \arg \max_{\bar{u}_0} \bar{J}_0,$

which is exactly the same as the zero-th order control problem considered in section 5.6.1.

Zero-th order fast response

The zero-th order fast response of x is governed by the equation

(5.133) $\dfrac{d\hat{x}_0(\tau)}{dt} = f(\bar{x}_0+\hat{x}_0,\bar{z}_0+\hat{z}_0,\bar{u}_0+\hat{u}_0,\nu,t)-f(\bar{x}_0,\bar{z}_0,\bar{u}_0,\nu,t),$

$\hat{x}_0(t_b/\varepsilon) = x(t_b) - \bar{x}_0(t_b) = 0,$

which after applying a time scaling transformation with $\tau = t/\varepsilon$ to (5.133) yields

(5.134) $\dfrac{d\hat{x}_0(\tau)}{d\tau} = \varepsilon[f(\bar{x}_0+\hat{x}_0,\bar{z}_0+\hat{z}_0,\bar{u}_0+\hat{u}_0,\nu,\varepsilon\tau) - f(\bar{x}_0,\bar{z}_0,\bar{u}_0,\nu,\varepsilon\tau)].$

Because order ε and higher effects are neglected in the zero-th order approximation, eqn. (5.134) reduces to

(5.135) $\dfrac{d\hat{x}_0(\tau)}{d\tau} = 0.$

On the fast time-scale τ, the dynamics of the fast sub-system are described by

(5.136) $$\frac{d\hat{z}_0^*(\tau)}{d\tau} = \frac{\partial\hat{\mathcal{H}}}{\partial\eta}(\bar{x}_0^*,\hat{x}_0^*,\bar{z}_0^*,\hat{z}_0^*,\bar{\lambda}_0^*,\hat{\lambda}_0^*,\bar{\eta}_0^*,\hat{\eta}_0^*,\bar{u}_0^*,\hat{u}_0^*,\nu,\varepsilon\tau),$$

$$\hat{z}_0^*(t_b/\varepsilon) = z(t_b) - \bar{z}_0^*(t_b).$$

The dynamics of the slow costates are governed by

(5.137) $$\frac{d\hat{\lambda}_0^*(\tau)}{d\tau} = \varepsilon\frac{\partial\hat{\mathcal{H}}}{\partial x}(\bar{x}_0^*,\hat{x}_0^*,\bar{z}_0^*,\hat{z}_0^*,\bar{\lambda}_0^*,\hat{\lambda}_0^*,\bar{\eta}_0^*,\hat{\eta}_0^*,\bar{u}_0^*,\hat{u}_0^*,\nu,\varepsilon\tau),$$

which reduces to

(5.138) $$\frac{d\hat{\lambda}_0^*(\tau)}{d\tau} = 0.$$

Finally, the dynamics of the fast costates are given by

(5.139) $$\frac{d\hat{\eta}_0^*(\tau)}{d\tau} = \frac{\partial\hat{\mathcal{H}}}{\partial z}(\bar{x}_0^*,\hat{x}_0^*,\bar{z}_0^*,\hat{z}_0^*,\bar{\lambda}_0^*,\hat{\lambda}_0^*,\bar{\eta}_0^*,\hat{\eta}_0^*,\bar{u}_0^*,\hat{u}_0^*,\nu,\varepsilon\tau),$$

$$\hat{\eta}_0^*(t_f/\varepsilon) = 0.$$

Due to Pontryagin's maximum principle, the necessary condition for optimality of the zero-th order fast control is

(5.140) $$\hat{\mathcal{H}}(\bar{x}_0^*,\hat{x}_0^*,\bar{z}_0^*,\hat{z}_0^*,\bar{\lambda}_0^*,\hat{\lambda}_0^*,\bar{\eta}_0^*,\hat{\eta}_0^*,\bar{u}_0^*,\hat{u}_0,\nu,\varepsilon\tau) \leq$$

$$\hat{\mathcal{H}}(\bar{x}_0^*,\hat{x}_0^*,\bar{z}_0^*,\hat{z}_0^*,\bar{\lambda}_0^*,\hat{\lambda}_0^*,\bar{\eta}_0^*,\hat{\eta}_0^*,\bar{u}_0^*,\hat{u}_0^*,\nu,\varepsilon\tau)$$

with the Hamiltonian

(5.141) $$\hat{\mathcal{H}}(\bar{x}_0^*,\hat{x}_0^*,\bar{z}_0^*,\hat{z}_0^*,\bar{\lambda}_0^*,\hat{\lambda}_0^*,\bar{\eta}_0^*,\hat{\eta}_0^*,\bar{u}_0^*,\hat{u}_0^*,\nu,\varepsilon\tau) =$$

$$\mathcal{H}(\bar{x}_0^*+\hat{x}_0^*,\bar{z}_0^*+\hat{z}_0^*,\bar{\lambda}_0^*+\hat{\lambda}_0^*,\bar{\eta}_0^*+\hat{\eta}_0^*,\bar{u}_0^*+\hat{u}_0^*,\nu,\varepsilon\tau)$$

$$- \mathcal{H}(\bar{x}_0^*+\hat{x}_0^*,\bar{z}_0^*,\bar{\lambda}_0^*,\bar{\eta}_0^*,\bar{u}_0^*,\nu,\varepsilon\tau) =$$

$$- L(\bar{x}_0^*+\hat{x}_0^*,\bar{z}_0^*+\hat{z}_0^*,\bar{u}_0^*+\hat{u}_0^*,\nu,\varepsilon\tau) + L(\bar{x}_0^*,\bar{z}_0^*,\bar{\lambda}_0^*,\bar{\eta}_0^*,\bar{u}_0^*,\nu,\varepsilon\tau)$$

$$+ \bar{\lambda}_0^{*T}(f(\bar{x}_0^*+\hat{x}_0^*,\bar{z}_0^*+\hat{z}_0^*,\bar{u}_0^*+\hat{u}_0^*,\nu,\varepsilon\tau) - f(\bar{x}_0^*,\bar{z}_0^*,\bar{u}_0^*,\nu,\varepsilon\tau))$$

$$+ \hat{\lambda}_0^{*T}f(\bar{x}_0^*+\hat{x}_0^*,\bar{z}_0^*+\hat{z}_0^*,\bar{u}_0^*+\hat{u}_0^*,\nu,\varepsilon\tau)$$

$$+ \bar{\eta}_0^{*T}(g(\bar{x}_0^*+\hat{x}_0^*,\bar{z}_0^*+\hat{z}_0^*,\bar{u}_0^*+\hat{u}_0^*,\nu,\varepsilon\tau) - g(\bar{x}_0^*,\bar{z}_0^*,\bar{u}_0^*,\nu,\varepsilon\tau))$$

$$+ \hat{\eta}_0^{*T} g(\overline{x}_0^* + \hat{x}_0^*, \overline{z}_0^* + \hat{z}_0^*, \overline{u}_0^* + \hat{u}_0^*, \nu, \varepsilon\tau).$$

Because in the zero-th order fast response both $d\hat{x}_0/d\tau = 0$ and $d\hat{\lambda}_0/d\tau = 0$, we obtain

(5.142)
$$\hat{\mathcal{H}}(\overline{x}_0^*, \overline{z}_0^*, \hat{z}_0^*, \overline{\lambda}_0^*, \overline{\eta}_0^*, \hat{\eta}_0^*, \overline{u}_0^*, \hat{u}_0^*, \nu, \varepsilon\tau) =$$
$$- L(\overline{x}_0^*, \overline{z}_0^* + \hat{z}_0^*, \overline{u}_0^* + \hat{u}_0^*, \nu, \varepsilon\tau) + L(\overline{x}_0^*, \overline{z}_0^*, \overline{u}_0^*, \nu, \varepsilon\tau)$$
$$+ \overline{\lambda}_0^{*T}(f(\overline{x}_0^*, \overline{z}_0^* + \hat{z}_0^*, \overline{u}_0^* + \hat{u}_0^*, \nu, \varepsilon\tau) - f(\overline{x}_0^*, \overline{z}_0^*, \overline{u}_0^*, \nu, \varepsilon\tau))$$
$$+ \overline{\eta}_0^{*T}(g(\overline{x}_0^*, \overline{z}_0^* + \hat{z}_0^*, \overline{u}_0^* + \hat{u}_0^*, \nu, \varepsilon\tau) - g(\overline{x}_0^*, \overline{z}_0^*, \overline{u}_0^*, \nu, \varepsilon\tau))$$
$$+ \hat{\eta}_0^{*T} g(\overline{x}_0^*, \overline{z}_0^* + \hat{z}_0^*, \overline{u}_0^* + \hat{u}_0^*, \nu, \varepsilon\tau).$$

To a first order approximation, z, η and u are approximated by $z_0(t) = \overline{z}_0(t) + \hat{z}_0(t/\varepsilon)$, $\eta_0(t) = \overline{\eta}_0(t) + \hat{\eta}_0(t/\varepsilon)$ and $u_0(t) = \overline{u}_0(t) + \hat{u}_0(t/\varepsilon)$. Then, rewriting eqn. (5.142) yields

(5.143)
$$\hat{\mathcal{H}}(\overline{x}_0^*, z_0^*, \overline{\lambda}_0^*, \eta_0^*, u_0^*, \nu, \varepsilon\tau) =$$
$$- L(\overline{x}_0^*, z_0^*, u_0^*, \nu, \varepsilon\tau) + L(\overline{x}_0^*, \overline{z}_0^*, \overline{u}_0^*, \nu, \varepsilon\tau)$$
$$+ \overline{\lambda}_0^{*T}(f(\overline{x}_0^*, z_0^*, u_0^*, \nu, \varepsilon\tau) - f(\overline{x}_0^*, \overline{z}_0^*, \overline{u}_0^*, \nu, \varepsilon\tau))$$
$$+ \eta_0^{*T}(g(\overline{x}_0^*, z_0^*, u_0^*, \nu, \varepsilon\tau) - g(\overline{x}_0^*, \overline{z}_0^*, \overline{u}_0^*, \nu, \varepsilon\tau)).$$

This equation can be related with the control problem

(5.144)
$$\frac{dz_0(\tau)}{d\tau} = g(\overline{x}_0^*, z_0, u_0, \nu, \varepsilon\tau),$$

(5.145)
$$\hat{J}_0(u_0) = \int_{t_b/\varepsilon}^{t_f/\varepsilon} \Big(-L(\overline{x}_0^*, z_0, u_0, \nu, \varepsilon\tau) + L(\overline{x}_0^*, \overline{z}_0^*, \overline{u}_0^*, \nu, \varepsilon\tau)$$
$$+ \overline{\lambda}_0^{*T} f(\overline{x}_0^*, z_0, u_0, \nu, \varepsilon\tau) - \overline{\lambda}_0^{*T} f(\overline{x}_0^*, \overline{z}_0^*, \overline{u}_0^*, \nu, \varepsilon\tau)\Big) d\tau,$$

(5.146)
$$u_0^*(\tau) = \arg\max_{u_0} \hat{J}_0(u_0).$$

In view of greenhouse climate control, the above stated control problem has the following interpretation. The Hamiltonian represents a momentary net economic return of the controlled process (see

section 5.4). Consequently, the integrand in eqn. (5.145) expresses the difference between the net economic return of the controlled crop production process in which the greenhouse climate dynamics have been considered, $\mathcal{H}(\bar{x}_0^*, z_0, \bar{\lambda}_0^*, \eta_0, u_0, v, \tau)$, and the net economic return of the controlled crop production process in which the greenhouse climate dynamics have not been considered, $\mathcal{H}(\bar{x}_0^*, \bar{z}_0^*, \bar{\lambda}_0^*, \bar{\eta}_0^*, \bar{u}_0^*, v, \tau)$. Thus, the objective of the control system is to maximize the benefits of controlling the greenhouse climate dynamics or alternatively, to minimize the losses due to neglecting the greenhouse climate dynamics in the zero-th order outer solution.

It can be observed that the slow and the fast dynamics are completely decoupled in the decomposition; first the control problem is solved in which the slow system dynamics are taken into account, then using the slow state and costate trajectories as a reference, the fast system dynamics are accounted for. The fast transients in the slow sub-system, *i.e.* $\hat{x}$ and $\hat{\lambda}$, are neglected in the zero-th order approximation. The fast transients can be arbitrarily large. If the zero-th order approximation fails to give an accurate solution, higher order corrections may be applied. Since in the fast sub-problem $L(\bar{x}_0^*, \bar{z}_0^*, \bar{u}_0^*, v, \tau)$ and $f(\bar{x}_0^*, \bar{z}_0^*, \bar{u}_0^*, v, \tau)$ constitute fixed reference trajectories, maximizing $\hat{\mathcal{H}}(\bar{x}_0^*, z_0, \bar{\lambda}_0^*, \eta_0, u_0, v, t)$ is equivalent with maximizing

(5.147) $\quad \tilde{\mathcal{H}}(\bar{x}_0^*, z_0, \bar{\lambda}_0^*, \eta_0, u_0, v, \varepsilon\tau) =$

$\qquad - L(\bar{x}_0^*, z_0, u_0, v, \varepsilon\tau) + \bar{\lambda}_0^{*T} f(\bar{x}_0^*, z_0, u_0, v, \varepsilon\tau)$

$\qquad + \eta_0^T g(\bar{x}_0^*, z_0, u_0, v, \varepsilon\tau),$

which is related to the control problem

(5.148) $\quad \dfrac{dz_0(\tau)}{d\tau} = g(\bar{x}_0^*, z_0, u_0, v, \varepsilon\tau),$

(5.149) $\quad J_0(u_0) = \displaystyle\int_{t_b/\varepsilon}^{t_f/\varepsilon} \left(-L(\bar{x}_0^*, z_0, u_0, v, \varepsilon\tau) + \bar{\lambda}_0^{*T} f(\bar{x}_0^*, z_0, u_0, v, \varepsilon\tau) \right) d\tau,$

(5.150) $\quad u_0^*(\tau) = \arg \max_{u_0} J_0(u_0).$

Eqns. (5.148) to (5.150) clarify the interpretation of the fast sub-

problem even further. Since in the problems considered in this thesis, $\bar{\lambda}_0^{*T}$ represents the marginal value of a unit crop growth, the objective of the fast sub-problem is to control the greenhouse climate such that an optimal trade-off between the operating costs $-L(\bar{x}_0^*, z_0, u_0, v, \varepsilon\tau)$ and the contribution of the control to the realisation of the final income valued at its marginal value $\bar{\lambda}_0^{*T} f(\bar{x}_0^*, z_0, u_0, v, \varepsilon\tau)$ is achieved. Economic optimal control of the greenhouse climate dynamics has already received some attention in the literature (Tchamitchan *et al.*, 1992; Tap *et al.*, 1992; Hwang, 1993), but the control problem stated by the previous authors was quite different from the control problem defined by eqns. (5.148) to (5.150). First of all, the previous authors included the slow crop growth dynamics in the control system design. For plausible reasons given above, in the present approach, the slow dynamics are neglected when dealing with optimal control of the greenhouse climate dynamics. Secondly, the performance criterion in the present approach follows directly from the performance criterion defined in the original full problem. Eqn. (5.149) shows that the contribution of a unit crop growth to the final return is valued at its marginal value $\bar{\lambda}$, which in turn is related to the gross return at harvest time through eqn. (5.31e) (see also section 5.4). In this way the difficulty of associating a value to a unit crop growth at a certain moment in the growing period, for instance encountered by Tchamitchan *et al.* (1992) and Tap *et al.* (1992) is solved in a transparent and straightforward way.

5.7. Numerical solution of the optimal control problem

In section 5.3, variational techniques were used to derive necessary conditions for the existence of an optimal control trajectory. The resulting two-point boundary value problem is generally hard to treat analytically and numerical tools are needed to generate a solution. In this section such an iterative numerical algorithm, based on the *steepest ascent* method, is described.

First, the general idea of the steepest ascent algorithm will be outlined (see *e.g.* Kirk, 1970). Secondly, since the basic steepest ascent algorithm is unable to cope with constraints on the controls, a modification of the algorithm is proposed which allows for the solution of optimal control problems with control constraints.

Suppose a nominal control trajectory $u^{(i)}(t)$, $t \in [t_b, t_f]$, is known and used to solve the differential equations

(5.151) $\dot{x}^{(i)} = \dfrac{\partial \mathcal{H}}{\partial \lambda}(x^{(i)},\lambda^{(i)},u^{(i)},t),$

(5.152) $-\dot{\lambda}^{(i)} = \dfrac{\partial \mathcal{H}}{\partial x}(x^{(i)},\lambda^{(i)},u^{(i)},t),$

satisfying the initial and final boundary conditions $x^{(i)}(t_b) = x_b$ and $\lambda^{(i)}(t_f) = \partial\Phi(x^{(i)}(t_f),t_f)/\partial x$. Here (i) denotes an iteration counter. If this nominal control trajectory satisfies

(5.153) $\dfrac{\partial \mathcal{H}}{\partial u}(x^{(i)}(t),u^{(i)}(t),\lambda^{(i)}(t),t) = 0,$

then $x^{(i)}(t)$, $u^{(i)}(t)$ and $\lambda^{(i)}(t)$ are extremal and $J(u^{(i)}(t))$ is said to be locally maximized. However, if eqn. (5.153) is not satisfied, the variation in the augmented performance criterion is

$$
(5.154) \quad \delta J_a(u^{(i)}) = \int_{t_b}^{t_f}\left\{[\frac{\partial \mathcal{H}}{\partial x}(x^{(i)},u^{(i)},\lambda^{(i)},t)+\dot{\lambda}^{(i)}]^T\delta x^{(i)}\right.
$$

$$
+ [\frac{\partial \mathcal{H}}{\partial u}(x^{(i)},u^{(i)},\lambda^{(i)},t)]^T\delta u^{(i)}
$$

$$
+ \left.[\frac{\partial \mathcal{H}}{\partial \lambda}(x^{(i)},u^{(i)},\lambda^{(i)},t)-\dot{x}^{(i)}]^T\delta\lambda^{(i)}\right\}dt
$$

$$
+ [\frac{\partial \Phi}{\partial x}(x^{(i)}(t_f),t_f)-\lambda^{(i)}(t_f)]^T\delta x^{(i)}(t_f)
$$

with $\delta x^{(i)}(t) = x^{(i+1)}(t)-x^{(i)}(t)$, $\delta u^{(i)}(t) = u^{(i+1)}(t)-u^{(i)}(t)$ and $\delta\lambda^{(i)}(t) = \lambda^{(i+1)}(t)-\lambda^{(i)}(t)$. If the state and costate equations (5.151) and (5.152) are satisfied, eqn. (5.154) becomes

$$
(5.155) \quad \delta J_a(u^{(i)}) = \int_{t_b}^{t_f}\frac{\partial \mathcal{H}^{(i)}}{\partial u}(t)\ dt =
$$

$$\int_{t_b}^{t_f} \frac{\partial \mathcal{H}}{\partial u}(x^{(l)}(t), u^{(l)}(t), \lambda^{(l)}(t), t) dt.$$

Because $\delta J_a(u^{(l)})$ is the linear part of the increment $\Delta J_a = J_a(u^{(l+1)}) - J_a(u^{(l)})$, for small values of the norm of δu, $\|u^{(l+1)} - u^{(l)}\|$, the sign of ΔJ_a will be determined by the sign of δJ_a (see section 5.3). To maximize J_a, a positive ΔJ_a should be chosen, which can be attained by selecting the change in u as

$$(5.156) \qquad \delta u(t) = u^{(l+1)} - u^{(l)} = \sigma \frac{\partial \mathcal{H}^{(l)}}{\partial u}(t), \qquad t \in [t_b, t_f],$$

with $\sigma > 0$. This results in

$$(5.157) \qquad \delta J_a = \sigma \int_{t_b}^{t_f} \left[\frac{\partial \mathcal{H}^{(l)}}{\partial u}(t) \right]^T \frac{\partial \mathcal{H}^{(l)}}{\partial u}(t) \ dt \geq 0$$

because the integrand is non-negative for all $t \in [t_b, t_f]$. The equality, *i.e.* $\delta J_a = 0$, holds only if

$$(5.158) \qquad \frac{\partial \mathcal{H}^{(l)}}{\partial u}(t) = 0$$

for all $t \in [t_b, t_f]$. Selecting δu in this manner, with $\|\delta u\|$ sufficiently small, ensures that each value of the performance criterion will be at least as large as the preceding value. Eventually, when J_a reaches a (local) maximum, the vector $\partial \mathcal{H}/\partial u$ will be zero for all $t \in [t_b, t_f]$.

Formulated in this way, the steepest ascent method is not able to deal with constraints on the controls. This can be seen as follows. If the control encounters a constraint, *i.e.* $u(t) = u_{max}(t)$ for some $t \in [t_b, t_f]$ and $\partial \mathcal{H}(t)/\partial u > 0$, then due to the fact that $\sigma > 0$, eqn. (5.156) yields a modification of the control

$u^{(l+1)} = u^{(l)} + \delta u(t) = \sigma \partial \mathcal{H}^{(l)}(t)/\partial u \geq u_{max}(t)$. Thus, a violation of the control constraint occurs. So, in case control constraints are encountered, not every variation in the control $\delta u(t)$ is allowed.

To circumvent this shortcoming, the following change of the algorithm is proposed. If control constraints are to be considered, the maximum permitted modification of the control is

$$(5.159) \quad \delta u_{max}(t) = \begin{cases} u_{max}(t) - u^{(l)}(t) \text{ if } \dfrac{\partial \mathcal{H}^{(l)}}{\partial u}(t) > 0, \\[4mm] u^{(l)}(t) - u_{min}(t) \text{ if } \dfrac{\partial \mathcal{H}^{(l)}}{\partial u}(t) < 0, \end{cases}$$

for all $t \in [t_b, t_f]$. Due to the boundedness of the control, the maximum control modification $\delta u_{max}^{(l)}(t)$ is positive and bounded. Basically, the algorithm is changed by putting a limitation on the control modification $\delta u(t)$. If the control modification is defined by

$$(5.160) \quad \delta u(t) = u^{(l+1)} - u^{(l)} = \sigma \, \frac{\partial \mathcal{H}^{(l)}}{\partial u}(t) \, \delta u_{max}^{(l)}(t),$$

then, because $|\partial \mathcal{H}/\partial u|$ can take very large values and $\delta u_{max}^{(l)}(t)$ is positive and bounded, the actual limitation of the control modification is established by limiting the choice of σ. For $\sigma > 0$, a control violation does occur if

$$\frac{|\delta u(t)|}{\delta u_{max}^{(l)}(t)} = \sigma |\frac{\partial \mathcal{H}^{(l)}}{\partial u}(t)| > 1.$$

So, by choosing $0 < \sigma \leq \bar{\sigma}_{max} = \min(\sigma_{j,max}(t))$ for every control $u_j(t)$, $j = 1,\ldots,m$, and all $t \in [t_b, t_f]$, with $\sigma_{j,max}(t)$ defined by

$$(5.161) \quad \sigma_{j,max}(t) = \frac{1}{|\partial \mathcal{H}^{(l)}(t)/\partial u_j|},$$

a limit on the control modification is obtained, which prevents

violation of the control constraints of all controls $u_j(t)$, $j = 1,\ldots,m$.

The previously described alteration of the algorithm does not affect its convergence properties. The increment in the augmented performance criterion due to a change in the control is

$$(5.162) \quad \delta J_a = \sigma \int_{t_b}^{t_f} \left[\frac{\partial \mathcal{H}^{(1)}}{\partial u}(t) \right]^T \frac{\partial \mathcal{H}^{(1)}}{\partial u}(t) \; \delta u_{max}^{(1)}(t) \; dt \geq 0,$$

with $0 < \sigma \leq \bar{\sigma}_{max}$ and $0 \leq \delta u_{max}^{(1)}(t) \leq a$, with a a positive real number. The equality $\delta J_a = 0$, is satisfied if $\delta u_{max}^{(1)}(t) = 0$ and/or $\partial \mathcal{H}^{(1)}(t)/\partial u = 0$ for all $t \in [t_b, t_f]$. Since the integrand is always larger or equal to zero, it is guaranteed that by selecting the control modification δu in this way, each value of the performance criterion will be at least as large as the preceding value. When J_a reaches a (local) maximum, $\partial \mathcal{H}/\partial u$ will be zero or $\delta u_{max}^{(1)}(t) \longrightarrow 0$ if a control constraint is encountered. If a local maximum is located on a control constraint, both $\delta u_{max}^{(1)}(t)$ and $\partial \mathcal{H}/\partial u$ will vanish ensuring that $\delta J_a \longrightarrow 0$.

For actual implementation in a digital computer, the algorithm has the following form.

[0] Set iteration number $i = 0$, choose a discrete approximation of the nominal control trajectory $u^{(0)}(t)$, $t \in [t_b, t_f]$ satisfying the control constraints and choose a desired value of the convergence criterion ε. Because the calculations are to be performed by a digital computer a discrete approximation of the control trajectory is required. A discrete approximation can be obtained by dividing the time interval $[t_b, t_f]$ into N subintervals (generally of equal length) and considering the control as being piece-wise constant during each of these subintervals; i.e. $u^{(0)}(t) = u^{(0)}(t_k)$, $t = [t_k, t_{k+1})$, $k = 0, 1,\ldots, N-1$.

[2] Integrate the state equations (5.151) from t_b to t_f using the nominal control trajectory $u^{(1)}(t)$ and the initial boundary

conditions $x(t_b) = x_b$ and   store   the   resulting   nominal   state trajectory $x^{(1)}(t)$.

[3] Calculate the performance criterion $J^{(1)}$.

[4] Integrate the costate equations (5.152) from t_f to t_b using the nominal control and state trajectories $x^{(1)}(t)$ and $u^{(1)}(t)$ and the final boundary conditions $\lambda^{(1)}(t_f) = \partial\Phi(x^{(1)}(t_f),t_f)/\partial x$ and store the resulting nominal costate trajectory $\lambda^{(1)}(t)$.

[5] Calculate the gradient $\dfrac{\partial\mathcal{H}^{(1)}}{\partial u}(t)$ and determine $\bar{\sigma}_{max}$ as well as $\delta u_{j,max}^{(1)}(t)$, $j = 1,...,m$,   for   all $t = [t_b,t_f]$ using   eqns. (5.159) and (5.161).

[6] Using $u^{(1+1)} = u^{(1)} + \sigma \dfrac{\partial\mathcal{H}^{(1)}}{\partial u}(t)\, \delta u_{max}^{(1)}(t)$,   perform   a   line   search for σ^* such that the performance criterion $J^{(1+1)}$ is maximized subject to the constraint $0 < \sigma^* \leq \bar{\sigma}_{max}$.

[7] If $0 < J^{(1+1)} - J^{(1)} < \varepsilon$ store   the   optimal   control   trajectory $u^{(1+1)}$ and go to step [8], else set $i = i+1$ and go to step [2].

[8] Stop.

Because the calculations are performed by a computer, discrete approximations of the continuous time control trajectories are required. The accuracy of the approximations depend on the length of the sampling interval $[t_k,t_{k+1})$. Usually the sampling interval is chosen such that it is smaller than the shortest dynamic response time involved in the process considered.

The performance of the steepest ascent algorithm is characterized by an easy start but a tendency to have a slow convergence rate, since as the maximum is approached the gradients become very small.

Constraints on the state variables are treated by extending the performance criterion with penalty functions as was described in

section 5.3.3.

In step [4], the costates are simulated in backward time. In optimal control problems, the costates may exhibit instabilities in forward time if the system's states, *e.g.* the greenhouse variables, are stable. The instabilities are circumvented by simulating the costates in backward time.

5.8. A sub-optimal feedback, feedforward control scheme

In this thesis, the objective of the control system design is to drive the greenhouse crop production process in such a way that the net economic return of crop production is maximized. Solution of the associated two-point boundary value problem derived in section 5.3 using a numerical tool like the steepest ascent algorithm described in section 5.7, yields so-called open-loop optimal control strategies. When these open-loop control strategies are applied in horticultural practice, a reduction in the performance of the controlled process is likely to occur due to modelling errors, errors in the measurements of the initial conditions and unmodelled exogenous dynamics. Under these circumstances, feedback and feedforward loops are needed in the control system to improve the performance of the controlled process.

For linear systems and quadratic performance criteria, the construction of optimal feedback laws has been established in the 1960's and in the early 1970's; see for instance Kwakernaak and Sivan (1972). However, for non-linear systems, the computation of analytic expressions of the optimal feedback law has been considerably more difficult and only recently have results in this field been reported (Rouff and Lamnabhi-Lagarrigue, 1986; Bourdache-Siguerdidjane and Fliess, 1987). These results were obtained through a differential geometric interpretation of the first-order necessary conditions for optimality. Alternatively, non-linear feedback laws can be computed numerically by solving the Hamilton–Jacobi–Bellman partial differential equation of the optimal cost (Fleming and Rishel, 1975). Results in this area have been reported by Gonzales and Rofman (1985[a,b]), Menaldi and Rofman (1986) and Van Henten and Chalabi (1994). Since the numerical computation of optimal non-linear feedback laws is numerically involved, in this thesis a different and much simpler approach is employed which is based on the 'sub-optimal' control algorithm reported by Friedland and Sarachnik (1966).

Essentially, the algorithm contains two parts. In the first part, off-line, a nominal solution of the optimal control problem is calculated by solving the two-point boundary value problem (see section 5.3), given a prediction of the disturbances $\bar{v}(t)$,

$t \in [t_b, t_f]$ and an estimate of the initial conditions of the process, $\bar{x}(t_b)$. The resulting nominal state and costate trajectories, $\bar{x}^*(t)$ and $\bar{\lambda}^*(t)$, and the nominal optimal control trajectories, $\bar{u}^*(t)$, are stored.

During the actual application of the open-loop optimal control strategies to the process, perturbations in the system's state will occur due to *e.g.* perturbations in the initial conditions, the model parameters and exogenous inputs around their nominal values. The second part of the algorithm, which is implemented on-line, modifies the control actions based on measurements of the perturbed system's state and the actual disturbances in the following way.

The nominal open-loop optimal control trajectories satisfy the general relation

(5.163) $\bar{u}^*(t) = \arg \max_u \mathcal{H}(\bar{x}^*, u, \bar{v}, \bar{\lambda}^*, t),$

subject to the control constraints (5.3), which is equivalent with saying that

(5.164) $\bar{u}^*(t) = \sigma(\bar{x}^*, \bar{\lambda}^*, \bar{v}, t).$

Eqn. (5.164) constitutes a non-linear control law which describes the optimal control action $\bar{u}^*(t)$ as a function of the system's state $\bar{x}^*$, the costate $\bar{\lambda}^*$, the exogenous inputs $\bar{v}$ and time t. If all the system's states as well as the disturbances can be measured, and for reasons stated above they deviate from their nominal values by taking the actual values $x(t)$ and $v(t)$, eqn. (5.164) will give the associated new control $u(t)$ once a value for the perturbed costate $\lambda(t)$ is available. In practice, however, the perturbed costate is hardly ever known. Therefore, an approximation of $\lambda(t)$ is constructed.

The perturbed system's state satisfies

(5.165) $x(t) = \bar{x}^*(t) + \delta x(t).$

If $\delta x(t)$ is small, it will induce a small change in the costate trajectory

(5.166) $\lambda(t) = \bar{\lambda}^*(t) + \delta \lambda(t).$

Substitution of (5.165) and (5.166) in the state equation and costate equations, (5.31a) and (5.31b) respectively, yields

(5.167) $\dfrac{dx}{dt} = \dfrac{d\bar{x}^*}{dt} + \dfrac{d}{dt}\delta x = \dfrac{\partial \mathcal{H}}{\partial \lambda}(\bar{x}^*,u,\bar{v},\bar{\lambda}^*,t) + \dfrac{\partial^2 \mathcal{H}}{\partial x \partial \lambda}(\bar{x}^*,u,\bar{v},\bar{\lambda}^*,t)\delta x$

$+ \dfrac{\partial^2 \mathcal{H}}{\partial \lambda^2}(\bar{x}^*,u,\bar{v},\bar{\lambda}^*,t)\delta \lambda + O(\delta x^2),$

(5.168) $-\dfrac{d\lambda}{dt} = -\dfrac{d\bar{\lambda}^*}{dt} - \dfrac{d}{dt}\delta \lambda = \dfrac{\partial \mathcal{H}}{\partial x}(\bar{x}^*,u,\bar{v},\bar{\lambda}^*,t) + \dfrac{\partial^2 \mathcal{H}}{\partial x^2}(\bar{x}^*,u,\bar{v},\bar{\lambda}^*,t)\delta x$

$+ \dfrac{\partial^2 \mathcal{H}}{\partial x \partial \lambda}(\bar{x}^*,u,\bar{v},\bar{\lambda}^*,t)\delta \lambda + O(\delta x^2),$

which, when the nominal state and costate trajectories satisfy the necessary conditions, reduce to a description of the perturbed state and costate trajectories up to order δx^2:

(5.169) $\dfrac{d}{dt}\delta x = \dfrac{\partial^2 \mathcal{H}}{\partial x \partial \lambda}(\bar{x}^*,u,\bar{v},\bar{\lambda}^*,t)\delta x + \dfrac{\partial^2 \mathcal{H}}{\partial \lambda^2}(\bar{x}^*,u,\bar{v},\bar{\lambda}^*,t)\delta \lambda,$

(5.170) $-\dfrac{d}{dt}\delta \lambda = \dfrac{\partial^2 \mathcal{H}}{\partial x^2}(\bar{x}^*,u,\bar{v},\bar{\lambda}^*,t)\delta x + \dfrac{\partial^2 \mathcal{H}}{\partial x \partial \lambda}(\bar{x}^*,u,\bar{v},\bar{\lambda}^*,t)\delta \lambda.$

Friedland and Sarachnik (1966) showed that eqns. (5.169) and (5.170) can be solved to obtain a linear relation between the state perturbation $\delta x(t)$ and the costate perturbation $\delta \lambda(t)$, *i.e.*

(5.171) $\delta \lambda(t) = M(t)\delta x(t),$

in which the $n{\times}n$-dimensional matrix $M(t)$ is defined as

(5.172) $M(t) = \dfrac{\partial \lambda}{\partial x}(\bar{x}^*,u,\bar{v},\bar{\lambda}^*,t),$

for all $t \in [t_b,t_f]$, which expresses the sensitivity of the costate for small perturbations in the states.

If the actual initial state, $x(t_b)$, is close to $\bar{x}(t_b)$, and the difference between the actual disturbances, $v(t)$, and the *a priori* estimated disturbances, $\bar{v}(t)$, are small, $\delta x(t)$ will remain small and thus the actual costate trajectory $\lambda(t)$ is well-approximated by

(5.173) $\lambda(t) = \bar{\lambda}^*(t) + M(t)\delta x(t).$

Using this approximation of the perturbed costate, the optimal control associated to the actual system's state $x(t)$ and the disturbances $v(t)$, is then approximated by

(5.174) $u^*(t) = \sigma(x,\lambda,v,t) = \arg \max_u \mathcal{H}(x,\lambda,u,v,t).$

The 'sub-optimal' control algorithm is summarized as follows:

[1.1]   Predict $\bar{v}(t)$, $t \in [t_b,t_f]$, and estimate $\bar{x}(t_b)$.

[1.2]   Calculate and store the nominal solution $\bar{x}^*(t)$, $\bar{\lambda}^*(t)$, $\bar{u}^*(t)$.

[1.3]   Calculate and store the sensitivity matrix $M(t)$.

[2.1]   Set $t = t_b$.

[2.2]   Take a measurement of the actual state, $x(t)$, and a measurement of the disturbance $v(t)$.

[2.3]   Calculate $\delta x(t) = x(t) - \bar{x}^*(t)$ and $\lambda(t) = \bar{\lambda}^*(t) + M(t)\delta x(t)$.

[2.4]   Solve $u^*(t) = \arg \max_u \mathcal{H}(x,\lambda,u,v,t) = \sigma(x,\lambda,v,t)$, subject to the control constraints $u_{i,min}(t) \leq u_i^*(t) \leq u_{i,max}(t)$, $i=1,\ldots,m$.

[2.5]   Apply $u^*(t)$ to the system.

[2.6]   If $t = t_f$, stop; else advance t one time step and go to [2.2].

In this algorithm steps [1.1] to [1.3] constitute the off-line part, and steps [2.1] to [2.6] are performed on-line. A block diagram of the 'sub-optimal' control scheme is depicted in figure 5.2.
    The algorithm has some appealing features. For instance it is easily implemented in an on-line environment. The computationally most involved part of the algorithm, *i.e.* the calculation of the nominal solution in steps [1.1] to [1.3], is performed off-line. Only step [2.4] in the on-line part of the algorithm, *i.e.* the maximization of the Hamiltonian with respect to the control inputs,

may take some computation time. However, an experiment with the climate control system at IMAG-DLO revealed that these calculations do not cause any timing problems with the currently available computer hardware and software (Van Meurs and Van Henten, 1994).

Fig. 5.2 shows that the control algorithm contains a state feedback loop and a feedforward of the exogenous inputs. The state feedback loop will deal with perturbations of the system's state due to modelling errors, errors in the estimates of the initial conditions of the process and errors in the weather prediction. In greenhouse climate control, the feedforward of the disturbances will be extremely important. Because of the slow response of the crop growth process, the effect of the exogenous inputs on crop growth and consequently on the economic return will become noticeable after quite a long time. Since exogenous inputs like solar radiation, wind speed and air temperature largely determine the operating costs of the climate conditioning equipment, favourable results are expected when the disturbances are dealt with immediately in a feedforward scheme instead of in a state feedback loop after their effects on the process have become visible.
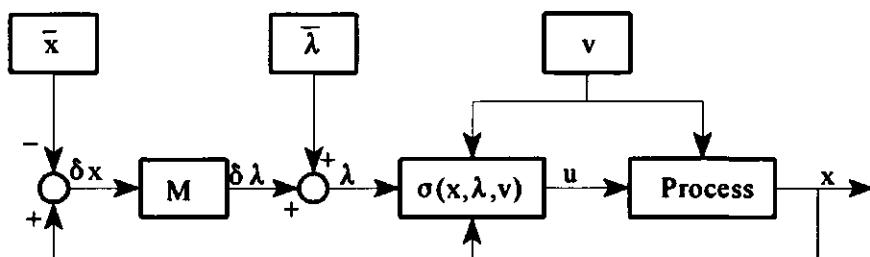

Fig. 5.2. The sub-optimal feedback, feedforward control algorithm in which $\bar{x}$ and $\bar{\lambda}$ are the nominal state and costate trajectories, M is the costate sensitivity matrix $\partial \lambda / \partial x$, x is the actual state of the process, v is the actual disturbance, λ is the approximation of the actual costate and $\sigma(x,\lambda,v)$ is the non-linear feedback law.

Feedback and feedforward control require measurements or at least estimates of the state variables and exogenous inputs. In greenhouse climate control measurements of inside and outside climatic conditions such as solar radiation, air temperature and

humidity, are readily available. Frequent measurements of the state of the crop are much more difficult to obtain, at least in a non-destructive way. In appendix A, a non-destructive method based on image processing to determine the dry matter content of a lettuce crop is described and evaluated.

For small perturbations in the system model, the initial conditions and the exogenous inputs, the algorithm will give near-optimum performance. One source of error which plays an important role in optimal greenhouse climate role is not considered in this control scheme, namely uncertainty in the performance criterion. The performance criterion used in this thesis is based on an estimate of the auction price of lettuce. As was illustrated in chapter 4, a considerable variance in the auction price of lettuce exists which makes its prediction to some extent inaccurate. The observed variance in the auction price may be included in the control system design within the framework of stochastic optimal control. A simpler and more practical approach will be to recalculate, say once every week, new nominal trajectories of the state, costate and control variables for the remaining part of the growing period once a new estimate of the auction price has become available. These new nominal trajectories are then stored in the control computer and used in the on-line part of the algorithm.

Friedland and Sarachnik (1966) stated that there exists a relationship between the algorithm outlined above and second variation or perturbation control algorithms. A more detailed description of these algorithms can be found in Bryson and Ho (1975) and Lewis (1986). In this thesis, this relation will not be elaborated upon. There is however one significant difference between the two approaches, namely that in the approach of Friedman and Sarachnik, control constraints can be included in a straightforward way, whereas in the perturbation control approach this is much more complicated.

6. SYNTHESIS

6.1. Introduction

This chapter contains a synthesis of the material presented so far. The optimal greenhouse climate control problem which was formulated in chapter 2 in general terms, will be restated in more detail in this chapter. Based on the observed differences in response times between crop growth and greenhouse climate (see chapter 3), the greenhouse climate control problem will be formulated as a singular perturbed control problem in which the state of the crop is considered as a slow state variable, denoted by X. The greenhouse climate variables, air temperature, carbon dioxide concentration and humidity are considered to be fast state variables, denoted by Z. It is assumed that in the group of slow state variables X as well as in the group of fast state variables Z no further differences in response times do exist.

In sections 6.2 and 6.3, two control problems will be defined. In the first problem (section 6.2), the state of the crop is represented by one state variable, *i.e.* total crop dry weight X_d. In the second problem (section 6.3), the state of the crop is represented by two state variables, namely non-structural dry weight, X_n, and structural dry weight, X_s. In both control problems, the greenhouse climate variables are air temperature Z_t, carbon dioxide concentration, Z_c, and humidity, Z_h. The model equations and parameters have been presented in chapter 3.

In section 6.2, necessary conditions will be presented for the full singularly perturbed control problem. Also the two time-scale decomposition, derived in section 5.6, will be illustrated using this control problem. Though the resulting equations are rather extensive, it is worth analysing them since they reveal some particularities of the control problem considered. Results of this analysis are presented in section 6.4.

6.2. Control problem 1

6.2.1. The full problem

The dynamics of the state variables are described by the differential equations

(6.1a) $\quad \dfrac{dX_d}{dt} = c_{\alpha\beta}\left(1-e^{-c_{pl,d}X_d}\right)\dfrac{c_1V_1(-c_{co2,1}Z_t^2+c_{co2,2}Z_t-c_{co2,3})(Z_c-c_\Gamma)}{c_1V_1+(-c_{co2,1}Z_t^2+c_{co2,2}Z_t-c_{co2,3})(Z_c-c_\Gamma)}$

$\qquad\qquad - c_{resp,1}X_d2^{(0.1Z_t-2.5)}$ kg m^{-2} s^{-1},

(6.1b) $\quad \varepsilon\dfrac{dZ_c}{dt} = \dfrac{1}{c_{cap,c}}\left(-\left(1-e^{-c_{pl,d}X_d}\right)\dfrac{c_1V_1(-c_{co2,1}Z_t^2+c_{co2,2}Z_t-c_{co2,3})(Z_c-c_\Gamma)}{c_1V_1+(-c_{co2,1}Z_t^2+c_{co2,2}Z_t-c_{co2,3})(Z_c-c_\Gamma)}\right.$

$\qquad\qquad \left. + c_{resp,2}X_d2^{(0.1Z_t-2.5)} + U_c - (U_v+c_{leak})(Z_c-V_c)\right)$ kg m^{-3} s^{-1},

(6.1c) $\quad \varepsilon\dfrac{dZ_t}{dt} = \dfrac{1}{c_{cap,q}}\left[U_q - (c_{cap,q,v}U_v+c_{al,ou})(Z_t-V_t) + c_{rad}V_1\right]$ ^{o}C s^{-1},

(6.1d) $\quad \varepsilon\dfrac{dZ_h}{dt} = \dfrac{1}{c_{cap,h}}\left(\left(1-e^{-c_{pl,d}X_d}\right)c_{v,pl,al}\left(\dfrac{c_{v,5}}{c_R(Z_t+c_{t,abs})}e^{\frac{c_{v,2}Z_t}{Z_t+c_{v,3}}}-Z_h\right)\right.$

$\qquad\qquad \left. - (U_v+c_{leak})(Z_h-V_h)\right)$ kg m^{-3} s^{-1},

with total crop dry weight, X_d [kg m^{-2}], carbon dioxide concentration, Z_c [kg m^{-3}], air temperature, Z_t [^{o}C], humidity, Z_h [kg m^{-3}], solar radiation, V_1 [W m^{-2}], outside air temperature, V_t [^{o}C], outside carbon dioxide concentration, V_c [kg m^{-3}], outside humidity, V_h [kg m^{-3}], energy supply by the heating system, U_q [W m^{-2}], ventilation rate, U_v [m s^{-1}], and the carbon dioxide supply rate U_c [kg m^{-2} s^{-1}]. To circumvent the complexity of finding a proper value for the time scaling parameter ε, in this research it is given a nominal value of 1. The actual value of ε does not play a role if in the computation of the optimal control for the singular perturbed system only the zero-th order terms are used. However,

knowledge of ε is required to decide whether higher-order corrections are necessary and to carry out these corrections (Shridar and Gupta, 1980; Shinar, 1983).

The performance criterion related to the above system is

$$(6.2) \qquad J(U_c, U_v, U_q) = c_{pri,1} + c_{pri,2} X_d(t_f) - \int_{t_b}^{t_f} c_{co2} U_c + c_q U_q \, dt \qquad \text{ct m}^{-2}.$$

The control inputs are constrained by

$$(6.3) \qquad U_{c,min} \le U_c \le U_{c,max}, \; U_{v,min} \le U_v \le U_{v,max}(V_W),$$
$$U_{q,min} \le U_q \le U_{q,max},$$

the greenhouse climate variables are constrained by

$$(6.4) \qquad Z_{c,min} \le Z_c \le Z_{c,max}, \; Z_{t,min} \le Z_t \le Z_{t,max},$$
$$Z_{h,min}(Z_t) \le Z_h \le Z_{h,max}(Z_t),$$

with $Z_{h,min}(Z_t) = RZ_{h,min} H_{sat}(Z_t)$, $Z_{h,max}(Z_t) = RZ_{h,max} H_{sat}(Z_t)$, $RZ_{h,min}$ and $RZ_{h,max}$ being a lower and an upper bound on the relative humidity and $H_{sat}(Z_t)$ is the saturated humidity level defined by

$$H_{sat}(Z_t) = \frac{c_{v,6}}{c_R(Z_t + c_{t,abs})} e^{\frac{c_{v,2} Z_t}{Z_t + c_{v,3}}} \qquad \text{kg m}^{-3}.$$

With these preliminaries, the control problem is defined as

$$(6.5) \qquad (U_c^*, U_v^*, U_q^*) = \arg \max_{U_c, U_v, U_q} J(U_c, U_v, U_q)$$

subject to the system equations (6.1) and the control and state constraints (6.3) and (6.4).

To account for the state constraints, the performance criterion is augmented with penalty functions conforming to eqn. (5.45):

(6.6) $J(U_c,U_v,U_q) = c_{pri,1} + c_{pri,2}X_d(t_f)$

$$- \int_{t_b}^{t_f} \left(c_{co2}U_c + c_qU_q + \zeta_c \left[\frac{2Z_c-Z_{c,max}-Z_{c,min}}{Z_{c,max}-Z_{c,min}} \right]^{2k} \right.$$

$$\left. + \zeta_t \left[\frac{2Z_t-Z_{t,max}-Z_{t,min}}{Z_{t,max}-Z_{t,min}} \right]^{2k} + \zeta_h \left[\frac{2Z_h-Z_{h,max}(Z_t)-Z_{h,min}(Z_t)}{Z_{h,max}(Z_t)-Z_{h,min}(Z_t)} \right]^{2k} \right) dt.$$

The parameterization of the performance criterion and state constraints is listed in table 6.1. The model parameters have been listed in tables 3.1, 3.3 and 3.6.

Table 6.1.   The parameterization of the performance criterion and state constraints.

Parameter	Value	Parameter	Value
$U_{c,min}$	0. kg m^{-2} s^{-1}	ζ_c	1×10^{-5}
$U_{c,max}$	1.2×10^{-6} kg m^{-2} s^{-1}	ζ_t	5×10^{-5}
$U_{v,min}$	0. m s^{-1}	ζ_h	1×10^{-2}
$U_{v,max}$	$7.5\times10^{-3}V_w$ m s^{-1}	k	20
$U_{q,min}$	0. W m^{-2}	$Z_{c,min}$	0. kg m^{-3}
$U_{q,max}$	150. W m^{-2}	$Z_{c,max}$	2.75×10^{-3} kg m^{-3}
$c_{pri,1}$	180. ct m^{-2}	$Z_{t,min}$	6.5 °C
$c_{pri,2}$	1600. ct kg^{-1}	$Z_{t,max}$	40. °C
c_{co2}	42. ct kg^{-1}	$RZ_{h,min}$	0.
c_q	6.35×10^{-7} ct J^{-1}	$RZ_{h,max}$	0.9

In the simulations presented in chapter 7, measured data of the control inputs and weather obtained during the second greenhouse

experiment in early 1992 will be used. This facilitates for instance a comparison of the performance of optimal greenhouse climate management with greenhouse climate control supervised by the grower. The maximum carbon dioxide supply rate, $U_{c,max}$, was taken to be equal to the supply rate installed in the experimental greenhouse. The maximum ventilation rate, $U_{v,max}$, depends on the outside wind speed and was determined from the first term in eqn. (3.28) setting the aperture of the lee and wind ward side ventilation windows at 100%. The maximum capacity of the heating system, $U_{q,max}$, was set equal to the design specifications of the experimental greenhouse.

Since the second greenhouse experiment ended in the 11th week of 1992, following the same approach as described in chapter 4, analysis of the auction price of lettuce during this week obtained from the Central Bureau of Fruit and Vegetable Auctions (CBT), yielded a linear relationship between the weight of a lettuce head and the price as shown in fig. 6.1. The intercept was found to be 10. ct head^{-1}, which yields $c_{pri,2}$ = 180. ct m^{-2}, at a plant density of 18 plants per square meter of soil. The additional income from a
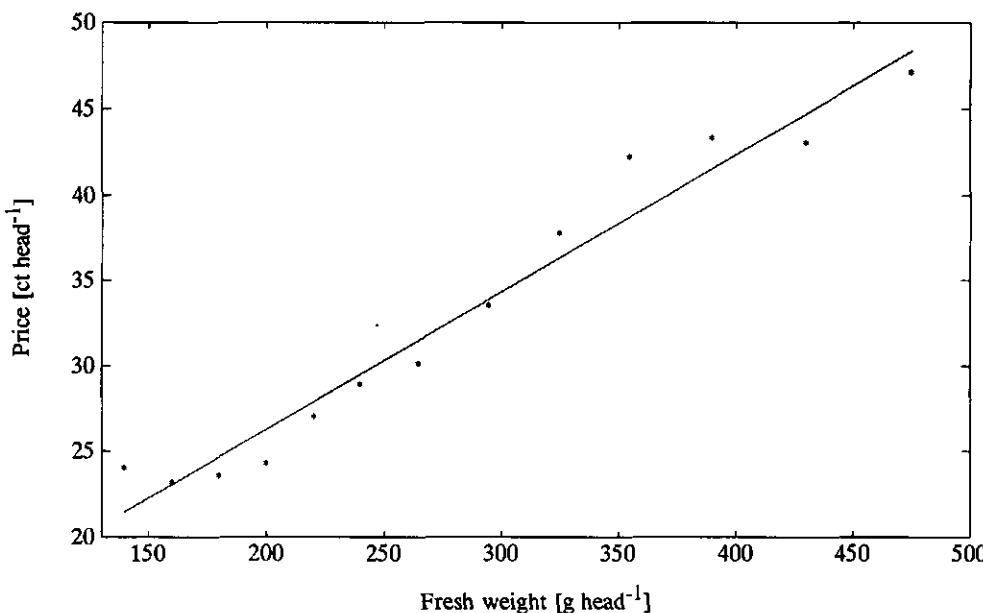

Fig. 6.1. The relation between the harvest fresh weight of lettuce and the auction price during the 11th week of 1992.

higher harvest fresh weight was found to be 0.08 ct g^{-1}. With the dry matter content of lettuce being approximately 4.5% and a shoot to total dry weight ratio of 0.93 this resulted in the additional revenue due to an additional amount of dry matter $c_{prl,2}$ = 1600. ct kg^{-1}. The price per unit energy consumption, c_q, was calculated on the basis of a price of natural gas of 20 ct m^{-3} and an energy conversion of 30×10^6 J m^{-3}.

The upper bound of the carbon dioxide concentration was defined as 1500 ppm which equals 2.75×10^{-3} kg m^{-3} for a density of carbon dioxide of 1.830 kg m^{-3}. Temperatures above 40 °C are considered lethal for crops like lettuce and therefore the upper bound on air temperature, $Z_{t,max}$, was defined accordingly. In practice, 5 °C is considered to be a minimum temperature for lettuce production. Since around that temperature numerical problems occur in the model (section 3.2.2.1), the lower bound on the temperature, $Z_{t,min}$, was defined slightly higher. In the greenhouse experiment, with respect to humidity control, the main objective of the grower was to prevent high humidity levels so only an upper bound on the relative humidity was used and $RZ_{h,min}$ = 0. It was suggested by Corver (1991) that a relative humidity exceeding 90% should be prevented during lettuce production and the upper limit on the relative humidity, $RZ_{h,max}$, was defined accordingly. Finally, the parameters ζ_c, ζ_t, ζ_h and k were given suitable values during test simulations.

For this particular problem the Hamiltonian is defined as

$$(6.7) \quad \mathcal{H} = - c_{co2}U_c - c_q U_q - \zeta_c \left(\frac{2Z_c - Z_{c,max} - Z_{c,min}}{Z_{c,max} - Z_{c,min}} \right)^{2k}$$

$$- \zeta_t \left(\frac{2Z_t - Z_{t,max} - Z_{t,min}}{Z_{t,max} - Z_{t,min}} \right)^{2k} - \zeta_h \left(\frac{2Z_h - Z_{h,max}(Z_t) - Z_{h,min}(Z_t)}{Z_{h,max}(Z_t) - Z_{h,min}(Z_t)} \right)^{2k}$$

$$+ \lambda_d \left(c_{\alpha\beta} \left(1 - e^{-c_{pl,d}X_d} \right) \frac{c_1 V_1 (-c_{co2,1}Z_t^2 + c_{co2,2}Z_t - c_{co2,3})(Z_c - c_\Gamma)}{c_1 V_1 + (-c_{co2,1}Z_t^2 + c_{co2,2}Z_t - c_{co2,3})(Z_c - c_\Gamma)} \right.$$

$$- c_{resp,1}X_d 2^{(0.1Z_t-2.5)}\Big)$$

$$+ \frac{\eta_c}{c_{cap,c}}\Bigg(-\Big(1-e^{-c_{pl,d}X_d}\Big)\frac{c_1V_1(-c_{co2,1}Z_t^2+c_{co2,2}Z_t-c_{co2,3})(Z_c-c_\Gamma)}{c_1V_1+(-c_{co2,1}Z_t^2+c_{co2,2}Z_t-c_{co2,3})(Z_c-c_\Gamma)}$$

$$+ c_{resp,2}X_d 2^{(0.1Z_t-2.5)} + U_c - (U_v+c_{leak})(Z_c-V_c)\Bigg)$$

$$+ \frac{\eta_t}{c_{cap,q}}\Bigg(U_q - (c_{cap,q,v}U_v+c_{al,ou})(Z_t-V_t) + c_{rad}V_1\Bigg)$$

$$+ \frac{\eta_h}{c_{cap,h}}\Bigg(\Big(1-e^{-c_{pl,d}X_d}\Big)c_{v,pl,al}\Big(\frac{c_{v,5}}{c_R(Z_t+c_{t,abs})}e^{\frac{c_{v,2}Z_t}{Z_t+c_{v,3}}}-Z_h\Big)$$

$$- (U_v+c_{leak})(Z_h-V_h)\Bigg) \qquad\qquad\qquad \text{ct m}^{-2}\text{ s}^{-1},$$

in which λ and η are costate variables related to the 'slow' state variables and the 'fast' state variables, respectively. The subscripts refer to the associated state variables in accordance with their definition.

A relation for the costate dynamics is obtained by taking the partial derivatives of the Hamiltonian with respect to the state variables:

$$(6.8a) \quad -\frac{d\lambda_d}{dt} = \frac{\partial \mathcal{H}}{\partial X_d} =$$

$$\lambda_d\Bigg(c_{\alpha\beta}c_{pl,d}e^{-c_{pl,d}X_d}\frac{c_1V_1(-c_{co2,1}Z_t^2+c_{co2,2}Z_t-c_{co2,3})(Z_c-c_\Gamma)}{c_1V_1+(-c_{co2,1}Z_t^2+c_{co2,2}Z_t-c_{co2,3})(Z_c-c_\Gamma)}$$

$$- c_{resp,1}2^{(0.1Z_t-2.5)}\Bigg)$$

$$+ \frac{\eta_c}{c_{cap,c}}\left(-c_{pl,d}e^{-c_{pl,d}X_d}\frac{c_1V_1(-c_{co2,1}Z_t^2+c_{co2,2}Z_t-c_{co2,3})(Z_c-c_\Gamma)}{c_1V_1+(-c_{co2,1}Z_t^2+c_{co2,2}Z_t-c_{co2,3})(Z_c-c_\Gamma)}\right.$$

$$\left. + c_{resp,2}2^{(0.1Z_t-2.5)}\right)$$

$$+ \frac{\eta_h}{c_{cap,h}}c_{pl,d}e^{-c_{pl,d}X_d}c_{v,pl,al}\left(\frac{c_{v,5}}{c_R(Z_t+c_{t,abs})}e^{\frac{c_{v,2}Z_t}{Z_t+c_{v,3}}}-Z_h\right)$$

$$\text{ct kg}^{-1}\text{ s}^{-1},$$

$$(6.8b)\quad -\varepsilon\frac{d\eta_c}{dt} = \frac{\partial\mathcal{H}}{\partial Z_c} = -\left(\frac{4k\zeta_c}{Z_{c,max}-Z_{c,min}}\right)\left(\frac{2Z_c-Z_{c,max}-Z_{c,min}}{Z_{c,max}-Z_{c,min}}\right)^{2k-1}$$

$$+ \lambda_d\frac{c_{\alpha\beta}\left(1-e^{-c_{pl,d}X_d}\right)\left(c_1V_1\right)^2(-c_{co2,1}Z_t^2+c_{co2,2}Z_t-c_{co2,3})}{\left(c_1V_1+(-c_{co2,1}Z_t^2+c_{co2,2}Z_t-c_{co2,3})(Z_c-c_\Gamma)\right)^2}$$

$$+ \frac{\eta_c}{c_{cap,c}}\left(-\frac{\left(1-e^{-c_{pl,d}X_d}\right)\left(c_1V_1\right)^2(-c_{co2,1}Z_t^2+c_{co2,2}Z_t-c_{co2,3})}{\left(c_1V_1+(-c_{co2,1}Z_t^2+c_{co2,2}Z_t-c_{co2,3})(Z_c-c_\Gamma)\right)^2}-(U_v+c_{leak})\right)$$

$$\text{ct m kg}^{-1}\text{ s}^{-1},$$

$$(6.8c)\quad -\varepsilon\frac{d\eta_t}{dt} = \frac{\partial\mathcal{H}}{\partial Z_t} = -\left(\frac{4k\zeta_t}{Z_{t,max}-Z_{t,min}}\right)\left(\frac{2Z_t-Z_{t,max}-Z_{t,min}}{Z_{t,max}-Z_{t,min}}\right)^{2k-1}$$

$$- 2k\zeta_h \left(\frac{2Z_h - Z_{h,max}(Z_t) - Z_{h,min}(Z_t)}{Z_{h,max}(Z_t) - Z_{h,min}(Z_t)} \right)^{2k-1} \left(\frac{-2Z_h(RZ_{h,max} - RZ_{h,min})}{\left(Z_{h,max}(Z_t) - Z_{h,min}(Z_t) \right)^2} \right)$$

$$\left(- \frac{c_{v,6}c_R}{\left(c_R(Z_t + c_{t,abs}) \right)^2} + \frac{c_{v,6}c_{v,2}c_{v,3}}{c_R(Z_t + c_{t,abs})\left(Z_t + c_{v,3} \right)^2} \right) e^{\frac{c_{v,2}Z_t}{Z_t + c_{v,3}}}$$

$$+ \lambda_d \left(\frac{c_{\alpha\beta}\left(1 - e^{-c_{pl,d}X_d} \right)\left(c_l V_l \right)^2 (Z_c - c_\Gamma)(-2c_{co2,1}Z_t + c_{co2,2})}{\left(c_l V_l + (-c_{co2,1}Z_t^2 + c_{co2,2}Z_t - c_{co2,3})(Z_c - c_\Gamma) \right)^2} \right.$$

$$\left. - 0.1\ln(2)c_{resp,1}X_d 2^{(0.1Z_t - 2.5)} \right)$$

$$+ \frac{\eta_c}{c_{cap,c}} \left(- \frac{\left(1 - e^{-c_{pl,d}X_d} \right)\left(c_l V_l \right)^2 (Z_c - c_\Gamma)(-2c_{co2,1}Z_t + c_{co2,2})}{\left(c_l V_l + (-c_{co2,1}Z_t^2 + c_{co2,2}Z_t - c_{co2,3})(Z_c - c_\Gamma) \right)^2} \right.$$

$$\left. + 0.1\ln(2)c_{resp,2}X_d 2^{(0.1Z_t - 2.5)} \right) - \frac{\eta_t}{c_{cap,q}} \left(c_{cap,q,v}U_v + c_{al,ou} \right)$$

$$+ \frac{\eta_h}{c_{cap,h}} \left(1 - e^{-c_{pl,d}X_d} \right) c_{v,pl,al} e^{\frac{c_{v,2}Z_t}{Z_t + c_{v,3}}}$$

$$\left(- \frac{c_{v,5}c_R}{\left(c_R(Z_t + c_{t,abs}) \right)^2} + \frac{c_{v,2}c_{v,3}c_{v,5}}{c_R(Z_t + c_{t,abs})\left(Z_t + c_{v,3} \right)^2} \right) \quad \text{ct m}^{-2}\ {}^\circ\text{C}^{-1}\ \text{s}^{-1},$$

(6.8d) $-\varepsilon\dfrac{d\eta_h}{dt} = \dfrac{\partial \mathcal{H}}{\partial Z_h} =$

$$-\left(\frac{4k\zeta_h}{Z_{h,max}(Z_t)-Z_{h,min}(Z_t)}\right)\left(\frac{2Z_h-Z_{h,max}(Z_t)-Z_{h,min}(Z_t)}{Z_{h,max}(Z_t)-Z_{h,min}(Z_t)}\right)^{2k-1}$$

$$+\frac{\eta_h}{c_{cap,h}}\left(-\left(1-e^{-c_{pl,d}X_d}\right)c_{v,pl,ai} - (U_v+c_{leak})\right) \qquad \text{ct m kg}^{-1}\text{ s}^{-1}.$$

According to the maximum principle of Pontryagin it is required that

(6.9) $\mathcal{H}(X^*,Z^*,U,V,\lambda^*,\eta^*) \leq \mathcal{H}(X^*,Z^*,U^*,V,\lambda^*,\eta^*)$

with $X = X_d,$ $Z = [Z_c,Z_t,Z_h]^T,$ $U = [U_c,U_v,U_q]^T,$ $\lambda = \lambda_d,$
$\eta = [\eta_c,\eta_t,\eta_h]^T$ and $V = [V_l,V_t,V_w,V_c,V_h]^T.$

Since the Hamiltonian is linear in the control, a so-called bang-singular-bang type of control is expected as the optimizing control strategy. The switching functions are obtained by taking the partial derivatives of the Hamiltonian with respect to the control inputs:

(6.10a) $\dfrac{\partial \mathcal{H}}{\partial U_c} = -c_{co2} + \dfrac{\eta_c}{c_{cap,c}}$ $\text{ct kg}^{-1},$

(6.10b) $\dfrac{\partial \mathcal{H}}{\partial U_v} = -\dfrac{\eta_c(Z_c-V_c)}{c_{cap,c}} - \dfrac{\eta_t c_{cap,q,v}(Z_t-V_t)}{c_{cap,q}} - \dfrac{\eta_h(Z_h-V_h)}{c_{cap,h}}$ $\text{ct m}^{-3},$

(6.10c) $\dfrac{\partial \mathcal{H}}{\partial U_q} = -c_q + \dfrac{\eta_t}{c_{cap,q}}$ $\text{ct J}^{-1}.$

If the switching function equals zero, the associated control is called singular.

6.2.2. The slow sub-problem

In this section, equations for the zero-th order slow sub-problem are presented (see section 5.6.2). In the slow sub-problem, only the crop growth dynamics are explicitly considered. They are described by

$$(6.11a) \quad \frac{d\bar{X}_d}{dt} = c_{\alpha\beta}\left(1-e^{-c_{pl,d}\bar{X}_d}\right)\frac{c_1V_1(-c_{co2,1}\bar{Z}_t^2+c_{co2,2}\bar{Z}_t-c_{co2,3})(\bar{Z}_c-c_\Gamma)}{c_1V_1+(-c_{co2,1}\bar{Z}_t^2+c_{co2,2}\bar{Z}_t-c_{co2,3})(\bar{Z}_c-c_\Gamma)}$$

$$- c_{resp,1}\bar{X}_d2^{(0.1\bar{Z}_t-2.5)} \qquad\qquad \text{kg m}^{-2} \text{ s}^{-1}.$$

The quasi steady-states for Z_c, Z_t and Z_h are solved from eqns. (6.1b) to (6.1d). Setting $\varepsilon = 0$ in eqn. (6.1b) yields

$$0 = -\left(1-e^{-c_{pl,d}\bar{X}_d}\right)\frac{c_1V_1(-c_{co2,1}\bar{Z}_t^2+c_{co2,2}\bar{Z}_t-c_{co2,3})(\bar{Z}_c-c_\Gamma)}{c_1V_1+(-c_{co2,1}\bar{Z}_t^2+c_{co2,2}\bar{Z}_t-c_{co2,3})(\bar{Z}_c-c_\Gamma)}$$

$$+ c_{resp,2}\bar{X}_d2^{(0.1\bar{Z}_t-2.5)} + U_c - (U_v+c_{leak})(\bar{Z}_c-V_c).$$

The solution of $\bar{Z}_c$ proceeds as follows. Define $\alpha = c_{rad}V_1$,

$$\rho = -c_{co2,1}\bar{Z}_t^2+c_{co2,2}\bar{Z}_t-c_{co2,3}, \qquad \omega = (1-e^{-c_{pl,d}\bar{X}_d}), \qquad \tau = U_v+c_{leak},$$

$$\delta = c_{resp,2}\bar{X}_d2^{(0.1\bar{Z}_t-2.5)}+U_c+(\bar{U}_v+c_{leak})(V_c-c_\Gamma) \text{ and } x = \bar{Z}_c-c_\Gamma \text{ then}$$

$$-\omega\frac{\alpha\rho x}{\alpha+\rho x}+\delta-\tau x = 0 \Rightarrow \tau\rho x^2+x(\omega\alpha\rho+\alpha\tau-\delta\rho)-\delta\alpha = 0$$

$$\Rightarrow x = \frac{-(\omega\alpha\rho+\alpha\tau-\delta\rho)\pm\sqrt{(\omega\alpha\rho+\alpha\tau-\delta\rho)^2+4\delta\alpha\tau\rho}}{2\tau\rho}.$$

So, actually two solutions satisfy the steady-state equation for Z_c. However, one of them is not valid, *i.e.* it yields $\bar{Z}_c < 0$. With $\alpha \geq 0$, $\rho \geq 0$ for $5 \leq \bar{Z}_t \leq 40$ °C, $\omega \geq 0$, $\tau \geq 0$ and $\delta \geq 0$ the valid solution is

(6.11b) $\bar{Z}_c = \dfrac{-(\omega\alpha\rho+\alpha\tau-\delta\rho)+\sqrt{(\omega\alpha\rho+\alpha\tau-\delta\rho)^2+4\delta\alpha\tau\rho}}{2\tau\rho} + c_\Gamma$ kg m^{-3}.

Setting $\varepsilon = 0$ in eqns. (6.1c) and (6.1d) results in

$$0 = U_q - (c_{cap,q,v}U_v+c_{al,ou})(\bar{Z}_t-V_t) + c_{rad}V_1,$$

and

$$0 = (1-e^{-c_{pl,d}\bar{X}_d})c_{v,pl,al}\left(\frac{c_{v,5}}{c_R(\bar{Z}_t+c_{t,abs})}e^{\frac{c_{v,2}\bar{Z}_t}{\bar{Z}_t+c_{v,3}}}-\bar{Z}_h\right)$$

$$- (U_v+c_{leak})(\bar{Z}_h-V_h),$$

which yield the following unique real solutions for $\bar{Z}_t$ and $\bar{Z}_h$:

(6.11c) $\bar{Z}_t = \dfrac{(c_{cap,q,v}\bar{U}_v+c_{al,ou})\bar{V}_t + c_{rad}\bar{V}_1 + \bar{U}_q}{(c_{cap,q,v}\bar{U}_v+c_{al,ou})}$ $^\circ$C,

(6.11d) $\bar{Z}_h = \dfrac{\dfrac{\left(1-e^{-c_{pl,d}\bar{X}_d}\right)c_{v,pl,al}c_{v,5}}{c_R(\bar{Z}_t+c_{t,abs})}e^{\frac{c_{v,2}\bar{Z}_t}{\bar{Z}_t+c_{v,3}}} + (\bar{U}_v+c_{leak})V_h}{\left(1-e^{-c_{pl,d}\bar{X}_d}\right)c_{v,pl,al} + (\bar{U}_v+c_{leak})}$ kg m^{-3}.

Since $\bar{Z}_t$ does not depend on $\bar{Z}_c$ and $\bar{Z}_h$, $\bar{Z}_t$ is calculated first. Secondly, $\bar{Z}_c$ and $\bar{Z}_h$ are calculated and the solution is substituted in eqn. (6.11a).

    In this particular example the valid solution of the steady-state equation is rather easily deduced. However, in case more complex multi-variable models are considered, mutual interactions between the state variables may require a numerical solution. Then the uniqueness of the solution is not guaranteed.

    In the zero-th order slow solution the constraints imposed on $\bar{U}$

and $\bar{Z}$ equal the control and state constraints as defined in eqns. (6.3) and (6.4). The performance criterion is defined as

$$(6.12) \quad \bar{J}(\bar{U}_c,\bar{U}_v,\bar{U}_q) = c_{prl,1} + c_{prl,2}\bar{X}_d(t_f)$$

$$- \int_{t_b}^{t_f} \left(c_{co2}\bar{U}_c + c_q\bar{U}_q + \zeta_c \left[\frac{2\bar{Z}_c - Z_{c,max} - Z_{c,min}}{Z_{c,max} - Z_{c,min}} \right]^{2k} \right.$$

$$\left. + \zeta_t \left[\frac{2\bar{Z}_t - Z_{t,max} - Z_{t,min}}{Z_{t,max} - Z_{t,min}} \right]^{2k} + \zeta_h \left[\frac{2\bar{Z}_h - Z_{h,max}(\bar{Z}_t) - Z_{h,min}(\bar{Z}_t)}{Z_{h,max}(\bar{Z}_t) - Z_{h,min}(\bar{Z}_t)} \right]^{2k} \right) dt$$

and the control problem is defined as to find

$$(6.13) \quad (\bar{U}_c^*,\bar{U}_v^*,\bar{U}_q^*) = \arg \max_{\bar{U}_c,\bar{U}_v,\bar{U}_q} \bar{J}(\bar{U}_c,\bar{U}_v,\bar{U}_q),$$

subject to the system equations (6.11) and the control constraints (6.3). For this problem the Hamiltonian is defined as:

$$(6.14) \quad \bar{\mathcal{H}} = -c_{co2}\bar{U}_c - c_q\bar{U}_q - \zeta_c \left[\frac{2\bar{Z}_c - Z_{c,max} - Z_{c,min}}{\bar{Z}_{c,max} - Z_{c,min}} \right]^{2k}$$

$$- \zeta_t \left[\frac{2\bar{Z}_t - Z_{t,max} - Z_{t,min}}{\bar{Z}_{t,max} - Z_{t,min}} \right]^{2k} - \zeta_h \left[\frac{2\bar{Z}_h - Z_{h,max}(\bar{Z}_t) - Z_{h,min}(\bar{Z}_t)}{Z_{h,max}(\bar{Z}_t) - Z_{h,min}(\bar{Z}_t)} \right]^{2k}$$

$$+ \bar{\lambda}_d \left(c_{\alpha\beta} \left(1 - e^{-c_{pl,d}\bar{X}_d} \right) \frac{c_l V_l (-c_{co2,1}\bar{Z}_t^2 + c_{co2,2}\bar{Z}_t - c_{co2,3})(\bar{Z}_c - c_\Gamma)}{c_l V_l + (-c_{co2,1}\bar{Z}_t^2 + c_{co2,2}\bar{Z}_t - c_{co2,3})(\bar{Z}_c - c_\Gamma)} \right.$$

$$\left. - c_{resp,1}\bar{X}_d 2^{(0.1\bar{Z}_t - 2.5)} \right)$$

$$+ \frac{\bar{\eta}_c}{c_{cap,c}}\Bigg(-\Big(1-e^{-c_{pl,d}\bar{X}_d}\Big)\frac{c_1 V_1(-c_{co2,1}\bar{Z}_t^2 + c_{co2,2}\bar{Z}_t - c_{co2,3})(\bar{Z}_c - c_\Gamma)}{c_1 V_1 + (-c_{co2,1}\bar{Z}_t^2 + c_{co2,2}\bar{Z}_t - c_{co2,3})(\bar{Z}_c - c_\Gamma)}$$

$$+ c_{resp,2}\bar{X}_d 2^{(0.1\bar{Z}_t - 2.5)} + \bar{U}_c - (\bar{U}_v + c_{leak})(\bar{Z}_c - V_c)\Bigg)$$

$$+ \frac{\bar{\eta}_t}{c_{cap,q}}\Bigg(\bar{U}_q - (c_{cap,q,v}\bar{U}_v + c_{al,ou})(\bar{Z}_t - V_t) + c_{rad}V_1\Bigg)$$

$$+ \frac{\bar{\eta}_h}{c_{cap,h}}\Bigg(\Big(1-e^{-c_{pl,d}\bar{X}_d}\Big)c_{v,pl,al}\Big(\frac{c_{v,5}}{c_R(\bar{Z}_t + c_{t,abs})}e^{\frac{c_{v,2}\bar{Z}_t}{\bar{Z}_t + c_{v,3}}} - \bar{Z}_h\Big)$$

$$- (\bar{U}_v + c_{leak})(\bar{Z}_h - V_h)\Bigg) \qquad\qquad ct\ m^{-2}\ s^{-1}.$$

The dynamics of the slow costate $\bar{\lambda}_d$ are governed by the equation

$$(6.15a)\quad -\frac{d\bar{\lambda}_d}{dt} = \bar{\lambda}_d\Bigg(c_{\alpha\beta}c_{pl,d}e^{-c_{pl,d}\bar{X}_d}\frac{c_1 V_1(-c_{co2,1}\bar{Z}_t^2 + c_{co2,2}\bar{Z}_t - c_{co2,3})(\bar{Z}_c - c_\Gamma)}{c_1 V_1 + (-c_{co2,1}\bar{Z}_t^2 + c_{co2,2}\bar{Z}_t - c_{co2,3})(\bar{Z}_c - c_\Gamma)}$$

$$- c_{resp,1}2^{(0.1\bar{Z}_t - 2.5)}\Bigg)$$

$$+ \frac{\bar{\eta}_c}{c_{cap,c}}\Bigg(-c_{pl,d}e^{-c_{pl,d}\bar{X}_d}\frac{c_1 V_1(-c_{co2,1}\bar{Z}_t^2 + c_{co2,2}\bar{Z}_t - c_{co2,3})(\bar{Z}_c - c_\Gamma)}{c_1 V_1 + (-c_{co2,1}\bar{Z}_t^2 + c_{co2,2}\bar{Z}_t - c_{co2,3})(\bar{Z}_c - c_\Gamma)}$$

$$+ c_{resp,2}2^{(0.1\bar{Z}_t - 2.5)}\Bigg)$$

$$+ \frac{\bar{\eta}_h}{c_{cap,h}}c_{pl,d}e^{-c_{pl,d}\bar{X}_d}c_{v,pl,al}\Big(\frac{c_{v,5}}{c_R(\bar{Z}_t + c_{t,abs})}e^{\frac{c_{v,2}\bar{Z}_t}{\bar{Z}_t + c_{v,3}}} - \bar{Z}_h\Big) \quad ct\ kg^{-1}\ s^{-1},$$

The quasi steady-state costates $\bar{\eta}_c$, $\bar{\eta}_t$ and $\bar{\eta}_h$ are derived from eqns. (6.8b) to (6.8d) by setting $\varepsilon = 0$ and rewriting the equations making use of their linear structure with respect to the costates. This procedure has been described in appendix C in some detail.

$$
(6.15b) \quad \bar{\eta}_c = \left\{ \frac{c_{\text{cap,c}}}{-\dfrac{\left(1-e^{-c_{\text{pl,d}}\bar{X}_d}\right)\left(c_lV_l\right)^2\left(-c_{\text{co2,1}}\bar{Z}_t^2+c_{\text{co2,2}}\bar{Z}_t-c_{\text{co2,3}}\right)}{\left[c_lV_l+(-c_{\text{co2,1}}\bar{Z}_t^2+c_{\text{co2,2}}\bar{Z}_t-c_{\text{co2,3}})(\bar{Z}_c-c_\Gamma)\right]^2} -(\bar{U}_v+c_{\text{leak}})} \right.
$$

$$
\left\{ \left(\frac{4k\zeta_c}{Z_{c,\max}-Z_{c,\min}}\right)\left(\frac{2\bar{Z}_c-Z_{c,\max}-Z_{c,\min}}{Z_{c,\max}-Z_{c,\min}}\right)^{2k-1} \right.
$$

$$
\left. - \bar{\lambda}_d c_{\alpha\beta} \frac{\left(1-e^{-c_{\text{pl,d}}\bar{X}_d}\right)\left(c_lV_l\right)^2\left(-c_{\text{co2,1}}\bar{Z}_t^2+c_{\text{co2,2}}\bar{Z}_t-c_{\text{co2,3}}\right)}{\left[c_lV_l+(-c_{\text{co2,1}}\bar{Z}_t^2+c_{\text{co2,2}}\bar{Z}_t-c_{\text{co2,3}})(\bar{Z}_c-c_\Gamma)\right]^2} \right\} \quad \text{ct m kg}^{-1},
$$

$$
(6.15c) \quad \bar{\eta}_t = \left(\frac{c_{\text{cap,q}}}{c_{\text{cap,q,v}}\bar{U}_v+c_{\text{ai,ou}})}\right)\left\{ -\left(\frac{4k\zeta_t}{Z_{t,\max}-Z_{t,\min}}\right)\left(\frac{2\bar{Z}_t-Z_{t,\max}-Z_{t,\min}}{Z_{t,\max}-Z_{t,\min}}\right)^{2k-1} \right.
$$

$$
- 2k\zeta_h\left(\frac{2\bar{Z}_h-Z_{h,\max}(\bar{Z}_t)-Z_{h,\min}(\bar{Z}_t)}{Z_{h,\max}(\bar{Z}_t)-Z_{h,\min}(\bar{Z}_t)}\right)^{2k-1}\left(\frac{-2\bar{Z}_h(RZ_{h,\max}-RZ_{h,\min})}{\left[Z_{h,\max}(\bar{Z}_t)-Z_{h,\min}(\bar{Z}_t)\right]^2}\right)
$$

$$
\left(-\frac{c_{v,6}c_R}{\left[c_R(\bar{Z}_t+c_{t,\text{abs}})\right]^2} + \frac{c_{v,6}c_{v,2}c_{v,3}}{c_R(\bar{Z}_t+c_{t,\text{abs}})\left[\bar{Z}_t+c_{v,3}\right]^2}\right)e^{\dfrac{c_{v,2}\bar{Z}_t}{\bar{Z}_t+c_{v,3}}}
$$

$$+ \bar{\lambda}_d \Bigg(\frac{c_{\alpha\beta}\left(1-e^{-c_{lar,d}\bar{X}_d}\right)\left(c_1 V_1\right)^2 (\bar{Z}_c - c_\Gamma)(-2c_{co2,1}\bar{Z}_t + c_{co2,2})}{\left[c_1 V_1 + (-c_{co2,1}\bar{Z}_t^2 + c_{co2,2}\bar{Z}_t - c_{co2,3})(\bar{Z}_c - c_\Gamma)\right]^2}$$

$$- 0.1\ln(2)c_{resp,1}\bar{X}_d 2^{\left(0.1\bar{Z}_t - 2.5\right)} \Bigg)$$

$$+ \frac{\bar{\eta}_c}{c_{cap,c}}\Bigg(\frac{\left(1-e^{-c_{lar,d}\bar{X}_d}\right)\left(c_1 V_1\right)^2 (\bar{Z}_c - c_\Gamma)(-2c_{co2,1}\bar{Z}_t + c_{co2,2})}{\left[c_1 V_1 + (-c_{co2,1}\bar{Z}_t^2 + c_{co2,2}\bar{Z}_t - c_{co2,3})(\bar{Z}_c - c_\Gamma)\right]^2}$$

$$+ 0.1\ln(2)c_{resp,2}\bar{X}_d 2^{\left(0.1\bar{Z}_t - 2.5\right)} \Bigg)$$

$$+ \frac{\bar{\eta}_h}{c_{cap,h}}\left(1-e^{-c_{pl,d}\bar{X}_d}\right)c_{v,pl,al}e^{\frac{c_{v,2}\bar{Z}_t}{\bar{Z}_t + c_{v,3}}}$$

$$\Bigg[-\frac{c_{v,5}c_R}{\left(c_R(\bar{Z}_t + c_{t,abs})\right)^2} + \frac{c_{v,5}c_{v,2}c_{v,3}}{c_R(\bar{Z}_t + c_{t,abs})\left(\bar{Z}_t + c_{v,3}\right)^2} \Bigg] \Bigg\} \qquad \text{ct m}^{-2}\ {}^{\circ}\text{C}^{-1},$$

$$(6.15d) \quad \bar{\eta}_h = \frac{\left(\dfrac{4k\zeta_h}{Z_{h,max}(\bar{Z}_t) - Z_{h,min}(\bar{Z}_t)}\right)\left(\dfrac{2\bar{Z}_h - Z_{h,max}(\bar{Z}_t) - Z_{h,min}(\bar{Z}_t)}{Z_{h,max}(\bar{Z}_t) - Z_{h,min}(\bar{Z}_t)}\right)^{2k-1}}{\dfrac{1}{c_{cap,h}}\left(-\left(1-e^{-c_{pl,d}\bar{X}_d}\right)c_{v,pl,ai} - (\bar{U}_v + c_{leak})\right)}$$

$$\text{ct m kg}^{-1}.$$

Since $\bar{\eta}_c$ and $\bar{\eta}_h$ do not depend on $\bar{\eta}_t$, they are calculated first and then substituted in eqn. (6.15c) to obtain $\bar{\eta}_t$. Finally, the gradient of the Hamiltonian with respect to the control inputs is defined as

$$(6.16a) \qquad \frac{\partial \bar{\mathcal{H}}}{\partial \bar{U}_c} = -c_{co2} + \frac{\bar{\eta}_c}{c_{cap,c}} \qquad\qquad \text{ct kg}^{-1},$$

$$(6.16b) \qquad \frac{\partial \bar{\mathcal{H}}}{\partial \bar{U}_v} = -\frac{\bar{\eta}_c(\bar{Z}_c - V_t)}{c_{cap,c}} - \frac{\bar{\eta}_t c_{cap,q,v}(\bar{Z}_t - V_t)}{c_{cap,q}} - \frac{\bar{\eta}_h(\bar{Z}_h - V_h)}{c_{cap,h}} \qquad \text{ct m}^{-3},$$

$$(6.16c) \qquad \frac{\partial \bar{\mathcal{H}}}{\partial \bar{U}_q} = -c_q + \frac{\bar{\eta}_t}{c_{cap,q}} \qquad\qquad \text{ct J}^{-1}.$$

6.2.3. The fast sub-problem

In this section, equations of the zero-th order fast sub-problem are given (see section 5.6.2). In the fast sub-problem the slow state variable $\bar{X}_d$, the slow costate variable $\bar{\lambda}_d$ and the slow control inputs $\bar{U}_c$, $\bar{U}_v$, $\bar{U}_q$ are used as slow reference inputs and the dynamics of the fast system's states are described by

$$(6.17a) \qquad \frac{dZ_c}{dt} = \frac{1}{c_{cap,c}}\left(-\left(1-e^{-c_{pl,d}\bar{X}_d}\right)\frac{c_l V_l(-c_{co2,1}Z_t^2 + c_{co2,2}Z_t - c_{co2,3})(Z_c - c_\Gamma)}{c_l V_l + (-c_{co2,1}Z_t^2 + c_{co2,2}Z_t - c_{co2,3})(Z_c - c_\Gamma)}\right.$$

$$\left. + c_{resp,2}\bar{X}_d 2^{(0.1Z_t - 2.5)} + U_c - (U_v + c_{leak})(Z_c - V_c)\right) \qquad \text{kg m}^{-3}\text{ s}^{-1},$$

$$(6.17b) \qquad \frac{dZ_t}{dt} = \frac{1}{c_{cap,q}}\left(U_q - (c_{cap,q,v}U_v + c_{al,ou})(Z_t - V_t) + c_{rad}V_l\right) \qquad {}^\circ\text{C s}^{-1},$$

$$(6.17c) \quad \frac{dZ_h}{dt} = \frac{1}{c_{cap,h}}\left(\left(\left(1-e^{-c_{pl,d}\bar{X}_d}\right)c_{v,pl,ai}\left(\frac{c_{v,5}}{c_R(Z_t+c_{t,abs})}e^{\frac{c_{v,2}Z_t}{Z_t+c_{v,3}}}-Z_h\right)\right.\right.$$

$$\left.\left. - (U_v+c_{leak})(Z_h-V_h)\right)\right] \qquad\qquad \text{kg m}^{-3}\text{ s}^{-1}.$$

The control inputs are constrained by the control constraint equations (6.3) and the state constraints are described by equation (6.4).

As shown in section 5.6.2, the performance criterion considered in the fast sub-problem is defined as:

$$(6.18) \quad \hat{J}(U_c,U_v,U_q) = \int_{t_b}^{t_f}\left(- c_{co2}U_c + c_{co2}\bar{U}_c - c_qU_q + c_q\bar{U}_q\right.$$

$$- \zeta_c\left(\frac{2Z_c-Z_{c,max}-Z_{c,min}}{Z_{c,max}-Z_{c,min}}\right)^{2k} + \zeta_c\left(\frac{2\bar{Z}_c-Z_{c,max}-Z_{c,min}}{Z_{c,max}-Z_{c,min}}\right)^{2k}$$

$$- \zeta_t\left(\frac{2Z_t-Z_{t,max}-Z_{t,min}}{Z_{t,max}-Z_{t,min}}\right)^{2k} + \zeta_t\left(\frac{2\bar{Z}_t-Z_{t,max}-Z_{t,min}}{Z_{t,max}-Z_{t,min}}\right)^{2k}$$

$$- \zeta_h\left(\frac{2Z_h-Z_{h,max}(\bar{Z}_t)-Z_{h,min}(\bar{Z}_t)}{Z_{h,max}(\bar{Z}_t)-Z_{h,min}(\bar{Z}_t)}\right)^{2k}$$

$$+ \zeta_h\left(\frac{2\bar{Z}_h-Z_{h,max}(\bar{Z}_t)-Z_{h,min}(\bar{Z}_t)}{Z_{h,max}(\bar{Z}_t)-Z_{h,min}(\bar{Z}_t)}\right)^{2k}$$

$$+ \bar{\lambda}_d \left\{ c_{\alpha\beta}(1-e^{-c_{pl,d}\bar{X}_d}) \frac{c_1 V_1(-c_{co2,1}Z_t^2+c_{co2,2}Z_t-c_{co2,3})(Z_c-c_\Gamma)}{c_1 V_1+(-c_{co2,1}Z_t^2+c_{co2,2}Z_t-c_{co2,3})(Z_c-c_\Gamma)} \right.$$

$$- c_{\alpha\beta}(1-e^{-c_{pl,d}\bar{X}_d}) \frac{c_1 V_1(-c_{co2,1}\bar{Z}_t^2+c_{co2,2}\bar{Z}_t-c_{co2,3})(\bar{Z}_c-c_\Gamma)}{c_1 V_1+(-c_{co2,1}\bar{Z}_t^2+c_{co2,2}\bar{Z}_t-c_{co2,3})(\bar{Z}_c-c_\Gamma)}$$

$$\left. - c_{resp,2}\bar{X}_d 2^{(0.1 Z_t - 2.5)} + c_{resp,2}\bar{X}_d 2^{(0.1\bar{Z}_t-2.5)} \right\} \bigg) dt \qquad\qquad \text{ct m}^{-2}.$$

The latter equation illustrates that in the fast sub-problem the optimal control is mainly involved with compensating the economic losses due to neglecting the dynamics of the fast state variables. The optimizing control is based on a trade-off between the additional costs required to excite the fast dynamics and the additional amount of growth of the economic return valued at its marginal value $\bar{\lambda}_d$.

The optimal control problem is defined as to find

$$(6.19) \qquad (U_c^*, U_v^*, U_q^*) = \arg \max_{U_c, U_v, U_q} J(U_c, U_v, U_q)$$

subject to the system equations (6.17) and the control constraints (6.3). For the fast sub-problem the Hamiltonian is defined as

$$(6.20) \qquad \hat{\mathcal{H}} = c_{co2}(\bar{U}_c - U_c) + c_q(\bar{U}_q - U_q) - \zeta_c \left(\frac{2Z_c - Z_{c,max} - Z_{c,min}}{Z_{c,max} - Z_{c,min}} \right)^{2k}$$

$$+ \zeta_c \left(\frac{2\bar{Z}_c - Z_{c,max} - Z_{c,min}}{Z_{c,max} - Z_{c,min}} \right)^{2k} - \zeta_t \left(\frac{2Z_t - Z_{t,max} - Z_{t,min}}{Z_{t,max} - Z_{t,min}} \right)^{2k}$$

$$+ \zeta_t \left(\frac{2\bar{Z}_t - Z_{t,max} - Z_{t,min}}{Z_{t,max} - Z_{t,min}} \right)^{2k} - \zeta_h \left(\frac{2Z_h - Z_{h,max}(Z_t) - Z_{h,min}(Z_t)}{Z_{h,max}(Z_t) - Z_{h,min}(Z_t)} \right)^{2k}$$

$$
+ \zeta_h \left[\frac{2\bar{Z}_h - Z_{h,max}(\bar{Z}_t) - Z_{h,min}(\bar{Z}_t)}{Z_{h,max}(\bar{Z}_t) - Z_{h,min}(\bar{Z}_t)} \right]^{2k}
$$

$$
+ \bar{\lambda}_d \Bigg\{ c_{\alpha\beta} \left(1 - e^{-c_{pl,d}\bar{X}_d} \right) \frac{c_1 V_1 (-c_{co2,1}Z_t^2 + c_{co2,2}Z_t - c_{co2,3})(Z_c - c_\Gamma)}{c_1 V_1 + (-c_{co2,1}Z_t^2 + c_{co2,2}Z_t - c_{co2,3})(Z_c - c_\Gamma)}
$$

$$
- c_{\alpha\beta} \left(1 - e^{-c_{pl,d}\bar{X}_d} \right) \frac{c_1 V_1 (-c_{co2,1}\bar{Z}_t^2 + c_{co2,2}\bar{Z}_t - c_{co2,3})(\bar{Z}_c - c_\Gamma)}{c_1 V_1 + (-c_{co2,1}\bar{Z}_t^2 + c_{co2,2}\bar{Z}_t - c_{co2,3})(\bar{Z}_c - c_\Gamma)}
$$

$$
- c_{resp,2}\bar{X}_d 2^{(0.1Z_t - 2.5)} + c_{resp,2}\bar{X}_d 2^{(0.1\bar{Z}_t - 2.5)} \Bigg\}
$$

$$
+ \frac{\eta_c}{c_{cap,c}} \Bigg(- \left(1 - e^{-c_{pl,d}\bar{X}_d} \right) \frac{c_1 V_1 (-c_{co2,1}Z_t^2 + c_{co2,2}Z_t - c_{co2,3})(Z_c - c_\Gamma)}{c_1 V_1 + (-c_{co2,1}Z_t^2 + c_{co2,2}Z_t - c_{co2,3})(Z_c - c_\Gamma)}
$$

$$
+ c_{resp,2}\bar{X}_d 2^{(0.1Z_t - 2.5)} + U_c - (U_v + c_{leak})(Z_c - V_c) \Bigg)
$$

$$
+ \frac{\eta_t}{c_{cap,q}} \Bigg[U_q - (c_{cap,q,v}U_v + c_{al,ou})(Z_t - V_t) + c_{rad}V_1 \Bigg]
$$

$$
+ \frac{\eta_h}{c_{cap,q}} \Bigg(\left(1 - e^{-c_{pl,d}\bar{X}_d} \right) c_{v,pl,al} \left(\frac{c_{v,5}}{c_R(Z_t + c_{t,abs})} e^{\frac{c_{v,2}Z_t}{Z_t + c_{v,3}}} - Z_h \right)
$$

$$
- (U_v + c_{leak})(Z_h - V_h) \Bigg) \qquad\qquad \text{ct m}^{-2}\text{ s}^{-1}.
$$

Taking the partial derivative of the Hamiltonian with respect to the fast state variables Z_c, Z_t and Z_h yields the equations describing the dynamics of the fast costates η_c, η_t and η_h:

$$(6.21a) \quad -\frac{d\eta_c}{dt} = \frac{\partial \mathcal{H}}{\partial Z_c} = -\left(\frac{4k\zeta_c}{Z_{c,max}-Z_{c,min}}\right)\left(\frac{2Z_c-Z_{c,max}-Z_{c,min}}{Z_{c,max}-Z_{c,min}}\right)^{2k-1}$$

$$+\ \bar{\lambda}_d \frac{c_{\alpha\beta}\left(1-e^{-c_{pl,d}\bar{X}_d}\right)\left(c_1 V_1\right)^2(-c_{co2,1}Z_t^2+c_{co2,2}Z_t-c_{co2,3})}{\left[c_1 V_1+(-c_{co2,1}Z_t^2+c_{co2,2}Z_t-c_{co2,3})(Z_c-c_\Gamma)\right]^2}$$

$$+\ \frac{\eta_c}{c_{cap,c}}\left(-\frac{\left(1-e^{-c_{pl,d}\bar{X}_d}\right)\left(c_1 V_1\right)^2(-c_{co2,1}Z_t^2+c_{co2,2}Z_t-c_{co2,3})}{\left[c_1 V_1+(-c_{co2,1}Z_t^2+c_{co2,2}Z_t-c_{co2,3})(Z_c-c_\Gamma)\right]^2}-(U_v+c_{leak})\right)$$

$$\text{ct m kg}^{-1}\text{ s}^{-1},$$

$$(6.21b) \quad -\frac{d\eta_t}{dt} = \frac{\partial \mathcal{H}}{\partial Z_t} = -\left(\frac{4k\zeta_t}{Z_{t,max}-Z_{t,min}}\right)\left(\frac{2Z_t-Z_{t,max}-Z_{t,min}}{Z_{t,max}-Z_{t,min}}\right)^{2k-1}$$

$$-\ 2k\zeta_h\left(\frac{2Z_h-Z_{h,max}(Z_t)-Z_{h,min}(Z_t)}{Z_{h,max}(Z_t)-Z_{h,min}(Z_t)}\right)^{2k-1}\left(\frac{-2Z_h(RZ_{h,max}-RZ_{h,min})}{\left(Z_{h,max}(Z_t)-Z_{h,min}(Z_t)\right)^2}\right)$$

$$\left(-\frac{c_{v,6}c_R}{\left(c_R(Z_t+c_{t,abs})\right)^2}+\frac{c_{v,6}c_{v,2}c_{v,3}}{c_R(Z_t+c_{t,abs})\left(Z_t+c_{v,3}\right)^2}\right)e^{\frac{c_{v,2}Z_t}{Z_t+c_{v,3}}}$$

$$+ \bar{\lambda}_d \Bigg(\frac{c_{\alpha\beta}\left(1-e^{-c_{pl,d}\bar{X}_d}\right)\left(c_1 V_1\right)^2 (Z_c-c_\Gamma)(-2c_{co2,1}Z_t+c_{co2,2})}{\left[c_1 V_1+(-c_{co2,1}Z_t^2+c_{co2,2}Z_t-c_{co2,3})(Z_c-c_\Gamma)\right]^2}$$

$$- \ 0.1\ln(2)c_{resp,1}\bar{X}_d 2^{(0.1Z_t-2.5)}\Bigg)$$

$$+ \frac{\eta_c}{c_{cap,c}}\Bigg(- \frac{\left(1-e^{-c_{pl,d}\bar{X}_d}\right)\left(c_1 V_1\right)^2 (Z_c-c_\Gamma)(-2c_{co2,1}Z_t+c_{co2,2})}{\left[c_1 V_1+(-c_{co2,1}Z_t^2+c_{co2,2}Z_t-c_{co2,3})(Z_c-c_\Gamma)\right]^2}$$

$$+ \ 0.1\ln(2)c_{resp,2}\bar{X}_d 2^{(0.1Z_t-2.5)}\Bigg)$$

$$- \frac{\eta_t}{c_{cap,q}}\Big(c_{cap,q,v}U_v+c_{al,ou}\Big)$$

$$+ \frac{\eta_h}{c_{cap,h}}\Big(1-e^{-c_{pl,d}\bar{X}_d}\Big)c_{v,pl,al}e^{\dfrac{c_{v,2}Z_t}{Z_t+c_{v,3}}}$$

$$\left[- \frac{c_{v,5}c_R}{\left(c_R(Z_t+c_{t,abs})\right)^2} + \frac{c_{v,5}c_{v,2}c_{v,3}}{c_R(Z_t+c_{t,abs})\left(Z_t+c_{v,3}\right)^2}\right] \qquad \text{ct m}^{-2}\ {}^{\circ}\text{C}^{-1}\ \text{s}^{-1},$$

$$(6.21\text{c}) \quad - \frac{d\eta_h}{dt} = \frac{\partial\mathcal{H}}{\partial Z_h} =$$

$$- \left[\frac{4k\zeta_h}{Z_{h,max}(Z_t)-Z_{h,min}(Z_t)}\right]\left[\frac{2Z_h-Z_{h,max}(Z_t)-Z_{h,min}(Z_t)}{Z_{h,max}(Z_t)-Z_{h,min}(Z_t)}\right]^{2k-1}$$

$$+ \frac{\eta_h}{c_{cap,h}}\left(-\left(1-e^{-c_{pl,d}\bar{X}_d}\right)c_{v,pl,al} - (U_v+c_{leak})\right) \qquad \text{ct m kg}^{-1}\text{ s}^{-1}.$$

Finally, the derivatives of the Hamiltonian with respect to the control inputs yield the switching functions governing the control inputs:

$$(6.22a) \qquad \frac{\partial \mathcal{H}}{\partial U_c} = -c_{co2} + \frac{\eta_c}{c_{cap,c}} \qquad \text{ct kg}^{-1},$$

$$(6.22b) \qquad \frac{\partial \mathcal{H}}{\partial U_v} = -\frac{\eta_c(Z_c-V_c)}{c_{cap,c}} - \frac{\eta_t c_{cap,q,v}(Z_t-V_t)}{c_{cap,q}} - \frac{\eta_h(Z_h-V_h)}{c_{cap,h}} \qquad \text{ct m}^{-3},$$

$$(6.22c) \qquad \frac{\partial \mathcal{H}}{\partial U_q} = -c_q + \frac{\eta_t}{c_{cap,q}} \qquad \text{ct J}^{-1}.$$

6.3. Control problem 2

In this control problem the dynamics of the state variables are described by the following differential equations:

$$(6.23a) \qquad \frac{dX_n}{dt} = c_\alpha\left(1-e^{-c_{pl,s}X_s}\right)\frac{c_1 V_1(-c_{co2,1}Z_t^2+c_{co2,2}Z_t-c_{co2,3})(Z_c-c_\Gamma)}{c_1 V_1+(-c_{co2,1}Z_t^2+c_{co2,2}Z_t-c_{co2,3})(Z_c-c_\Gamma)}$$

$$- \frac{c_{gr}X_n X_s}{X_s+X_n}1.6^{(0.1Z_t-2.)} - c_{resp,3}X_s2^{(0.1Z_t-2.5)} \qquad \text{kg m}^{-2}\text{ s}^{-1},$$

$$(6.23b) \qquad \frac{dX_s}{dt} = \frac{c_{r,gr,max}X_n X_s}{X_s+X_n}1.6^{(0.1Z_t-2.)} \qquad \text{kg m}^{-2}\text{ s}^{-1},$$

$$(6.23c) \qquad \varepsilon\frac{dZ_c}{dt} = \frac{1}{c_{cap,c}}\left(-\left(1-e^{-c_{pl,s}X_s}\right)\frac{c_1 V_1(-c_{co2,1}Z_t^2+c_{co2,2}Z_t-c_{co2,3})(Z_c-c_\Gamma)}{c_1 V_1+(-c_{co2,1}Z_t^2+c_{co2,2}Z_t-c_{co2,3})(Z_c-c_\Gamma)}\right.$$

$$+ \; c_{resp,2}X_s 2^{(0.1Z_t - 2.5)} \;\; + \; \frac{c_{resp,4}X_nX_s}{X_s + X_n}1.6^{(0.1Z_t - 2.)}$$

$$\left. + \; U_c \; - \; (U_v + c_{leak})(Z_c - V_c) \right] \hspace{5cm} \text{kg m}^{-3} \text{ s}^{-1},$$

(6.23d) $\displaystyle \varepsilon\frac{dZ_t}{dt} = \frac{1}{c_{cap,q}} \left[U_q - (c_{cap,q,v}U_v + c_{al,ou})(Z_t - V_t) + c_{rad}V_1 \right] \hspace{1cm} {}^{\circ}\text{C s}^{-1},$

(6.23e) $\displaystyle \varepsilon\frac{dZ_h}{dt} = \frac{1}{c_{cap,h}} \left[\left(\left[1 - e^{-c_{pl,s}X_s} \right] c_{v,pl,al} \left(\frac{c_{v,5}}{c_R(Z_t + c_{t,abs})} e^{\frac{c_{v,2}Z_t}{Z_t + c_{v,3}}} - X_h \right) \right. \right.$

$$\left. - \; (U_v + c_{leak})(Z_h - V_h) \right] \hspace{5cm} \text{kg m}^{-3} \text{ s}^{-1}.$$

For this system the performance criterion is

(6.24) $\displaystyle J(U_c, U_v, U_q) = c_{prl,1} + c_{prl,2}(X_n(t_f) + X_s(t_f)) - \int_{t_b}^{t_f} c_{co2}U_c + c_q U_q dt.$

The control inputs and fast state variables are constrained as described in eqns. (6.3) and (6.4). Finally, the control problem is defined as to find

(6.25) $\displaystyle (U_c^*, U_v^*, U_q^*) = \arg \max_{U_c, U_v, U_q} J(U_c, U_v, U_q)$

subject to the system equations (6.23a) to (6.23e) and the control and state constraints.

6.4. Analysis

Using the interpretation of optimal control problems introduced in section 5.4, in this section the equations presented in section 6.2 will be analysed for understanding of the operation of economic

optimal greenhouse climate control. The analysis will serve as a basis for the interpretation of simulations presented in chapter 7.

The performance criterion J, eqn. (6.2), expresses a net economic return of crop production, evaluated over the whole production period. In the process of dynamic optimization, the performance criterion J, is replaced by a local performance criterion, the Hamiltonian, eqn. (6.7). The Hamiltonian, $\mathcal{H} = -L + \lambda^T f$, accounts for the momentary contribution of a control action to the running costs, L, and long term revenues from a change in the state due to a control action, $\lambda^T f$. The revenues of an investment in a change of the state is determined by the costate or marginal value of a state variable, λ.

The marginal value of a state variable at a certain moment during the growing period is equivalent with the sensitivity of the economic return at harvest time, *i.e.* J, to a small variation of that particular state at that time in the growing period. In view of this interpretation, the absolute value and sign of a costate are of special interest. A positive costate indicates benefits from a positive change in the associated state, a negative costate value indicates that losses will result from an increment of the state. A large (small) positive costate value indicates large (small) benefits from a positive change in the associated state. If at a given moment in time a costate equals zero, the performance of the controlled process is not affected by a change of the associated state variable at that time.

So, from the value and sign of the costate it can be deduced whether or not a change in the associated state will result in an improvement or a loss of economic performance of the controlled process. The economic feasibility of a controlled change of the state, however, is determined by the stationarity condition conforming eqn. (5.19c)

$$(6.26) \quad \frac{\partial \mathcal{H}}{\partial u} = -\frac{\partial L}{\partial u} + \left(\frac{\partial f}{\partial u}\right)^T \lambda = 0.$$

This equation asserts that an optimal greenhouse climate control action is characterized by the fact that its marginal contribution to the gross economic return expressed by $[\partial f/\partial u]^T \lambda$ just outweighs its marginal contribution to the momentary operating costs, $\partial L/\partial u$. This notion is depicted in fig. 6.2 for $\lambda = 1$ and $\lambda = 2$. Since $\partial f/\partial u > 0$, a higher marginal value yields a higher optimal control and vice-versa.
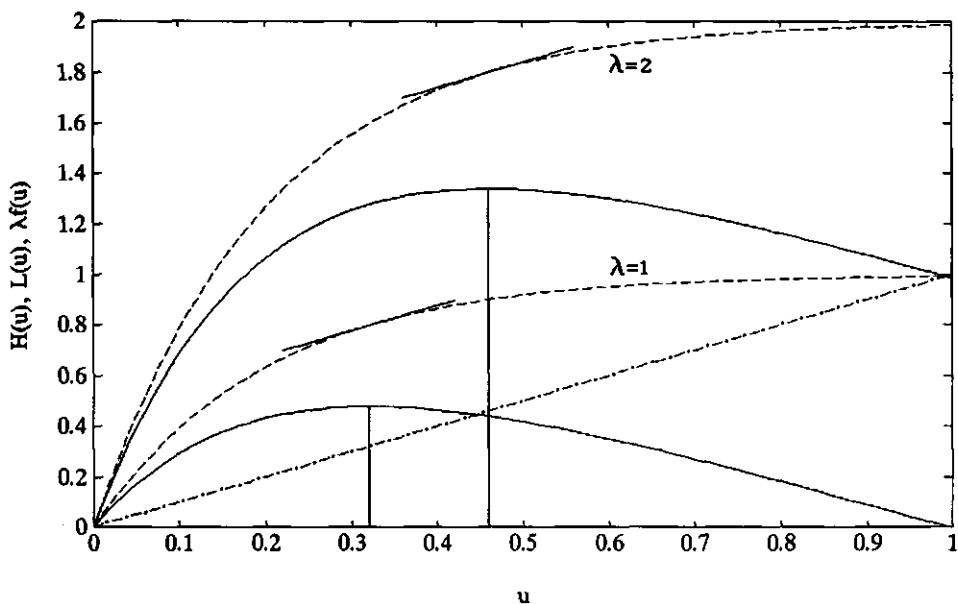
Fig. 6.2. Optimal control: the balance between additional gross income, $\lambda \partial f/\partial u$, and additional costs, $\partial L/\partial u$, yields the optimal net return; (—) denotes the Hamiltonian $\mathcal{H}$, (-·) denotes the operating costs L and (--) denotes the gross income λf for $\lambda = 1$ and $\lambda = 2$; the tangents at the gross income curve indicate where $\lambda \partial f/\partial u = \partial L/\partial u$ i.e. where $\mathcal{H}$ is maximized, the maximum of $\mathcal{H}$ is indicated by vertical lines.

For unconstrained control problems, the stationarity condition coincides with the Maximum Principle of Pontryagin, which asserts that a maximizing control should satisfy

(6.27) $\mathcal{H}(x^*,u^*,\lambda^*,t) \geq \mathcal{H}(x^*,u,\lambda^*,t)$.

However, if the control is constrained by e.g. inequality constraints of the form $0 = u_{min} \leq u \leq u_{max}$, then a control which satisfies the maximum principle does not automatically satisfy the stationarity condition. This can be seen as follows. Assume that at a certain moment during the growing period the marginal value of the state is zero, i.e. $\lambda = 0$, then we may see in fig. 6.2 that the maximizing control will be $u = u_{min} = 0$ since any increase in the control will yield smaller values of the Hamiltonian. With eqn. (6.27) satisfied,

eqn. (6.26) is not satisfied by the maximizing control, because $-\partial L/\partial u < 0$, which contradicts the requirement defined in eqn. (6.26). An identical argument will show the limitation of the stationarity condition if an upper bound u_{max} is encountered. Still, for controls lying between the constraint boundaries, both eqn. (6.26) and eqn. (6.27) constitute the same necessary condition for optimality of the control and may be used simultaneously in an analysis for understanding of the optimal control problems.

The partial derivatives of the Hamiltonian, eqn. (6.7), with respect to the control inputs, eqns. (6.10a) to (6.10c), being the basis of the stationarity condition, reveal the following. The economic optimal operation of the carbon dioxide supply is solely determined by the marginal value of the carbon dioxide concentration in the greenhouse, *i.e.* η_c. Equivalently, the operation of the heating system is determined by the marginal value of the air temperature η_t. However, since the ventilation affects all three greenhouse climate states, carbon dioxide concentration, air temperature and humidity, the operation of the ventilation windows is affected by their respective costates, η_c, η_t and η_h. The dry matter production is not affected by the control inputs as can be seen in table 3.7a and eqn. (6.1), and therefore the marginal value of crop dry weight, λ_d, does not influence the operation of the climate conditioning equipment directly. However, λ_d is indirectly involved in the operation of the climate conditioning equipment by means of its impact on the marginal values of carbon dioxide concentration, air temperature and humidity (eqns. (6.8b) to (6.8d)).

Concentrating on carbon dioxide supply and heating first, eqns. (6.1b) and (6.1c) reveal the trivial observation that carbon dioxide supply increases the carbon dioxide concentration and heating increases the temperature, both effects being effectively summarized by saying that $\partial f/\partial u > 0$ in which f is the system equation or model. If the costates related with the carbon dioxide concentration and air temperature are less than zero, *i.e.* η_c, $\eta_t < 0$, then the marginal contribution of the control to the economic return at the end of the growing period will be less than zero, *i.e.* $[\partial f/\partial u]\eta < 0$, since $\partial f/\partial u > 0$. Additionally, application of carbon dioxide and heating energy to the greenhouse yields higher running costs of the climate conditioning equipment, *i.e.* $\partial L/\partial u > 0$. Consequently, using the arguments in line with the maximum principle of Pontryagin (eqn. (6.27)), this implies that the control input resulting in the largest value of the Hamiltonian will be $U_c = 0$, $U_q = 0$. *Summarizing, carbon dioxide and heating energy will not be supplied to the greenhouse if the marginal contribution of the carbon dioxide concentration and air*

temperature in the greenhouse to the final economic return is less than zero.

However, if η_c and $\eta_t > 0$, *i.e.* if the carbon dioxide concentration and air temperature positively affect the final economic return, application of carbon dioxide and heating energy to the greenhouse may be economically feasible. Then, referring to fig. 6.2 and the interpretation of the stationarity condition given at the beginning of this section, the marginal contribution of the control to the economic return should outweigh its marginal contribution to the costs. From eqns. (6.10a) and (6.10b) it is deduced that for an optimizing control U_c and U_q larger than zero, the costates should have values $\eta_c \geq c_{co2}c_{cap,c}$ and $\eta_t \geq c_q c_{cap,q}$. This requirement illustrates that if the running costs of the climate conditioning equipment, *i.e.* c_{co2} and c_q, increase, the marginal contribution of the carbon dioxide concentration and air temperature to the final economic return, need to be higher before actual operation of the climate conditioning equipment becomes economically feasible. *In other words, the control strategies have an energy conservation attitude in situations with high energy costs. Alternatively, a reduction of the running costs will yield a more generous operation of the climate condition equipment.* Also, $\eta_c \geq c_{co2}c_{cap,c}$ and $\eta_t \geq c_q c_{cap,q}$ indicate that for economic optimal greenhouse climate operation the mass and heat capacity of the greenhouse ($c_{cap,c}$ and $c_{cap,q}$), *i.e.* the greenhouse volume, should be kept as small as possible, since the equations show that with a higher energy and mass capacity the marginal contribution of the carbon dioxide concentration and the air temperature to the final economic return need to be higher before heating energy or carbon dioxide is supplied to the greenhouse. With large mass and heat capacities, it will require more energy and carbon dioxide to attain a unit increase of the carbon dioxide concentration in the greenhouse.

For the ventilation, the analysis yields a slightly different picture, since no operating costs are related with the ventilation and the impact of ventilation on the indoor climate is different from the influence of the heating and carbon dioxide supply. Generally, the air temperature, carbon dioxide and humidity levels in the greenhouse are higher than outside the greenhouse and a higher ventilation rate results in a reduction of the air temperature, carbon dioxide concentration and humidity in the greenhouse, *i.e.* $\partial f/\partial u < 0$. Sometimes, however, it may happen that due to a very high crop photosynthesis rate, the carbon dioxide concentration in the greenhouse air is lower than the carbon dioxide concentration in the outside air (Schapendonk and Gaastra, 1984). Then, a higher

ventilation rate will yield a higher carbon dioxide concentration in the greenhouse, *i.e.* $\partial f/\partial u > 0$.

If the carbon dioxide concentration and air temperature have a positive contribution to the final economic return, *i.e.* η_c, $\eta_t > 0$, for an optimal ventilation rate the marginal contribution of the control to the final economic return, *i.e.* $[\partial f/\partial u]\eta$, should be larger or equal to zero. If the carbon dioxide concentration and air temperature in the greenhouse exceed the outside conditions, any increment in the ventilation rate will yield a loss of carbon dioxide and energy from the inside air ($\partial f/\partial u < 0$). Thus the ventilation rate which yields the largest value of the Hamiltonian is $U_v = 0$. If, however, $\eta_c > 0$ and the carbon dioxide concentration in the outside air exceeds the concentration in the greenhouse, then ventilation may be used to open a 'cheap' carbon dioxide source to improve the inside climate. The optimal ventilation rate will equalize the inside carbon dioxide concentration with the outside concentration such that $\partial f/\partial u = 0$ thus satisfying the stationarity condition (see eqn. (6.1b)).

A positive value of the humidity costate, η_h, is not considered here, since it will be shown below and in section 7.2 that the marginal value of humidity never exceeds zero in the control problems considered in this research.

If the marginal contribution of the carbon dioxide concentration, air temperature and humidity is less than zero, *i.e.* $\eta_c < 0$, $\eta_t < 0$, $\eta_h < 0$, and the inside climatic conditions exceed the outside conditions, the previous line of reasoning will yield exactly the opposite result. If for instance $\eta_t < 0$, a reduction of the air temperature will yield a positive contribution to the performance. If the inside temperature is higher than the outside temperature, an increment in the ventilation flux will contribute to a reduction of the air temperature, *i.e.* $\partial f/\partial u < 0$. Since the marginal contribution of the control to the final economic return should be larger or equal to zero, the ventilation rate will be increased until $\eta_t = 0$ or the inside temperature equals the outside temperature thus resulting in $\partial f/\partial u = 0$ (see eqn. (6.1c)). For the carbon dioxide concentration and humidity similar arguments can be used.

The previous analysis has shed some light on the operation of the climate conditioning equipment depending on the marginal values of carbon dioxide concentration, air temperature and humidity. What remains is to get some insight into how the costates η_c, η_t and η_h, are affected for instance by the state of the crop and the outside climatic conditions.

In the control problem considered, eqn. (6.2) shows that the

gross economic return is solely determined by the state of the crop at harvest time, *i.e.* $X_d(t_f)$. It is expected that the costates associated with the air temperature, carbon dioxide concentration and humidity will be determined by their effect on dry matter production and consequently the final gross economic return.

In this research it is assumed that humidity does not directly affect crop growth. And if, for the moment, the humidity constraint is neglected, for instance by requiring $\zeta_h = 0$, humidity is eliminated from the Hamiltonian and does not affect the economic performance of the controlled process any more. Consequently, $\eta_h = 0$. The effect of constraints on the costates will be investigated below.

Fig. 6.3 shows the response of the rate of dry matter production, *i.e.* eqn. (6.1a), to the carbon dioxide concentration in the greenhouse at different light levels. During the day, any increment in carbon dioxide concentration contributes to an increase in dry matter production which suggests that during the day $\eta_c > 0$.
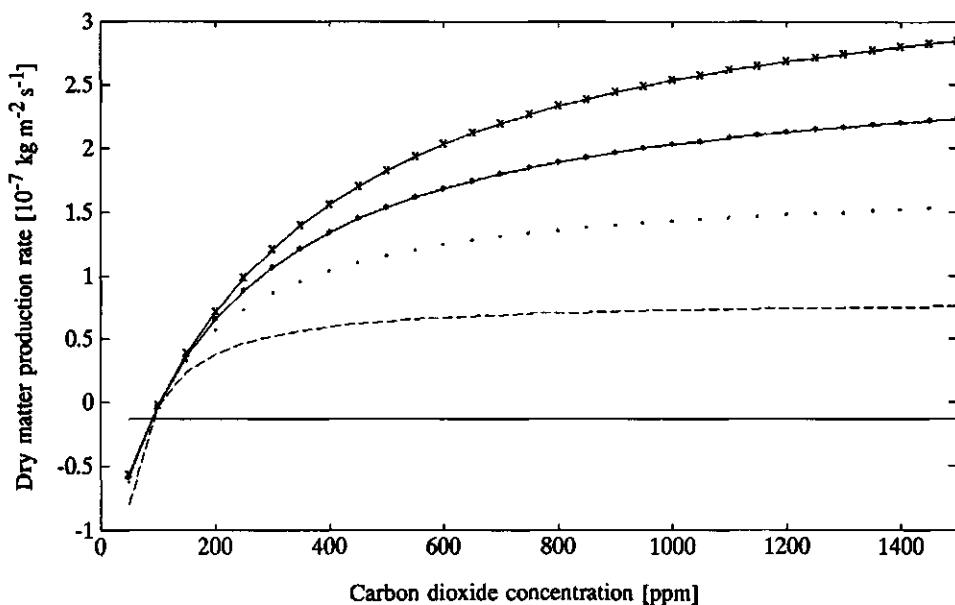

Fig. 6.3. The response of the dry matter production rate to the carbon dioxide concentration, after canopy closure, under different light regimes (—: 0 W m^{-2}, --: 50 W m^{-2}, ...: 100 W m^{-2}, -*-: 150 W m^{-2}, -x-: 200 W m^{-2}).

If the radiation level increases, an increment in the carbon dioxide level in the greenhouse yields an even higher dry matter production rate, which indicates that η_c is positively related with the radiation level. At night the carbon dioxide concentration does not affect dry matter production since the photosynthesis rate is zero, and the marginal value of carbon dioxide is then zero.
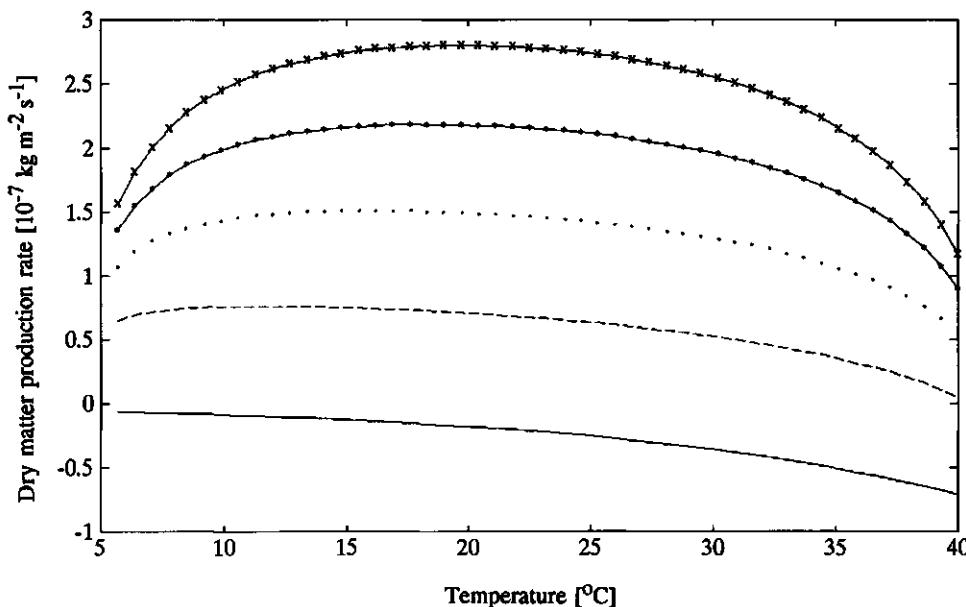
Fig. 6.4. The response of the dry matter production rate to the air temperature, after canopy closure, under different light regimes (—: 0 W m^{-2}, --: 50 W m^{-2}, ...: 100 W m^{-2}, -*-: 150 W m^{-2}, -x-: 200 W m^{-2}).

In fig. 6.4, the response of crop growth rate to air temperature is shown. This rate has an optimum response to temperature during the day. Below the optimum temperature an increment in the air temperature contributes to a higher dry matter production and consequently to a higher gross economic return. So, during the day the marginal value of the air temperature is expected to be larger than zero, *i.e.* $\eta_t > 0$. However, for an air temperature exceeding the optimum temperature, the marginal value of the air temperature will be less than zero since any increment in the air temperature will yield a reduction in the dry matter production rate. Observe that at

low temperatures the slope of the response curve is positively correlated with the radiation level which suggests a positive correlation of η_t with radiation. At night a temperature raise will result in higher respiratory losses of dry matter, thus affecting the gross economic return in a negative way. Therefore, the marginal value of air temperature is expected to be less than zero at night. Consequently, additional heating does not seem to be profitable at night. This seems to contradict standard horticultural practice where during lettuce production the greenhouse is heated at night to achieve a minimum temperature between 7 and 10 $^{\circ}$C (see section 3.2.1) and indicates a possible flaw in the crop growth model used. In section 7.3 this issue is further elaborated upon.

In the examples considered in this thesis, the marginal value of humidity, *i.e.* η_h, is completely determined by the constraint imposed on the humidity level in the greenhouse. If constraints are imposed on the humidity level in the greenhouse, *i.e.* $\zeta_h > 0$, the humidity affects the performance through a penalty function. If the humidity stays within the constraint boundaries, the penalty on the performance will be almost zero and consequently the marginal value of humidity will be approximately zero. However, if the humidity level approaches for instance the constraint boundary $Z_{h,max}$, then any increase in the humidity level will yield a reduction of the performance criterion J (see eqn. (6.6)), which will result in a distinct negative marginal value of the humidity, *i.e.* $\eta_h < 0$ at that time.

For the carbon dioxide concentration and air temperature, the constraints have the same impact on the respective costates. Constraint violations will have a strong negative influence on the marginal value.

It has been shown that the costates η_t and η_c uniquely determine the operation of heating and CO_2 supply, respectively. In the operation of the ventilation windows, however, contradicting objectives are encountered. It may occur during the day that $\eta_c > 0$ demands a reduction in ventilation rate to reduce losses of carbon dioxide to the outside air, whereas at the same time $\eta_h < 0$ demands a higher ventilation rate to reduce the humidity level in the greenhouse climate and consequently the penalty on the performance of the controlled process. Obviously, a trade-off between both objectives will result in an optimum ventilation rate under the current conditions.

Until now, the effect of single variable analysis of the operation of the climate conditioning equipment was performed. A

closer inspection of the costate equations (6.8a) to (6.8d) reveals that the marginal values of the various state variables are determined by a complex interaction of effects of state variables, costates and external inputs. A clear example is eqn. (6.8c) describing the dynamics of η_t. Analysis of eqn. (6.8c) will reveal, for instance, that the humidity constraint has a positive effect on the marginal value of the air temperature. A higher temperature will result in a reduction of the relative humidity and consequently a reduction of the humidity constraint penalty. This positive effect of humidity on the marginal value of air temperature suggests that heating may be used as a means to reduce the relative humidity in the greenhouse. When humidity control is considered, this positive costate of air temperature results in contradicting objectives with respect to ventilation. Eqn. (6.10b) reveals that the positive η_t induces a reduction of ventilation whereas, at the same time the negative η_h will demand a higher ventilation rate. Possibly heating and ventilation will be used simultaneously to achieve the single objective of controlling humidity in the greenhouse.

7. SIMULATIONS

7.1. Introduction

In this chapter optimal greenhouse climate management is investigated using simulations. The simulations can be divided into two groups. In the first set of three simulations, presented in sections 7.2 to 7.4, efficient control of the slow crop growth dynamics is studied. For the four state variable crop production model, as an example, equations of this so-called zero-th order slow sub-problem have been presented in section 6.2.2. In the slow sub-problem, the greenhouse climate is described by a quasi-steady-state model. Such a model description is expected to be quite accurate if the crop production process is driven by slowly varying external and control inputs. Therefore, in the first three simulations only the slow trends in the outside climatic conditions are considered. In view of the hierarchical decomposition of greenhouse climate management presented in chapter 1 (table 1.1), sections 7.2 to 7.4 emphasize optimization of the crop production process at level 2. In section 7.2, the optimal control approach and the grower's approach to greenhouse climate management are compared. Section 7.3 evaluates the effect of using different crop growth models, namely the one state variable and the two state variable lettuce growth model, on the solution of the optimal control problem. In section 7.4, the feedback-feedforward scheme introduced in section 5.8 is evaluated.

In the second set of three simulations, presented in sections 7.5 to 7.7, the greenhouse climate dynamics as well as rapid fluctuations of the outside climatic conditions will be considered in economic optimal greenhouse control. In section 7.5, the two time-scale decomposition of optimal greenhouse climate management will be evaluated. In section 7.6, the performance sensitivity of open-loop optimal greenhouse climate control is evaluated. The sensitivity analysis is intended to give more insight into optimal greenhouse climate control and the relative impact of parameters, initial conditions and external inputs thereon. Finally, in section 7.7, using the results of the two time-scale decomposition reported in section 7.5, greenhouse climate control using an explicit economic criterion is compared with a greenhouse climate set-point tracking approach.

7.2. Optimal control versus grower

7.2.1. Introduction

In this section the performance and characteristics of the optimal control approach are compared with greenhouse climate control supervised by the grower.

In horticultural practice, greenhouse climate control resembles the hierarchical concept discussed in chapter 1. At level 2, to control crop growth and production, the grower decides on the set-points or set-point trajectories of the greenhouse climate variables such as air temperature, carbon dioxide concentration and humidity. These set-points are usually not defined as fixed values. They may change during actual operation of the climate conditioning equipment in response to changes in the outside climatic conditions. Such adaptations of the set-points include for instance a radiation dependent change of the air temperature set-point and radiation and ventilation dependent adaptation of the carbon dioxide set-point. These set-points are then used at level 1 and 0 for actual greenhouse climate control. Besides these set-points and their adaptation, the grower also acts on greenhouse climate control at level 1 by means of bounds on the control inputs such as a minimum temperature of the heating valves, minimum and maximum values for the aperture of the ventilation windows.

In modern greenhouse climate control equipment, a large number of parameters need to be specified by the grower. They determine the afore mentioned set-points, their adaptation in relation to the outside climatic conditions as well as various bounds on the control inputs. Using a complex mental model of crop growth and production based on experience, knowledge about plant growing and results from empirical research, the grower decides about the proper values for these parameters.

It would be an interesting exercise to compare the rules laid down in the mental model of the grower with the optimal control approach to assess the benefits or limitations of either approach. But the deduction of the mental model of the grower is complicated and it is a well known fact that among growers significant differences may occur as to the outcome of the mental process of decision making. Instead, in this thesis, the performance and characteristics of the optimal control approach is evaluated by comparing the calculated state and control trajectories with measurements of a crop production process supervised by the grower. These measured data are considered to represent the outcome of the decisions made by the grower in relation to, for instance, the state of the process and the outside climatic conditions.

7.2.2. Methodology

In this section the control problem concerning the four state variable crop production process is used as an example. It is assumed that most of the decisions made by the grower are intended to control the relatively slow crop growth response. Therefore, in the present analysis, emphasis lies on the evaluation of optimal control of the slow crop growth dynamics and the fast greenhouse climate dynamics were neglected. The system equations and control problem were presented in section 6.2.2. The various parameters defining the running cost, and the state and control constraints were listed in table 6.1. In the simulations, measured data of the outside climatic conditions obtained during the second greenhouse experiment in early 1992 were employed. Since for the present analysis only the slow trends in these data are of interest, the data consisting of two minute measurements of the outside climatic conditions, the control inputs and the greenhouse climate, were averaged over periods of half an hour.

The grower's approach to greenhouse climate management was evaluated by simulating the system equation (6.11a) together with the quasi-steady-state equations (6.11b) to (6.11d), using half hour averages of the measured data of the control inputs.

The performance of greenhouse climate control according to the grower was compared with three optimization runs. First, in 'run 1', the optimal control problem defined in section 6.2.2 was solved including the constraints on air temperature, humidity and carbon dioxide concentration. In horticultural practice the operation of the ventilation windows is largely determined by considerations on the humidity level in the greenhouse. Since a time invariant constraint on the relative humidity is possibly not a prudent way of dealing with humidity in optimal greenhouse climate control, in a second run, hereafter referred to as 'run 2', optimal control trajectories were calculated for heating and carbon dioxide supply only, omitting the humidity constraint and using the measured ventilation implemented by the grower instead, to control the humidity level in the greenhouse. Finally, to get a clearer picture of the effect of the constraints on relative humidity and carbon dioxide concentration, in a third optimization run, hereafter referred to as 'run 3', both constraints were omitted by setting $\zeta_c = 0$ and $\zeta_h = 0$. The lower bound on the temperature was maintained for numerical reasons mentioned in section 6.2.

The state and costate equations were integrated with a time step of half an hour using a fourth order Runge-Kutta algorithm described by Press *et al.* (1986). The steepest ascent algorithm, described in section 5.7, was used for the iterative solution of the optimal

control problems. The search for the optimizing control strategy was stopped once the improvement in the performance criterion was less than 1.0×10^{-3} during at least three consecutive iterations.

7.2.3. Results and discussion

In fig. 7.1, performance data of the four control approaches are presented on a relative basis. The data include the simulated harvest weight, energy and carbon dioxide consumption and net economic return which, in the context of the present research, is defined as the difference between the value of the crop at harvest time and the
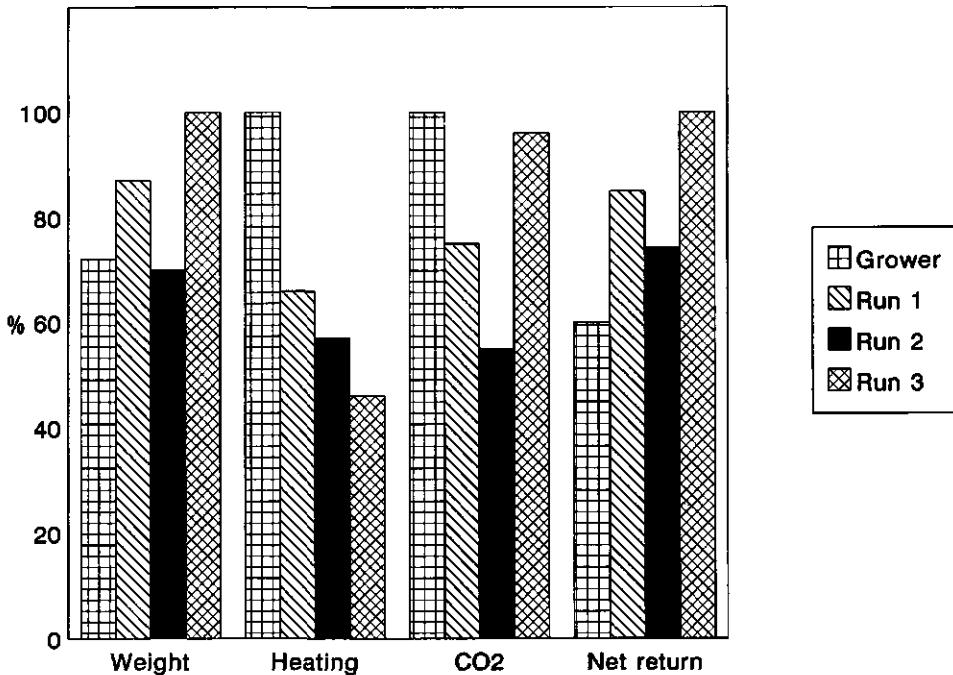
Fig. 7.1. Performance of the controlled crop production process using climate control supervised by the grower (Grower), optimal carbon dioxide supply, heating and ventilation with a humidity constraint (Run 1), optimal heating and carbon dioxide supply but ventilation according to grower (Run 2) and optimal heating, carbon dioxide supply and ventilation without humidity and carbon dioxide constraints (Run 3).

climate conditioning costs integrated over the whole growing period. In terms of net return, a considerable difference in performance between greenhouse climate control according to the grower and the three optimal control approaches can be observed. The results of run 1, in which the relative humidity was limited by an upper constraint of 90%, are characterized by a higher dry matter production and less energy and carbon dioxide consumption than with greenhouse climate control supervised by the grower. In run 2, in which ventilation according to the grower was used instead of the humidity constraint to control the relative humidity in the greenhouse, the energy and carbon dioxide consumption was much smaller than with heating, ventilation and carbon dioxide supply according to the grower. Although dry matter production was approximately the same as with the grower's control, the reduced carbon dioxide and energy consumption yielded a higher net economic return. Apparently, with optimal control, heating energy and carbon dioxide are used more efficiently. Run 3 revealed the very strong impact of constraints on carbon dioxide concentration and relative humidity on the performance of optimal control. Carbon dioxide consumption was about the same as in run 1, but less energy was used and due to the much higher dry matter production, a higher net economic return was obtained.

Table 7.1, showing total carbon dioxide and energy consumption, and ventilation during a full production cycle, partly clarifies how the performance of the different control approaches was achieved. In run 1, a lower ventilation rate during the day was calculated than was used by the grower. On the contrary at night, optimal ventilation was much higher. Though in run 1 less carbon dioxide was consumed than the grower had used, the reduced ventilation rate during the day will have resulted in a higher carbon dioxide concentration in the greenhouse, thus yielding the observed higher dry matter production. Another distinct difference between optimal control and climate control according to the grower is the reduced energy consumption during the day and, to a lesser extent, during the night (table 7.1). Using ventilation according to the grower (run 2), during both day and night less heating energy and about half the amount of carbon dioxide was used. Omitting the constraints on the carbon dioxide concentration and humidity (run 3), resulted in a significant reduction of the ventilation during both day and night. This indicates that in run 1 ventilation was mainly used to control the relative humidity. In run 3, ventilation occurred occasionally during the day. Because the reduced ventilation rate resulted in less energy losses to the outside air, less energy was needed for greenhouse heating. The reduced ventilation rate and slightly higher carbon dioxide consumption will have resulted in higher carbon dioxide concentrations in the greenhouse which have had the distinct positive

Table 7.1. Total carbon dioxide consumption, energy consumption and
            ventilation during the whole growing period in early 1992
            with greenhouse climate control according to the grower
            (Grower), optimal control with humidity constraint
            (Run 1), optimal control without humidity constraint using
            the measured ventilation trajectories implemented by the
            grower (Run 2) and optimal control without humidity and
            carbon dioxide constraint (Run 3).

	Carbon dioxide consumption $kg\ m^{-2}$		Energy consumption $MJ\ m^{-2}$		Ventilation $m^3\ m^{-2}$	
	Day	Night	Day	Night	Day	Night
Grower	1.23	–	105	127	5439	2955
Run 1	0.94	–	43	110	3519	6298
Run 2	0.68	–	45	88	5439	2955
Run 3	1.18	–	27	80	467	–

effect on dry matter production shown in fig. 7.1.

Further insight into the characteristics of the grower's approach and the optimal control approach to greenhouse climate management is obtained by inspection of the measured and calculated control and state trajectories. In fig. 7.2 simulations of the dry matter production are presented. In run 2, dry matter accumulation closely followed dry matter production with greenhouse climate control according to the grower. In run 1, a higher dry matter production is found from the start.

Fig. 7.3 (p. 190) presents the averaged measured data of solar radiation, temperature, wind speed and humidity outside the greenhouse during a period of 5 days. Carbon dioxide supply, ventilation and heating according to the grower and the optimal control trajectories calculated with the humidity constraint in run 1, are depicted in fig. 7.4 (p. 191). The simulated greenhouse climate variables resulting from these outside climatic conditions and control inputs are shown in fig. 7.5 (p. 192). The state and control trajectories calculated in runs 2 and 3 are not shown.

Figs. 7.3 to 7.5 clarify some of the differences found in fig. 7.1 and table 7.1. For instance, fig. 7.4a shows that with optimal control, the carbon dioxide supply responds to the solar radiation in a different way than in the grower's control approach. Due to the unfavourable radiation conditions as well as the high ventilation
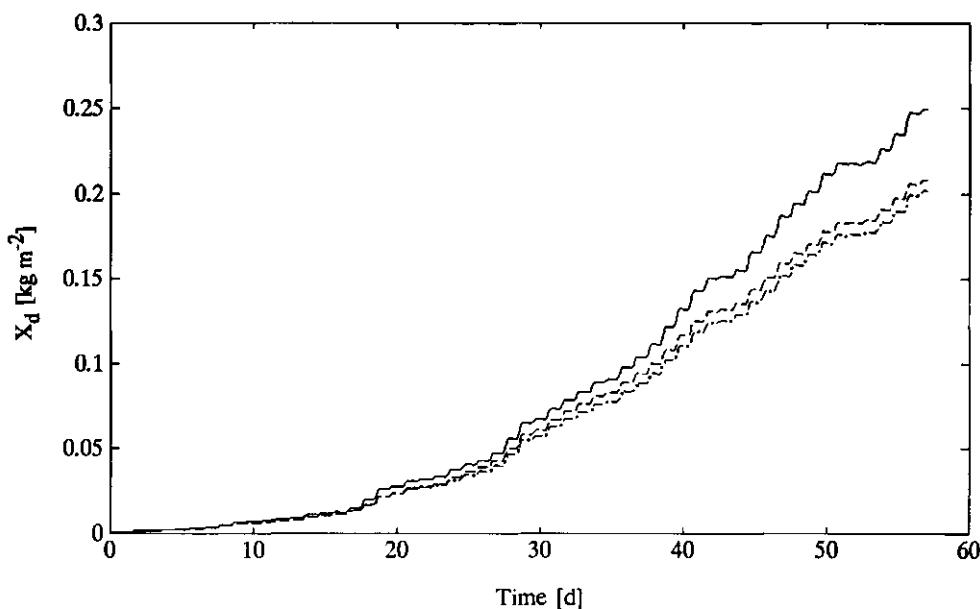
Fig. 7.2. Dry matter production simulated with climate control according to the grower (Grower: --), optimal control with humidity constraint (Run 1: —) and optimal control without humidity constraint and ventilation according to grower (Run 2: -·).

rate during days 2 and 3, in the optimal control approach the supply of carbon dioxide to the greenhouse air was not considered profitable. In greenhouse climate control implemented by the grower, the carbon dioxide set-point was adapted to the solar radiation as well as the ventilation rate (Corver, 1991), but compared with optimal control, during days 2 and 3, carbon dioxide was too abundantly supplied. On the contrary, the control implemented by the grower was reluctant with carbon dioxide supply under favourable radiation conditions during days 4 and 5. At that time, the grower seemed to prefer a high ventilation rate to reduce the relative humidity in the greenhouse (see fig. 7.5c, p. 192) and consequently reduced the carbon dioxide supply rate to prevent excessive losses of carbon dioxide to the outside air.

In fig. 7.5a it can be seen that under favourable circumstances, using optimal control, the carbon dioxide concentration in the greenhouse exceeded 1000 ppm whereas the grower used an upper limit of 750 ppm on the carbon dioxide concentration in the greenhouse to
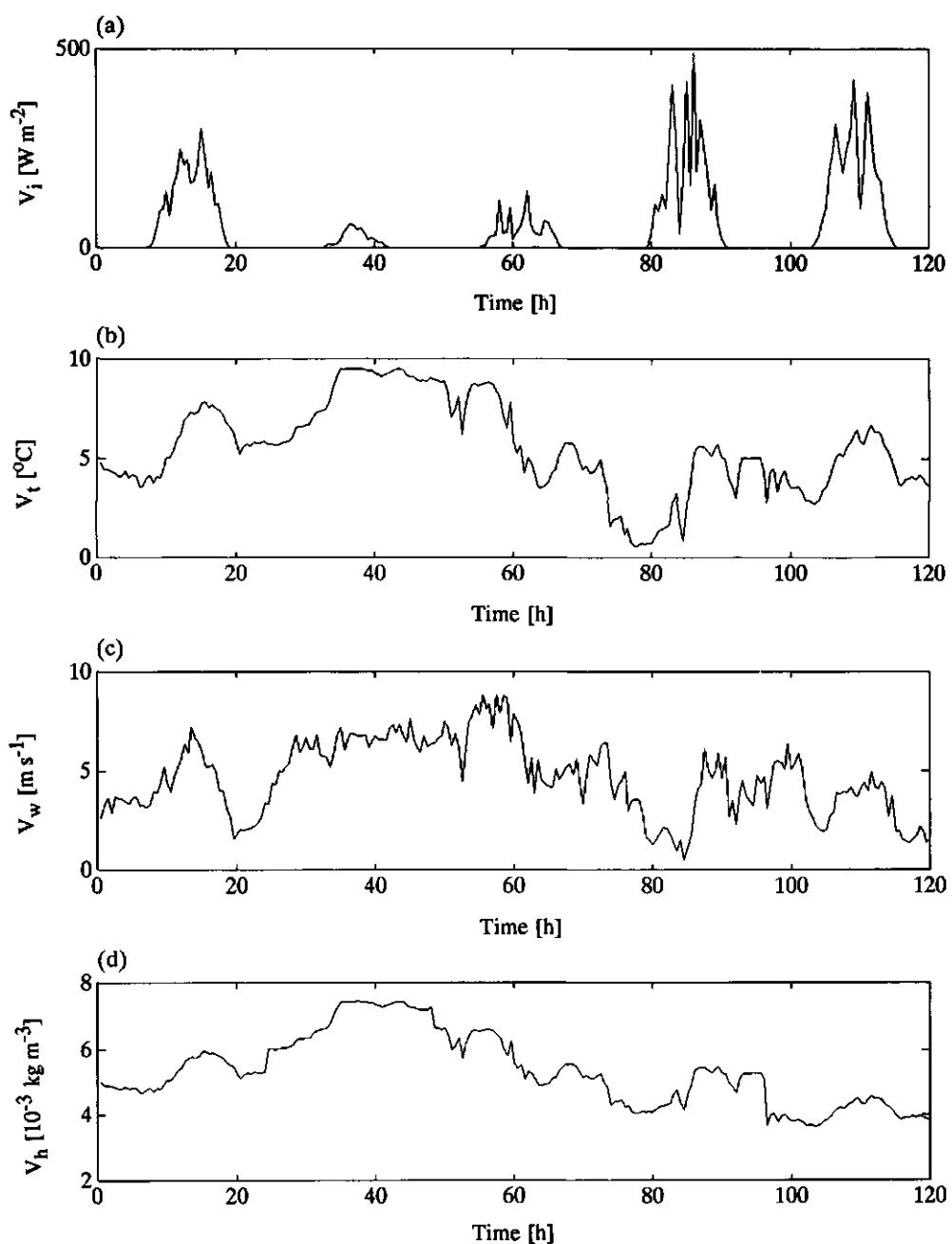
Fig. 7.3.   Outside climatic conditions during a five days period:
(a) solar radiation, (b) temperature, (c) wind speed and
(d) absolute humidity.
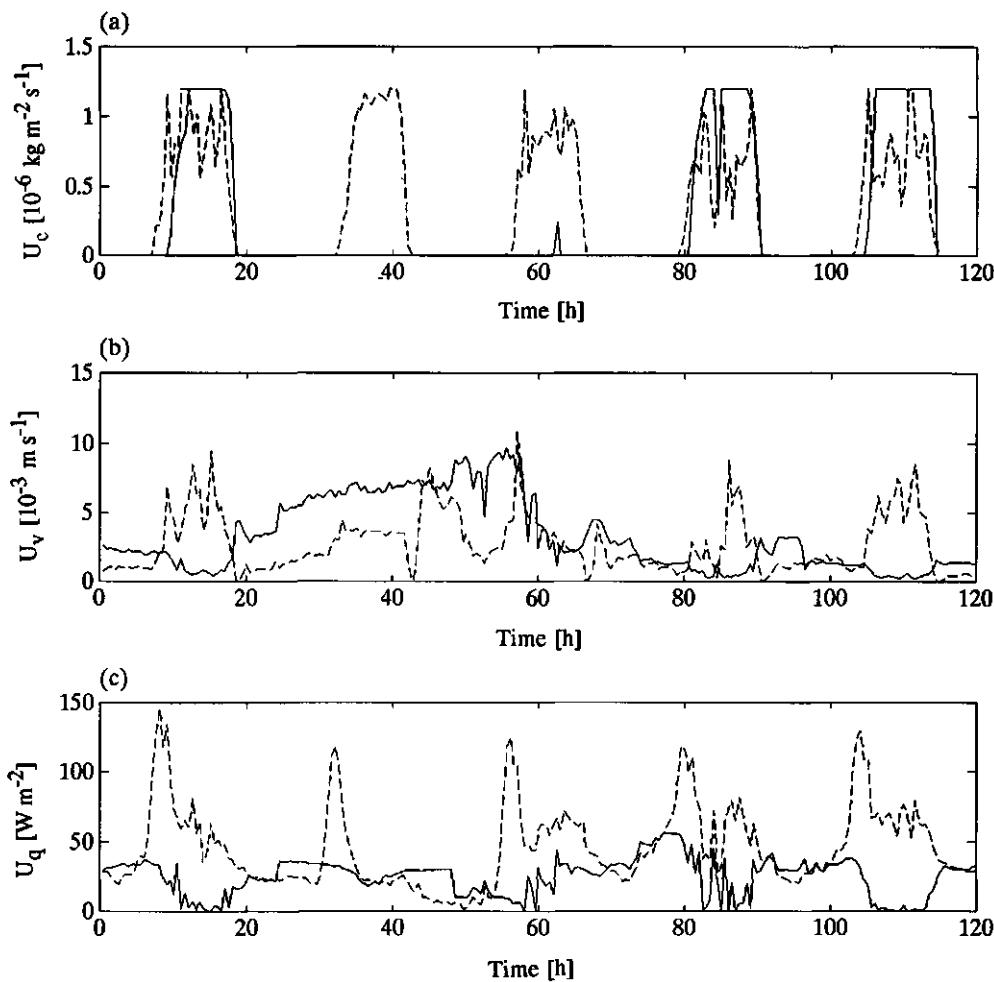
Fig. 7.4. Carbon dioxide supply rate (a), ventilation rate (b) and heating (c), according to grower (--) and optimal control of run 1 (—).

limit the carbon dioxide consumption (Corver, 1991).

The high ventilation rate implemented by the grower during the day was mainly intended to reduce the humidity level in the greenhouse and consequently to prevent fungal diseases and physiological damage, such as marginal spot (Corver, 1991). A simulated relative humidity as low as 60% can be seen in fig. 7.5c. In the optimal control approach, however, the ventilation rate was reduced during the day to achieve a more efficient use of the carbon
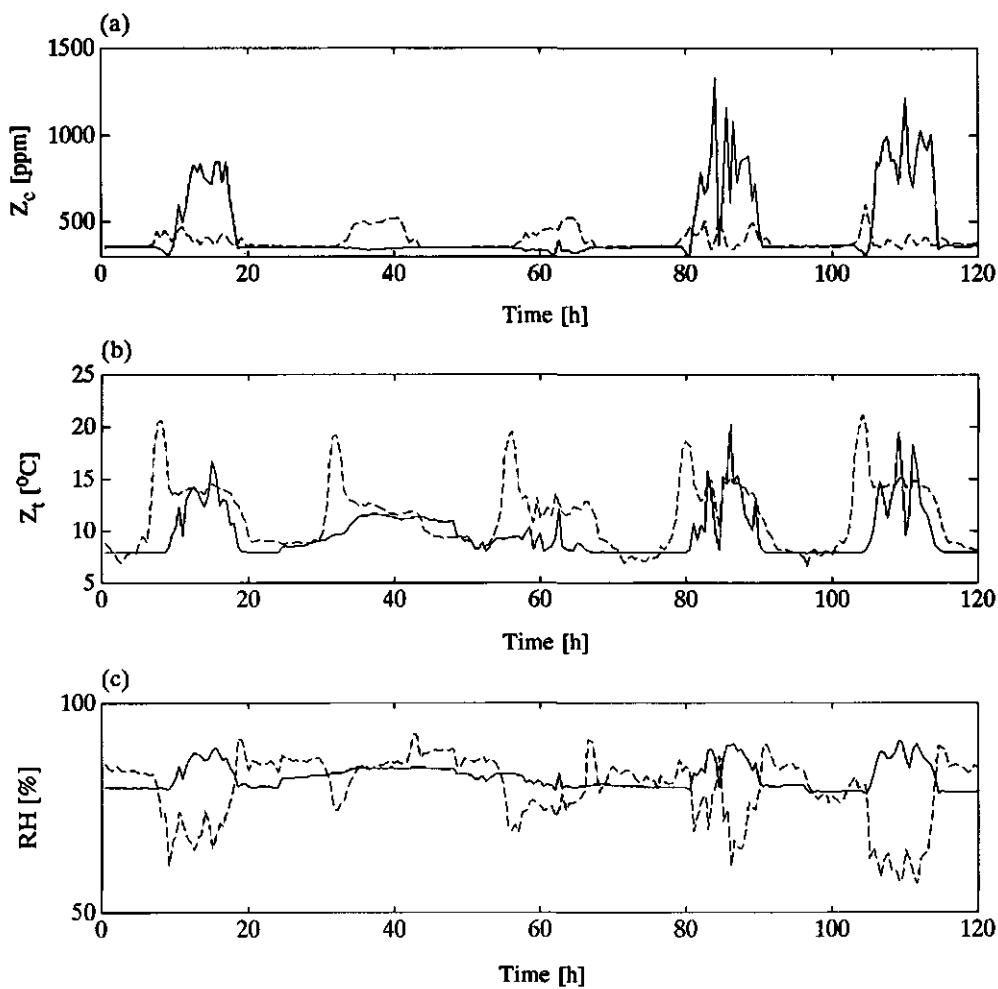
Fig. 7.5. Carbon dioxide concentration (a), air temperature (b) and
relative humidity (c), simulated with climate control
according to the grower (--) and optimal control of run 1
(—).

dioxide supplied. Consequently, a higher relative humidity (90%) was
encountered than in practice. At night the differences in the
humidity level were found to be rather small.

For the air temperature in the greenhouse, the grower used a
minimum value of 14 °C during the day. On average, in this example,
this set-point was almost equivalent to the calculated optimal air
temperature during the five days shown. Due to the higher ventilation

rate used by the grower during the day, more heating energy was needed to realize the air temperature set-point which largely explains the higher day time energy consumption by the grower observed in table 7.1. The optimal air temperature trajectories in fig. 7.5b also suggest that adjustment of the indoor temperature anticipating the outside climatic conditions such as solar radiation may improve the efficiency of greenhouse climate management.

The difference in energy consumption at night is partly explained by the fact that, especially during the first two weeks of the growing period, the grower used an air temperature set-point of 14 $^\circ$C. It was observed in section 6.4 that, with the one state variable lettuce growth model, heating is not considered profitable at night. The resulting higher air temperature has a negative effect on the dry matter production due to the temperature related increase in maintenance respiration. Therefore at night the air temperature was determined by the lower bound constraint so that values as low as 7 $^\circ$C were simulated. Also in the optimal control approach, the heat pulse at sun rise, implemented by the grower to 'activate' the crop, was not considered economically feasible since the possible benefits in terms of crop quantity or quality of this approach were not described by the models used. Clearly, the heat pulse implemented by the grower contributed to a higher energy consumption.

In a qualitative sense, the characteristics of the control strategies calculated in run 2 (not shown) were much the same as the strategies calculated in run 1. The improved efficiency of greenhouse climate control was achieved by a more efficient use of carbon dioxide and a reduction of the energy consumption due to the absence of the heat pulse at sun rise and the lower air temperature at night. Although less heating energy was used during the day, given the ventilation implemented by the grower, only a slightly higher humidity level in the greenhouse was reached than with greenhouse climate management supervised by the grower.

The control strategies calculated in run 3 were quite different (not shown). The main difference was the very low ventilation rate during both day and night which resulted in relative humidity levels continuously exceeding 90%. The carbon dioxide supply, combined with the low ventilation rate during the day, sometimes yielded carbon dioxide concentrations in the greenhouse well in excess of 2000 ppm. It seems that, in this example, ventilation was hardly used for temperature control. But this may be due to the fact that in early 1992 low outside temperatures and radiation levels occurred, and high temperatures in the greenhouse were not reached.

The marginal value of total crop dry weight calculated in runs 1 and 3, shown in fig. 7.6a, presents further insight into optimal
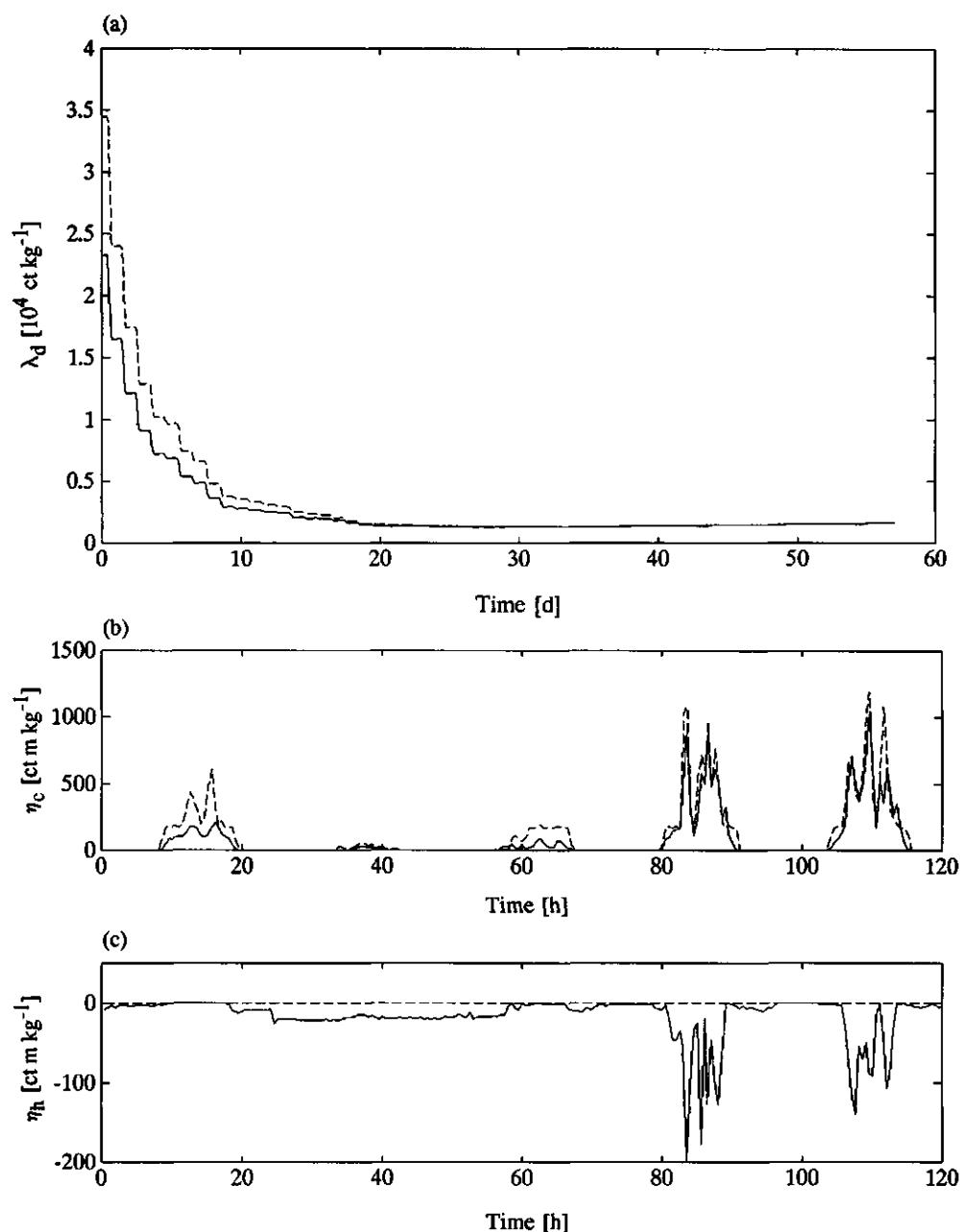
Fig. 7.6. Marginal value of total crop dry weight (a), carbon dioxide
          concentration (b) and absolute humidity (c), calculated
          with constraints on the carbon dioxide concentration and
          humidity in run 1 (—) and calculated without constraints
          in run 3 (--).

greenhouse climate management. The marginal value of crop dry weight is positive throughout the whole growing period, indicating the positive effect of an increment in crop dry weight on the economic return at harvest time. Also, the marginal value of crop dry weight is high during the early stages of growth and gradually reduces towards the end of the growing period. In other words, during the early stages of growth a small increment in crop dry weight contributes more to the final economic return than at a later stage in the crop production period. The high marginal value of crop dry weight in the beginning of the growing period is caused by the fact that then light interception is a limiting factor for crop growth. Since the light interception is related with the dry matter present (eqn. (6.11a)), any increment in crop dry matter yields a higher light interception, earlier canopy closure and thus more dry matter production and a higher economic return at harvest time. It is interesting to note that this observation has been recognized in horticultural practice. It was exactly for the reason of rapid canopy closure that in the two growth experiments high day and night temperature set-points were maintained in the first two weeks to stimulate leaf area expansion (Corver, 1991).

Fig. 7.6c shows that, as observed in section 6.4, the humidity constraint results in a marginal value of humidity less than zero. If the humidity constraint is omitted, the marginal value is zero, since then humidity does not affect the performance of the crop production process any more.

In fig. 7.6a it can be seen that the humidity constraint has a negative effect on the marginal value of crop dry weight. Before canopy closure, dry matter production results in an expansion of leaf area and consequently an expansion of the transpiring canopy surface (eqns. (6.11a) and (6.11d)). The resulting increase in canopy transpiration leads to higher humidity levels in the greenhouse and more control effort is required to maintain the humidity below the constraint bound. The negative effect of the humidity constraint suggests to reduce the investment in dry matter production and leaf area expansion and thus counteracts the objective of rapid canopy closure to achieve a higher dry matter production also encountered in horticultural practice. Fig. 7.6b illustrates that, since the humidity constraint reduces the marginal value of crop dry weight, the marginal value of the carbon dioxide concentration is also reduced (see eqn. (6.15b)). At night the marginal value of carbon dioxide is zero, because then the photosynthesis rate is zero.

The differences in efficiency between the optimal control approach and the grower's approach to greenhouse climate management are quite large and one may argue whether such large improvements in efficiency of greenhouse climate control can be achieved in practice.

With respect to the origin of these large differences the following observations can be made. First of all, in this section, the optimal control approach represented an ideal situation since the control trajectories were calculated after the greenhouse experiment had ended using complete knowledge about the outside climatic conditions as well as the auction price. In practice, these external factors have to be predicted and errors in these predictions may reduce the benefits of optimal control suggested in this section. Secondly, in the present analysis the greenhouse climate dynamics were neglected based on the premise that only the slow trends in the outside climatic conditions were considered. In reality, rapid fluctuations in the outside climatic conditions do occur and their impact on greenhouse climate management as well as the role of the greenhouse climate dynamics thereon needs further attention. Finally, the crop growth model used for the calculation of the optimal control strategies only described crop dry matter production and other aspects related to crop quality, such as head formation, and the occurrence of physiological damage and fungal diseases under humid conditions, were not covered by the model.

In section 7.4 it will be shown that the problem of long term weather prediction is largely alleviated using the sub-optimal feedback-feedforward control scheme presented in section 5.8. In section 7.5 it will be shown that using the two time-scale decomposition proposed in section 5.6, the greenhouse climate dynamics and rapid fluctuations in the outside climatic conditions are efficiently dealt with. In horticultural practice, the high humidity levels calculated in run 1 with the time invariant constraint on the humidity during the day may be unfavourable for the quality of a lettuce crop. However, run 2, in which ventilation according to the grower was used to control the humidity level in the greenhouse showed that then carbon dioxide as well as heating energy were still more efficiently used. Furthermore, the optimal carbon dioxide concentrations and air temperatures, calculated in run 1, looked reasonable and are not expected to have an adverse effect on lettuce growth. Therefore, using optimal control with a more appropriately chosen humidity constraint, an improvement in efficiency of greenhouse climate management seems possible through a better adjustment of the greenhouse climate to the outside climatic conditions. But, clearly, the merits of optimal control are best tested in full scale validation experiments in the greenhouse.

7.2.4. Concluding remarks

From the single example considered in this section the following

conclusions are derived:

(1) in optimal greenhouse climate management, the ventilation windows are mainly operated to control the humidity level in the greenhouse,

(2) since humidity control has a very strong impact on the performance of optimal greenhouse climate control, an accurate assessment of the effect of humidity on the quality and quantity of crop production, either in terms of model equations or in terms of (time variant) constraints is required,

(3) the observation, that in optimal greenhouse climate management at night greenhouse heating beyond a minimum constraint on the air temperature is not profitable during lettuce cultivation, does not agree with standard horticultural practice; this probably points at a limitation of the growth model used in describing the effect of temperature on lettuce growth,

(4) using optimal control with a more appropriately defined constraint on relative humidity, an improvement in efficiency of greenhouse climate management is expected through a better adjustment of the greenhouse climate to the outside climatic conditions.

7.3. The effect of different crop growth models on optimal heating in greenhouse climate control

7.3.1. Introduction

In section 6.4, it was concluded that with the one state variable lettuce growth model, heating would not be profitable at night, since any increment in the air temperature would result in higher maintenance losses of dry matter thus affecting the final economic return in a negative sense. In the simulations presented in the previous section, the calculated optimal control trajectories included heating at night, but this was due to the minimum temperature constraint and the humidity constraint. Possibly, the model used does not correctly describe the temperature effects on crop growth. The same observation was made by Tchamitchan *et al.* (1992), who considered optimal greenhouse climate control during tomato production. They suggested an extension of the crop growth model with a carbohydrate buffer, since the transformation of carbohydrates to structural dry matter is an enzymatic process largely dependent on temperature. The two state variable model of lettuce growth, described and analysed in chapter 3, contains such a

carbohydrate buffer, namely the non-structural dry weight, X_n. In this section the effect of this carbohydrate buffer on optimal greenhouse climate control is investigated.

7.3.2. Methodology

Two optimal control problems, one with the one state variable lettuce growth model and one with the two state variable lettuce growth model, were solved. These control problems were stated in sections 6.2 and 6.3, respectively. In the present analysis, emphasis lies on control of the slow crop growth dynamics; the fast greenhouse climate dynamics are not considered. The various parameters defining the running costs, and the state and control constraints were listed in table 6.1. In the simulations, measured data of the outside climatic conditions obtained during the second greenhouse experiment in early 1992 were employed. Since only the slow trends in these data were of interest, the data consisting of two minute measurements of the outside climatic conditions, the control inputs and the greenhouse climate, were averaged over periods of half an hour. For further details about the integration of the state and costate equations as well as the solution of the control problems refer to section 7.2.2.

7.3.3. Results and discussion

In fig. 7.7, performance data of optimal greenhouse climate control calculated with the two models are presented. With the two state variable lettuce growth model slightly less dry matter production was simulated using more heating energy and less carbon dioxide. The differences, however, are rather small. A more pronounced difference can be observed in the total ventilation during a full production cycle, as shown in table 7.2. With both models, during day and night approximately the same energy consumption was calculated.

In fig. 7.8 (p. 200), the dry matter accumulation described by both models is shown. This figure explains the lower ventilation rate calculated with the two state variable model. In this model, canopy transpiration is related to the amount of structural dry matter present (eqn. (6.23e)), which is smaller than the total dry matter simulated with the one state variable lettuce growth model. Therefore, before canopy closure, a smaller effective transpiring canopy surface was simulated with the two state model. So, in the simulation with the two state variable model, the humidity level in the greenhouse was less affected by canopy transpiration and consequently less ventilation was needed to maintain the relative
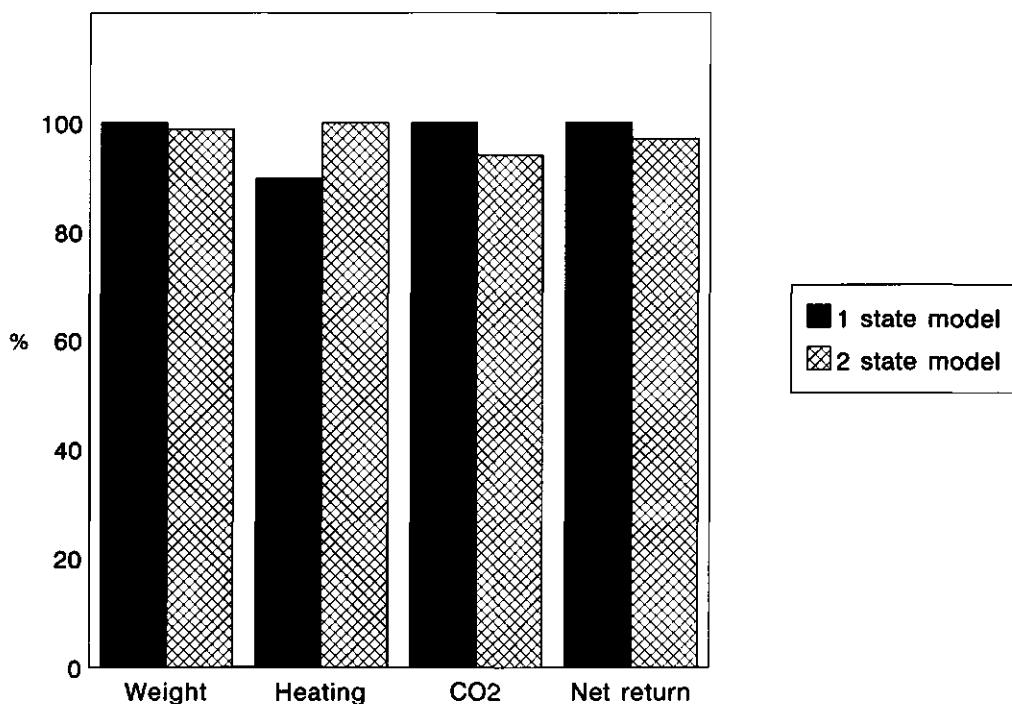
Fig. 7.7.   Performance of the controlled crop production process
calculated with the one state variable lettuce growth model
and the two state variable lettuce growth model.

Table 7.2.   Total carbon dioxide consumption, energy consumption and
ventilation during the whole growing period, calculated
with the one state variable lettuce growth model and the
two state variable lettuce growth model.

|	Carbon dioxide consumption $kg\ m^{-2}$		Energy consumption $MJ\ m^{-2}$		Ventilation $m^3\ m^{-2}$	
	Day	Night	Day	Night	Day	Night
1 state model	0.94	–	43	110	3519	6298
2 state model	0.88	–	56	114	2563	5241
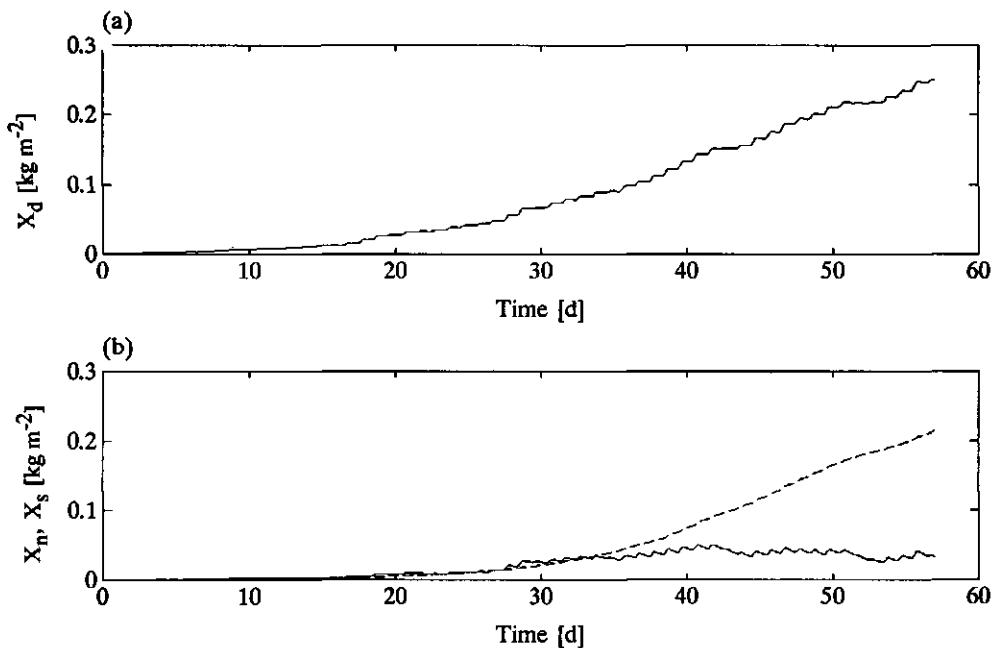
Fig. 7.8. Dry matter accumulation simulated with the one state
variable model (a) and the two state variable model (b); in
fig. (b) non-structural dry matter is denoted by (—) and
structural dry matter is denoted by (--).

humidity below the constraint. After canopy closure, the effective
transpiring canopy surfaces simulated with both models was the same.

In fig. 7.9 the costate trajectories related to crop dry matter
calculated in both control problems are depicted. The marginal values
of total crop dry weight (X_d), non-structural dry weight (X_n) and
structural dry weight (X_s) are positive throughout the whole growing
period, indicating that the economic return at harvest time will
benefit from an increment in crop dry weight. The marginal value of
crop dry weight is high during the early stages of growth and
gradually reduces towards the end of the growing period. Note, the
relatively high marginal value of the structural dry weight compared
with the marginal value of non-structural material. Since in the two
state variable model the light interception by the canopy is
determined by the amount of structural dry matter present; total crop
dry matter production is most strongly influenced by an increment of
the structural dry matter before canopy closure. This is indicated by
the relatively high marginal value. For growth of structural
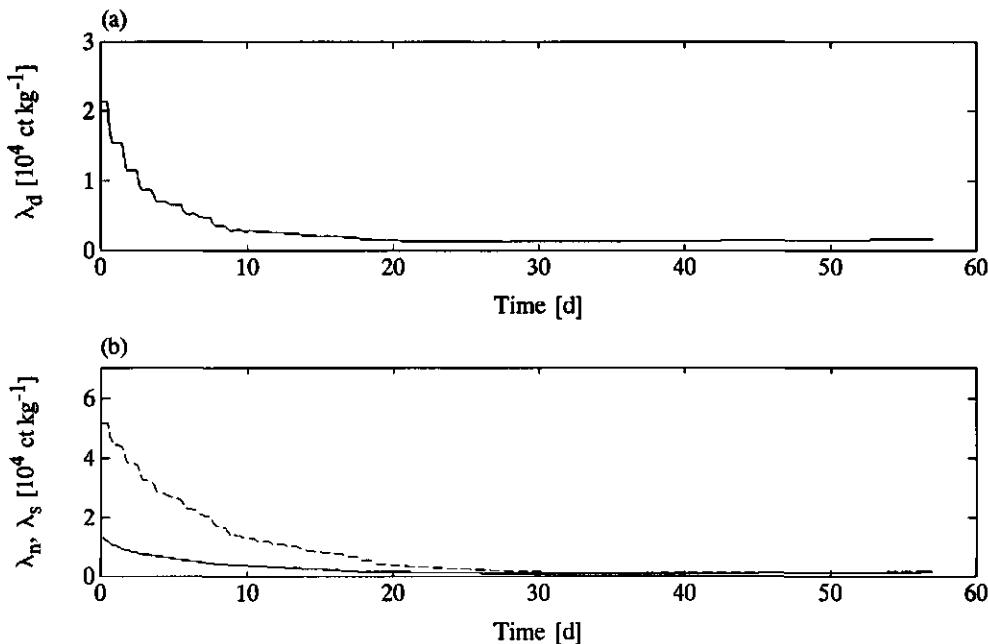
Fig. 7.9. Marginal value of total crop dry weight (a), non-structural dry weight (b: —) and structural dry weight (b: --).

material, however, non-structural material is required and therefore an increment in the non-structural dry matter will also contribute significantly to a higher gross economic return. This explains the increased marginal value of the non-structural dry weight before canopy closure.

The comparably high marginal value of the structural dry weight indicates that the performance would benefit from an enhanced transformation of non-structural dry matter into structural dry matter by means of a higher air temperature and that these benefits are most pronounced before canopy closure. Therefore, inspection of the calculated optimal state and control trajectories during the first days of the growing period, calculated with both models, were expected to reveal possible differences.

Fig. 7.10 shows the outside climatic conditions during the first five days of the growing period, in early 1992. In fig. 7.11 (p. 203) the optimal control strategies are presented. Since the relative humidity in the greenhouse was below the upper bound constraint, the ventilation windows were closed. Calculated with the two models, the
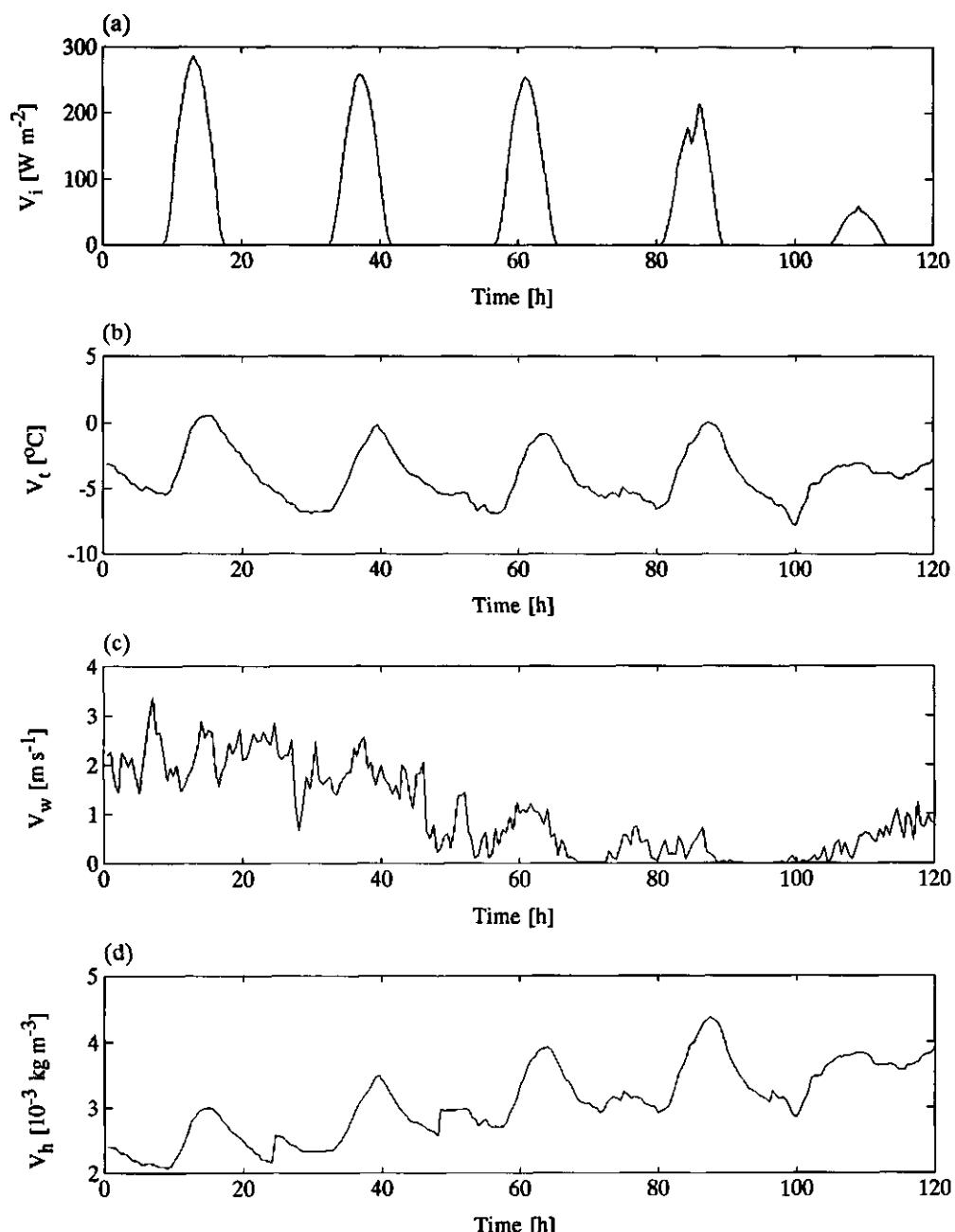
Fig. 7.10. Outside climatic conditions during the first five days of the growing period in early 1992: (a) solar radiation, (b) temperature, (c) wind speed and (d) absolute humidity.
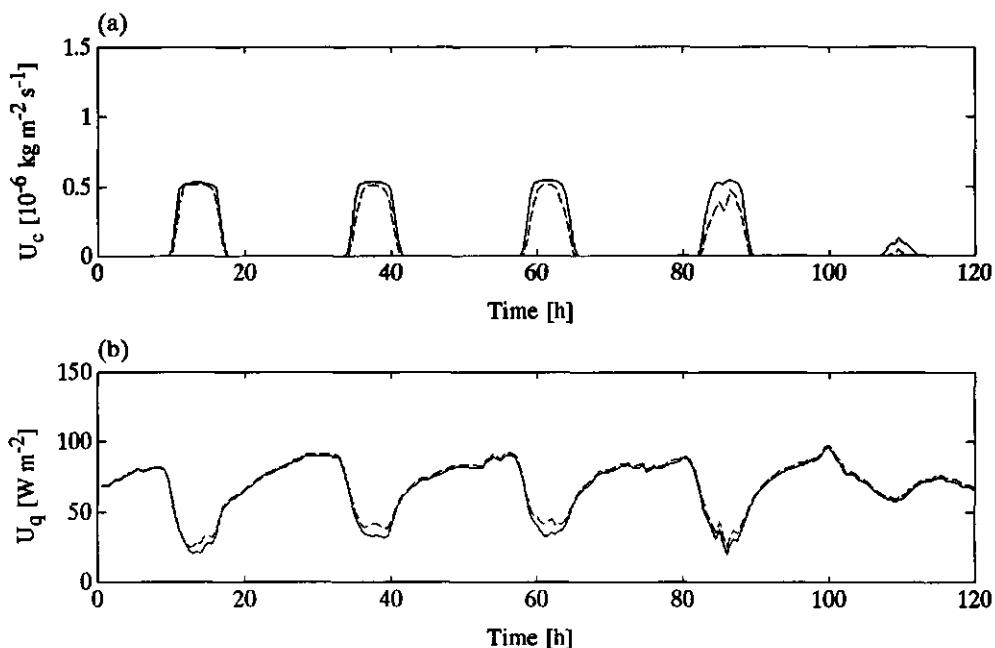
Fig. 7.11. Optimal carbon dioxide supply rate (a) and heating (b), simulated with the one state variable model (—) and the two state variable model (--).

optimal carbon dioxide supply rate and heating were found to be quite similar. Since the ventilation windows were closed in the simulations with both models, the differences in the greenhouse climate are largely explained by differences in the carbon dioxide supply rate and heating. The higher carbon dioxide supply rate calculated with the one state variable model resulted in a higher carbon dioxide concentration, whereas the slightly higher energy input calculated with the two state variable model yielded a somewhat higher air temperature. The differences, however, are small as can be seen in fig. 7.12. The lower relative humidity level calculated with the two state variable model largely explains the observed difference in ventilation rate as described before.

Differences in the energy consumption and air temperature were expected to occur at night, but fig. 7.12 clearly illustrates that the two growth models yielded almost the same result. At night, the air temperature was maintained around the minimum temperature. Due to the parameterization of the penalty function the calculated minimum

temperature was approximately 1.5 $^{\circ}$C higher than the minimum
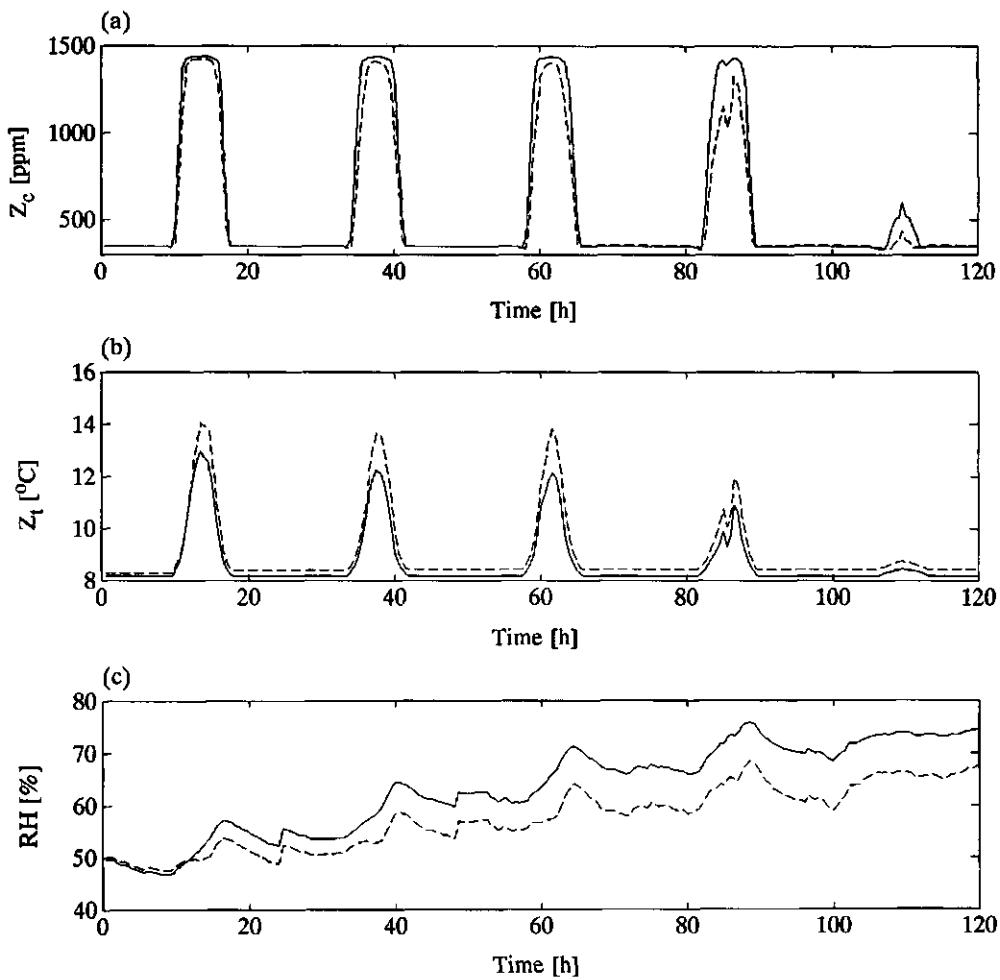
Fig. 7.12.   Optimal carbon dioxide concentration (a), air temperature
(b) and relative humidity (c), simulated with one state
variable model (—) and two state variable model (--).

temperature constraint of 6.5 $^\circ$C. Beyond this minimum temperature
additional heating did not seem to be profitable.

Fig. 7.13 sheds some new light on the effect of the two crop
growth models. This figure shows the marginal value of the air
temperature simulated with the previously calculated optimal control
trajectories. However, in the simulation the state constraint
penalties were omitted by setting the scaling parameters ζ_c, ζ_t and
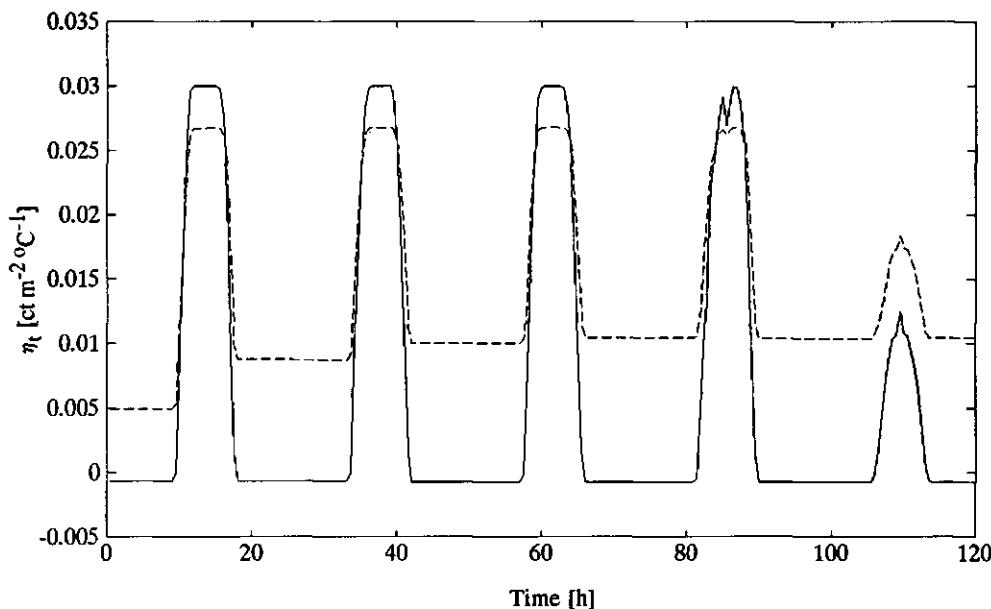
Fig. 7.13. Marginal value of air temperature simulated with the one state variable model (—) and the two state variable model (--), omitting the state constraints.

ζ_h equal to zero. Confirming the observations made in section 6.4, the marginal value of the air temperature, simulated with the one state variable model, is less than zero at night since any increment in the air temperature will yield higher maintenance respiration losses and thus a reduction of the gross economic return. Simulated with the two state variable model, the marginal value of the air temperature is positive at night indicating that an increment in the air temperature contributes positively to the gross economic return as was expected. This positive effect which is determined by the positive effect of the temperature on the transformation of non-structural dry matter to structural dry matter, however, is small. Although the costate is larger than zero, the necessary conditions for optimality described in eqn. (6.16c) require that, for the given price of a unit amount of energy, the costate should at least have a value of $c_q c_{cap,q} = 0.02$ for heating to be profitable. Since the costate is smaller than 0.02, the revenues of additional heating do not outweigh the additional costs.

These results clearly demonstrate a distinguishing feature of optimal greenhouse climate management compared with horticultural practice, namely that, during the whole production cycle, the

benefits of greenhouse climate control are constantly weighed against
the costs of operating the climate conditioning equipment.

The results obtained in this section confirm the observations
made in the sensitivity analysis of the two state variable model in
section 3.3, since there it was found that given the climate
conditions during the second growth experiment in early 1992, the
transformation of non-structural to structural dry matter was not a
limiting factor for total dry matter production. The fact that in the
optimal control problem, the final return is based on total crop dry
weight and no distinction is made between non-structural and
structural dry weights, does not encourage the transformation of non-
structural to structural dry weight by means of raising the
temperature in the greenhouse. It is expected that for a crop like
tomatoes and cucumbers this may be different, since fruit growth is
largely dependent on the carbohydrates produced in the leaves and
their temperature dependent transformation into structural material.

In the models used in this thesis, the temperature effects were
included in the photosynthesis rate, maintenance respiration rates
and the transformation of non-structural material into structural
material, but it was found that the costs of heating the greenhouse
did not outweigh the benefits of higher dry matter production. The
temperature effects on morphogenetic aspects of lettuce growth such
as leaf area expansion and head formation (Bensink, 1971), have not
been considered in this thesis. A higher temperature yields a higher
leaf area ratio and will result in earlier canopy closure. The
influence of this on the results obtained in the present research is
not completely clear. First of all, using a fixed leaf area ratio,
dry matter production during the two greenhouse experiments was quite
successfully simulated. Secondly, the sensitivity analysis in section
3.3 revealed that the leaf area ratio has a strong impact on dry
matter production during the early stages of growth, but this effect
diminishes towards the end of the growing period. Therefore, it is
questionable whether the additional revenues obtained from increasing
the leaf area ratio by adapting the air temperature would outweigh
the considerable costs of heating the greenhouse. After canopy
closure, head formation of the crop largely determines the quality of
the crop. For head formation, however, low air temperatures are
preferred.

Finally, in view of the time-scale decomposition of greenhouse
climate management advocated in this thesis, it is interesting to see
in fig. 7.8 that even in the two state variable crop production model
different response times do exist; the non-structural dry weight
responds relatively quickly showing a clear diurnal pattern whereas
structural dry weight responds comparatively slowly.

7.3.4. Concluding remarks

From the results obtained in this section and section 3.3 it is concluded that:

(1) due to small benefits of the temperature driven transformation of non-structural to structural dry matter compared with the considerable costs of heating the greenhouse, the extension of the model with a carbohydrate buffer does not significantly alter the heating strategies in optimal greenhouse climate control during lettuce cultivation,

(2) since, when evaluated under practical circumstances, total dry matter production was sensitive to small changes in the leaf area ratio, it is possible that temperature effects on crop morphology (leaf area ratio, head formation) are more important than the temperature effects already included in the model and need further attention in future climate control research,

(3) in optimal greenhouse climate control, the benefits of greenhouse climate control in terms of a higher yield and gross income of the crop production, are constantly weighed against the operating costs of the climate conditioning equipment. Therefore a change of the greenhouse climate, though having a positive effect on crop growth, may not be profitable due to the costs of climate conditioning needed to achieve this change.

7.4. Sub-optimal feedback, feedforward control of the slow crop growth dynamics

7.4.1. Introduction

Application of optimal control in greenhouse climate management requires an accurate model description of the crop production process, an accurate assessment of the economic revenues at harvest time as well as, in principle, detailed knowledge about the outside climate conditions during the whole growing period considered. Since these requirements are not met in practice, the value of the open-loop solution of the optimal control problem for actual implementation in practice is limited (Challa and Van Straten, 1991). Van Henten and Bontsema (1991) investigated a state feedback approach to deal with errors in the weather prediction while controlling the slow crop growth dynamics. The results were not very encouraging and it was suggested that a feedforward approach would improve the

performance. The sub-optimal control scheme presented in section 5.8, meets these requirements; it includes a state feedback loop as well as feedforward control based on the outside climatic conditions. The algorithm is based on the framework of optimal control theory, it is easily implemented in an on-line environment and it is expected to yield sub-optimal performance under perturbations of the system's state and external inputs from their nominal trajectories. In this section the sub-optimal control scheme is evaluated by simulations.

7.4.2. Methodology

In this section the control problem concerning the four state variable crop production process is used as an example. The example focuses on economic optimal control of the slow crop growth dynamics and the greenhouse climate dynamics will be neglected for the moment. The system equations and control problem were presented in section 6.2.2. The various parameters defining the running cost, and the state and control constraints were listed in table 6.1. To be able to compare the results with the previous sections, only the slow trends in the outside climatic conditions were considered. The sub-optimal control algorithm was evaluated using half hour averages of the measured weather data obtained during the 1992 greenhouse experiment.

As described in section 5.8, the sub-optimal control scheme contains two steps. First, a so-called nominal solution of the optimal control problem is derived using a prediction of the outside climatic conditions for the whole growing period considered and an estimation of the initial state of the system (Steps [1.1] and [1.2]). In this section average values of weather recordings, collected from 1975 to 1989 by the Department of Meteorology of the Wageningen Agricultural University, were used as long term weather prediction. These data included the daily solar radiation sum, average, minimum and maximum air temperatures, wind speed and relative humidity. Using these daily data diurnal trends were reconstructed as described in appendix B. In this section, perturbations in the initial state are not considered.

The costate sensitivity to perturbations in the state trajectory, eqn. (5.172), was calculated in a backward integration of the partial derivative of the costate equation (eqn. (6.11a)), with respect to the state variable X_d using $\partial\lambda/\partial x = 0$ at $t = t_f$ (Step [1.3]).

Then, secondly, the system equations were simulated using the measured weather data obtained during the second greenhouse experiment in early 1992. Using the previously calculated nominal state and costate trajectories as time varying references, at every

time step, the costate was modified using the calculated perturbation in the state and a new sub-optimal control was calculated based on the value of the actual (perturbed) state of the system and a one step, *i.e.* half hour, ahead prediction of the outside climatic conditions. In the simulations with the sub-optimal control algorithm exact prediction of the weather was assumed; the one step ahead prediction was set equal to the next measurement in the 1992 data. Hereafter this simulation is referred to as 'sub-optimal 1'.

Two other simulations were performed using an alternative implementation of the sub-optimal control scheme. In a simulation, hereafter referred to as 'sub-optimal 2', the costate modification in step [2.3] was omitted and the sub-optimal control algorithm employed the unmodified nominal costate trajectory. Finally, to evaluate the effect of the time variant character of the costate trajectory on the optimization, in a third simulation referred to as 'sub-optimal 3', a constant costate trajectory was employed which was set equal to the marginal value of the crop at harvest time.

To evaluate the performance of the sub-optimal control scheme, the optimal control problem was also solved using the measured outside climatic conditions in the 1992 greenhouse experiment. This simulation run, representing the ideal case of having complete knowledge about the weather during the whole growing period considered is referred to as 'optimal'. As an additional reference, in a simulation of the crop production system, the nominal control trajectories were used together with the outside climatic conditions measured during the 1992 greenhouse experiment. This simulation is referred to as 'open-loop', since it does not use any information about the actual state of the process, nor about the real outside climatic conditions.

For the technical details of the simulation and solution of the optimal control problems refer to section 7.2.2.

7.4.3. Results and discussion

The costate sensitivity for perturbations in the state of the crop is shown in fig. 7.14. The negative sensitivity implies that positive deviations in the state of the crop reduce the marginal value of the crop dry weight. The influence of the state deviations on the evolution of the costate are most pronounced during the early stages of crop growth.

The nominal, optimal and sub-optimal costate trajectories are presented in fig. 7.15 (p. 211). There is a rather large difference between the nominal costate trajectory and the optimal costate trajectory. Also, it can be seen that in the simulation
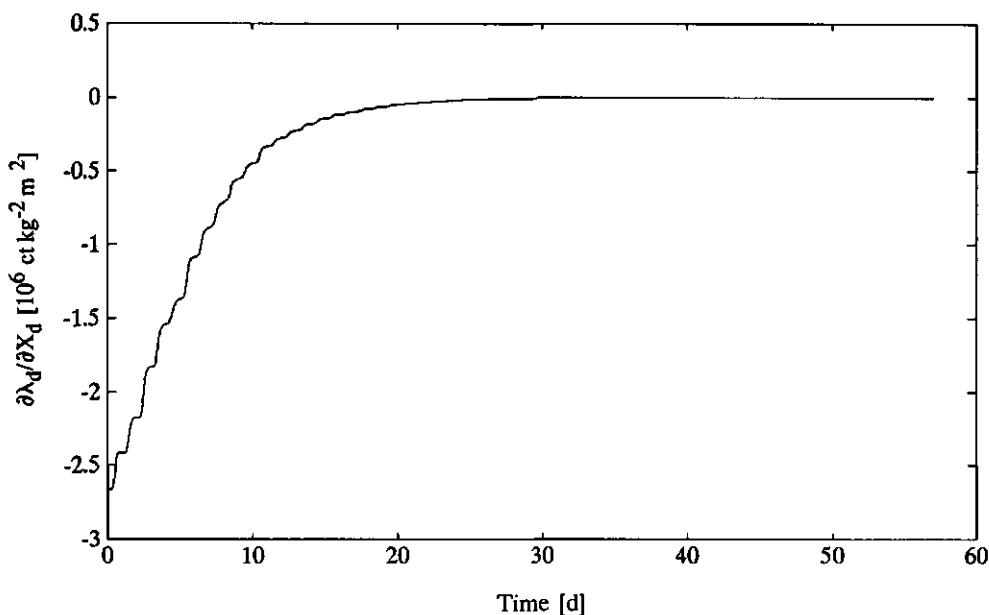
Fig. 7.14.   Sensitivity of the costate of crop dry weight with respect
              to perturbations in the crop dry weight, evaluated around
              the nominal optimal costate trajectory.

'sub-optimal 1', the costate modification due to perturbations in the
dry matter content of the crop does not cover the gap between the
optimal and the nominal costate trajectories.
        Fig. 7.16 (p. 212), in which the nominal and optimal dry matter
accumulation as well as dry matter accumulation using open-loop and
sub-optimal control are shown, illustrates that the sub-optimal
control algorithm actually yields a slightly higher dry matter
production than in the optimal solution. Using open-loop control a
distinct reduction in dry matter production is obtained.
        Fig. 7.17 (p. 213) produces some more insight into the
performance of the sub-optimal control algorithm. For a realistic
comparison the value of the performance criterion J is mentioned as
well, since J also includes the penalties on state constraint
violations. Comparing the performance criterion J of the sub-optimal
control approach with the performance of the optimal solution and
open-loop solution, reveals the favourable characteristics of the
sub-optimal control scheme. Only in run 'sub-optimal 3', using a
constant costate trajectory, is a reduction in the performance
criterion found. Actually, with a higher carbon dioxide consumption
in runs 'sub-optimal 1' and 'sub-optimal 2' a slightly higher dry
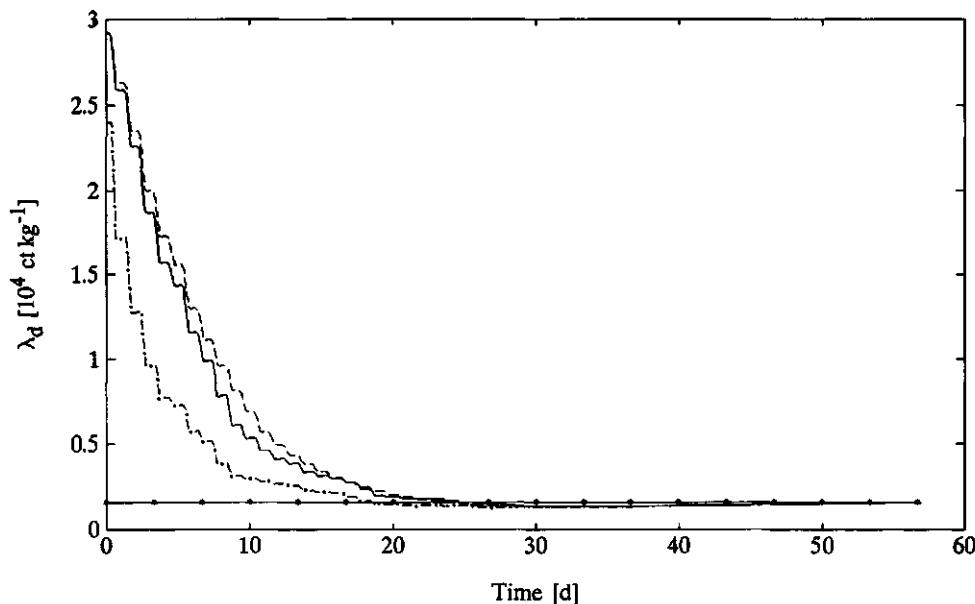
Fig. 7.15. Nominal costate trajectory (--), optimal costate trajectory (-·), sub-optimal costate trajectory with adaptation (——) and constant costate trajectory (-*-).

matter production was achieved. With open-loop control, heating and carbon dioxide were not used efficiently. A negative value of the performance criterion J was found, possibly due to considerable violations of the constraint on the relative humidity.

The characteristics of the sub-optimal feedback, feedforward control scheme compared with open-loop control are illustrated in figs. 7.18 to 7.20 for a five day period in the beginning of the growing season. As shown in fig. 7.18 (p. 214), the nominal and the actually measured weather are quite different. Optimal, open-loop and sub-optimal control trajectories, calculated with costate adaptation, are presented in fig. 7.19 (p. 215) and the simulated greenhouse climate is shown in fig. 7.20 (p. 216). These figures clearly show that the sub-optimal control scheme exploits the opportunities in the weather conditions and adapts the indoor climate in response to changes in the outdoor climate. The open-loop control, however, does not make use of this actual weather information and the greenhouse climate is not very efficiently controlled. Open-loop control resulted, for instance, in very high humidity levels yielding the negative value of the performance measure found in fig. 7.17 (p. 213).
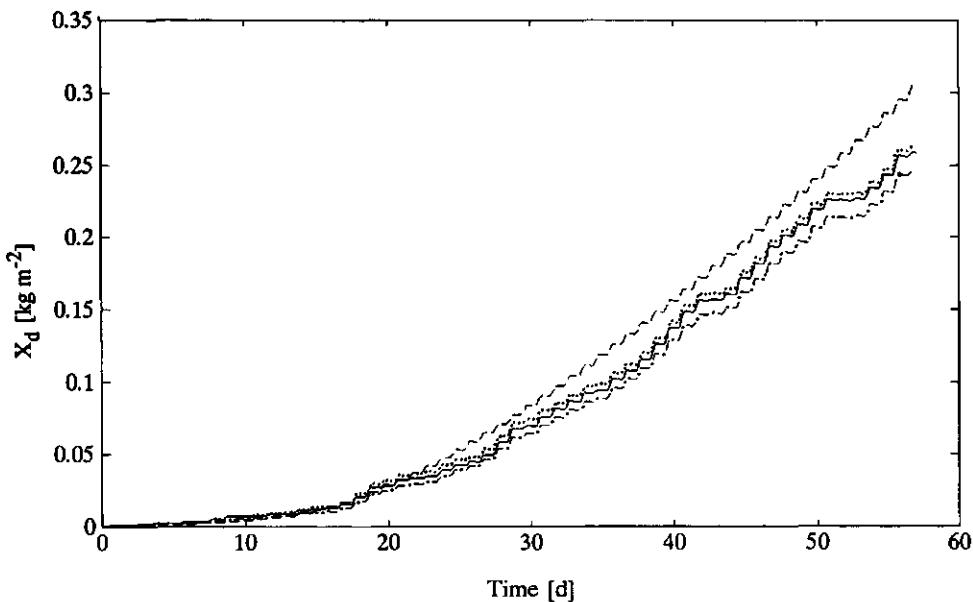
Fig. 7.16.   Nominal   dry   matter   accumulation   (- -),   and   dry   matter
             accumulation   simulated   with   optimal   control   (—),   sub-
             optimal   control   with   costate   adaptation   (...)   and   open-
             loop control (- ·).

The sub-optimal control algorithm calculated a higher carbon dioxide
supply and ventilation rate than the optimal solution, which is
explained by the fact that the marginal value of crop dry weight used
in the sub-optimal control strategies was higher than the optimal
marginal value. Since the marginal value of crop dry weight affects
the marginal value of the carbon dioxide concentration (see eqn.
(6.15b)), a higher carbon dioxide supply rate was calculated. The
differences between the optimal and sub-optimal heating were found to
be small. With optimal control and sub-optimal control, the
trajectories of the humidity and air temperature in the greenhouse
are almost the same, as shown in fig. 7.20 (p. 216).
       The favourable results of the sub-optimal control scheme has a
very interesting implication. Until quite recently the long term
weather prediction required for optimal control of the slow crop
growth dynamics was felt to be a major complication for successful
application of optimal control in horticultural practice. In this
section, using an exact one step ahead prediction of the weather,
near optimal performance was achieved with the feedback-feedforward
algorithm. Although a reduction in performance is expected to occur
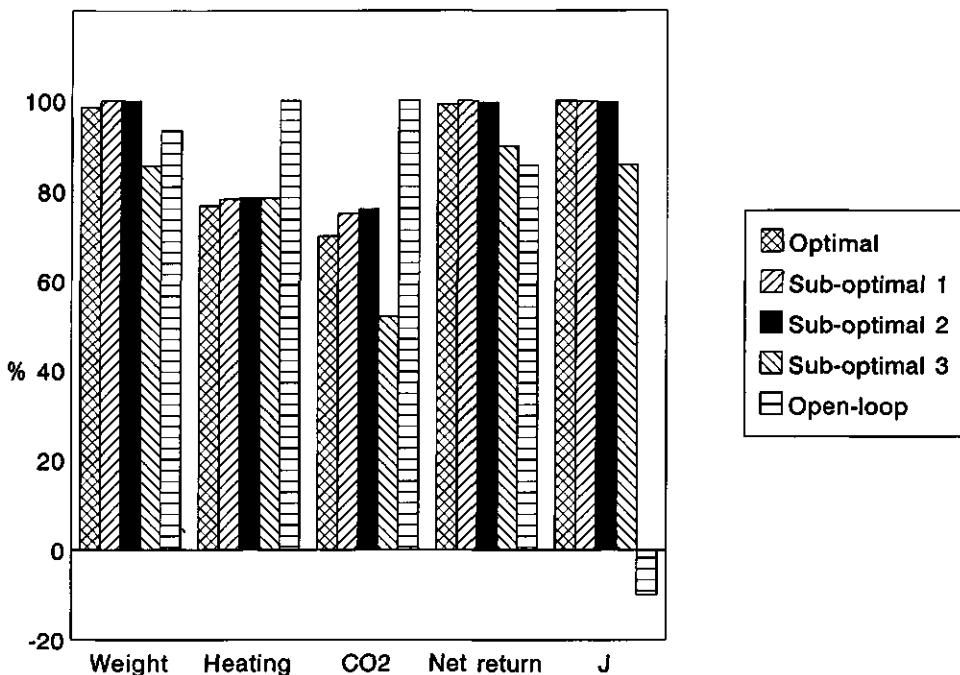
Fig. 7.17. Performance of the sub-optimal control algorithm.

if the weather prediction is very inaccurate, the results clearly illustrate that for economic optimal control of the relatively slow crop growth dynamics, the problem of generating long term weather predictions is largely alleviated and a short term weather prediction of at most a few hours ahead seems sufficient. From a practical point of view this is very attractive.

The results obtained in this section put the results of section 7.2 into a better perspective. The fact that near optimal performance can be achieved with sub-optimal feedback-feedforward control, indicates that, in practice, the weather is no longer a limiting factor in obtaining the improved efficiency of greenhouse climate management found in section 7.2.

An important step in the sub-optimal control algorithm is the maximization of the Hamiltonian with respect to the control inputs. As eqn. (6.14) shows, the Hamiltonian contains the non-linear dynamics of the system and therefore the sub-optimal control approach generates a non-linear feedback, feedforward control law which exploits the non-linear characteristics of the controlled process.
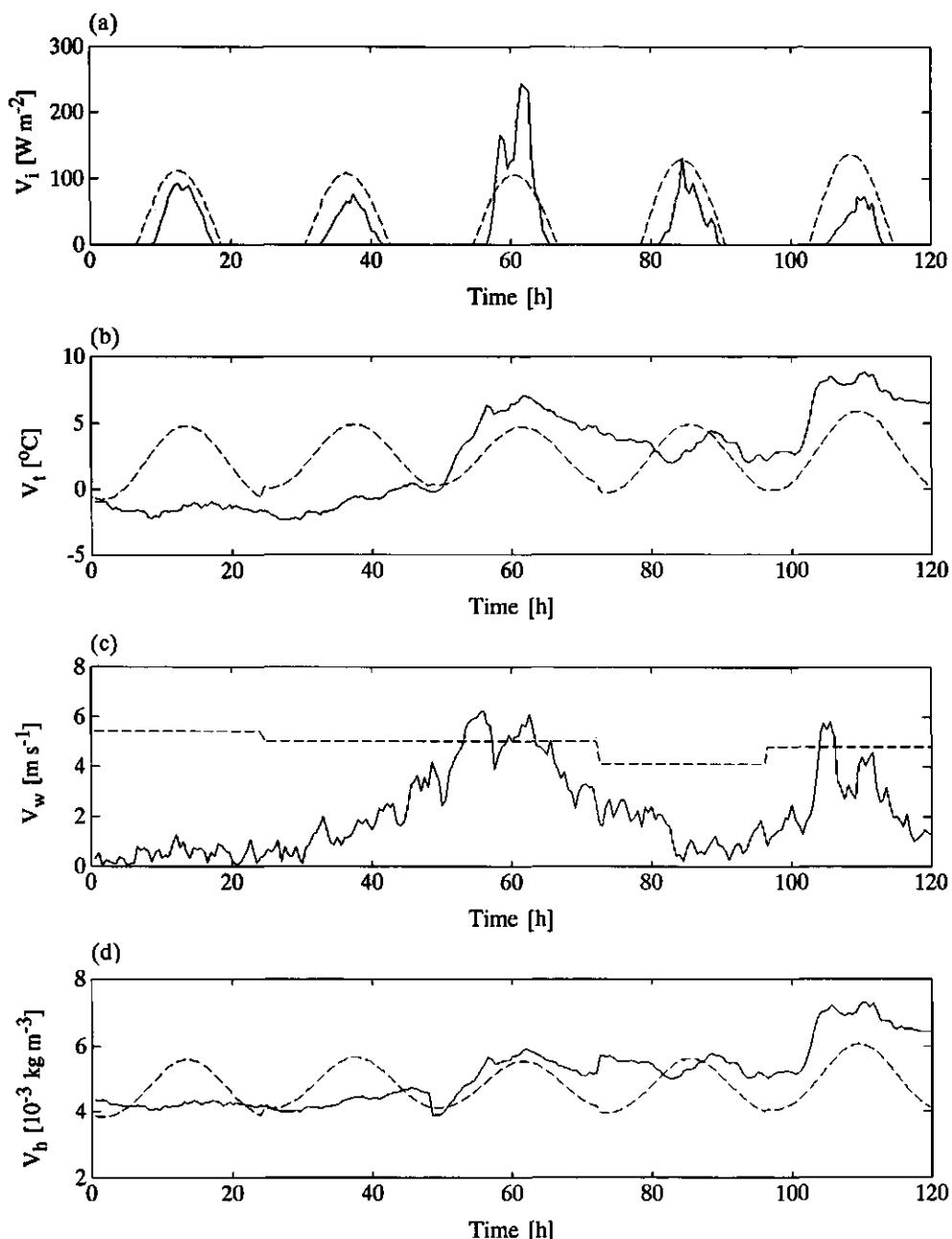
Fig. 7.18.   Nominal (- -) and measured (—) outside climatic conditions during a five day period: (a) solar radiation, (b) air temperature, (c) wind speed and (d) absolute humidity.
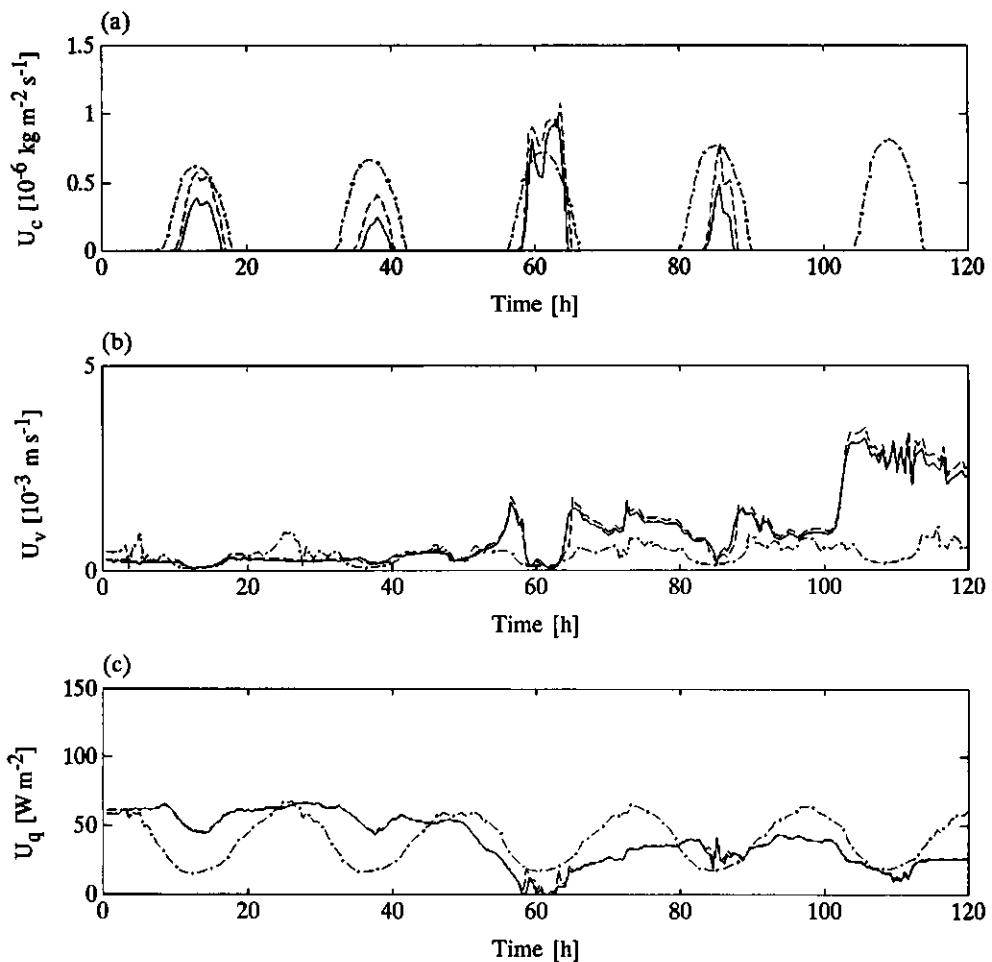
Fig. 7.19. Optimal (—), sub-optimal (−−) and open−loop control (−·)
trajectories of carbon dioxide supply rate (a),
ventilation rate (b) and heating (c).

This interesting feature requires more attention in future research.

The performance of the sub-optimal control algorithm is essentially determined by the sensitivity of the Hamiltonian and the optimal control with respect to the costate. From the fact that the sub-optimal controller without state induced costate modification yielded near optimal performance, it is concluded that, in the control problem considered, the optimal control is not very sensitive to variations in the costate variables. However, the application of a
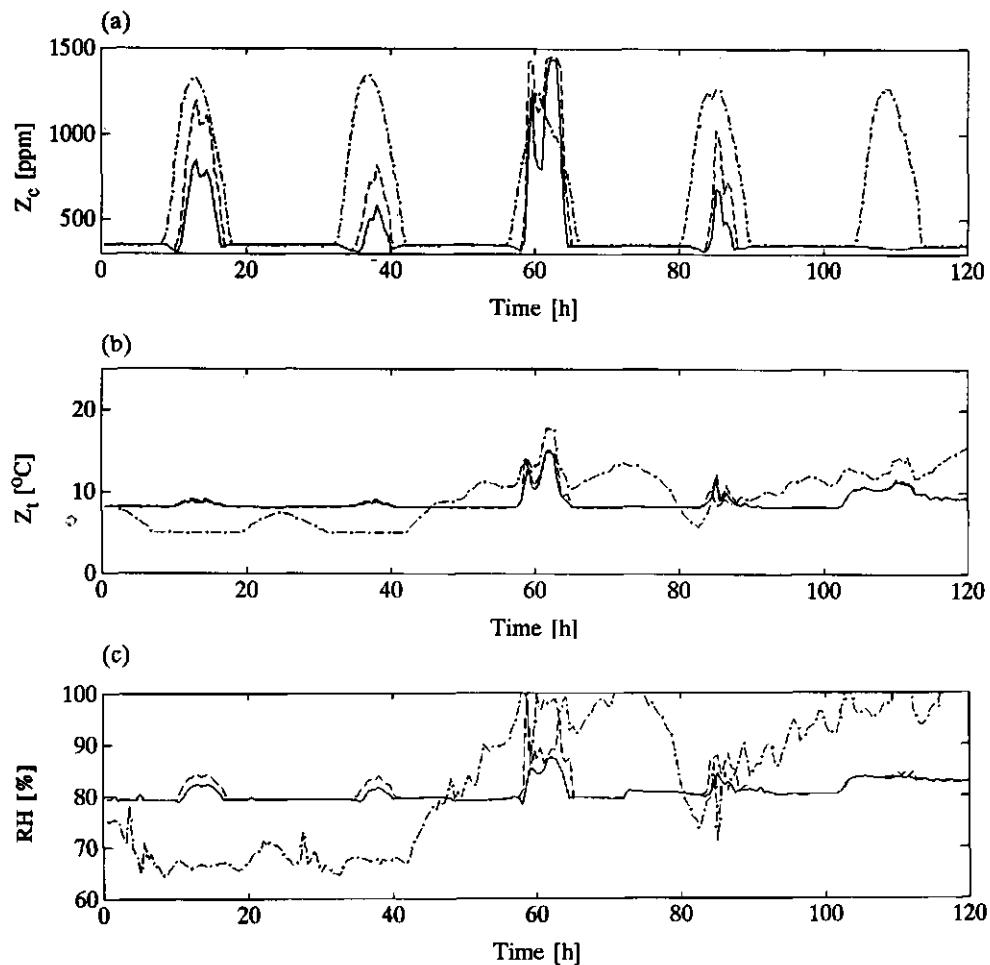
Fig. 7.20. State trajectories of carbon dioxide concentration (a),
air temperature (b) and relative humidity (c), simulated
with optimal control (—), sub-optimal control using
costate adaptation (--) and open-loop control (-·).

constant costate value resulted in a reduction in performance of the
controller. Therefore, for a general successful application of this
sub-optimal scheme in crop growth control, it seems crucial to
account for the fundamental trend in the costate trajectory assigning
a higher marginal value to crop dry weight before canopy closure. The
generality of these trends has been investigated briefly by solving
the optimal control problem with the two state variable lettuce
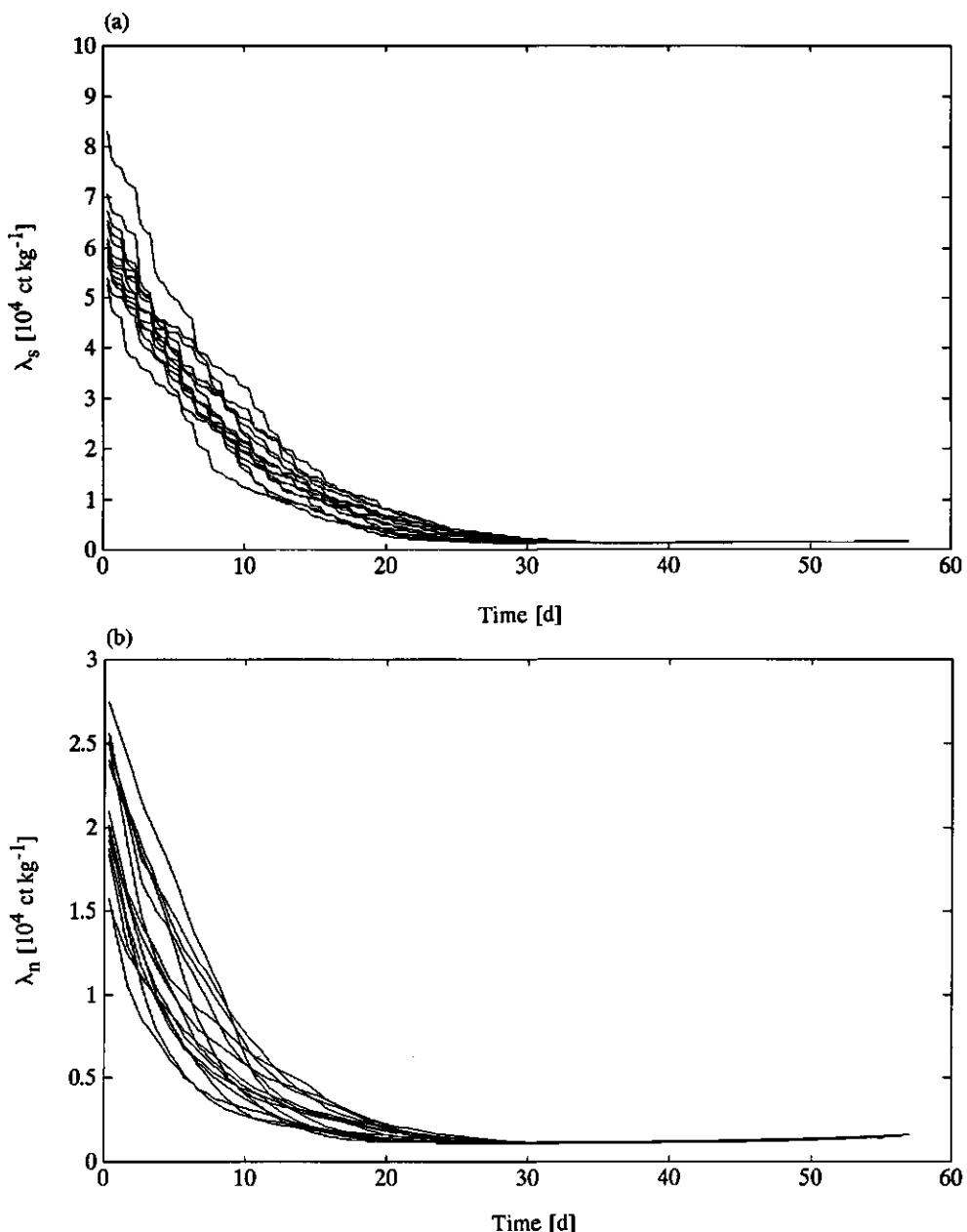
Fig. 7.21. Optimal costate trajectories of structural dry weight (a) and non-structural dry weight (b), calculated for the first 57 days of 1975 to 1989 with the two state variable lettuce growth model.

growth model (see section 6.3), for the individual years in the 1975 to 1989 weather data set. The calculated costate trajectories for non-structural and structural dry weights are shown in fig. 7.21. Differences do exist amongst these trajectories, but they all contain the same fundamental trend. Since these differences may affect the performance of the algorithm, in practice it may be necessary to recalculate the nominal solution during the growing period using a measurement of the state of the crop and a new (long term) weather prediction. Recalculation of the nominal solution may also be needed if a better prediction of the auction price becomes available, since this will affect the marginal value of the crop during the growing period.

Since the marginal value of crop dry weight is high during the first few weeks of the growing period, it seems that accurate state feedback control is important at that time. For the state feedback loop, measurements of the state of the crop are required. Usually destructive measurements are used to determine crop dry weight and other crop related state variables. In Appendix A, a non-destructive method for the measurement of crop dry matter using image processing techniques is described and evaluated.

7.4.4. Concluding remarks

From the results obtained in this section it is concluded that:

(1) using state feedback and feedforward of the weather conditions, the sub-optimal control algorithm is able to produce near optimal performance under rather large perturbations of the state and external inputs from the nominal trajectories,

(2) in the feedback, feedforward control scheme the costate serves as an investment policy for greenhouse climate control and therefore, it is important to have a description of the fundamental trends in the costate trajectory; in the example considered the performance of the control scheme was not much affected by small errors in the costate value,

(3) the results indicate that for application in horticultural practice using the sub-optimal feedback, feedforward controller weather, predictions for a period of only a few hours ahead are sufficient for on-line control,

(4) the weather prediction is no longer a limiting factor in obtaining, in horticultural practice, the improved efficiency of

greenhouse climate management found in section 7.2.

7.5. Validation of the two time-scale decomposition

7.5.1. Introduction

In this section, the validity of the two time-scale decomposition of optimal control problems with rapidly fluctuating external inputs, proposed in section 5.6, will be evaluated. In view of greenhouse climate management, the essential feature of the two time-scale decomposition is that the solution of the control problem in which both greenhouse climate dynamics and crop growth dynamics are included, hereafter referred to as the full problem, is replaced by the sequential solution of two sub-problems. First, an optimal control problem concerning the slow crop growth dynamics is solved. In this control problem, referred to as the 'slow sub-problem', the greenhouse climate dynamics are neglected. Then, secondly, the 'fast sub-problem' aiming at economic optimal control of the greenhouse climate dynamics is solved, using the state, costate and control trajectories calculated in the slow sub-problem as reference inputs. Besides the validity of the two time-scale decomposition, the importance of considering both the slow crop growth dynamics and the fast greenhouse climate dynamics in economic optimal greenhouse climate control will be addressed. Moreover, since the control strategies resulting from the solution of the full problem and the two time-scale decomposition can be used for minute by minute control of the greenhouse climate dynamics, their behaviour will be analysed with respect to application in horticultural practice.

7.5.2. Methodology

In the literature, the validation of the time-scale decomposition of singularly perturbed optimal control problems without external inputs has been established in a formal way by means of determining the convergence properties of the power series approximations of the state, costate and control variables as well as the performance criterion. It was found that the zero-th order terms of the power series produce an $O(\varepsilon)$ approximation of the state variables and performance criterion of the full system (Freedman and Granoff, 1976; Freedman and Kaplan, 1976; Belokopytov and Dmitriev, 1986; Benssousan, 1988). Without further proof it was suggested by Kokotovic *et al.* (1986) that these results also apply to singularly perturbed systems affected by slowly varying external inputs.

However, they are not applicable to singular perturbed systems
disturbed by rapidly fluctuating inputs such as the greenhouse crop
production process. The reason is that, in the above mentioned
convergence proofs, it is assumed that the fast system variables
rapidly converge to the zero-th order slow reference trajectories,
the so-called outer solution $\bar{z}_0$. Since in the greenhouse crop
production process the fast state variables, *i.e.* the greenhouse
climate variables, are continuously exited by exogenous inputs, they
are not expected to converge to their outer solution $\bar{z}_0$.
Consequently, a straightforward extension of the previously mentioned
convergence proofs to the problems considered in this thesis is not
available.

In this thesis, the validity of the time-scale decomposition is
evaluated by means of a qualitative and quantitative comparison of
simulations of the slow and fast sub-problems with the solution of
the full control problem. The decomposition is considered successful
if (i) the optimal performance of the full problem is approximated by
the sum of the optimal performances of the slow sub-problem and the
fast sub-problem, *i.e.* $J^* \cong \bar{J}_0^* + \hat{J}_0^*$ and (ii) the control, state and
costate trajectories resulting from the solution of the full problem
are closely approximated by the trajectories obtained in the solution
of the slow and the fast sub-problems. For the latter criterion a
visual check will supply some insight into the similarity of the
control strategies, but a more stringent test will be to simulate the
full system dynamics with the control strategies resulting from the
two time-scale decomposition and to compare the performance of the
controlled process with the optimal performance of the full problem.

The decomposition is illustrated and evaluated for the control
problem concerning the four state variable crop production process,
stated in section 6.2. The equations governing the full problem were
defined and necessary conditions were derived in section 6.2.1. In
sections 6.2.2 and 6.2.3, equations of the slow and fast sub-problems
were given. The various parameters defining the running cost, and the
state and control constraints were listed in table 6.1. First the
full problem was solved. Then, secondly, the slow sub-problem was
solved and the calculated state, costate and control trajectories
were stored. Finally, using the state, costate and control
trajectories of the slow sub-problem, the fast sub-problem was
solved.

In the simulations, measured data of the outside climatic
conditions obtained during the second greenhouse experiment in early
1992 were employed. These data consisted of two minute measurements
which were not filtered before use in the simulations. Though in the
second greenhouse experiment the growing period lasted for 57 days,

in the simulations a growing period of only 50 days was considered because of limitations in the available workspace on the VAX mainframe computer used for the solution of the control problem. The state and costate equations of the full problem, the slow sub-problem and the fast sub-problem were simulated in double precision with an integration time step of half a minute using a fourth order Runge-Kutta algorithm described by Press *et al.* (1986). The steepest ascent algorithm, described in section 5.7, was used for the iterative solution of the three control problems. The search for the optimizing control strategy was stopped once the improvement in the performance criterion was less than 1.0×10^{-6} during at least three consecutive iterations.
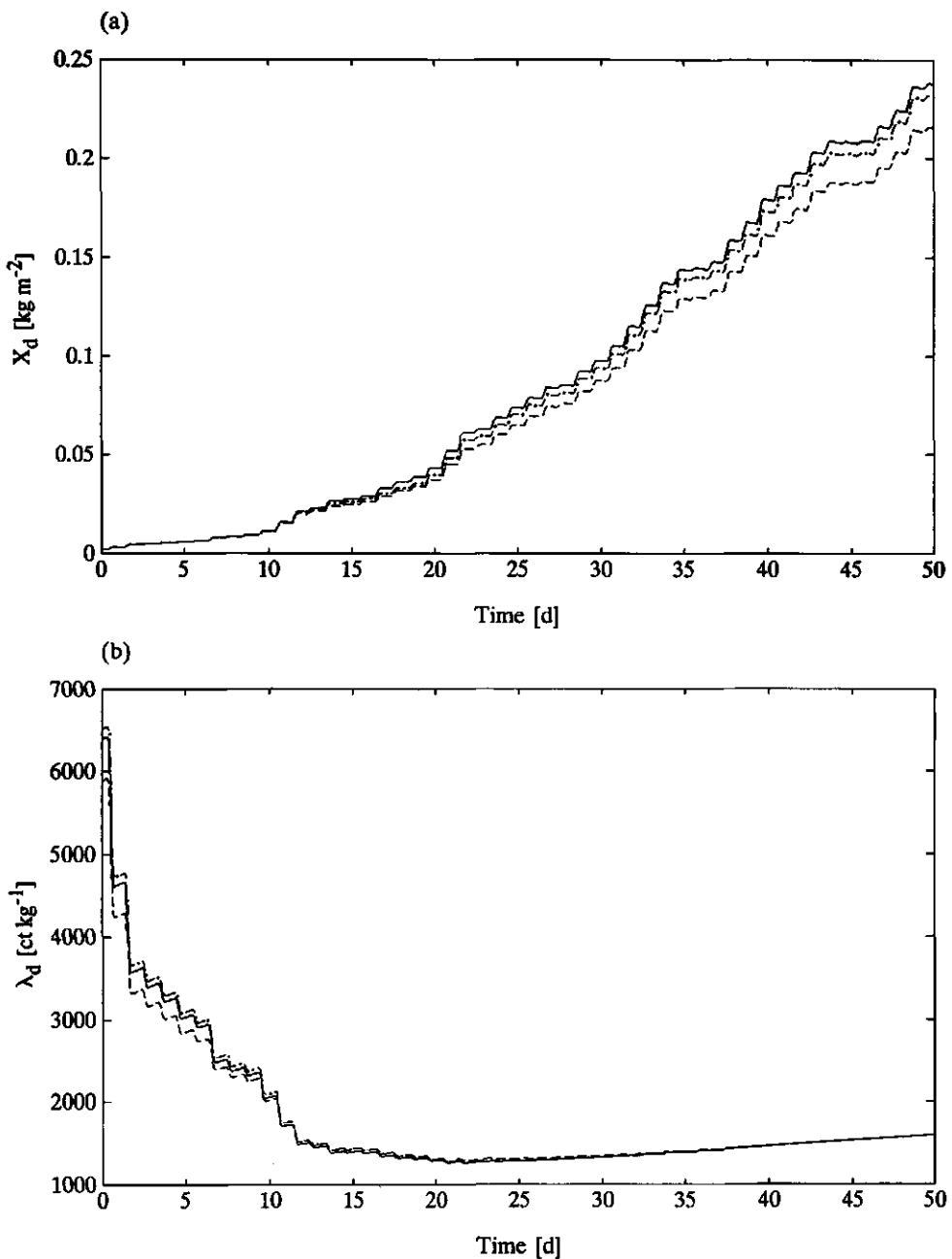
7.5.3. Results and discussion

The solution of the full problem, the slow sub-problem and the fast sub-problem yielded the absolute values of the performance criteria listed in table 7.3. For the two time-scale decomposition to be successful, the performance of the full problem (J) should be approximated by the sum of the performances of the slow sub-problem ($\bar{J}_0$) and the fast sub-problem ($\hat{J}_0$). With a value of 238.2, this sum is higher than the performance of the full problem having a value of 231.9. Still, these results suggest that, in the example considered, the two time-scale decomposition produces a successful approximation of the full control problem.

Table 7.3. Optimal performance (absolute values) of the full problem (J), the slow sub-problem ($\bar{J}_0$) and the fast sub-problem ($\hat{J}_0$) including penalties on constraint violations.

Simulation	Performance
Full problem (J)	231.9
Slow sub-problem ($\bar{J}_0$)	204.9
Fast sub-problem ($\hat{J}_0$)	33.3

The accuracy of this approximation as well as possible sources of error will become clear in a comparison of the calculated control, state and costate trajectories. Fig. 7.22 presents the evolution of

(a)

(b)

Fig. 7.22.   Simulated dry matter accumulation (a) and marginal value
of crop dry weight (b), obtained in the solution of the
full control problem (—) and the slow sub-problem (--)
and a simulation of the full system dynamics using the
optimal control trajectories of the fast sub-problem (-·).

crop dry weight (X_d) and the associated costate (λ_d) obtained in the solution of the full problem and the slow sub-problem. In the slow sub-problem, the simulation of crop dry weight and its marginal value approximates the trajectories simulated in the full problem, though the approximation is not very accurate. In the slow sub-problem, a smaller costate is found during the early stages of growth. This difference, however, vanishes towards the end of the growing period. At harvest, the difference becomes zero since at that time, in both control problems, the costate should satisfy the same condition $\lambda_d(t_f) = \partial\phi/\partial X_d = c_{prl,2}$. Also less dry matter production is simulated in the slow sub-problem; an increasing error towards the end of the growing period can be observed.

The fast sub-problem emphasizes the control of the fast greenhouse climate dynamics and the control, state and costate trajectories obtained in the solution of the slow sub-problem are used as reference trajectories. The optimal control strategies found in the fast sub-problem should approximate the optimal control strategies calculated in the full problem. Their equivalence was first checked by simulating the full system dynamics with the control strategies obtained in the fast sub-problem. The resulting trajectories of the slow state (X_n) and costate (λ_d) are shown in fig. 7.22 as well. A close approximation of the state and costate trajectories calculated in the full problem is found, suggesting that the control strategies calculated in the two time-scale decomposition accurately approximate the optimal control strategies calculated in the full problem.

More insight into the accuracy of the two time-scale decomposition is given in figs. 7.23 (p. 224) to 7.32 (p. 233), showing for a two day period half-way through the growing period the evolution of the control inputs, fast state variables and associated costates obtained in the solution of the full control problem and the slow and fast sub-problems. In fig. 7.23, measurements of the outside climatic conditions, *i.e.* solar radiation, temperature, wind speed and humidity are presented. It is worth noticing that besides a diurnal trend, the solar radiation contains high frequency variations. The impact of these high frequencies on the optimal control strategies of the full problem and the two sub-problems becomes clear in the subsequent figures.

Figs. 7.24 to 7.32 show that, as expected, the solution of the slow sub-problem is not a very accurate approximation of the solution of the full control problem. For instance, the optimal carbon dioxide supply rate calculated in the slow sub-problem rapidly fluctuates in accordance with variations in the solar radiation. Because, in the slow sub-problem, the greenhouse climate is described by a
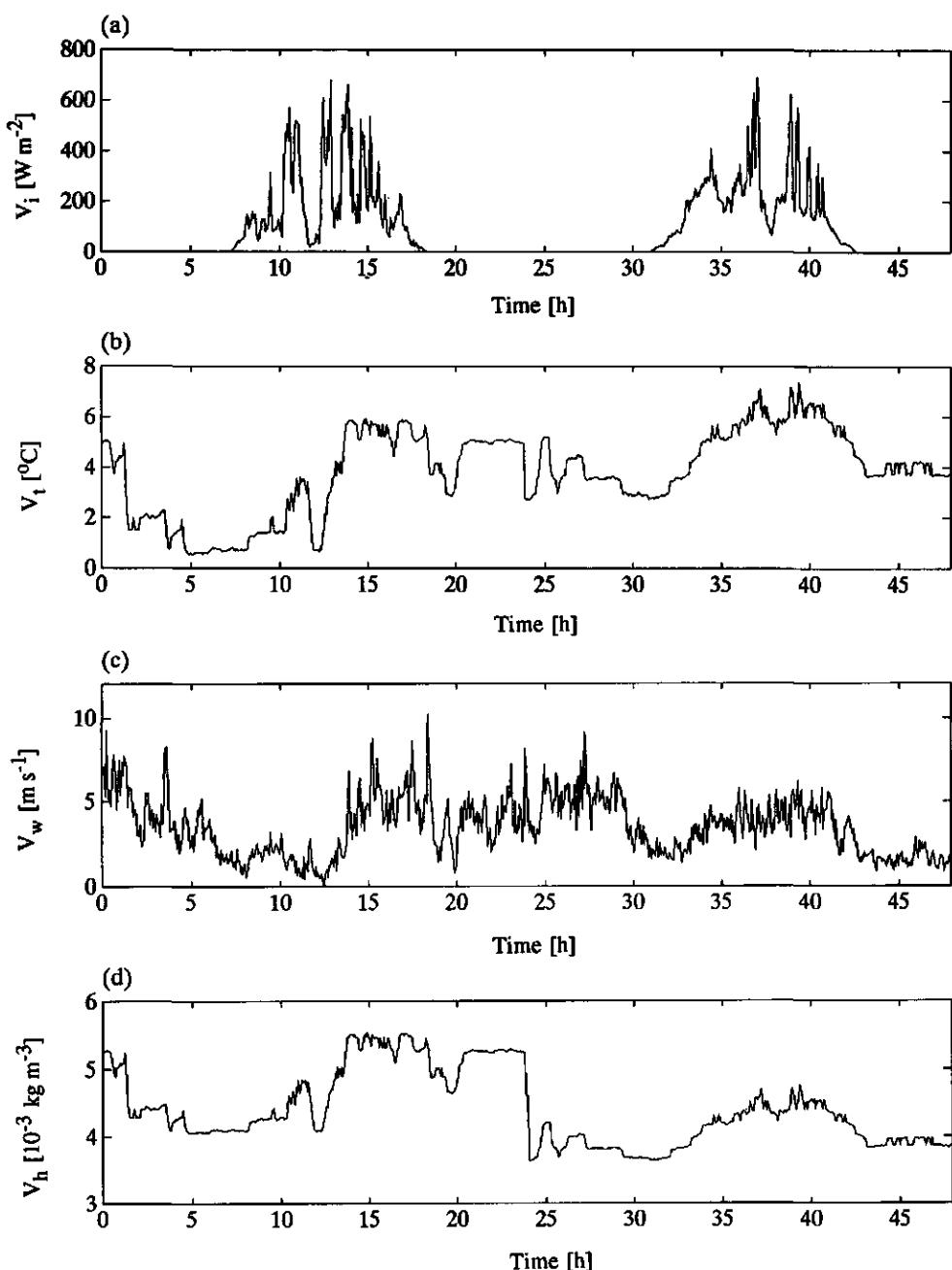
Fig. 7.23.   Outside climatic conditions during two days of the 50 days
             growing   period: (a)   solar   radiation,   (b)   temperature,
             (c) wind speed and (d) absolute humidity.
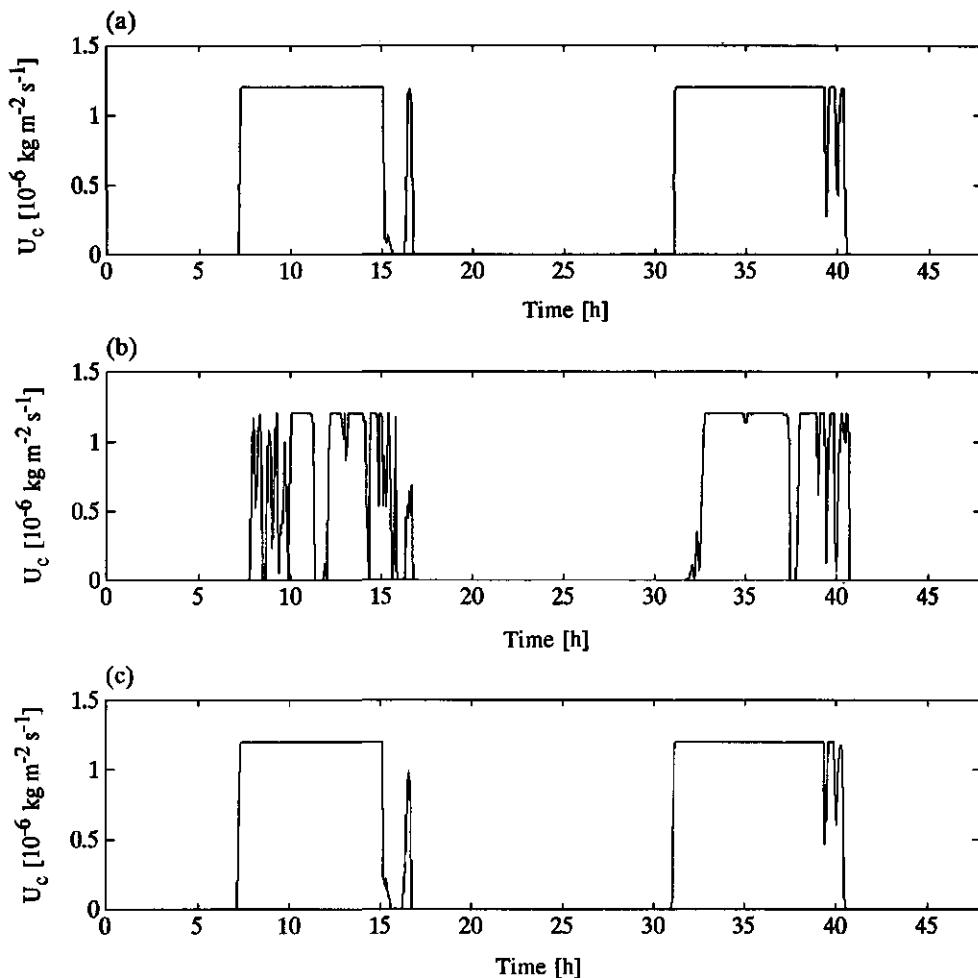
Fig. 7.24. Optimal carbon dioxide supply rate calculated in the full problem (a), slow sub-problem (b), fast sub-problem (c).

quasi-steady-state model, any control action will have an immediate effect on the system and consequently on the economic return, which largely explains the instantaneous response of the optimal control strategies to the solar radiation. The same kind of behaviour is found in the other control, state and costate trajectories calculated in the slow sub-problem. The largest differences with the solution of the full problem are found during the day under rapidly varying external input conditions which induce rapid fluctuations in the quasi-steady-state description of the greenhouse climate. At night,
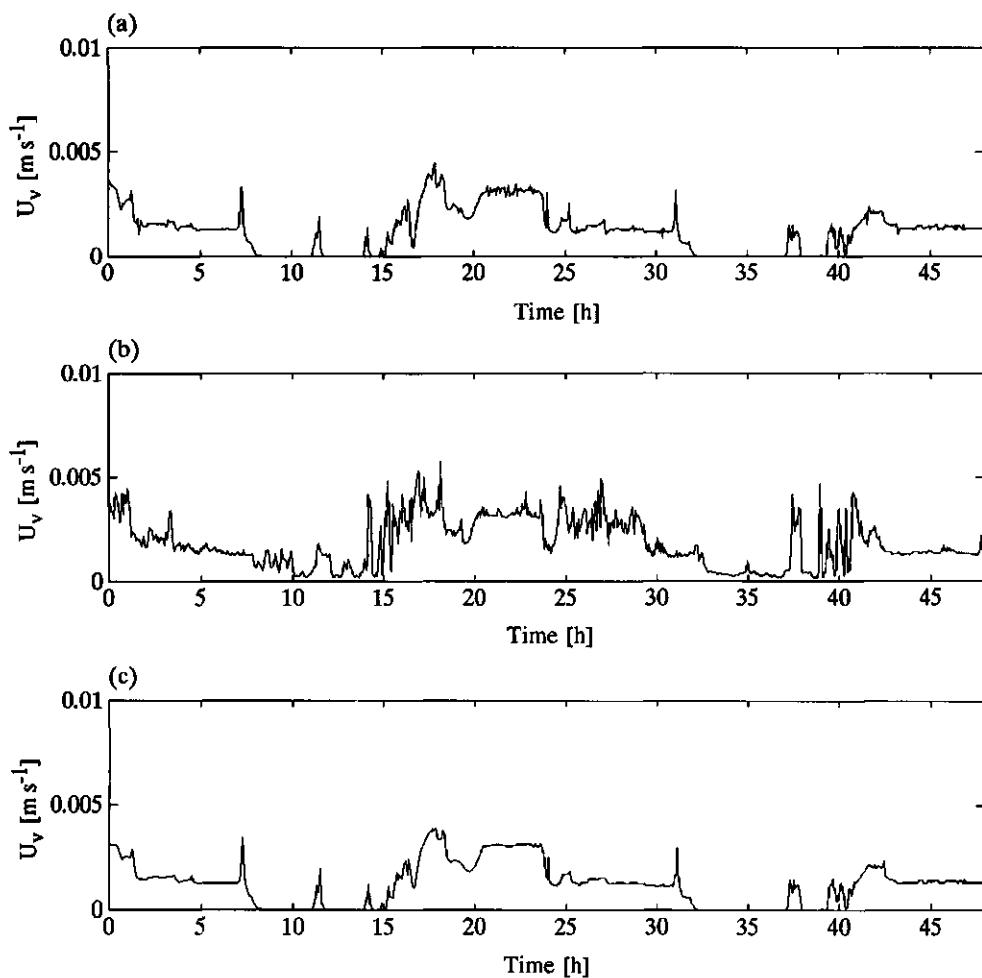
Fig. 7.25. Optimal ventilation rate calculated in the full problem (a), slow sub-problem (b) and fast sub-problem (c).

when the crop production system is relatively at rest, the differences between the various strategies are less pronounced and the quasi–steady–state model produces a fairly accurate description of the greenhouse climate.

Figs. 7.24 to 7.32 clearly reveal that, during the two days shown, a remarkable similarity of the solution of the fast sub-problem and the solution of full control problem is obtained. To circumvent a cumbersome visual inspection of all the control, state and costate trajectories, in fig. 7.33 (p. 234) aggregated
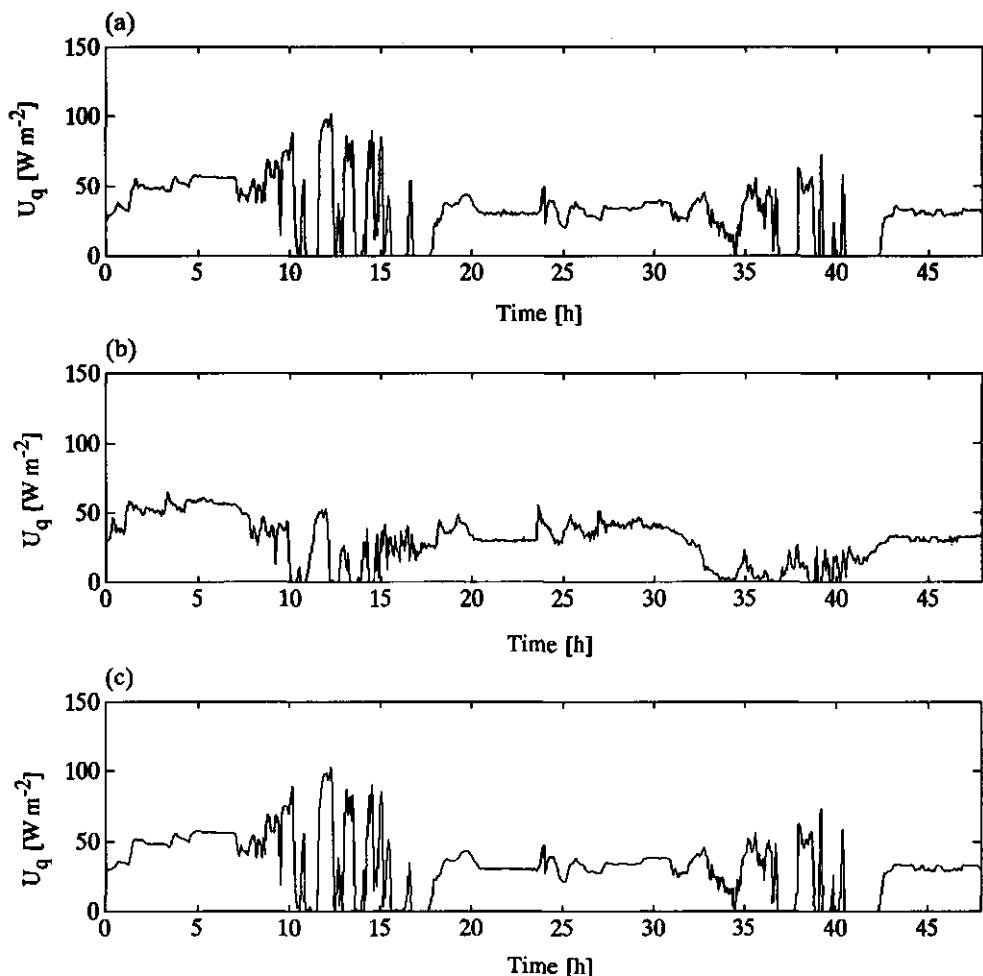
Fig. 7.26. Optimal heating calculated in the full problem (a), slow sub-problem (b) and fast sub-problem (c).

performance data of the three control strategies evaluated over the 50 days growing period are presented. These data were obtained in simulations of the full system dynamics using the control strategies calculated in the full control problem, the slow sub-problem and the fast sub-problem.

Fig. 7.33 (p. 234) shows that the control strategies obtained in the slow sub-problem, neglecting the greenhouse climate dynamics, are not very useful approximations of the optimal control strategies of the full problem. Though the use of heating energy and carbon dioxide
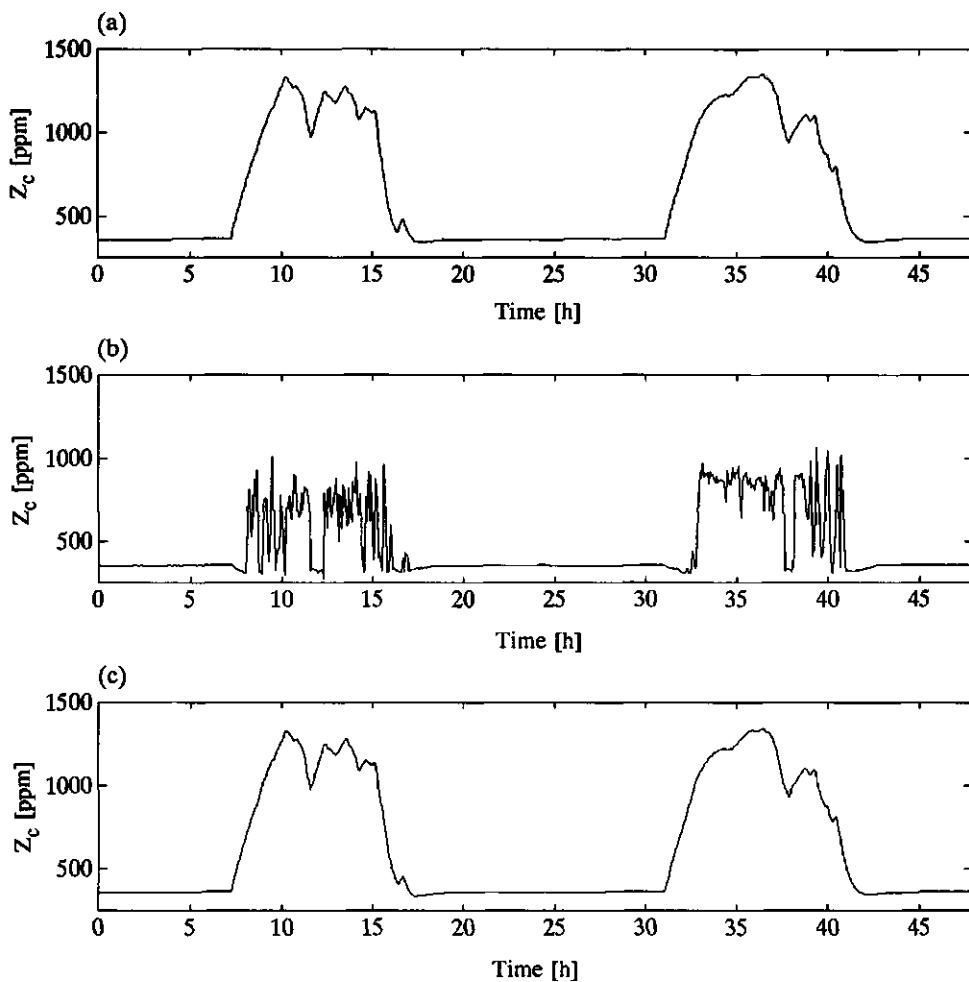
Fig. 7.27.   Optimal CO_2 concentration simulated in the full problem (a), slow sub-problem (b) and fast sub-problem (c).

is much less than in the full solution, a significant reduction in dry matter production is achieved which results in a reduction of the net economic return of just over 15%. An equivalent result was reported by Tap *et al.* (1993). If, using the results obtained in the slow sub-problem, in the fast sub-problem new control strategies are calculated taking the greenhouse climate dynamics explicitly into account, a significant improvement of the performance is obtained. The new control strategies yield almost the same dry matter production, also shown in fig. 7.22a, and energy consumption as in
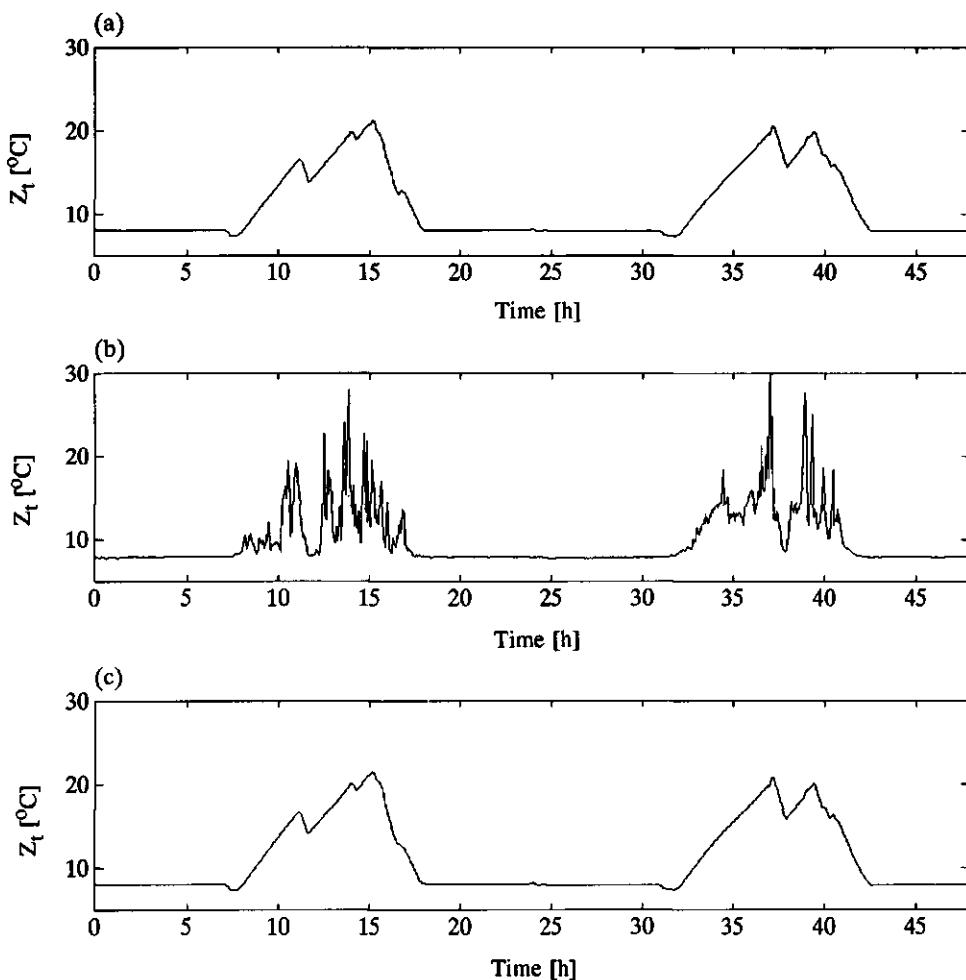
Fig. 7.28. Optimal air temperature simulated in the full problem (a), slow sub-problem (b) and fast sub-problem (c).

the full problem. The carbon dioxide consumption is about 10% smaller, but the overall reduction in the net economic return amounts to only about 2%.

A possible source of the observed error in the performance of the two time-scale decomposition may be the relatively inaccurate trajectories of the slow state (X_d) and costate (λ_d) obtained in the solution of the slow sub-problem. It was shown in fig. 7.22 that, in the slow sub-problem, the marginal value of a unit crop dry weight is underestimated in comparison with the marginal value found in the
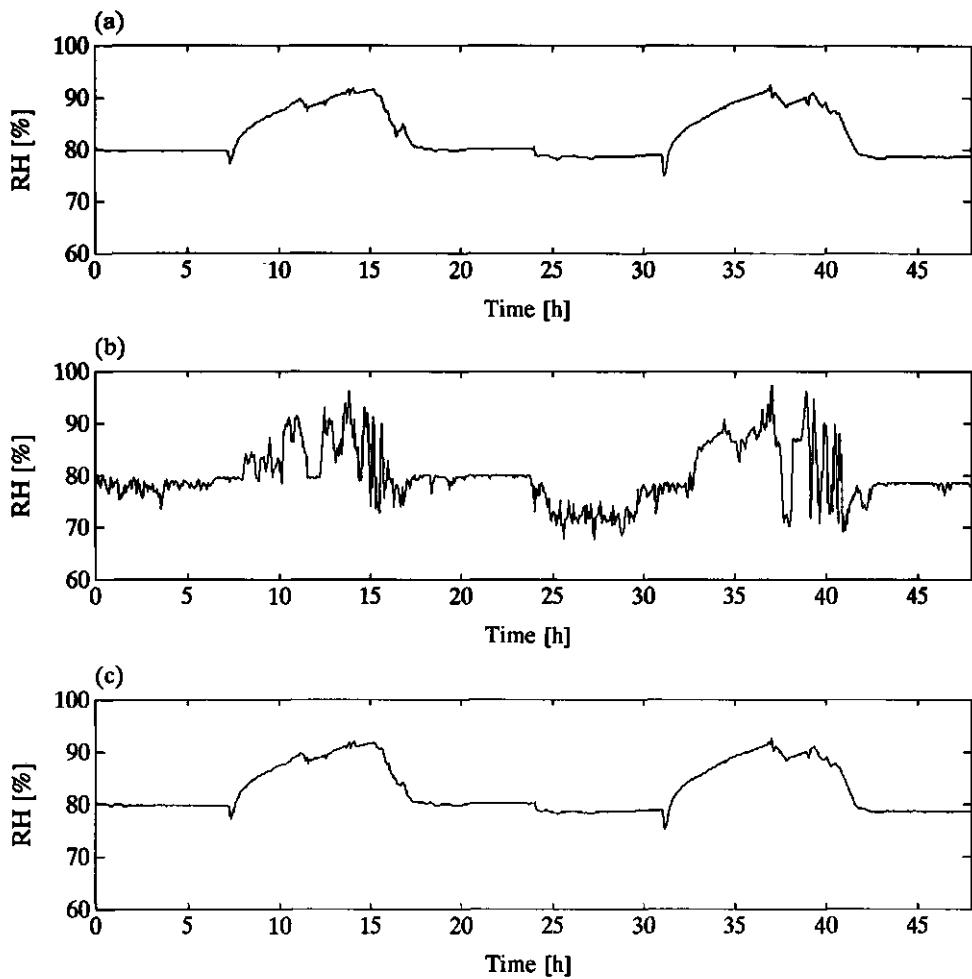
Fig. 7.29.   Optimal relative humidity simulated in the full problem
            (a), slow sub-problem (b) and fast sub-problem (c).

solution of the full problem. According to eqn. (6.21a), λ_d has a
positive effect on the marginal value of the carbon dioxide (η_c)
during the day. In turn, a higher value of η_c suggests a more
generous carbon dioxide supply (eqn. (6.22a)), leading to a higher
carbon dioxide concentration in the greenhouse and, consequently, a
higher dry matter production. So, underestimation of λ_d will result
in a less abundant carbon dioxide supply and less dry matter
production, which is in line with the observations made in fig. 7.33.
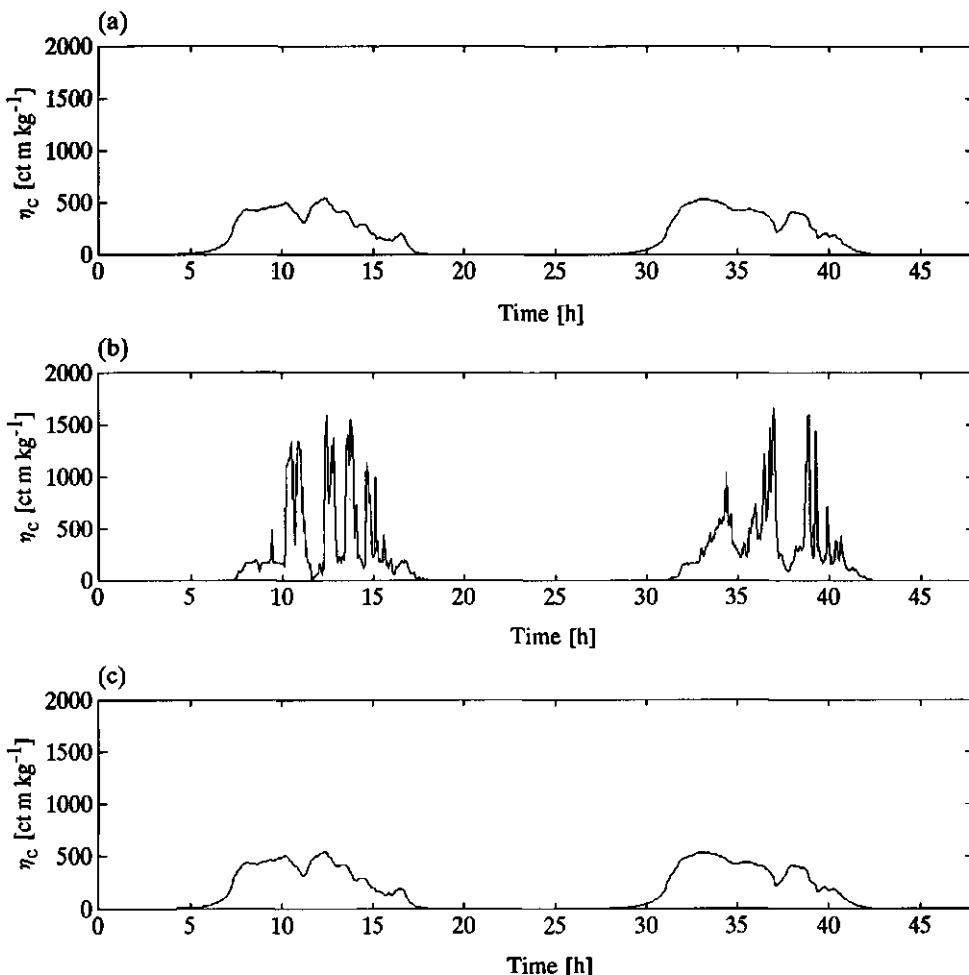
Fig. 7.30. Marginal value of the carbon dioxide concentration simulated in the full problem (a), slow sub-problem (b) and fast sub-problem (c).

Underestimation of the dry matter production in the slow sub-problem will also affect the solution of the fast sub-problem. But since these errors occur after canopy closure, their effect on dry matter production and the humidity balance in the fast sub-problem seems small.

The results of the two time-scale decomposition reveal the interesting fact that the performance of the slow sub-problem $(\bar{J}_0)$ claims the major part of the performance (J) of the full problem.
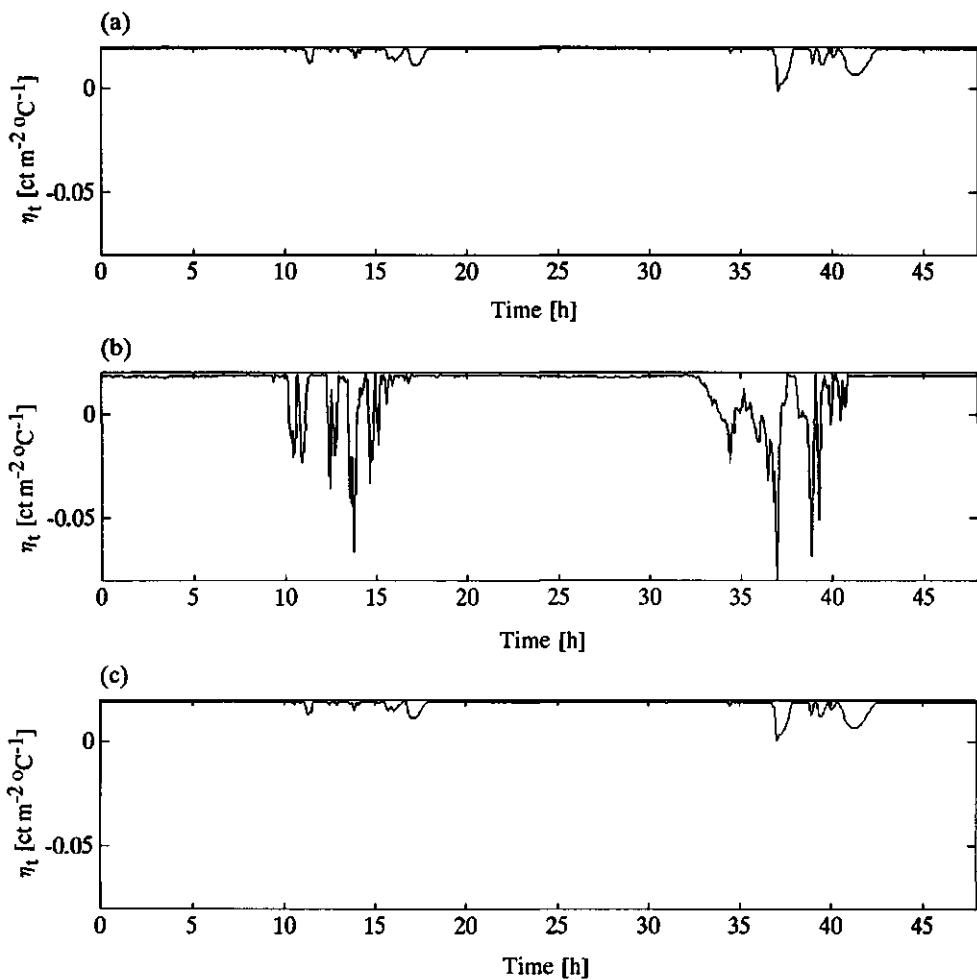
Fig. 7.31.   Marginal value of air temperature obtained in full problem
             (a), slow sub-problem (b) and fast sub-problem (c).

Also, in the simulations, the marginal value of crop dry weight is
significantly higher than the marginal value of carbon dioxide
concentration, air temperature and humidity. Since the costate
expresses the sensitivity of the performance criterion for small
changes in the associated state, these observations suggest that, in
greenhouse climate management during lettuce production, efficient
control of the relatively slow crop growth dynamics should be
emphasized first. Then, secondly, further improvements in the
performance can be obtained by economic optimal control of the
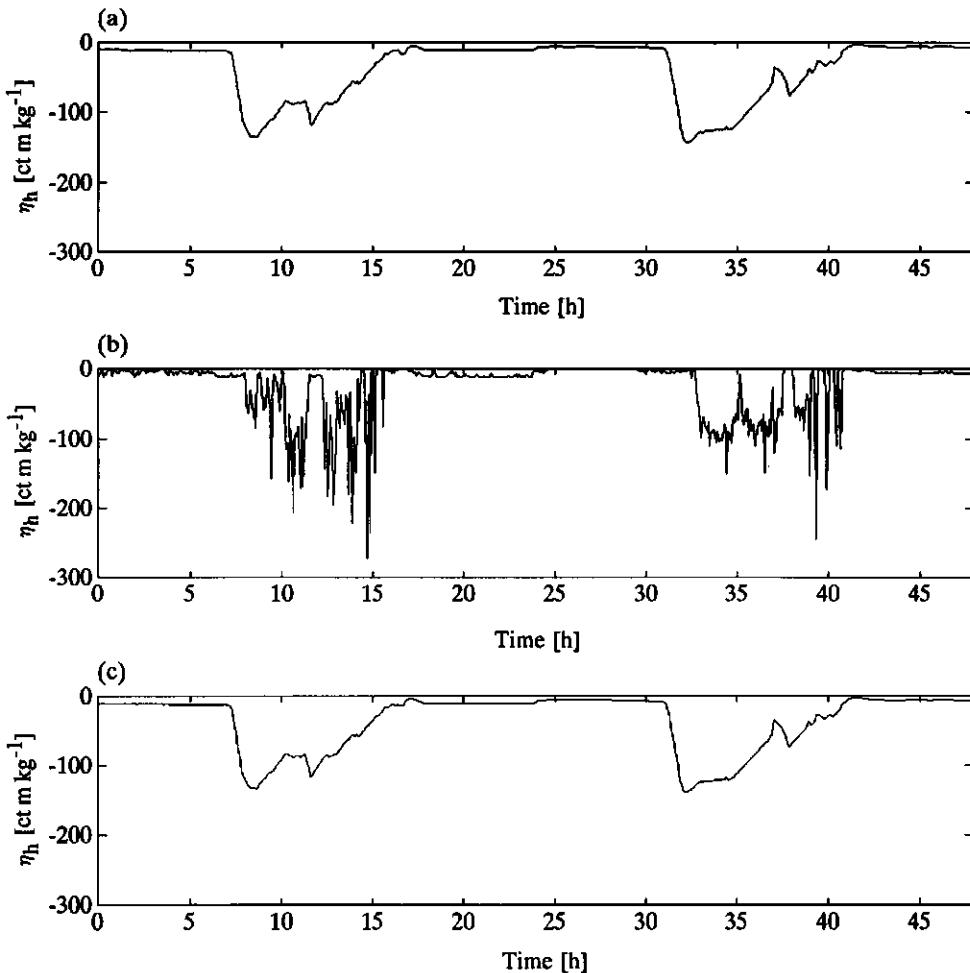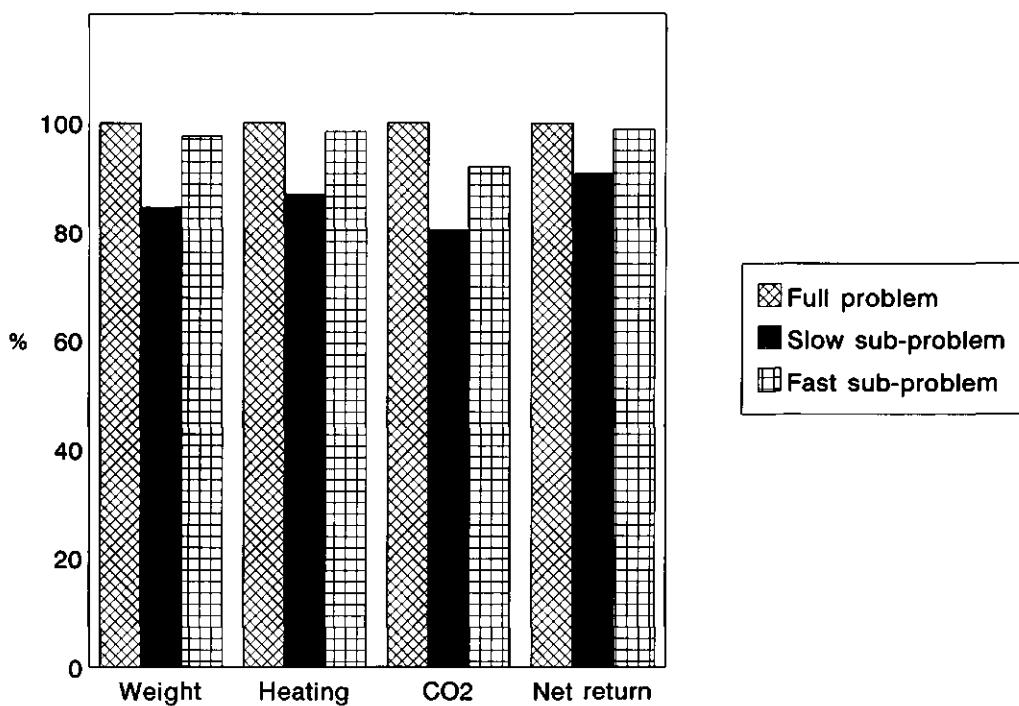
Fig. 7.32. Marginal value of absolute humidity simulated in the full problem (a) and the slow (b) and fast (c) sub-problems.

greenhouse climate dynamics. This agrees with the predominant approach in research on optimal greenhouse climate management focusing on the efficient control of the crop growth dynamics (see chapter 1).

It is worth noticing that despite the fact that rapid changes in the outside climatic conditions occur, the optimal greenhouse climate variables show a rather smooth evolution. Only when relatively long-term changes in for instance solar radiation occur, the indoor climate is adapted accordingly. On the contrary, the optimal control

Fig. 7.33. Performance of the controlled process evaluated with the full system description over the 50 days growing period, using the optimal control trajectories calculated in the full problem, slow sub-problem and fast sub-problem.

trajectories exhibit rapid (minimum energy) adaptations anticipating the external inputs such as solar radiation.

The control strategies resulting from the solution of the full problem and the two time-scale decomposition can be used for minute by minute control of the greenhouse climate dynamics and therefore, with their application to horticultural practice in mind, it is worth having a second look at their behaviour.

Control problems in which both the system equations and the performance measure are linear in the control and the control strategies are required to stay in a bounded region, often have (or are assumed to have) a bang-bang type solution in which the optimal control switches between its lower and upper bound and vice-versa. These bang-bang solutions may not be very practical since extreme switching will result in wear and breakdown of the valves and servo motors used in the climate conditioning equipment. Figs. 7.23 to 7.32
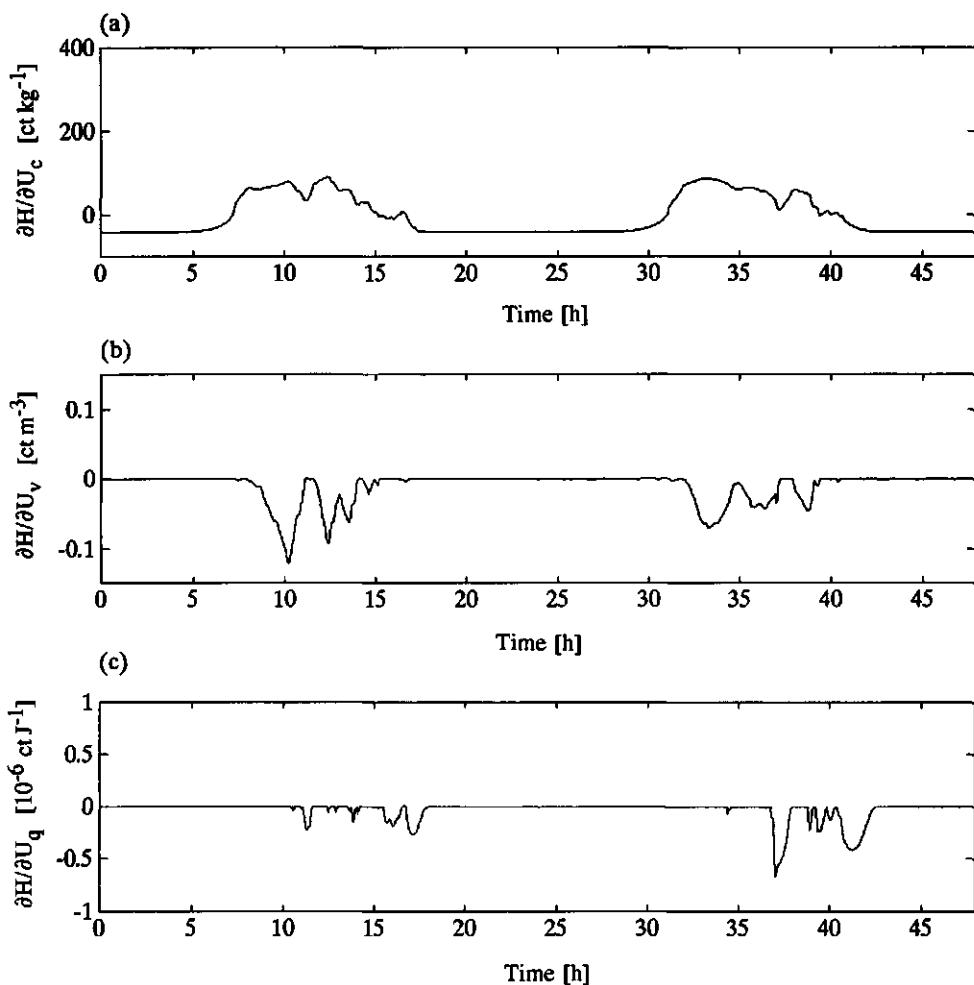
Fig. 7.34. Switching functions of carbon dioxide supply rate (a), ventilation rate (b) and heating (c), calculated in the full optimal control problem.

show that the control problem considered in this thesis yields a much smoother bang-singular-bang type behaviour in which the control takes values on the lower and upper bounds but also between these bounds, rather than a bang-bang behaviour. The singularities do occur when the switching function, *i.e.* the gradient of the Hamiltonian with respect to the control, equals zero. In fig. 7.34 it is shown that the observed singularities in the carbon dioxide supply, heating and ventilation, actually do coincide with zero values of the switching
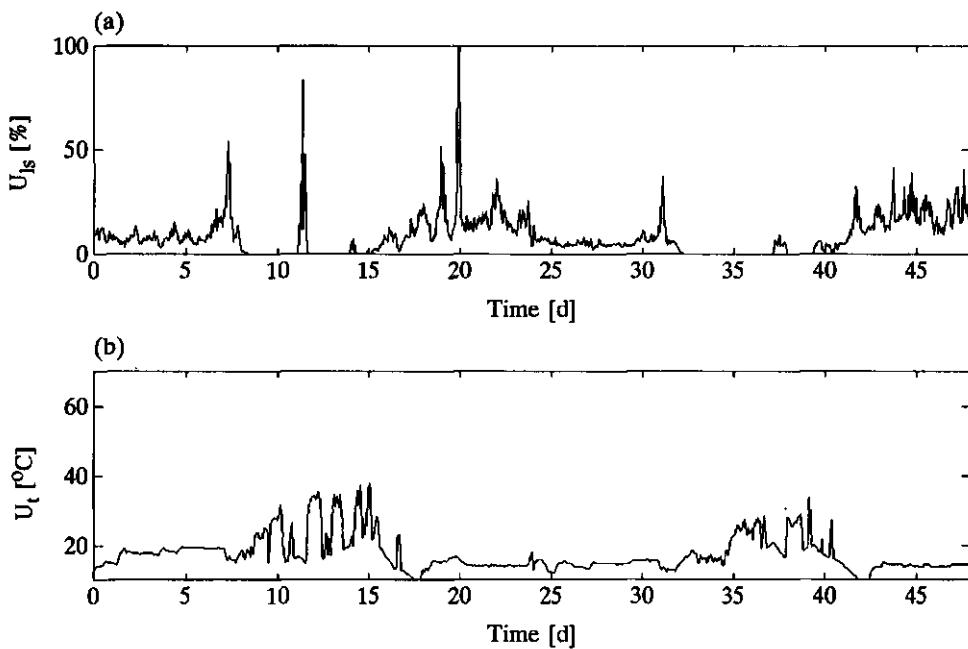
Fig. 7.35. Optimal aperture of lee side vents (a) and pipe temperature (b) calculated from the optimal ventilation and heating trajectories of the full control problem.

functions. They do occur in the control strategies, not only at night but also during the day under dynamically changing outside climatic conditions. Only carbon dioxide supply exhibits an almost bang-bang type of behaviour, but in horticultural practice, on-off switching of the carbon dioxide supply valve is commonly used. The rather smooth optimal heating and ventilation strategies are acceptable for implementation in horticultural practice.

In horticultural practice, instead of ventilation rate and energy supply by the heating system, the aperture of the ventilation windows and temperature of the heating pipes are used as control inputs. Using eqns. (3.68) and (3.69a) the aperture of the windows and temperature of the heating system has been calculated from the ventilation rate and heating. For the two day period considered in this section the resulting trajectories are shown in fig. 7.35 for the full problem. Also these control strategies look acceptable for use in horticultural practice.

7.5.4. Concluding remarks

From the results obtained in this section it is concluded that:

a) for the particular control problem considered, the solution of the full control problem in which both greenhouse climate dynamics and crop growth dynamics are included, is accurately approximated by the solution of two sub-problems; one sub-problem emphasizes optimal control of the slow crop growth dynamics, the other emphasizes economic optimal control the greenhouse climate dynamics,

b) in greenhouse climate management during lettuce production, efficient control of the (slow) crop growth dynamics establishes the major part of the performance of the controlled process; an additional improvement in the performance of the controlled production process can be obtained by using economic criteria to control the greenhouse climate dynamics,

c) the resulting optimal greenhouse climate control strategies have such (smooth) characteristics that they can be used in horticultural practice with the commonly used climate conditioning hardware.

7.6. Sensitivity analysis of open-loop optimal greenhouse climate control

7.6.1. Introduction

In this section, the performance sensitivity of open-loop optimal greenhouse climate control strategies to perturbations in the model parameters, external inputs and initial conditions of the state variables is evaluated. The first-order sensitivity analysis is expected to produce further insight into the operation of optimal greenhouse climate control as well as the impact of inaccurate parameterization and measurement errors in the initial conditions of the states.

7.6.2. Methodology

In section 5.5, a numerical scheme for the calculation of the performance sensitivity of open-loop optimal control strategies to small changes in the initial conditions and model parameters was presented. Basically, this first order sensitivity analysis contains two steps. First of all, the optimal control problem is solved.

Secondly, the effect of small perturbations of the model parameters on the performance measure is evaluated using a first-order measure of the performance sensitivity with respect to parameter perturbations. This first-order measure is obtained by integrating the partial derivatives of the Hamiltonian with respect to the model parameters over the whole optimization interval considered (eqn. (5.69)). The performance sensitivity for small changes in the initial conditions of the state variables is determined by the value of the associated costates at the starting time t_b (eqn. (5.68)). To assess the relative importance of the model parameters and initial conditions, a relative sensitivity measure conforming to eqn. (5.70) is used instead of the afore mentioned absolute performance measure.

In this section, the performance sensitivity is evaluated and analysed for the control problem concerning the four state variable crop production process, stated in section 6.2.1. In this analysis both the greenhouse climate dynamics and the crop growth dynamics will be considered. The parameters defining the running cost, and the state and control constraints listed in table 6.1 were used.

First the optimal control problem was solved using measured data of the outside climatic conditions obtained during the second greenhouse experiment in early 1992. These data consisted of two minute measurements which were not filtered before use in the simulations. A growing period of only 50 days was considered. The state and costate equations were simulated in double-precision with an integration time step of half a minute using a fourth order Runge-Kutta algorithm described by Press *et al.* (1986). The steepest ascent algorithm, described in section 5.7, was used for the iterative solution of the three control problems. The search for the optimizing control strategy was stopped once the improvement in the performance criterion was less than 1.0×10^{-6} during at least three consecutive iterations.

Secondly, the performance sensitivity was calculated by integrating the partial derivatives of the Hamiltonian with respect to the model parameters. In the actual computation, these partial derivatives can be calculated analytically or numerically with a central difference approximation (see section 3.3). Here analytical derivatives were calculated and implemented in the simulation software based on FORTRAN.

Besides the performance sensitivity with respect to variations in the initial conditions and model parameters, the performance sensitivity with respect to small perturbations in the external inputs has been evaluated. In the model equations, a time invariant perturbation parameter $c_{V,i}$ having a nominal value of 1 was introduced for every external input (*e.g.* $V_i = c_{V,i}V_i$). Clearly, the

effect of this perturbation parameter is that throughout the whole optimization interval the external inputs are perturbed by the same amount. In the sensitivity analyses, these perturbation parameters are treated as normal model parameters.

The interpretation of the results is straightforward. If the relative sensitivity measure is larger (less) than zero, a small positive perturbation in the parameter yields an increase (decrease) of the value of the performance criterion. If the performance measure has an absolute value of 1, a change of 1% is expected to result in a 1% change of the value of the performance criterion. For a relative performance sensitivity measure having a value larger or smaller than unity, the interpretation changes accordingly. Because the first-order sensitivity analysis is based on a first-order Taylor series approximation of the change in the performance due to a change in a parameter, the validity of the previous interpretation of the performance sensitivity with respect to parameter variations is limited to small parameter variations only. Still, the relative performance sensitivity measure will provide valuable insight into the contribution of certain model parameters to the control strategies calculated.

7.6.3. Results and discussion

Results of the sensitivity analysis are presented in table 7.4. The constraint on the relative humidity seems to play a primary role in the optimal state and control trajectories. This was already observed in the previous sections, but it is clearly confirmed in the present sensitivity analysis. The importance of the humidity state constraint is indicated by the large sensitivity measure of c_R, $c_{t,abs}$, $c_{v,2}$, $c_{v,3}$ and $c_{v,6}$, parameterizing the saturation water vapour pressure used in the definition of the constraint on the relative humidity. Although they are also involved in the description of the canopy transpiration, their effect on the performance of the control strategies through the canopy transpiration seems to be of secondary importance. This can be inferred from the sign of the sensitivity measure. Taking c_R as an example, this can be seen as follows. An increment in the value of c_R results in a reduction of the saturation water vapour pressure (see section 6.2.1). When the humidity constraint is encountered, the costate η_H takes large negative values indicating the required reduction of the humidity in the greenhouse (see fig. 7.32). Focusing on the humidity balance in the Hamiltonian equation (eqn. (6.7)), we can see that given $\eta_H < 0$ and assuming the saturation water vapour pressure to be larger than the absolute

Table 7.4. Relative performance sensitivity to small variations in the model parameters, control inputs, external inputs and initial conditions.

Parameter	Relative sensitivity	Parameter	Relative sensitivity
$c_{v,2}$	5.4178	$c_{pl,d}$	-0.1542
$c_{v,6}$	4.5173	$c_{co2,3}$	-0.1399
$c_{v,3}$	-3.9328	c_{leak}	-0.1116
$c(V_c)$	1.6637	$c_{cap,q,v}$	-0.0958
$c_{\alpha\beta}$	1.7807	$c(V_t)$	0.0963
$c(V_1)$	1.2627	$c_{cap,h}$	0.0919
c_i	1.1783	$X_d(t_b)$	0.0600
$c(V_h)$	-1.0804	$c_{cap,c}$	-0.0500
c_R	-1.0800	$c_{resp,2}$	0.0148
$c_{t,abs}$	-1.0349	c_Γ	-0.0123
$c_{co2,2}$	0.8742	$c_{cap,q}$	-0.0095
$c_{co2,1}$	-0.3668	$c_{v,5}$	-0.0064
c_q	-0.3617	$Z_T(t_b)$	0.0007
$c_{al,ou}$	-0.3418	c_{rad}	0.0004
$c_{v,pl,al}$	-0.3313	$Z_h(t_b)$	-0.0003
$c_{resp,1}$	-0.2772	$Z_c(t_b)$	0.0001
c_{co2}	-0.1672		

humidity level in the greenhouse, any reduction in the water vapour pressure would result in a larger value of the Hamiltonian, thus suggesting a positive effect of an increment in c_R on the performance measure. The sign of the sensitivity measure, however, is negative. Therefore another effect of c_R is dominating. Close to the humidity constraint, the partial derivative of the penalty function takes very large positive values. Then, any reduction of the saturation water vapour pressure will result in an increasing penalty, thus yielding the negative effect on the performance measure observed in the sensitivity analysis. Apparently, the penalty function related to the humidity constraint dominates the Hamiltonian, thus emphasizing the importance of an accurate definition of the humidity constraint in optimal greenhouse climate control.

Because the constraint on the relative humidity is of such great importance in the control strategies, an accurate description of the humidity balance in the greenhouse, including processes like canopy transpiration, seems required. This is confirmed by the relatively large performance sensitivity of parameter $c_{v,pl,al}$ expressing the mass transfer coefficient for evaporative water vapour transport from the leaves to the ambient air. Under equal circumstances, a small positive increment in this parameter will result in a higher canopy transpiration and consequently will result in an earlier conflict with the humidity constraint. The accompanying increment in the value of the penalty results in the negative sensitivity measure in table 7.4.

As was observed in the sensitivity analysis of the two dimensional crop growth model of lettuce in section 3.3, the parameters determining crop growth include the yield factor c_β, the light use efficiency c_ε, the extinction coefficient c_k, the leaf area ratio $c_{lar,s}$, and a parameter expressing a linear effect of the temperature on the leaf conductance for carbon dioxide $c_{g,car,2}$. Since the performance of the economic optimal control is largely determined by dry matter production, the results of section 3.3 suggest a significant performance sensitivity with respect to the associated parameters $c_{\alpha\beta}$, $c_{pl,d}$, c_l and $c_{co2,2}$. Apart from the parameter $c_{pl,d}$, table 7.4 shows the expected relatively large performance sensitivity for these parameters, thus emphasizing the fact that for optimal greenhouse climate control their accurate parameterization is required.

The performance sensitivity for parameter $c_{pl,d}$, however, is much less distinct than was expected. The reason for this is the fact that $c_{pl,d}$ is also involved in the humidity balance of the greenhouse in which it describes the effective surface of the canopy. Before canopy closure, any increment in the effective canopy surface will result in an increment of the canopy transpiration and consequently more frequent conflicts with the humidity constraints will occur. This has a negative effect on the performance measure, thus partly outweighing the positive effects of early canopy closure on dry matter production of the canopy.

Table 7.4 shows that most of the crop growth related parameters more or less affect the performance of the control strategies. Since the important role of humidity has been discussed in some detail above, the analysis will now be focused on the parameters in the energy and carbon dioxide balance.

Parameters that most clearly affect the dynamic behaviour of the carbon dioxide concentration and air temperature in the greenhouse

are the mass and heat capacities $c_{cap,c}$ and $c_{cap,q}$ respectively. Table 7.4 reveals that the effect of a perturbation in their values on the performance is small. The heat and mass capacities of the greenhouse air determine to a large extent the dynamic rate with which the greenhouse climate can be modified: a larger capacity will result in a longer response time. The small performance sensitivity suggests that the greenhouse climate system is fast enough to deal with fast fluctuations in the exogenous inputs in an economic optimal fashion. This can be seen as follows. If large benefits can be obtained by rapid modifications of the greenhouse climate in accordance with or anticipating rapid fluctuations in the exogenous inputs (*e.g.* solar radiation) any decrease in the response time will contribute to a significant improvement of the economic performance. Then, a pronounced performance sensitivity with respect to these parameters is expected. Compared with for instance crop growth related parameters, however, $c_{cap,c}$ and $c_{cap,q}$ have a small impact on the performance. Apparently, the response time of the greenhouse climate is not a limiting factor in the economic optimal control of the crop production process. Or alternatively, the relatively small performance sensitivity to changes in the heat and mass capacity of the greenhouse air suggests that in economic optimal greenhouse climate control very fast modifications of the greenhouse climate do not contribute significantly to an improvement of the economic performance.

These observations are in line with the results of the sensitivity analysis in section 3.3. There it was found that crop growth is much more sensitive to changes in the long term average of, for instance, the carbon dioxide concentration than to rapid fluctuations. Since in this example the performance of optimal greenhouse climate control is largely determined by the dry matter production, this would suggest a large performance sensitivity for parameters affecting the average indoor climate. In the present sensitivity analysis this is confirmed by the significant sensitivity of the performance measure to a change in the carbon dioxide concentration in the outside air induced by $c(V_c)$. Clearly, such a change does affect the long term average carbon dioxide concentration in the greenhouse air, but not the rate of change of the carbon dioxide concentration in the greenhouse.

In section 3.3 it was concluded that during the day lettuce growth is not strongly influenced by the air temperature in the greenhouse. Due to this relatively low temperature sensitivity of crop growth and the comparably high heating costs, the greenhouse air is rarely heated during the day. Still, parameter $c_{ai,ou}$, describing the energy losses to the outside air by means of transmission through

the greenhouse cover and natural ventilation through the windows, shows a high performance sensitivity. During the major part of the growing period, heating energy is supplied to the greenhouse at night to satisfy the minimum temperature constraint. This minimum temperature constraint determines the total energy consumption. Any reduction in the energy loss to the outside air will result in a reduction of the energy consumption required for heating the greenhouse which results in a negative performance sensitivity. Because the greenhouse climate is not exposed to rapid changes in the outside conditions during night time, economic optimal control does not require extremely fast modifications of the greenhouse air temperature, thus explaining the low performance sensitivity of the heat capacity $c_{cap,q}$.

The very large positive performance sensitivity for perturbations in the solar radiation and outside carbon dioxide concentration is explained by the large sensitivity of crop growth for these climatic conditions. The large negative sensitivity for an increase in the outside humidity is due to the constraint on the relative humidity which will then be more difficult to satisfy. The large performance sensitivities emphasize the need for accurate assessment, *i.e.* prediction and measurement, of these outside climatic conditions.

The total operating costs of the climate conditioning equipment (±100 ct m^{-2}) is relatively small compared with the gross economic return of the crop production (±525 ct m^{-2}). Therefore a relatively small performance sensitivity for the operating costs expressed by the c_{co2} and c_q is found. Since in the simulations the overall heating costs exceed the costs for carbon dioxide supply, the performance sensitivity for c_{co2} is smaller than for c_q.

Finally, for all state variables the performance sensitivity to a perturbation in their initial conditions is relatively small. For the greenhouse climate variables this is explained by the fact that due to the fast system dynamics a small perturbation in the greenhouse climate has a very short duration which does not affect the performance of the system significantly.

7.6.4. Concluding remarks

From the results obtained in this section it is concluded that:

(1) the first-order sensitivity analysis supplies a simple and straightforward way of getting deeper insight into the operation of

the optimal control problem and the relative importance of the model parameters, initial conditions of the state variables and the external inputs, without having to go through extensive recalculations of the optimal control strategies,

(2) in the example considered, the constraint on the humidity strongly influences the performance of optimal greenhouse climate management,

(3) in optimal greenhouse climate management, the dynamics of crop growth play a dominant role,

(4) the outside climatic conditions such as solar radiation, carbon dioxide concentration and humidity, and to a lesser extent the air temperature, are important in optimal greenhouse climate management; consequently their accurate measurement and prediction is required.

7.7. Set-point tracking control versus optimal control of the greenhouse climate dynamics

7.7.1. Introduction

In chapter 1, it was observed that in the literature on greenhouse climate management, optimization was most often considered at the level of controlling the crop growth dynamics whereas the greenhouse climate dynamics were commonly neglected. In that research only slow variations in the outside climatic conditions were considered, assuming that these would not interfere with the dynamic response of the greenhouse. The calculated optimal climate strategies were intended for use as set-point strategies for on-line greenhouse climate control.

In practice, however, the weather exhibits rapid fluctuations. This gives rise to the following two observations. First, it is not clear whether the above mentioned set-point trajectories represent the optimal greenhouse climate trajectories when the system is driven by rapidly fluctuating weather and when applied to the actual dynamic greenhouse climate. Secondly, the above mentioned approach assumes that the climate set-point trajectories are realized by the set-point tracking controller with some accuracy using heating energy and carbon dioxide supply in an economically efficient way. For that reason, recently control algorithms using an economic criterion for the control of the greenhouse climate dynamics were introduced (Tchamitchan *et al.*, 1992; Tap *et al.*, 1992; Hwang, 1993).

Using the results of the two time-scale decomposition (section

7.5), in this section, the benefits of using an explicit economic criterion for the control of the greenhouse climate dynamics instead of the set-point tracking approach is briefly investigated.

7.7.2. Methodology

In this section, the control problem concerning the four state variable crop production process, stated in section 6.2, is used as an example. The various parameters defining the running cost, and the state and control constraints have been listed in table 6.1.

In the simulations, measured data of the outside climatic conditions obtained during the second greenhouse experiment in early 1992 were used. Climate set-points were generated by solving the slow sub-problem with inputs from which rapid fluctuations were eliminated using a moving average filter with a window of half an hour. To facilitate a comparison with the results presented in section 7.5, a growing period of 50 days was considered. The slow state and costate equations (eqns. (6.11a) and (6.15a)) were integrated in double precision with an integration time step of half a minute using a fourth order Runge-Kutta algorithm described by Press *et al.* (1986). The steepest ascent algorithm, described in section 5.7, was used for the solution of the control problem. The search for the optimizing control strategy was stopped once the improvement in the performance criterion was less than 1.0×10^{-3} during at least three consecutive iterations.

The performance of the calculated control strategies was evaluated in a simulation in which they were applied to the full system including both greenhouse climate and crop growth dynamics (eqns. (6.1a) to (6.1d)); unfiltered external inputs were used. As a reference, the solution of the full optimal control problem, presented in section 7.5, was used.

Secondly, by inversion of the system's equations (6.1b) to (6.1d), a dead-beat controller was derived so that control strategies were calculated using (i) the greenhouse climate trajectories as set-point trajectories and (ii) the unfiltered external input data, satisfying the control constraints. Since ventilation and heating have counteracting effects on air temperature, in the dead-beat controller the ventilation rate was used to control humidity. Given the previously calculated ventilation rate, the carbon dioxide supply rate and heating were calculated. The resulting control strategies were applied to the full system and the performance was evaluated in comparison with the performance of the full problem.
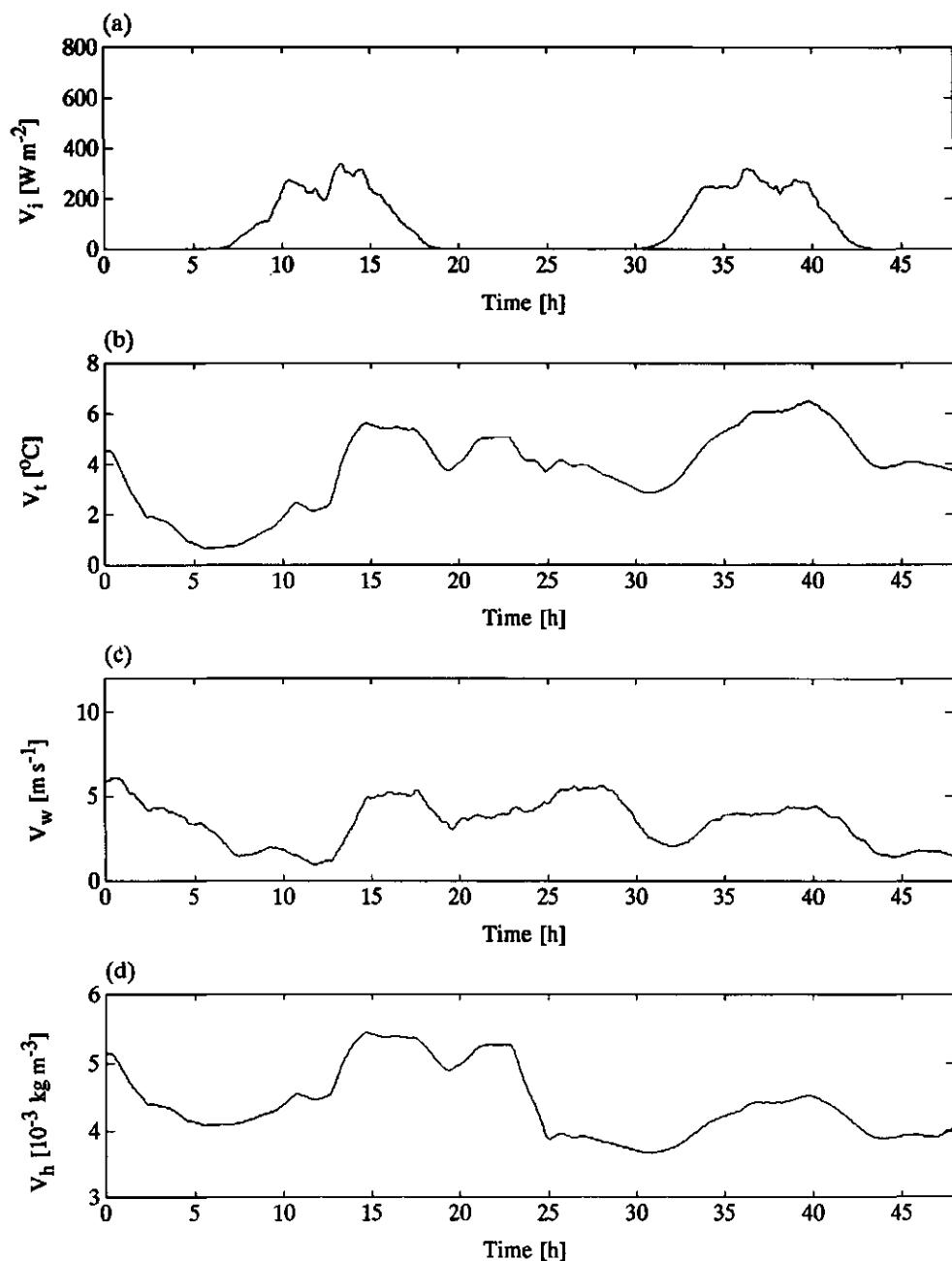
Fig. 7.36.   Filtered external inputs during two days of the 50 days
             growing   period: (a)   solar   radiation,   (b)   temperature,
             (c) wind speed and (d) absolute humidity.

7.7.3. Results and discussion

The filtered data of the external inputs are shown in fig. 7.36 for the same two days shown in section 7.2. The calculated optimal control and state trajectories are shown in figs. 7.37 and 7.38. A distinct difference with the optimal trajectories of the full problem shown in figs. 7.24a to 7.29a can be seen.
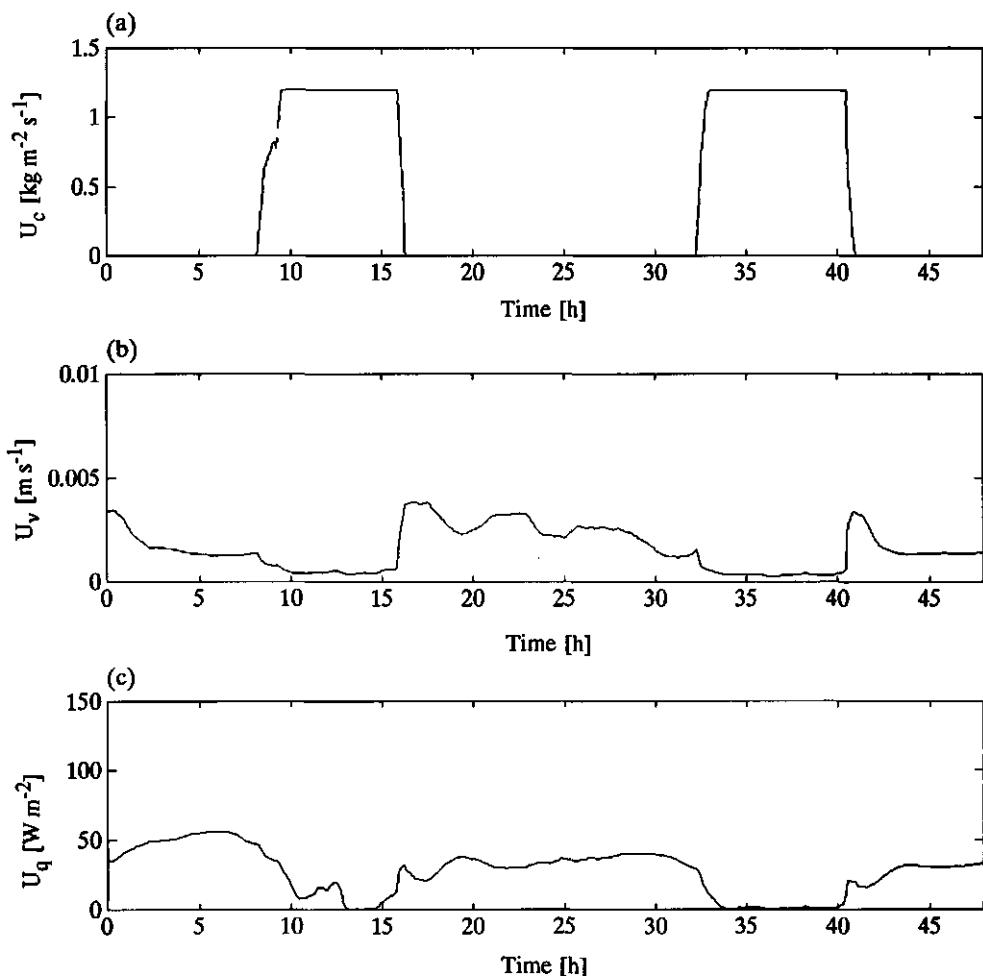
Fig. 7.37. Optimal carbon dioxide supply rate (a), ventilation rate (b) and heating (c).
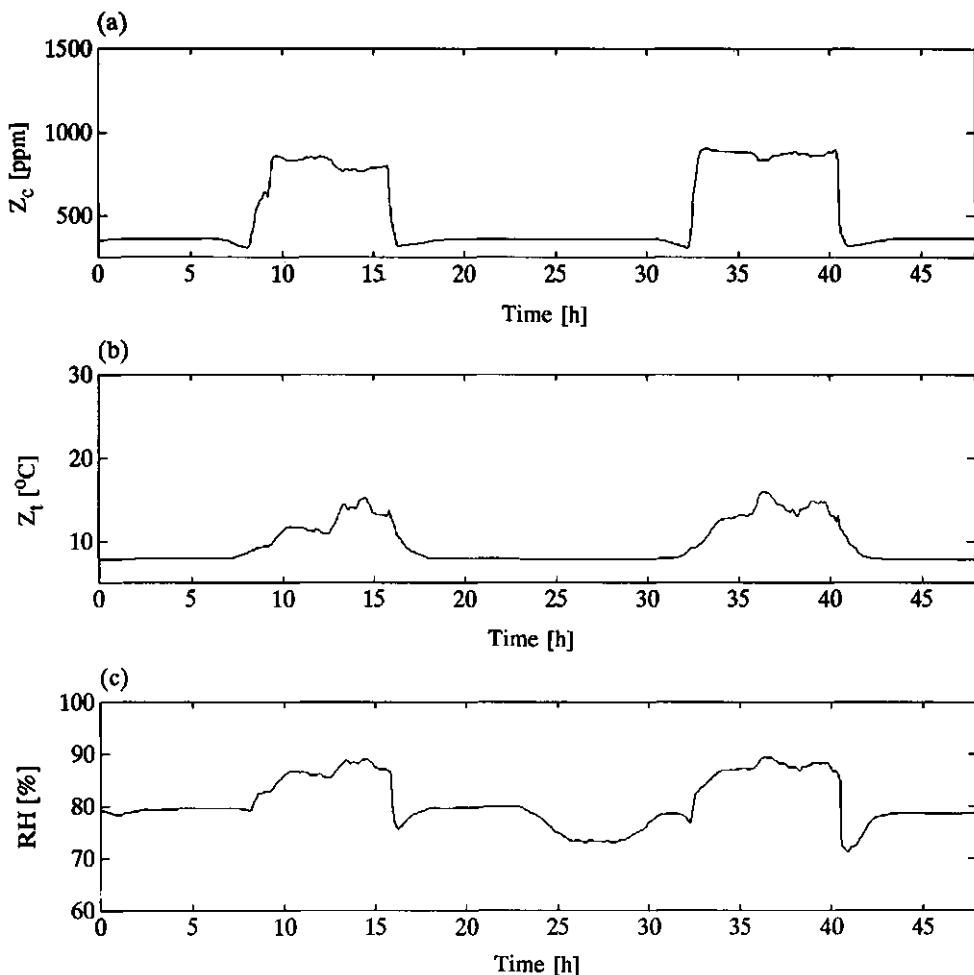
Fig. 7.38.   Optimal carbon dioxide concentration (a), air temperature
(b) and relative humidity (c).

In line with the observations of Tap *et al.* (1992), applying the
control inputs shown in fig. 7.37 to the full system dynamics yields
a poor performance of the controlled process (fig. 7.39). Comparison
of the control trajectories shown in fig. 7.37 with figs. 7.24 to
7.26 reveals, for instance, that the carbon dioxide supply is both
switched on and switched off too late, and therefore, under dynamic
conditions, the carbon dioxide concentration in the greenhouse will
lag behind the optimal trajectory shown in fig. 7.27. Moreover, the
ventilation rate and heating do not anticipate the rapid fluctuations
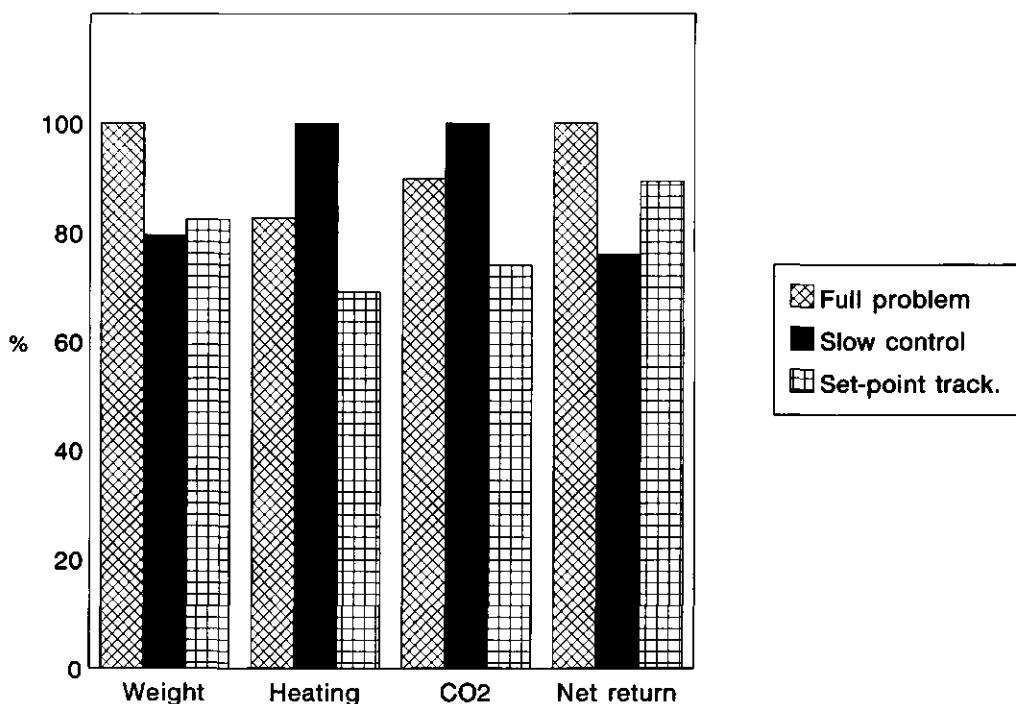
Fig. 7.39. Performance of the controlled process using the set-point tracking approach, compared with the true optimal solution calculated in the full problem and the performance of the optimal control trajectories calculated in the slow sub-problem.

in the outside climatic conditions. Consequently, the crop production process is driven in a rather inefficient way.

The set-point tracking approach, however, yields a better performance as shown in fig. 7.39. The reason is that the climate set-point trajectories shown in fig. 7.38, resemble the optimal greenhouse climate trajectories shown in figs. 7.27 to 7.29. Since the dead-beat controller anticipates the outside climatic conditions, energy and carbon dioxide are more efficiently applied.

Yet, there is still a loss in performance compared with the solution of the full problem. The set-point trajectories of the greenhouse climate do not exactly match the optimal trajectories calculated in the full problem. Secondly, it is still arguable whether these trajectories can be realized in practice using standard controllers. Clearly, the dead-beat controller is not a practicable

concept. In practice an appropriately designed multivariable feedback controller should be used instead.

7.7.4. Concluding remarks

From the results presented in the section it is concluded that:

(1) as expected, the control strategies calculated without taking the greenhouse climate dynamics into account have a poor performance when applied to the full system and therefore are not useful for actual greenhouse climate control,

(2) the state trajectories calculated without taking the greenhouse climate dynamics into account can be used as set-point trajectories for on-line tracking, but compared with the optimal performance of the full system a reduction in performance is found and therefore,

(3) benefits are expected from the control of the greenhouse climate dynamics using an economic performance criterion. The decomposition, outlined in section 5.6 and successfully evaluated in section 7.5, provides valuable information as to the appropriate form of the necessary objective function to be used for the control of the greenhouse climate dynamics.

8. FINAL SYNTHESIS AND DISCUSSION

In this chapter two concepts for an optimal greenhouse climate control system will be presented and discussed with respect to application in horticultural practice. Besides the methodological side of these concepts, their contribution to an improvement of the efficiency of horticultural crop production will be addressed.

A hierarchical greenhouse climate management system: concept 1

The first concept, presented in fig. 8.1, is based on the two time-scale decomposition of optimal control problems, described in section 5.6 and validated in section 7.5. In the example shown in fig. 8.1, the control system contains two loops, an outer loop controlling the (slow) crop growth dynamics and an inner loop controlling the (fast) greenhouse climate dynamics. Later on, it will be shown that, in this concept, the control system is easily extended with more control loops if in the crop production process more significantly different response times exist.
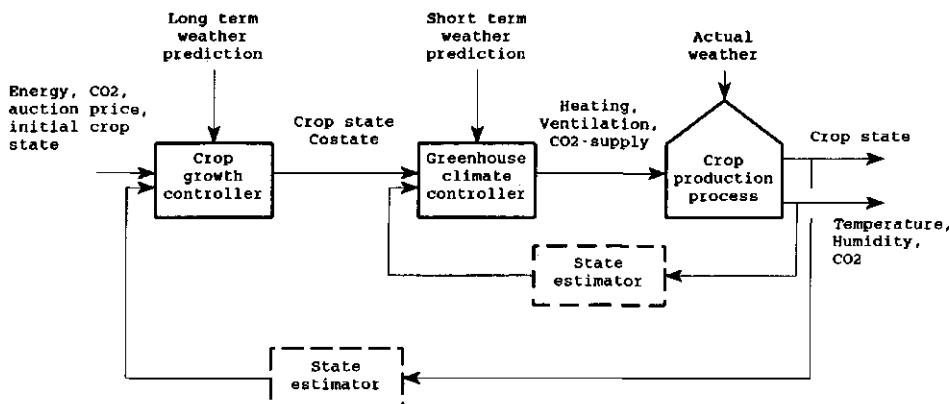
Fig. 8.1. Optimal greenhouse climate management, concept 1.

In the outer control loop, using a long term weather prediction, a prediction of the auction price and measurements or estimates of the (initial) state of the crop, the optimal control problem

concerning the slow crop growth dynamics is solved. Refer to section
6.2.2 for a definition of such a slow control problem. Since crop
growth is not very sensitive to rapid fluctuations in the
environmental conditions (figs. 3.11 and 3.12), the weather data
should describe the main diurnal and seasonal trends. Also due to the
relatively slow dynamics involved, the control problem can be solved
using large time steps of the order of half an hour. The calculated
nominal trajectories of the state of the crop and the costates are
stored in the control computer for efficient control of the
greenhouse climate dynamics in the inner control loop.

As shown in eqn. (6.12), in the outer loop, the performance
criterion used is quite similar to the objective criterion employed
for efficient control of the full greenhouse crop production process
(eqn. (6.6)).

Due to modelling errors and errors in the prediction of the
weather, the state of the crop may deviate from the nominal optimal
trajectory. Modelling errors, and errors in the prediction of the
weather and the auction price also affect the evolution of the
marginal value of the crop. Fig. 7.14 revealed that, for a lettuce
crop, the effect of perturbations in the state on the marginal value
of the state are most pronounced before canopy closure. In fig. 7.21
it was shown that under different weather conditions the evolution of
the marginal value of the crop may vary considerably. The impact of
the auction price on the trajectories of the costate has not been
shown, but follows directly from the necessary conditions (eqn.
(5.31e)). A change in the auction price will shift the final value of
the costate and thus the whole trajectory. Since errors in the
trajectories of the crop and its marginal value will affect the
performance of the inner control loop and consequently of the whole
greenhouse climate management system, a regular update of the state
and costate trajectories is needed. Using a measurement or estimate
of the actual state of the crop, a renewed long term weather
prediction and a renewed prediction of the auction price, the slow
control problem is solved again. Fig. 7.22 indicates that due to the
rather slow dynamics involved, solution of the control problem should
be repeated once a day or every few days, depending on the
availability of new information.

Repeated solution of the optimal control problem in the outer
control layer results in the state feedback loop in fig. 8.1. In the
state feedback loop measurements or estimates of the state of the
crop are needed. Crop measurements can be obtained destructively or
in a non-destructive way using for instance image processing
techniques as will be illustrated in appendix A. Usually not all
state variables will be equally easy to measure. Lettuce for example,
the total dry matter content of the crop is rather simple to

determine under practical circumstances, but it is much more difficult to obtain a measurement of the non-structural and the structural components. In such cases, state estimation techniques are needed to reconstruct the state of the process from the available measurements.

Using the trajectories of the slow states and costates obtained in the outer layer as reference trajectories, the inner control loop is aimed at efficient control of the greenhouse climate dynamics. Refer to section 6.2.3 for a definition of such a fast control problem. Since the state equations are generally non-linear, and the performance criterion used at this level is non-quadratic (eqn. (6.18)), a state feedback law is not easily deduced. Therefore, at this level, the control problem is best put into the framework of Receding Horizon Optimal Control (RHOC) (Richalet *et al.*, 1978; Garcia and Morari, 1989). In RHOC, using a prediction of the weather over a short horizon, an open-loop solution of the control problem is calculated. The control trajectory is applied to the system for some time after which the procedure is repeated. For RHOC, the performance criterion in the inner control layer, eqn. (6.18), has a favourable property. It evaluates the costs of operating the climate conditioning equipment and the revenues of crop growth by controlling the greenhouse climate dynamics. Although eqn. (6.18) suggests that this performance criterion should be optimized over the whole growing period, in practice it will be sufficient to consider only the time span during which a control action affects the dynamics of the greenhouse climate. In horticultural practice this time span will in general not exceed one hour. This favourable characteristic of the control problem in the inner loop reduces the amount of computation needed as well as the horizon of the weather prediction (Tap *et al.*, 1994[a], 1994[b]).

Also at this level, modelling errors and errors in the short term weather prediction will affect the performance of the controlled process. With the relatively short response times of the greenhouse climate in mind, the optimization should be repeated about once every minute. The RHOC approach automatically implies a state feedback loop for which measurements or estimates of the greenhouse climate variables are needed.

The time scale decomposition has an inherent flexibility and is easily extended to account for more than two different groups of dynamic responses. In fig. 7.8 it was shown that, even in crop growth, differences in response times do exist. The non-structural dry weight showed a distinct diurnal trend, whereas the structural dry weight only showed a slow evolution, not affected much by the environmental conditions. Based on these differences in response times, separate loops for control of the structural and non-

structural dry matter production may be added to the greenhouse
climate management system. The general idea is shown in fig. 8.2,
omitting some of the details shown in fig. 8.1. The response times
involved suggest a time step of about an hour for the control of the
non-structural dry matter production, whereas a time step of a few
days seems sufficient for control of the structural dry matter
production.
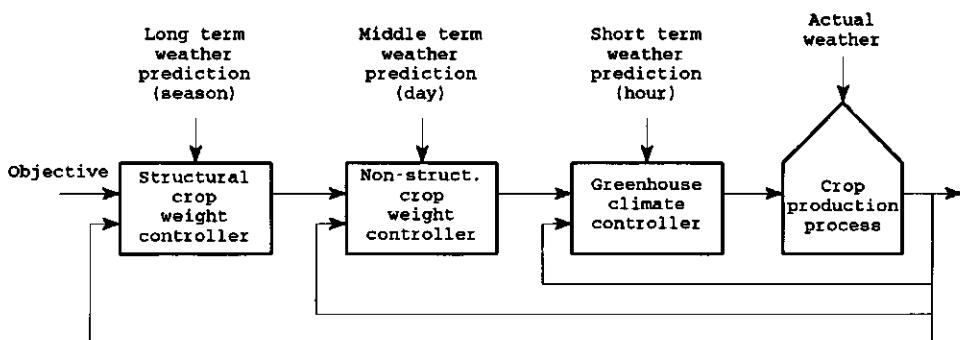
Fig. 8.2. Optimal greenhouse climate management, concept 1,
           accounting for differences in response times between non-
           structural dry matter production and structural dry matter
           production.

The layout of the control scheme presented in fig. 8.2 looks
quite similar to the hierarchical schemes proposed by Bot *et al.*
(1978), Udink ten Cate *et al.* (1983) and Challa (1985). But there are
some important differences:

(i) While referring to the hierarchical schemes, Udink ten Cate
(1983) observed that it was difficult to deal with the short term
crop responses within the hierarchical framework of optimal crop
growth control since these responses do not seem to have a direct
relationship with the long term objective of optimal crop growth
control during a whole growing period. As shown in sections 5.6.2 and
6.2, in the present framework, at all levels performance criteria are
used which have a direct relationship with the main objective of
optimal greenhouse crop production.

(ii) In some hierarchical schemes reported in literature (e.g.
Challa, 1985), the short term crop responses refer to individual
processes in crop production such as crop photosynthesis and
transpiration. Since these processes do not have a dynamic character

on the time scale used for greenhouse climate control, they are difficult to deal with in control system design. The time-scale decomposition proposed in this thesis focuses on the control of dynamic state variables, such as for instance the non-structural dry weight, rather than on the control of individual sub-processes such as photosynthesis, maintenance and growth respiration involved in dynamics of non-structural dry matter production (see eqn. (3.10)).

(iii) In contrast to the previously mentioned hierarchical schemes, the interaction between the individual control layers is clearly defined in the present concept. The state trajectories calculated in the outer layer are used as reference trajectories in the inner control loop. Additionally, the marginal value of the state variables is transferred from the outer layer to the inner layer, and used as a sort of investment policy during the realization of the crop growth trajectory in the inner layer by means of greenhouse climate control.

A hierarchical greenhouse climate management system: concept 2

The second concept is shown in fig. 8.3. Again, the control system contains an outer loop for crop growth control and an inner loop for greenhouse climate control.
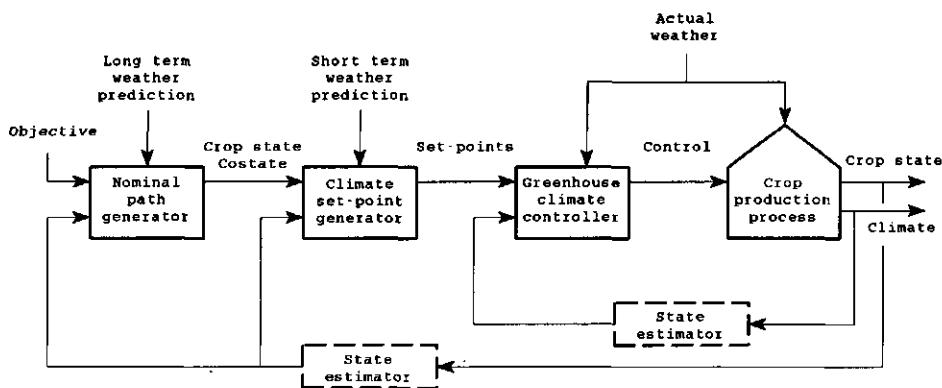
Fig. 8.3. Optimal greenhouse climate management, concept 2.

The main difference with the scheme presented in fig. 8.1 is that, in the outer control loop, set-point trajectories are generated for the greenhouse climate variables such as humidity, temperature and carbon

dioxide concentration. These set-point trajectories are then used in the inner loop for on-line greenhouse climate control.

In sections 7.2 and 7.4, it was found that fixed set-point trajectories based on an inaccurate long term prediction of the weather, do not result in efficient control of the crop production process. In stead, the greenhouse climate set-points should be adapted to the outside climatic conditions. For this purpose, in the outer loop, the sub-optimal feedback-feedforward control scheme presented in section 5.8 and validated in section 7.4 can be used. Employing a long term weather prediction and a prediction of the auction price, the slow optimal control problem (see section 6.2.2) is solved and the trajectories of the state of the crop as well as its marginal value are stored in the control computer. Using short term weather predictions, the sub-optimal feedback-feedforward controller generates set-points for the greenhouse climate variables adapted to the outside climatic conditions. Like in the concept shown in fig. 8.1, modelling errors, errors in the long term weather prediction as well as in the prediction of the auction price may require repeated calculation of the slow sub-problem using new information about the actual state of the crop, the auction price and weather. As illustrated in section 7.4, the marginal value of the state of the crop plays an important role in the feedback-feedforward control scheme.

The climate set-points calculated in the outer control layer need to be realized by the greenhouse climate controller. In the greenhouse climate, strong interactions exist between the greenhouse climate variables; take for instance humidity and air temperature. Also, the ventilation rate, as an example of the control inputs, affects both state variables. Due to this multivariable character of the greenhouse climate, the single-loop controllers presently used in horticultural practice will not be sufficient for the realization of the set-points. New multivariable greenhouse climate control concepts such as proposed by Van Henten (1989) and further developed by Young et al. (1993) are needed.

In fig. 7.20 it was shown that adaptation of the greenhouse climate set-points to the outside climatic conditions improved the efficiency of greenhouse climate control. Since in the weather rapid fluctuations do occur, the generation of the greenhouse climate set-points should be given some care. Because rapid adaptations of set-points interfere with the dynamics of the greenhouse climate, the calculated set-points will not represent the optimal indoor climate (see figs. 7.27 to 7.29) and will not be realizable in practice. Consequently, in the outer control loop only slow trends in the weather conditions should be considered and information about realizable dynamic changes in the controlled greenhouse climate

process should be included.

Comparison of both concepts in terms of efficiency

In terms of efficiency of greenhouse climate control, the simulations in section 7.6 and 7.7 revealed some evidence about the differences between the two concepts of greenhouse climate management. In section 7.7 it was found that a set-point tracking approach, as proposed in concept 2 in fig. 8.3, may yield a loss in performance compared with optimal control of the full system dynamics, including the crop response and the dynamic response of the greenhouse climate, as proposed in concept 1 in fig. 8.1. Fig. 7.38 revealed that the set-points, generated while neglecting the greenhouse climate dynamics, do not fully resemble the optimal greenhouse climate trajectories when the greenhouse climate dynamics are explicitly considered in the control system design (see figs. 7.27 to 7.29). This may result in a loss in performance of the controlled crop production process when using the scheme of fig. 8.3. Also, the simulations in section 7.6 revealed that when the greenhouse climate dynamics are explicitly considered in optimal greenhouse climate control, the greenhouse climate variables show a rather smooth trajectory even under rapidly fluctuating outside climatic conditions (see figs. 7.27 to 7.29). The control inputs, however, show an immediate reaction to changes in the outside weather, which implies that in the multivariable controller used in the second concept (fig. 8.3) for the realization of the climate set-points, feedforward of the outside climatic conditions should be used. In the multivariable control schemes presented in the literature, feedforward control has not been considered (Van Henten, 1989; Young *et al.*, 1993).

Hardware and software implementation

The currently available computer hardware and software is no longer limiting the implementation of both control concepts in horticultural practice. In both concepts, the solution of the slow control sub-problem in the outer control layer consumes most CPU-time, but these computations do not have to be frequently repeated. Moreover, since the results do not have a direct and strong impact on the process controlled, they can be performed off-line. Clearly, efficient numerical algorithms are needed to limit the amount of computation time for the solution of the open-loop control problem. Conjugate gradient algorithms (Gill et al., 1981) or sequential quadratic programming algorithms (Bartholomew-Biggs, 1987) are expected to

perform better than the steepest ascent algorithm used in the present research. In the first concept (fig. 8.1), the inner loop will be implemented in an on-line environment. The available CPU-time may cause a limitation in this control layer. However, no such problems were encountered with RHOC of the greenhouse climate during the

tomato production (Tap *et al.*, 1994[a]). In the second concept (fig. 8.3), the maximization of the Hamiltonian in the sub-optimal feedback-feedforward set-point generator will be time consuming. An experiment with carbon dioxide optimization during tomato production using the climate control system at IMAG-DLO, revealed that these calculations do not cause any timing problems with the currently available computer control hardware and software (Van Meurs and Van Henten, 1994). A multivariable control algorithm in the inner control loop of the second concept (fig. 8.3) will only need a few matrix-vector multiplications.

The benefits of optimal greenhouse climate control

In section 7.2, the performance of greenhouse climate control by the grower and optimal control were compared assuming complete knowledge about the weather throughout the growing period as well as the auction price. The results suggested that, in theory, a significant improvement in efficiency of greenhouse climate management can be achieved by using optimal control. In practice, the performance of optimal greenhouse climate control will largely depend on the ability of the control system to deal with modelling errors, and errors in the predictions of the weather and auction prices.

To deal with modelling errors in both greenhouse climate and crop growth models, state feedback loops have been included in both concepts for greenhouse climate management. In section 7.4 it was shown that using information about the actual state of the crop, near optimal performance could be achieved in the presence of large perturbations of the crop state from a precalculated nominal trajectory.

Until quite recently, long term weather predictions were considered to be a major drawback for the application of optimal greenhouse climate control in horticultural practice. In section 7.4, however, it was shown that the issue of accurate long term weather prediction for on-line optimal greenhouse climate control is largely alleviated when a feedforward control scheme, based on the framework of optimal control, is used. It was shown that, using such a feedforward control scheme, only short term weather predictions are needed for optimal greenhouse climate control. This observation has

been confirmed by Tap *et al.* (1994[b]), who investigated RHOC of the greenhouse climate dynamics.

The effect of errors in the prediction of the auction price have not been investigated in this research. The results of the analysis of the auction price of lettuce in chapter 4 indicated an opportunity for predicting the auction price. Also, a repeated optimization in the outer control loops in figs. 8.1 and 8.3, will deal with new information about the auction prices in an efficient way.

Finally, unmodelled behaviour of the greenhouse crop production process may affect the performance of optimal greenhouse climate control. To illustrate the methodology developed, in this research rather simple models were used to describe crop growth and the greenhouse climate. In chapter 3, a validation experiment revealed that the crop growth models as well as the greenhouse climate model quite accurately describe the dynamics of the processes involved during the greenhouse experiment considered. Quality aspects of crop growth, however, were not considered in the crop growth model, and humidity control was achieved in an indirect way by imposing a fixed constraint on the relative humidity. Since the humidity constraint was found to be of great importance in optimal greenhouse climate control, a more detailed description of the humidity balance in terms of canopy transpiration and condensation may be needed.

Still, the calculated carbon dioxide concentration and temperature trajectories look quite reasonable and are not expected to have a direct adverse effect on crop growth. Therefore, with a more appropriately defined constraint on the humidity an improvement in efficiency of greenhouse climate management is expected when using optimal control. Due to modelling errors and uncertainty in the weather and auction prices, the benefits of optimal greenhouse climate control may not be as large as suggested by the results reported in section 7.2. The improvement in efficiency may be in the order of 5 to 10%. But clearly, the benefits of optimal greenhouse climate management are best evaluated in full scale experiments in the greenhouse.

Compared with standard horticultural practice, a distinguishing and favourable feature of optimal greenhouse climate management is that throughout the whole production cycle the benefits of greenhouse climate control in terms of a higher yield and income of the crop production are constantly weighed against the costs of operating the climate conditioning equipment. Therefore, a modification of the greenhouse climate, though it may have a positive effect on crop growth and development, may not be profitable due to the costs of climate conditioning needed to achieve this change in the greenhouse climate. An example of this behaviour was given in section 7.3. In sections 6.4 and 7.2, it was shown that optimal control greenhouse

climate control algorithm has energy conserving properties, which results in an efficient adaptation of heating, carbon dioxide supply and ventilation to the energy and CO_2 prices and outside climatic conditions.

The role of the grower in optimal greenhouse climate management

Though the control schemes presented in figs. 8.1 to 8.3 have been presented as relatively independently operating control systems, there is still an important role for the grower in greenhouse climate management. For instance, the grower has to define the duration of the production cycle. Also, the grower is able to influence the operation of the greenhouse climate management system by supplying a prediction of the auction price and defining the type and importance of bounds on the state constraints. The scaling parameter in the penalty function offers a way to define the importance of a particular constraint and to scale the priority of the state constraints in relation to other objectives in greenhouse climate management.

 The flexibility of the theoretical framework of optimal control allows for the inclusion of unmodelled dynamics in terms of complex state constraints, e.g. a constraint on the canopy transpiration shown in section 5.3, or additional integral terms representing for instance temperature integrals to describe development aspects of greenhouse crop production (Pierre, 1969; Kirk, 1970; Sage and White, 1977).

Optimal greenhouse climate management with multiple harvest crops

The methodology presented in this thesis is not only applicable to single harvest crops like lettuce, but can be used during the production of a multiple harvest crop like tomato as well. Besides a different and possibly more complex crop production model (De Koning, 1994), a different performance criterion will then be used in optimal greenhouse climate control. The performance criterion needs to account for the multiple harvests of the fruits and will look like:

$$J = \sum_{i=1}^{n} \phi(x_i(t_i), t_i) - \int_{t_b}^{t_f} L(x, z, u, v, t) dt$$

where n is the number of harvests during the growing period, t_1 is the harvest time, t_b is the planting date, t_f is the end of the growing period, $\phi(x_1(t_1),t_1)$ is the gross return of an individual harvest which will depend on the amount of fruits harvested and the auction price, and $L(x,z,u,v,t)$ is the operating costs of the climate conditioning equipment. This definition will alter the solution of the control problem. However, since in the tomato production process differences in response times do exist in much the same way as in the lettuce production process, the hierarchical decomposition of the greenhouse climate management system is expected to be applicable to tomato production as well.

9. CONCLUSIONS AND SUGGESTIONS

The research presented in this thesis has led to the following conclusions.

(1) Exploiting the differences in response times of crop growth and greenhouse climate, a hierarchical decomposition of the optimal greenhouse climate control problem can be achieved in which the upper control level has the objective of economic optimal control of the crop growth dynamics and the lower control level emphasizes efficient control of the greenhouse climate dynamics. This decomposition means a major breakthrough in the field of optimal greenhouse climate management since, compared with hierarchical schemes reported in the literature, the hierarchical control scheme presented in this thesis is transparent, has an inherent flexibility because it is easily extended to contain more than two control loops if differences in response times occur, and uses performance criteria at all control levels which have a straightforward relationship with the main objective of efficient control of greenhouse crop production. The hierarchical decomposition of the control problem simplifies the implementation of optimal greenhouse climate management in horticultural practice.

(2) Benefits are expected from the control of the greenhouse climate dynamics using an explicit economic performance criterion. The hierarchical decomposition provides valuable information on the appropriate form of the objective function to be used for control of the greenhouse climate dynamics.

(3) Using a feedforward control scheme based on the framework of optimal control, for on-line control of the crop production process, only a short term weather prediction for a period of the order of an hour ahead is needed. This is an important result since the generation of accurate long term weather predictions was long considered to be a major obstacle to the application of optimal greenhouse climate control in horticultural practice.

(4) Compared with standard horticultural practice, optimal greenhouse climate management has the distinguishing and favourable feature that throughout the whole production cycle the benefits of greenhouse climate control in terms of a higher yield and income of crop production, are constantly weighed against the costs of operating the climate conditioning equipment. Therefore, modification of the greenhouse climate, though it may have a positive effect on crop

growth and development, may not be profitable due to the costs of climate conditioning needed to achieve this change in the greenhouse climate. In this way, optimal greenhouse climate control will result in an efficient adaptation of heating, carbon dioxide supply and ventilation to the energy and CO_2 prices as well as the outside climatic conditions.

(5) With a more appropriately defined constraint on the (relative) humidity, using optimal control, an improvement in efficiency of greenhouse climate management can be achieved through a better adjustment of the greenhouse climate to the outside climatic conditions.

(6) The costate variables and necessary conditions derived in optimal control theory, have a meaningful interpretation in economic optimal greenhouse climate management and can be used to inform the grower about the particular operation of the greenhouse climate conditioning equipment.

(7) In optimal greenhouse climate management, humidity control will largely determine the operation of the ventilation windows.

In this research project much insight has been gained into economic optimal greenhouse climate management. However, it is clear that this important problem is far from being completely solved or understood. Therefore research effort in the following areas is suggested.

The performance of optimal greenhouse climate control is largely determined by the model used to describe the process considered. To generalize the concepts presented in this thesis, further research in the field of dynamic modelling of the greenhouse climate and crop growth and production is required. Research should put emphasis on sensitivity and uncertainty analysis, simplification and validation of existing and new models.

In economic optimal greenhouse climate control it is important to have an accurate assessment of revenues of the crop at harvest time. The analysis in chapter 4 provided some insight into the predictability of the auction price of lettuce, but more research in this direction is needed.

To determine the benefits of optimal control in horticultural practice, it is necessary to perform full scale experiments in the greenhouse in which the optimal control approach is compared with greenhouse climate control supervised by the grower. The layout of experiments should receive considerable attention since the results may be influenced by the inherent variability present in crops grown

in practice and mutual interaction between the compartments in experimental greenhouses. In these experiments it is important to have a good representation of greenhouse climate control in horticultural practice. Since amongst growers different attitudes towards greenhouse climate management are known to exist, this may require some attention.

In optimal greenhouse climate control many sources of uncertainty exist, for instance in the model, the weather and the auction prices. More insight into the impact of these uncertainties on the solution of the control problem is expected from investigating optimal greenhouse climate control within the framework of non-linear stochastic optimal control.

The non-linear characteristics of the crop production models used in this thesis complicate the analysis of the optimal control problem. Symbolic processing techniques may contribute to a better understanding of the particular characteristics of the control problem.

The introduction of feedback loops in crop growth control emphasizes the need for, preferably non-destructive, measurement techniques to determine the state of the crop. Since it is not always possible to measure all the states of the process, measurement techniques and (non-linear) state estimation techniques have to be developed for use in feedback control. The issue of (non-linear) state estimation has not yet been addressed in horticultural engineering research as far as the author is aware.

REFERENCES

Acock, B., D.A. Charles-Edwards, D.J. Fitter, D.W. Hand, L.J. Ludwig, J. Warren Wilson and A.C. Withers, 1978. The contribution of leaves from different levels within a tomato crop to canopy net photosynthesis: an experimental examination of two canopy models. Journal of Experimental Botany, 29: 815-827.

Anonymous, 1989. PC-MATLAB User's Guide. The MathWorks Inc., South Natick, MA.

Arnold, E., 1988. Zur optimalen Steuerung zeitdiskreter dynamischer Prozesse mittels nichtlinearer Optimierung mit Anwendungen auf die Klimasteuerung von Gewächshäusern [in German]. Ph.D. Thesis, Technische Hochschule, Ilmenau, Germany.

Bakker, J.C., 1991. Analysis of humidity effects on growth and production of glasshouse fruit vegetables. Ph.D. Thesis, Wageningen Agricultural University, Wageningen.

Bartholomew-Biggs, M.C., 1987. Recursive quadratic programming methods based on the augmented lagrangian. Mathematical Programming Study, 31: 21-41.

Beers, G., 1983. Optimalisering van de teeltstrategie [in Dutch]. IMAG Report 101, Wageningen.

Bellman, R., 1957. Dynamic programming. Princeton University Press, Princeton, New Jersey.

Belokopytov, S.V. and M.G. Dmitriev, 1986. Direct scheme in optimal control problems with fast and slow motions. Systems and Control Letters, 8: 129-135.

Bensink, J., 1971. On morphogenesis of lettuce leaves in relation to light and temperature. Mededelingen Landbouwhogeschool, Wageningen, 71: 1-93.

Bensoussan, A., 1988. Perturbation methods in optimal control. John Wiley and Sons, New York.

Bot, G.P.A., J.J. van Dixhoorn and A.J. Udink ten Cate, 1978. Beheersing van de teelt in kassen met behulp van de computer [in Dutch]. Bedrijfsontwikkeling, 9 (10): 729-731.

Bot, G.P.A., 1983. Greenhouse climate: from physical process to a dynamic model. Ph.D. Thesis, Wageningen Agricultural University, Wageningen.

Bourdache-Siguerdidjane, H. and M. Fliess, 1987. Optimal feedback control of non-linear systems. Automatica, 23: 365-372.

Bryson, A.E. and Y.C. Ho, 1975. Applied optimal control. Hemisphere, New York.

Chalabi, Z.S. and B.J. Bailey, 1991. Sensitivity analysis of a non-steady state model of the greenhouse microclimate. Agricultural and Forest Meteorology, 56: 111-127.

Chalabi, Z.S., 1992. A generalized optimization strategy for dynamic CO_2 enrichment in a greenhouse. European Journal of Operational Research, 59: 308-312.

Challa, H., 1985. Report of the working party "Crop growth models". Acta Horticulturae, 174: 169-174.

Challa, H., G.P.A. Bot, E.M. Nederhoff and N.J. van de Braak, 1988. Greenhouse climate control in the nineties. Acta Horticulturae, 230: 459-470.

Challa, H. and G. van Straten, 1991. Reflections about optimal climate control in greenhouse cultivation. In: Hashimoto, Y. and W. Day (eds.). Mathematical and control applications in agriculture and horticulture. IFAC Workshop Series, 1: 13-18.

Challa, H. and G. van Straten, 1993. Optimal diurnal climate control in greenhouses as related to greenhouse management and crop requirements. In: Hashimoto, Y., G.P.A. Bot, W. Day, H.J. Tantau, H. Nonami (eds.). The computerized greenhouse. Automatic control application in plant production. Academic Press, New York: 119-137.

Chotai, A., P.C. Young, P. Davis and Z.S. Chalabi, 1991. True digital control of glasshouse systems. In: Hashimoto, Y. and W. Day, 1991. Mathematical and control applications in agriculture and horticulture. IFAC Workshop Series, 1: 41-46.

Corver, F.J.M., 1991. Personal communication.

Courtin, P. and J. Rootenberg, 1971. Performance index sensitivity of optimal control systems. IEEE Transactions on Automatic Control, AC-16: 275-277.

Critten, D.L., 1991. Optimization of CO_2 concentration in greenhouses: A modelling analysis for the lettuce crop. Journal of Agricultural Engineering Research, 48: 261-271.

Dorfman, R., 1969. An economic interpretation of optimal control theory. American Economic Review, 59: 817-831.

Doyle, J.C., B.A. Francis and A.R. Tannenbaum, 1992. Feedback control theory. MacMillan, New York.

Evers, A.H., 1979. Sensitivity analysis of optimal control problems. Ph.D. Thesis, Technical University, Enschede.

Evers, A.H., 1980. Sensitivity analysis in dynamic optimization. Journal of Optimization Theory and Applications, 32: 17-37.

Farquhar, G.D., S. von Caemmerer and J.A. Berry, 1980. A biochemical model of photosynthetic CO_2 assimilation in leaves of C_3 species. Planta, 149: 78-90.

Fleming, W.H. and R.W. Rishel, 1975. Deterministic and stochastic optimal control. Springer Verlag, New York.

France, J. and J.H.M. Thornley, 1984. Mathematical models in agriculture. Butterworths, London.

Frank, P.M., 1978. Introduction to system sensitivity theory. Academic Press, New York.

Freedman, M.I., and B. Granoff, 1976. Formal asymptotic solution of a singularly perturbed nonlinear optimal control problem. Journal of Optimization Theory and Applications, 19 (2): 301-325.

Freedman, M.I. and J.L. Kaplan, 1976. Singular perturbations of two-point boundary value problems arising in optimal control. SIAM Journal on Control and Optimization, 14 (2): 189-215.

Friedland, B. and P.E. Sarachnik, 1966. A unified approach to suboptimum control. In: Proceedings of the 3rd Congress of the IFAC, London, 1: 13A.1-13A.8.

Garcia, C.E. and M. Morari, 1989. Model predictive control: theory and practice - A survey, Automatica, 25 (3): 335-348

Gill, P.E., W. Murray and M.H. Wright, 1981. Practical optimization. Academic Press, London.

Gonzales, R. and E. Rofman, 1985[a]. On deterministic control problems: an approximation procedure for the optimal cost. I. The stationary problem. SIAM Journal on Control and Optimization, 23: 242-266.

Gonzales, R. and E. Rofman, 1985[b]. On deterministic control problems: an approximation procedure for the optimal cost. II. The nonstationary case. SIAM Journal on Control and Optimization, 23: 267-285.

Goudriaan, J., 1977. Crop meteorology: a simulation study. Pudoc, Wageningen.

Goudriaan, J. and H.H. van Laar, 1978. Calculation of daily totals of the gross CO_2 assimilation of leaf canopies. Netherlands Journal of Agricultural Science, 26: 373-382.

Goudriaan, J., 1987. Simulatie van gewasgroei [in Dutch]. MsC Course Theoretical Production Ecology, Wageningen Agricultural University, Wageningen.

Goudriaan, J., H.H. van Laar, H. van Keulen and W. Louwerse, 1985. Photosynthesis, CO_2 and plant production. In: Day, W. and R.K. Atkin (eds.). Wheat growth and modelling. NATO Asi Series, Series A, 86., Plenum Press, New York: 107-122.

Goudriaan, J. and J.L. Monteith, 1990. A mathematical function for crop growth based on light interception and leaf area expansion. Annals of Botany, 66: 695-701.

Henten, E.J. van, 1989. Model based design of optimal multivariable climate control systems. Acta Horticulturae, 248: 301-306.

Henten, E.J. van and J. Bontsema, 1991. Optimal control of greenhouse climate. In: Hashimoto, Y. and W. Day (eds.). Mathematical and control applications in agriculture and horticulture. IFAC Workshop Series, 1: 27-32.

Henten, E.J. van and J. Bontsema, 1992. Singular perturbation methods applied to variational problem in greenhouse climate control. Proceedings 31st IEEE Congress on Decision and Control, Tucson, Arizona: 3068-3069.

Henten, E.J. van, 1994. Validation of a dynamic lettuce growth model for greenhouse climate control. Agricultural Systems, 45: 55-72.

Henten, E.J. van and G. van Straten, 1994. Sensitivity analysis of a dynamic growth model of lettuce. Journal of Agricultural Engineering Research, 59: 19-31.

Henten, E.J. van and Z.S. Chalabi, 1994. Optimal feedback control of nonlinear dynamic systems. Optimal Control Applications and Methods. *Submitted for publication.*

Henten, E.J. van and J. Bontsema, 1994. A two time-scale decomposition of greenhouse climate management. Acta Horticulturae. *Submitted for publication.*

Holsteijn, H.M.C. van, 1981. Growth and photosynthesis of lettuce. Ph.D. Thesis, Wageningen Agricultural University, Wageningen.

Holtzman, J.M., 1992. On using perturbation analysis to do a sensitivity analysis: derivatives versus differences. IEEE Transactions on Automatic Control, AC-37 (2): 243-247.

Hoppensteadt, F., 1971. Properties of solutions of ordinary differential equations with small parameters. Communications on Pure and Applied Mathematics, 24: 807-840.

Hwang, Y., 1993. Optimization of greenhouse temperature and carbon dioxide in subtropical climate. Ph.D. Thesis, University of Florida, Florida.

Jacobson, D.H. and M.M. Lele, 1969. A transformation technique for optimal control problems with a state variable inequality constraint. IEEE Transactions on Automatic Control, AC-14: 457-464.

Jacobson, D.H., M.M. Lele and J.L. Speyer, 1971. New necessary conditions of optimality for control problems with state-variable inequality constraints. Journal of Mathematical Analysis and Applications, 35: 255-284.

Janecke, T., 1989. Market models for analyzing and forecasting the prices of horticultural crops. Acta Horticulturae, 248: 151-157.

Jansen, M.L.E., 1992. A policy for efficient use of energy in Dutch glasshouse-industries. Acta Horticulturae, 312: 13-18.

Janssen, P.H.M., W. Slob and J. Rotmans, 1990. Gevoeligheidsanalyse en onzekerheidsanalyse: een inventarisatie van ideeën, methoden en technieken [in Dutch]. RIVM Rapport nr. 958805001, Bilthoven.

Jong, T. de, 1990. Natural ventilation of large multi-span greenhouses. Ph.D. Thesis, Wageningen Agricultural University, Wageningen.

Kamien, M.I., Schwartz, N.L., 1981. Dynamic Optimization: The

calculus of variations and optimal control in economics and management. North Holland, New York.

Keulen, H. van, F.W.T. Penning de Vries and E.M. Drees, 1982. A summary model for crop growth. In: Penning de Vries, F.W.T. and H.H. van Laar (eds.). Simulation of plant growth and crop production. Pudoc, Wageningen.

Kirk, D.E., 1970. Optimal control theory. Prentice-Hall, Englewood Cliffs, New Jersey.

Kokotovic, P.V. and P. Sannuti, 1968. Singular perturbation method for reducing the model order in optimal control design. IEEE Transactions on Automatic Control, AC-13: 377-384.

Kokotovic, P.V., J.J. Allemong, J.R. Winkelman and J.H. Chow, 1980. Singular perturbation and iterative separation of time scales. Automatica, 16: 23-33.

Kokotovic, P.V., H.K. Khalil and J. O'Reilly, 1986. Singular perturbation methods in control: analysis and design. Academic Press, London.

Koning, A.N.M. de., 1994. Development and dry matter distribution in glasshouse tomato: a quantitative approach. Ph.D. Thesis, Wageningen Agricultural University, Wageningen.

Kreindler, E., 1982. Additional necessary conditions for optimal control with state-variable inequality constraints. Journal of Optimization Theory and Applications, 38: 241-250.

Kwakernaak, H. and R. Sivan, 1972. Linear optimal control systems. John Wiley and Sons, New York.

Lentz, W., 1987. Bestimmung von Temperaturstrategien für Gewächshauskulturen mittels bio-ökonomischer Modelle und Numerischer Suchverfahren [in German]. Ph.D. Thesis, University of Hannover, Hannover.

Lewis, F.L., 1986. Optimal control. John Wiley and Sons, New York.

Lorenz, H.P. and H.J. Wiebe, 1980. Effect of temperature on photosynthesis of lettuce adapted to different light and temperature conditions. Scientia Horticulturae, 13: 115-123.

Markert, A., 1990. Aggregation pflanzenphysiologischer Wachstumsmodelle und Berechnung von Steuerstrategien für das Gewächshausinnenklima mittels Verfahren der nichtlinearen Optimierung [in German]. Ph.D. Thesis, Technische Hochschule, Ilmenau.

Maurer, H. and M. Wiegand, 1992. Numerical solution of a drug displacement problem with bounded state variables. Optimal Control Applications and Methods, 13: 43-55.

Menaldi, J.-L. and E. Rofman, 1986. An algorithm to compute the viscosity solution of the Hamilton-Jacobi-Bellman equation. In: Byrnes, C.I. and A. Lindquist (eds.), Theory and Applications of Nonlinear Control Systems. Elsevier Science Publishers: 461-467.

Meurs, W.Th.M. van, 1980. The climate control computer system at the IMAG, Wageningen. Acta Horticulturae, 106: 77-83.

Meurs, W.Th.M. van and E.J. van Henten, 1994. An experiment on the optimization of CO_2 in greenhouse climate control. Acta Horticulturae, 366: 201-208.

O'Flaherty, T., B.J. Gaffney and J.A. Walsh, 1973. Analysis of the temperature control characteristics of heated glasshouses using an analogue computer. Journal of Agricultural Engineering Research, 18: 117-132.

Penning de Vries, F.W.T., A.H.M. Brunsting and H.H. van Laar, 1974. Products, requirements and efficiency of biosynthesis: a quantitative approach. Journal of Theoretical Biology, 45: 339-377.

Pierre, D.A., 1969. Optimization theory with applications. John Wiley and Sons Inc., New York.

Pontryagin, L.S., V.G. Boltyanski and R.V. Gamkrelidze, 1962. The mathematical theory of optimal process. John Wiley and Sons, New York.

Press, W.H., B.P. Flannery, S.A. Teukolsky and W.T. Vetterling, 1986. Numerical recipes. Cambridge University Press, Cambridge.

Reinisch, K., E. Arnold, A. Markert and H. Puta, 1989. Development of strategies for temperature and CO_2 control in the greenhouse production of cucumbers and tomatoes based on model building and optimization. Acta Horticulturae, 260: 67-75.

Richalet, J., A. Rault, J.L. Testud and J. Papon, 1978. Model predictive heuristic control: application to industrial process. Automatica, 14: 413-428.

Rinaldi, S., R. Sonani-Sessa, H. Stehfest and H. Tamura, 1979. Modeling and control of river quality. McGraw-Hill, New York.

Rouff, M. and F. Lamnabhi-Lagarrigue, 1986. A new approach to nonlinear feedback law. Systems and Control Letters, 7: 411-417.

Sage, A.P., and C.C. White, 1977. Optimum systems control. Prentice-Hall, Englewood Cliffs, New Jersey.

Schapendonk, A.H.C.M. and P. Gaastra, 1984. A simulation study on CO_2 concentration in protected cultivation. Scientia Horticulturae, 23: 217-229.

Schmidt, M., K. Reinisch, H. Puta and A. Markert, 1987. Determining climate strategies for greenhouse cucumber production by means of optimization. In: Preprints 10th IFAC World Congress, Munich, Germany: 350-355.

Seginer, I., G. Angel, S. Gal and D. Kantz, 1986. Optimal CO_2 enrichment strategy for greenhouses: a simulation study. Journal of Agricultural Engineering Research, 34: 285-304.

Seginer, I., 1989. Optimal greenhouse production under economic

constraints. Agricultural Systems, 29: 67-80.

Seginer, I., G. Shina, L.D. Albright and L.S. Marsh, 1991[a]. Optimal temperature setpoints for greenhouse lettuce. Journal of Agricultural Engineering Research, 49: 209-226.

Seginer, I., 1991[b]. Optimal greenhouse temperature trajectories for a multi-state-variable tomato model. In: Hashimoto, Y. and W. Day (eds.). Mathematical and control applications in agriculture and horticulture. IFAC Workshop Series, 1: 73-79.

Shina, G. and I. Seginer, 1989. Optimal management of tomato growth in greenhouses. Acta Horticulturae, 248: 307-313.

Shinar, J., 1983. On applications of singular perturbation techniques in nonlinear optimal control. Automatica, 19: 203-211.

Shridar, B. and N.K. Gupta, 1980. Missile guidance laws based on singular perturbation methodology. Journal on Guidance and Control, 3 (2): 158-165.

Spitters, C.J.T., H. van Keulen and D.W.G. van Kraalingen, 1989. A simple and universal crop growth simulator: SUCROS87. In: Rabbinge, R., S.A. Ward and H.H. van Laar (eds.). Simulation and system management in crop production. Pudoc, Wageningen.

Spitters, C.J.T, H.A.J.M. Toussaint and J. Goudriaan, 1986. Separating the diffuse and direct component of global radiation and its implications for modelling canopy photosynthesis. Part I. Components of incoming radiation. Agricultural and Forest Meteorology, 38: 217-229

Stanghellini, C., 1987. Transpiration of greenhouse crops. Ph.D. Thesis, Wageningen Agricultural University, Wageningen.

Stanghellini, C., 1993. Personal communication.

Sweeney, D.G., D.W. Hand, G. Slack and J.H.M. Thornley, 1981. Modelling the growth of winter lettuce. In: Rose, D.A. and D.A. Charles-Edwards (eds.). Mathematics and plant physiology. Academic Press, New York.

Tantau, H.J., 1985. Greenhouse climate control using mathematical models. Acta Horticulturae, 174: 449-459.

Tantau, H.J., 1991. Optimal control for plant production in greenhouses. In: Hashimoto, Y. and W. Day (eds.). Mathematical and control applications in agriculture and horticulture. IFAC Workshop Series, 1: 1-6.

Tantau, H.J., 1993. Optimal control for plant production in greenhouses. In: Hashimoto, Y., G.P.A. Bot, W. Day and H.J. Tantau and H. Nonami (eds.). The computerized greenhouse. Automatic control application in plant production. Academic Press, New York: 139-152.

Tap, R.F., L.G. van Willigenburg, G. van Straten, and E.J. van Henten, 1993. Optimal control of greenhouse climate:

computation of the influence of fast and slow dynamics. Proceedings 12th IFAC World Congress, Sydney, Australia, 10: 321-324.

Tap, R.F., L.G. van Willigenburg and G. van Straten, 1994[a]. Experimental results of receding horizon optimal control of the greenhouse climate. *In preparation.*

Tap, R.F., L.G. van Willigenburg and G. van Straten, 1994[b]. Receding horizon optimal control of greenhouse climate based on the lazy man weather prediction. *In preparation.*

Tchamitchan, M., L.G. van Willigenburg and G. van Straten, 1992. Short term dynamic optimal control of greenhouse climate. MRS Report 29-3, Wageningen Agricultural University, Wageningen.

Thornley, J.H.M. and R.G. Hurd, 1974. An analysis of the growth of young tomato plants in water culture at different light integrals and CO_2 concentrations. Annals of Botany, 38: 389-400.

Udink ten Cate, A.J., G.P.A. Bot and J.J. van Dixhoorn, 1978. Computer control of greenhouse climates. Acta Horticulturae, 87: 265-272.

Udink ten Cate, A.J. and J. van de Vooren, 1978. Adaptive control of a greenhouse heating system. Acta Horticulturae, 87: 265-272.

Udink ten Cate, A.J., and J. van Zeeland, 1981. A modified PI-algorithm for a glasshouse heating system. Acta Horticulturae, 115 (1): 351-358.

Udink ten Cate, A.J., 1983. Modelling and (adaptive) control of greenhouse climates. Ph.D. Thesis, Wageningen Agricultural University, Wageningen.

Valentin, J. and J. van Zeeland, 1980. Adaptive split range control of a glasshouse heating system. Acta Horticulturae, 106: 109-115.

Verwaayen, P.W.T, Th.H. Gieling and W.Th.M. van Meurs, 1985. Measurement and control of the climate in a greenhouse, where a heated concrete-floor is used as low temperature energy source. Acta Horticulturae, 174: 469-475.

Young, P.C., M. Lees, A. Chotai and W. Tych, 1993. The modelling and multivariable control of glasshouse systems. Proceedings of 12th World Congress IFAC, Sydney, 10: 313-316.

APPENDIX A. NON-DESTRUCTIVE CROP MEASUREMENTS BY IMAGE PROCESSING FOR CROP GROWTH CONTROL

E.J. Van Henten[*] and J. Bontsema[**]

[*]
Institute of Agricultural and Environmental Engineering
(IMAG-DLO)
P.O. Box 43, NL-6700 AA Wageningen
The Netherlands

[**]
Agricultural University
Department of Agricultural Engineering and Physics
Bomenweg 4, NL-6703 HD Wageningen
The Netherlands

ABSTRACT

A non-destructive way of measuring the state of a crop by means of image processing is presented. Three models which describe the relation between the relative soil coverage by the crop canopy and the dry weight are discussed. The accuracy of the method and of the models is determined from two experiments in lettuce growth. It is shown that the best model can estimate the dry weight from the relative soil coverage with an accuracy of about 5%. It is also shown for lettuce that there is a linear relation between the leaf area and the dry weight of the plant.

A.1. Introduction

Climate control in greenhouses can be made more efficient by explicitly taking the crop development into account. A dynamic optimal control scheme balances the benefits associated with the marketable produce against the costs associated with its production (Seginer *et al.*, 1991; Van Henten and Bontsema, 1991). Such a scheme requires among others an appropriate model of the crop progression in time as a function of the indoor climate. Some special cases excluded, the application of optimal control theory (see *e.g.* Kirk, 1970) generally results in so-called open loop control strategies, which means that, when optimal greenhouse climate control is

considered, no references with respect to the actual status of the crop and the greenhouse climate are employed in the control strategy. Consequently, successful application of the control strategies are strongly dependent on the accuracy of the process models employed. Validation experiments showed the accuracy but also some limitations of a dynamic growth model in describing dry matter accumulation and leaf area expansion of a lettuce crop (Van Henten, 1994). On-line adaptation of the control strategies, by means of repeated optimization (see *e.g.* Van Henten and Bontsema, 1991) using information about the actual status of the crop may improve the controller performance, but requires measurements of the crop variables relevant for control. Destructive measurements of crop dry weight, fresh weight and leaf area are very laborious and reduce the economic revenues of the crop produced. Therefore non-destructive measurements are preferred.

Image processing can be used as an indirect non-destructive measurement of the status of the crop. Favourable results of this approach were reported by Hack (1989) and Tantau and Hack (1993), but for single plants only. In this paper, results are presented of the application of image processing to detect crop growth of lettuce in a full scale experiment in a greenhouse.

The paper is organized as follows. First the methodology is described. Then the results are presented. Finally, the results are analyzed and implication for future research on greenhouse climate control are addressed.

A.2. Materials and methods

During two consecutive experiments, plants were sown and raised at a nursery in peat blocks and then planted in gutters on the soil surface at a density of 18 plants/m^2 using a nutrient film technique (NFT) system in an experimental greenhouse with an area of 300 m^2. Both the soil surface and gutters of the NFT system were covered with white plastic. The greenhouse was heated by a hot water system consisting of pipes mounted parallel to the gutters at a heigth of 2.0 m (fig. A.1). Because comparative studies of, for instance Van Holsteijn (1981) revealed that different lettuce cultivars have distinct growth responses, in the two successive experiments different lettuce cultivars were used. In agreement with Dutch horticultural practice, during the first experiment, which started on 17 October 1991, cultivar 'Berlo' was used. In the second experiment, starting on 21 January 1992, cultivar 'Norden' was employed. 'Norden' is frequently cultivated in winter and spring. The greenhouse climate

was controlled according to the rules followed in normal horticultural practice. During the first two weeks of the cultivation period the day temperature and night temperature were kept at 14 $^\circ$C. The night temperature was then lowered to 10 $^\circ$C, whereas the day time temperature set point was at least 14 $^\circ$C and increased dependent on the radiation level. During day time, pure CO_2 was supplied up to a maximum level of 750 ppm depending on the amount of solar radiation and the aperture of the ventilation windows. The nutrient solution had an electrical conductivity (EC) of around 2.3 mS and a pH of around 6.

Every 5 to 7 d throughout the growing period, five plants were selected at random and dry weight of the shoot and plant leaf area were determined destructively for each plant. Dry weights were obtained after oven drying the plants at a temperature of 105 $^\circ$C for 24 h. At the same time, images were recorded of a fixed group of 24 plants in the same experimental block. The number of plants in the camera's field of view did not alter during the experiment. Furthermore, during a limited period in the second experiment, images of the canopy were recorded at daily intervals.

The image recording system (fig. A.1) consisted of a charge coupled device (CCD) camera, connected to a girder of the greenhouse about 2.5 m perpendicularly above the canopy, a monitor and a video recorder. The monitor was used for adjusting the setting of the
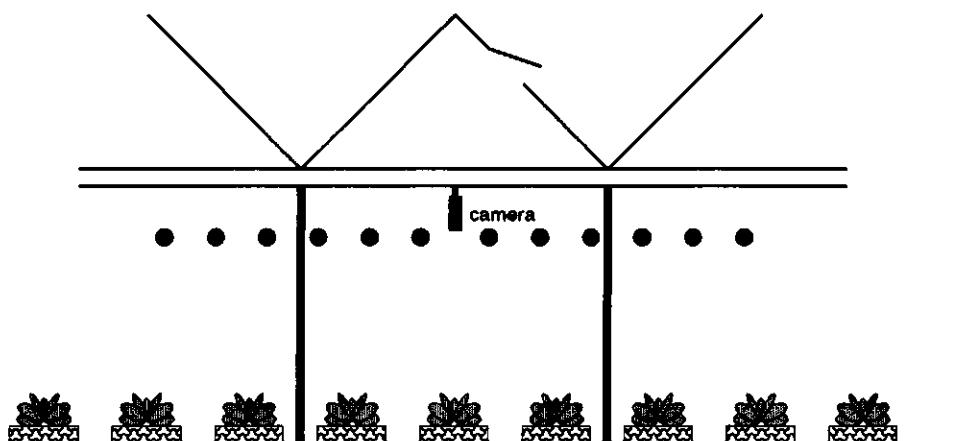
Fig. A.1. The image recording system.

camera. The video picture was converted to a digital picture with maximally 256 grey levels and a resolution of 512 by 512 pixels. Digitization logic and A/D converters were located on an image processing board in a microcomputer. The software package TCL-Image was used for processing the digitized picture. Images were recorded during daylight. Without additional filtering, an image was obtained with a sufficient amount of contrast between the canopy and the background under a wide range of radiation conditions.

The relative soil coverage was calculated by dividing the pixels of the images among two sets, namely a set representing the crop canopy and a set representing the background (soil, gutters), according to their grey value. Since a suitable algorithm was not available at the time of the experiment, a threshold value (grey level) for the separation of the pixels among these two sets was chosen manually. Though the threshold value varied with the radiation conditions, the white plastic film covering the soil and the gutters insured that good contrast between canopy and background was obtained. The fraction of image pixels belonging to the set of canopy pixels was taken as a value for the fraction of soil covered by the crop canopy.

The destructive measurements and the results of the image processing are analyzed for a possible relation between relative soil coverage and the dry weigth of the plants.

A.3. Models

In order to describe the relation between the relative soil coverage (x_{rsc}) and the dry weight (y_{dw}) of the plants we introduce three models.

The first model is derived from the so-called closing canopy model (Goudriaan and Monteith, 1990), which describes the relation between the dry weight and the soil coverage. This model is given by:

$$(A.1) \qquad x_{rsc} = (1 - e^{-py_{dw}}),$$

where x_{rsc} is the fraction of the soil which is covered by the plants, y_{dw} is the plant dry weight and p is a parameter. The model describes the feature that after a certain time the canopy is closed and that all light will be intercepted by the canopy. Inversion of the model gives a relation between x_{rsc} and y_{dw}:

(A.2) $\qquad y_{dw} = q\ln(1 - x_{rsc})$, $q = -\dfrac{1}{p}$.

This model is linear in the parameter q and if we consider x_{rsc} as a deterministic variable then standard regression analysis can be applied.

The second model (the volume/surface ratio model) is based on the assumption that for a spherical plant the relation between volume (V) and surface (S) is given by (Mohsenin, 1980):

$$V = \frac{1}{6\sqrt{\pi}} S^{3/2}.$$

If furthermore it is assumed that the mass of the plant is homogeneously distributed, the relation between the relative soil coverage and the dry weight is given by:

(A.3) $\qquad y_{dw} = \beta(x_{rsc})^{3/2}$.

Again this model is linear in the parameter β and standard linear regression can be applied.

The third model which will be considered is taken from Hack (1989). The relation between relative soil coverage and dry weight is given by:

(A.4) $\qquad y_{dw} = p_1 e^{p_2 x_{rsc}}$.

This model is clearly non-linear in the parameter p_2, so that standard regression methods only can be applied if this model is transformed to a linear one, by taking the logarithm of both sides of eqn. (A.4):

(A.5) $\qquad z_{dw} = q_1 + q_2 x_{rsc}$,

where $z_{dw} = \ln(y_{dw})$, $q_1 = \ln(p_1)$ and $q_2 = p_2$. The model given by eqn. (A.5) is linear in the parameters, so here standard linear regression can be applied, but one should be careful in translating these results to the nonlinear model given by eqn. (A.4).

A.4. Linear regression

The three models of the previous section given by the eqns. (A.2), (A.3) and (A.5) can be written as:

$$(A.6) \qquad y_1 = x_1^T p,$$

where p is the parameter vector, y_1 is the ith measurement and x_1^T is the transpose of the ith regression vector x_1.

In order to express the uncertainty in the measurement y_1, eqn. (A.6) is replaced by:

$$y_1 = x_1^T p + \varepsilon_1,$$

where ε_1 is the additive uncertainty in the ith measurement and the ε_1's are assumed to be mutually independent and have all the same Gaussion distribution with mean 0 and standard deviation σ.

If all the measurement are collected in the vector Y and the regression variables x_1 are collected in the matrix X, the following equations holds:

$$Y = Xp + e.$$

Using standard regression analysis we have the following properties (Montgomery and Peck, 1982):

The least squares estimate of the parameter vector p is given by:

$$\hat{p} = \left[X^T X \right]^{-1} X^T Y.$$

The estimate for the variance σ^2 is given by:

$$\hat{\sigma}^2 = \left(Y - X\hat{p} \right)^T \left(Y - X\hat{p} \right) / (N - n_p),$$

where N is the number of measurements and n_p is the number of parameters.

The $100(1 - \alpha)\%$ confidence interval for the j'th parameter p_j is given by:

$$(A.7) \qquad \hat{p}_j - t_{\alpha/2,N-n_p}\sqrt{\hat{\sigma}^2(X^TX)^{-1}_{jj}} \leq p_j \leq \hat{p}_j + t_{\alpha/2,N-n_p}\sqrt{\hat{\sigma}^2(X^TX)^{-1}_{jj}},$$

where $t_{\alpha/2,N-n_p}$ is the upper $\alpha/2$ percentage point of the Students t-distribution with $N - n_p$ degrees of freedom and $(X^TX)^{-1}_{jj}$ is the j'th diagonal element of $(X^TX)^{-1}$.

The $100(1 - \alpha)\%$ confidence interval for the measurement y_1 is given by:

$$(A.8) \qquad x_1^T\hat{p} - t_{\alpha/2,N-n_p}\sqrt{\hat{\sigma}^2 x_1^T(X^TX)^{-1}x_1} \leq y_1 \leq x_1^T\hat{p} + t_{\alpha/2,N-n_p}\sqrt{\hat{\sigma}^2 x_1^T(X^TX)^{-1}x_1}.$$

The $100(1 - \alpha)\%$ confidence interval for predictions of y_1, that means the values of y_1's corresponding to values of the regression variables x_1 which were not measured is given by:

$(A.9)$

$$x_1^T\hat{p} - t_{\alpha/2,N-n_p}\sqrt{\hat{\sigma}^2\left(1 + x_1^T(X^TX)^{-1}x_1\right)} \leq y_1 \leq x_1^T\hat{p} + t_{\alpha/2,N-n_p}\sqrt{\hat{\sigma}^2\left(1 + x_1^T(X^TX)^{-1}x_1\right)}.$$

Note that the confidence intervals for prediction are larger than those for the actual measurements.

For other research purposes, we measured, in addition to the block where x_{rsc} was measured, also the dry weight in three other blocks. Since these measurements were available we used the results from all four blocks to estimate the mean dry weight of the plants in the greenhouse compartment. If the total number of measurements equals M, then the confidence interval for the mean dry weight is given by:

$$(A.10) \qquad \hat{y}_1 - t_{\alpha/2,M-1}\hat{\sigma}_1/\sqrt{M} \leq \bar{y}_1 \leq \hat{y}_1 + t_{\alpha/2,M-1}\hat{\sigma}_1/\sqrt{M},$$

with M the number of measurements and $\hat{\sigma}_1$ is the estimated standard deviation of the measured dry weights in the ith experiment given by:

$$\hat{\sigma}_1^2 = \frac{1}{M-1}\sum_{j=1}^{M}(y_1 - \hat{y}_1)^2.$$

In our experiment the leaf area was also measured. The measurements indicated strong evidence for a linear relationship between the dry weight (y_{dw}) and the leaf area (y_{lai}). We will use the coefficient of determination R^2 to verify if this is true. Here R^2 is given by:

$$R^2 = \frac{\sum_{j=1}^{M}(\hat{y}_j - \overline{y})^2}{\sum_{j=1}^{M}(\hat{y}_j - \overline{y})^2 + \sum_{j=1}^{M}(y_j - \hat{y}_j)^2},$$

where y_j, $\hat{y}_j$ and $\overline{y}_j$ are the measured, estimated and mean leaf area respectively.

A.5. Results

In fig. A.2, as a representative example, the relative distribution of the pixels among the 256 grey values is shown for an image taken at 10 February 1992. In the images, the canopy is represented by the dark grey pixels whereas the soil contains the light grey values, respectively the left and the right part of the distribution shown in fig. A.2. The deep valley in the relative distribution around grey value 150 represents the pronounced contrast between canopy and background. In this specific example the pixels were divided into two sets by selecting a grey value of 150 as a threshold level, which resulted in a relative soil coverage of 54%.

By measuring artificial test objects for which the soil coverage was known, the error in these measurements was found to be less than 5%. This means that we can assume that the measurement of the relative soil coverage is deterministic. Since a lettuce crop is relatively small, it was assumed that the effect of plants being of
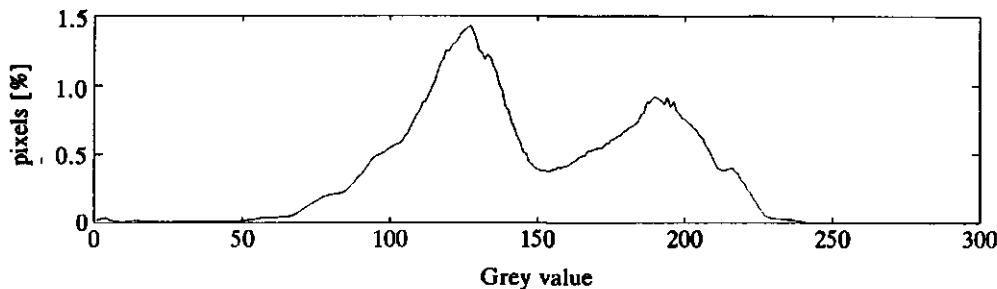
Fig. A.2. The relative distribution of the pixels of a crop image taken on February 10, 1992.

the focal axis of the camera could be neglected.

For both crops on five days measurements were performed before the canopy was closed. For crop 2 only, the measurements of the first 4 d were used. The measurement for the fifth day was too close to the closing of the canopy. The measurements are shown in fig. A.3.
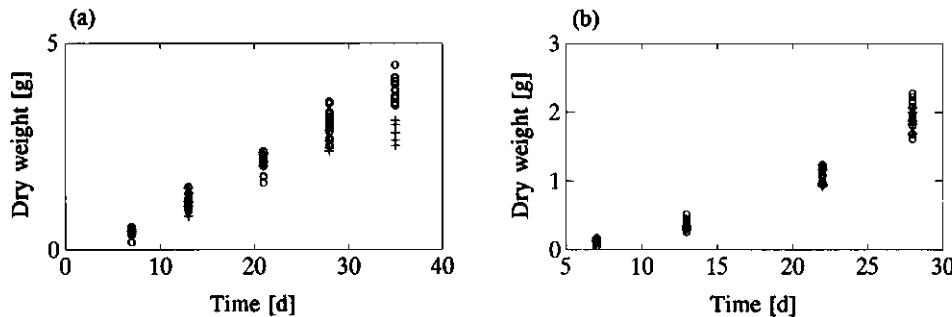
Fig. A.3. The destructive measurements of the dry weights: (a) crop 1, (b) crop 2; '+' denotes measurements from the block from which the images were taken, 'o' denotes measurements from three other blocks.

From this figure is can be seen that there is an enormous spread in the destructive measurements. Partly this can be explained by the fact that in the neighbouring compartments tomatoes were growing. Maybe this has caused some shading at the borders of the canopy. Also differences in the seedlings will contribute to this effect.

For the first crop we get the following results. The resulting closing canopy model (model 1) is:

$$y_{dw} = q\ln(1 - x_{rsc}), \text{ with } q = -0.983.$$

The 95% confidence interval for q, according to eqn. (A.7) is:

$$-1.037 < q < -0.929.$$

The volume/surface ratio model (model 2) is given by:

$$y_{dw} = \beta(x_{rsc})^{3/2}, \text{ with } \beta = 2.797.$$

The 95% confidence interval for β according to eqn. (A.7) is:

$$2.632 < \beta < 2.962.$$

The third model is given by:

$$y_{dw} = p_1 e^{p_2 x_{rsc}}, \text{ with } p_1 = 0.163 \text{ and } p_2 = 2.983.$$

The 95% confidence intervals for p_1 and p_2 calculated from the transformed linear model are:

$$0.134 < p_1 < 0.198 \text{ and } 2.733 < p_2 < 3.233.$$

The estimated dry weights (eqn. (A.8)), the predicted dry weights (eqn. (A.9)), their confidence intervals for the three models and the mean dry weights and their confidence intervals are listed in table A.1. Here $\hat{y}_{dw}$ is the estimated dry weight, $\Delta\hat{y}_{dw,est}$ is the estimation error in $\hat{y}_{dw}$ according to the 95% confidence interval eqn. (A.8). $\Delta\hat{y}_{dw,pred}$ is the prediction error in $\hat{y}_{dw}$ according to the 95% confidence interval eqn. (A.9), $\bar{y}_{dw}$ is the mean dry weight and $\Delta\bar{y}_{dw}$ is the estimation error in $\bar{y}_{dw}$ according to the 95% confidence interval eqn. (A.10). For model 3 the confidence interval is not symmetric. The largest deviation is taken (this was the upper bound).

From table A.1 some interesting features about the models can be determined. The relative error for the estimated dry weight is constant for models 1 and 2. This can easily be explained from eqn. (A.8) and the fact that there is only one regression variable. In that case the relative error is given by $t_{\alpha/2,N-1}\sqrt{\hat{\sigma}^2(X^TX)^{-1}}$ and this is independent of individual measurements. The absolute error in the predicted dry weights for models 1 and 2 turns out to be almost

Table A.1. Results for crop 1.

		model 1	model 2	model 3	mean dry weight
$x_{rsc}=0.335$	$\hat{y}_{dw}$	0.401	0.542	0.442	$\bar{y}_{dw}=0.446$
	$\Delta\hat{y}_{dw,est}$	0.022; 5.5%	0.032; 5.8%	0.055; 13%	$\Delta\bar{y}_{dw}=0.041$
	$\Delta\hat{y}_{dw,pred}$	0.561; 139%	0.597; 110%	0.159; 36%	
$x_{rsc}=0.685$	$\hat{y}_{dw}$	1.136	1.586	1.255	$\bar{y}_{dw}=1.163$
	$\Delta\hat{y}_{dw,est}$	0.063; 5.5%	0.093; 5.8%	0.076; 6%	$\Delta\bar{y}_{dw}=0.083$
	$\Delta\hat{y}_{dw,pred}$	0.564; 50%	0.603; 38%	0.422; 34%	
$x_{rsc}=0.840$	$\hat{y}_{dw}$	1.802	2.153	1.992	$\bar{y}_{dw}=2.104$
	$\Delta\hat{y}_{dw,est}$	0.100; 5.5%	0.127; 5.8%	0.126; 6%	$\Delta\bar{y}_{dw}=0.095$
	$\Delta\hat{y}_{dw,pred}$	0.570; 32%	0.610; 28%	0.672; 34%	
$x_{rsc}=0.935$	$\hat{y}_{dw}$	2.687	2.529	2.645	$\bar{y}_{dw}=2.963$
	$\Delta\hat{y}_{dw,est}$	0.149; 5.5%	0.149; 5.8%	0.201; 8%	$\Delta\bar{y}_{dw}=0.174$
	$\Delta\hat{y}_{dw,pred}$	0.580; 22%	0.615; 24%	0.902; 34%	
$x_{rsc}=0.950$	$\hat{y}_{dw}$	2.945	2.590	2.766	$\bar{y}_{dw}=3.636$
	$\Delta\hat{y}_{dw,est}$	0.163; 5.5%	0.152; 5.8%	0.218; 8%	$\Delta\bar{y}_{dw}=0.262$
	$\Delta\hat{y}_{dw,pred}$	0.584; 20%	0.615; 24%	0.945; 34%	

constant. This can be explained from eqn. (A.9). If there is only one regression variable, then the absolute error is given by $t_{\alpha/2,N-1}\sqrt{\hat{\sigma}^2\left[1+x_1^2(X^TX)^{-1}\right]}$ and since x_1^2 is in general much smaller than X^TX the term $x_1^2(X^TX)^{-1}$ will give only a small contribution.

We see also the remarkable difference in the errors for the estimated and the predicted dry weights. The latter ones are significantly larger. From table A.1 it can be concluded that models 1 and 2 are comparable and both are to be preferred over model 3, also owing to the fact that for model 3 we are not allowed to draw any statistical conclusions.

Near the closing of the canopy, all three models underestimate the dry weight.

For the second crop we get the following results. The resulting closing canopy model (model 1) is:

$y_{dw} = q\ln(1 - x_{rsc})$, with $q = -0.799$.

The 95% confidence interval for q, according to eqn. (A.7) is:

-0.869 < q < -0.729.

The volume/surface ratio model (model 2) is given by:

$y_{dw} = \beta(x_{rsc})^{3/2}$, with $\beta = 2.165$.

The 95% confidence interval for β according to eqn. (A.7) is:

2.070 < β < 2.260.

The third model is given by:

$y_{dw} = p_1 e^{p_2 x_{rsc}}$, with $p_1 = 0.104$ and $p_2 = 3.375$.

The 95% confidence intervals for p_1 and p_2 calculated from the transformed linear model are:

0.079 < p_1 < 0.137 and 2.883 < p_2 < 3.867.

The estimated dry weights (eqn. (A.8)), the predicted dry weights (eqn. (A.9)), their confidence intervals for the three models and the mean dry weights and their confidence intervals are listed in table A.2. Here $\hat{y}_{dw}$ is the estimated dry weight, $\Delta\hat{y}_{dw,est}$ is the estimation error in $\hat{y}_{dw}$ according to the 95% confidence interval eqn. (A.8). $\Delta\hat{y}_{dw,pred}$ is the prediction error in $\hat{y}_{dw}$ according to the 95% confidence interval eqn. (A.9), $\bar{y}_{dw}$ is the mean dry weight and $\Delta\bar{y}_{dw}$ is the estimation error in $\bar{y}_{dw}$ according to the 95% confidence interval eqn. (A.10).

Again we see the same features as for the first crop. Now model 2 is clearly better than the other two. Model 3 is not able to predict the dry weights. Both models 1 and 2 have problems in predicting the dry weight in the beginning of the crop.

For the second crop, daily image recordings of the canopy were made. The resulting dry weights and their confidence limits according to eqn. (A.9) for model 1 and 2 are shown in figs. A.4 and A.5. From these figures it is clear that model 2 performs better than model 1. The absolute error (*i.e.* the difference between the mean dry weight and the 95% confidence limit) in the dry weight is for model 1 about

Table A.2. The results for crop 2.

		model 1	model 2	model 3	mean dry weight
x_{rsc}=0.115	$\hat{y}_{dw}$	0.098	0.084	0.153	$\bar{y}_{dw}$=0.127
	$\Delta\hat{y}_{dw,est}$	0.009; 8.8%	0.004; 4.4%	0.041; 26%	$\Delta\bar{y}_{dw}$=0.014
	$\Delta\hat{y}_{dw,pred}$	0.425; 435%	0.214; 254%	0.162; 106%	
x_{rsc}=0.270	$\hat{y}_{dw}$	0.251	0.304	0.258	$\bar{y}_{dw}$=0.362
	$\Delta\hat{y}_{dw,est}$	0.022; 8.8%	0.013; 4.4%	0.052; 20%	$\Delta\bar{y}_{dw}$=0.029
	$\Delta\hat{y}_{dw,pred}$	0.425; 169%	0.215; 70%	0.266; 103%	
x_{rsc}=0.601	$\hat{y}_{dw}$	0.734	1.009	0.790	$\bar{y}_{dw}$=1.083
	$\Delta\hat{y}_{dw,est}$	0.065; 8.8%	0.044; 4.4%	0.141; 18%	$\Delta\bar{y}_{dw}$=0.049
	$\Delta\hat{y}_{dw,pred}$	0.430; 59%	0.219; 22%	0.805; 102%	
x_{rsc}=0.919	$\hat{y}_{dw}$	2.007	1.907	2.310	$\bar{y}_{dw}$=1.935
	$\Delta\hat{y}_{dw,est}$	0.177; 8.8%	0.084; 4.4%	0.704; 30%	$\Delta\bar{y}_{dw}$=0.082
	$\Delta\hat{y}_{dw,pred}$	0.460; 23%	0.230; 12%	2.497; 108%	

0.45 g and for model 2 this is about 0.22 g.

The relation between the dry weight x_{dw} and leaf area y_{lal} is given by:

$$y_{lal} = \alpha x_{dw},$$ with α = 600.1 for crop 1 and α = 532 for crop 2.

The 95% confidence intervals for α are given by:

$$519.6 < \alpha < 608.6$$ for crop 1 and $525.7 < \alpha < 538.3$ for crop 2.

The coefficient of determination R^2 is given by:

$$R^2 = 0.98$$ for crop 1 and $R^2 = 0.99$ for crop 2.

The measured values and the linear relations are shown in figs. A.6 and A.7. From these figures and from the the fact that values of R^2 for both crops are close to 1 is clear that it reasonable to assume that the leaf area is linearly proportional to the dry weight. For future tests this is interesting since destructive measurements of the leaf area are very time consuming compared with measuring the dry weights.
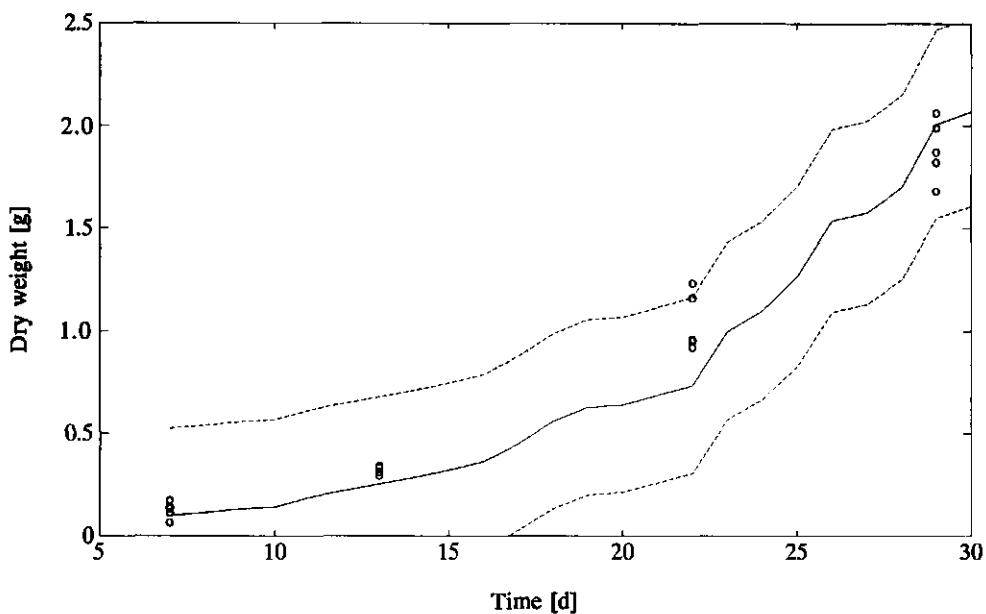
Fig. A.4. Crop 2, model 1: (——) predicted dry weights and (——) their
95% confidence limits, 'o' destructive measurements.
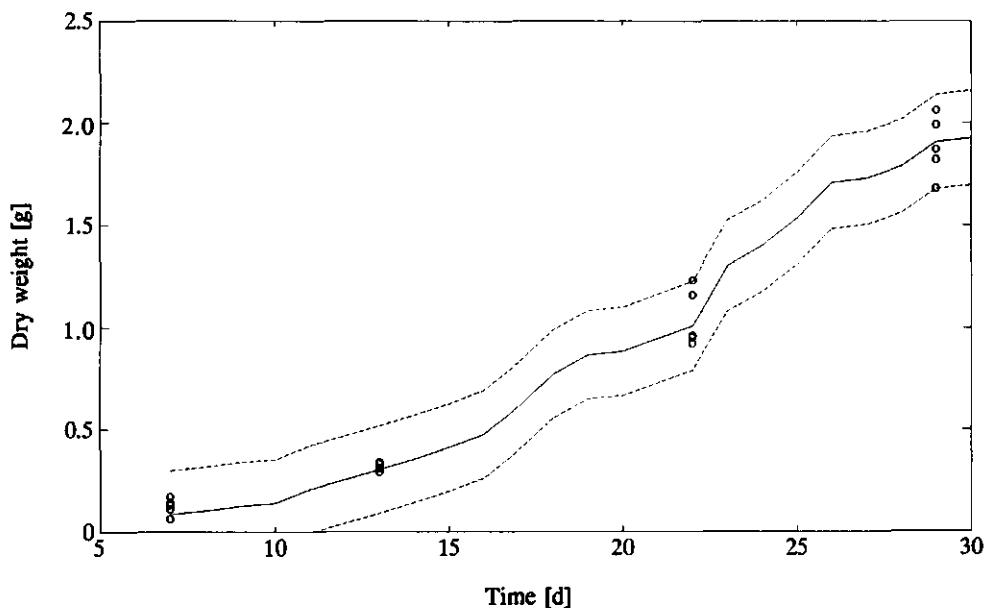

Fig. A.5. Crop 2, model 2: (——) predicted dry weights and (——) their
95% confidence limits, 'o' destructive measurements.
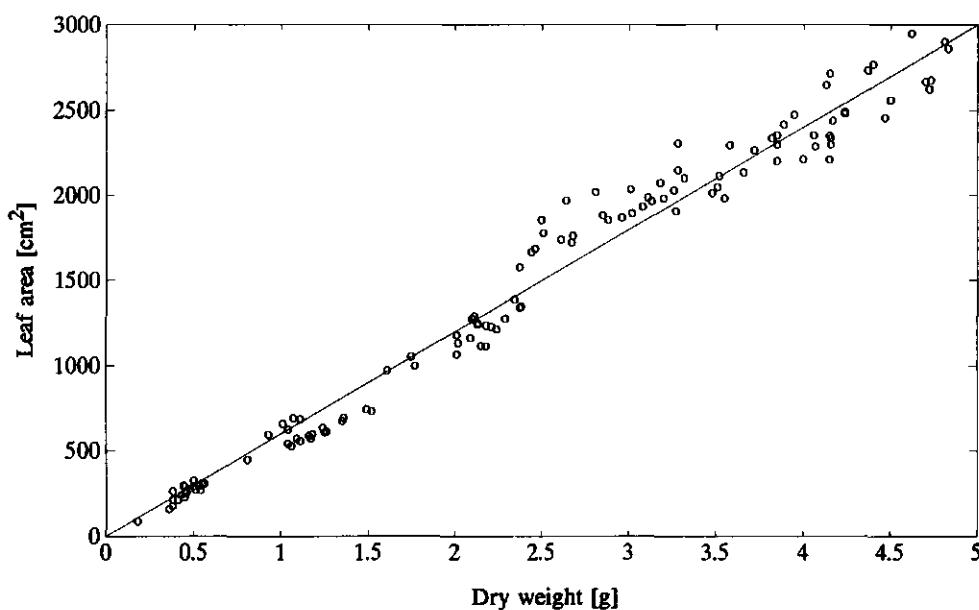
Fig. A.6. Crop 1. The relation between dry weight and leaf area (—), 'o' denotes destructive measurements.
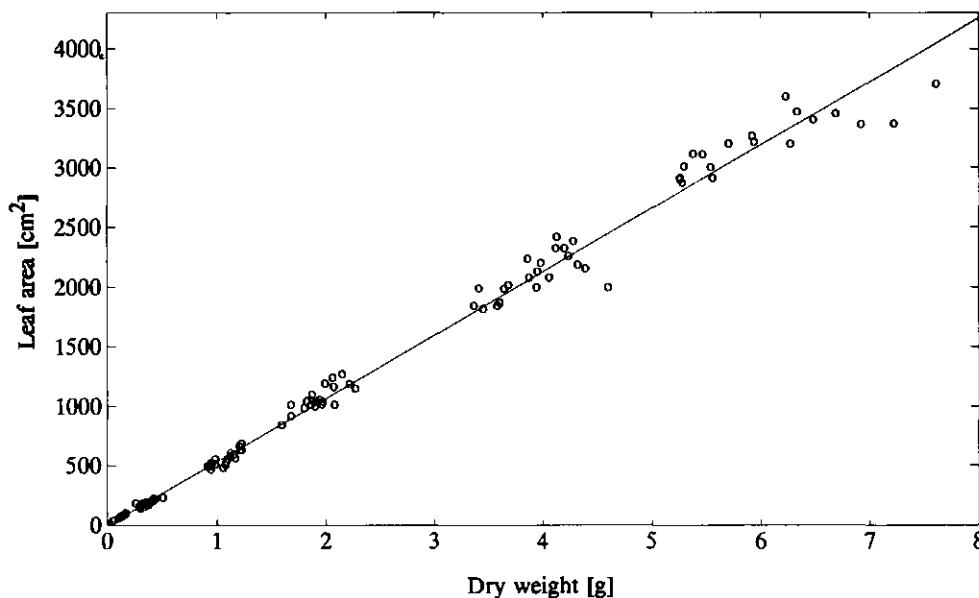
Fig. A.7. Crop 2. The relation between dry weight and leaf area (—), 'o' denotes destructive measurements.

A.6. Discussion

The applicability of optimal crop growth control in practice is limited, among others, by the accuracy of the dynamic growth models employed. The performance of these optimal controllers can be improved by modifying the control strategies using information about the actual status of the crop. Then accurate and preferably automatic non-destructive measurements of the crop status are required. However, using the Kalman filter approach (Lewis, 1986), the main issue is not that the measurements are accurate but how accurate they are. Knowing the accuracy of the measurements and the uncertainty of the growth model this approach balances between faith in the model and faith in the measurement. If we consider figs. A.4 and A.5 this means that as long as the dry weight predicted by the growth model lies between the confidence limits the value of the model is used, otherwise this value will be corrected according to the measurements. With this in mind it is also clear from the figures that in the case of crop 2 the volume/surface ratio model has to be preferred.

Image processing can be used as an indirect non-destructive measurement of the status of the crop. Since this method is based on the detection of the relative soil coverage by the canopy, it is only applicable to the growing period before canopy closure, *i.e.* about 30 d in both experiments. However, the relative importance of crop growth control in this growing period was emphasized in both empirical research on the relation between greenhouse climate and crop growth (Bierhuizen *et al.*, 1973) and more theoretical climate optimization studies (Seginer *et al.*, 1991; Van Henten, 1994). During the early stages of growth, dry matter production is limited by the light interception of the canopy. Any postponement of canopy closure can be seen as a loss of valuable crop production time and will reduce the final harvest weight of the crop (Goudriaan and Monteith, 1990). Nevertheless, for the remaining part of the cultivation period, different ways of monitoring crop growth should be exploited.

The accuracy with which the state of the crop can be estimated from measurements of the relative soil coverage is essentially determined by the accuracy of the measurement system and the accuracy of the correlation between the relative soil cover and the variables related to the state of the crop. Furthermore, it depends on the variability of the states of the individual plants in the crop. In using the image processing system, a reasonable accuracy of 5% was encountered. However, small errors in the measured soil residue cover can cause large errors in the estimated crop state shortly before canopy closure, especially for model 1 (see eqn. (A.2)). For model 2, this effect is much smaller. During the early stages of growth the effect of measurement errors is much less distinct.

Although we showed that it is possible to find a relation between the relative soil cover and crop dry weight, the reconstruction of the crop state from measured relative soil coverage contains a lot of uncertainty, as can be seen from tables A.1 and A.2. This is due to the variability encountered in the destructive and non-destructive measurements. The variability in the destructive measurements is a consequence of the inherent variability of the canopy, commonly encountered in crops grown under practical circumstances, and measurement errors. The variation in the non-destructive measurements is caused by morphological adaptations (head formation) and leaf overlap, and measurement errors due to the fact that shortly before canopy closure it is hard to determine the relative soil coverage under daylight conditions because of lack of contrast. Due to these sources of variation the confidence limits for the predicted dry weights are quite large.

Although most of the times good contrast between canopy and background was obtained, the accuracy of the non-destructive measurements could be improved by increasing the contrast using infrared-filters (Han and Hayes, 1986) and artificial lighting. Furthermore, higher resolution may contribute to a reduction of the 5% measurement error.

Finally, more experiments should be conducted to obtain more insight into the sources of variation.

Non-destructive measurements of the crop state by means of image processing is much less laborious than destructive measurements. The process can even be improved further when image recording and analysis is automated. Furthermore, non-destructive measurements do not reduce the economic value of the crop, which is of utmost importance when application in horticultural practice is considered.

A.7. Conclusion

A non-destructive way of measuring the state of the crop by means of image processing is presented. The method is not laborious when compared with destructive crop measurements and does not reduce the economic value of the canopy.

Three relations between the measured relative soil coverage and the destructive measured dry weight were considered and it has been shown that the volume/surface model gave the best results in both experiments. This model can estimate the dry weight from the relative soil coverage with an accuracy of about 5%. The parameters in all three models are dependant on the cultivar used. Furthermore it has been shown for lettuce that there is a linear relation between the leaf area index and the dry weight of the plant.

The applicability of this method depends on the accuracy with which the state of the crop has to be determined when crop growth control is considered. Further experimentation is needed to get more insight into the sources of error.

Acknowledgements

References

Bierhuizen, J.F., J.L. Ebbens and N.C.A. Koomen, 1973. Effects of temperature on lettuce growing. Netherlands Journal Agricultural Science, 21: 110-116.

Goudriaan, J. and J.L. Monteith, 1990. A mathematical function for crop growth based on light interception and leaf area expansion. Annals of Botany, 66: 695-701.

Hack, G, 1989. The use of image processing under greenhouse conditions for growth and climate control. Acta Horticulturae, 230: 215-220.

Han, Y.J. and J.C. Hayes, 1986. Evaluation of image processing methods for measuring crop cover. ASAE Paper no. 88-2540, ASAE, St. Joseph.

Kirk, D.E., 1970. Optimal Control Theory. Prentice Hall.

Lewis, F.L., 1986. Optimal estimation. John Wiley & Sons, New York.

Mohsenin, N.N., 1980. Physical properties of plant and animal material, Gordon and Breach, New York.

Montgomery, D.G. and E.A. Peck, 1982. Introduction to linear regression analysis, John Wiley & Sons, New York.

Seginer, I., G. Shina, L.D. Albright, L.S. Marsh, 1991. Optimal temperature set points for greenhouse lettuce. Journal of Agricultural Engineering Research, 49: 209-226.

Tantau, H.J., G. Hack, 1993. On-line measurement of plant growth in the greenhouse. Proceedings IFAC World Congress, 1: 311-312.

Van Henten, E.J. and J. Bontsema, 1991. Optimal control of greenhouse climate. In: Mathematical and control applications in agriculture and horticulture. Hashimoto, Y. and W. Day (eds.). IFAC Workshop Series 1: 27-32.

Van Henten, E.J., 1994. Validation of a dynamic lettuce growth model for greenhouse climate control. Agricultural Systems, 45: 55-72.

Van Henten, E.J., 1994. Analysis of a variational problem in greenhouse climate control. Ph.D. Thesis, Wageningen

Agricultural University, Wageningen.

Van Holsteijn, H.M.C., 1981. Growth and photosynthesis of lettuce. Ph.D. Thesis, Wageningen Agricultural University, Wageningen.

APPENDIX B. RECONSTRUCTION OF OUTDOOR CLIMATE DATA FROM HISTORICAL RECORDS

B.1. Introduction

Historical data have been used in the development and evaluation of the climate controller. Because in the optimal control problem the whole growing period is considered but essential subprocesses related to crop growth and greenhouse climate show a dynamic behaviour within the time scale of a day, the data were required to contain both the long term trends observable throughout the year as well as diurnal variations. Data from the period 1975 to 1989 including the daily solar radiation sum, daily minimum and maximum temperatures, the mean wind speed, and humidity were used to describe the long term trends which will be demonstrated in section B.2. In section B.3 the reconstruction of the diurnal trajectories from these data is described.

B.2. Annual trends

Long term trends in the outdoor climate were extracted from data of a measurement site of the Department of Meteorology of the Wageningen Agricultural University from the period 1975 to 1989. The measurements included daily values of the solar radiation sum, the maximum and minimum air temperature and daily average wind speed and relative humidity.

For the design and evaluation of the control algorithm, the time series data of the individual years 1975 to 1989 were used as well as time series containing the mean values of the 1975 to 1989 data. Because the latter data were essentially used to study the effect of the annual trend in the outdoor climate variables on the controller performance, small fluctuations in the data were eliminated by fitting the following periodic function through the data

(B.1) $$f(t_d) = p_1 + p_2 \sin(\frac{2\pi(t_d - p_3)}{365}),$$

where t_d denotes time in days starting at 1 January and p_1, p_2 and p_3 are parameters.

For the solar radiation sum, the minimum and maximum temperature, and the daily average wind speed and relative humidity, fitting eqn. (B.1) to all 1975 to 1989 data resulted in the

parameters listed in table B.1.

Table B.1. Parameters of eqn. (B.1) describing the annual trend in the daily solar radiation sum, the minimum and maximum air temperature and the daily mean mean wind speed and relative humidity.

Climate variable	P_1	P_2	P_3
Solar radiation sum, $\sum V_1$) [J cm^{-2}]	928.9	810.6	81.5
Maximum air temperature, $V_{t,max}$ [$^\circ$C]	13.2	8.9	111.0
Minimum air temperature, $V_{t,min}$ [$^\circ$C]	5.2	6.4	120.6
Average wind speed, V_w [m s^{-1}]	3.9	-0.8	113.3
Average relative humidity, V_{rh} [%]	80.8	-6.0	60.7

In fig. B.1 accumulated data of the solar radiation sum between 1975 and 1989 and the fitted curve are shown as an example.
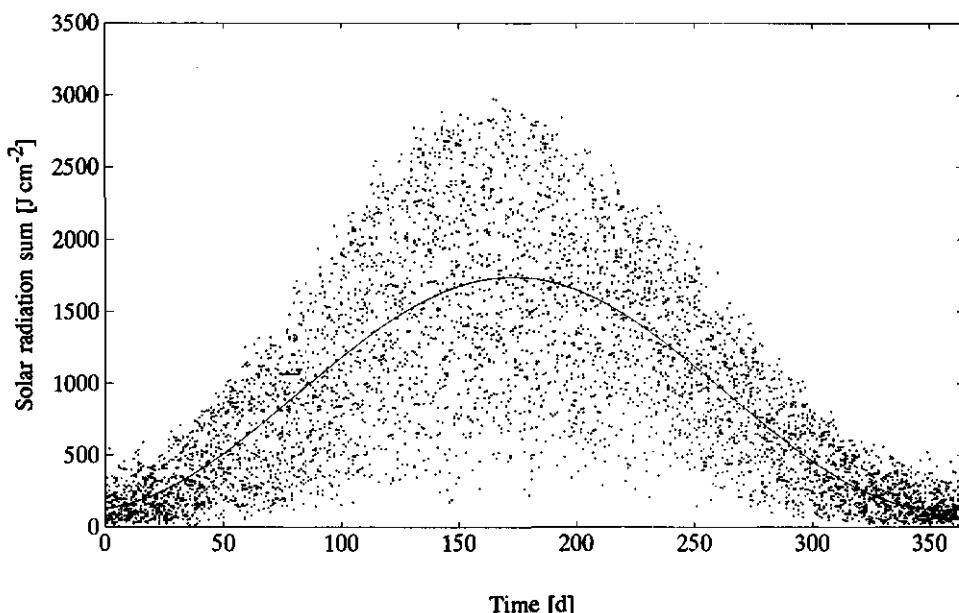
Fig. B.1. Accumulated data of the solar radiation sum between 1975 and 1989

B.3. Diurnal trends

The annual trends described in section B.2 do not contain any information about trends in these climate variables throughout the day. During the day both low as well as high frequency variations in the solar radiation, wind speed and relative humidity are known to occur. For the derivation and analysis of long term optimal climate control strategies, it is sufficient to focus on the low frequency components in the outdoor climate variables. However when on-line, i.e. short term, control is emphasized, this will not suffice and high frequency fluctuations need to be considered.

Slow diurnal trajectories of the solar radiation, air temperature, wind speed and relative humidity were reconstructed from the annual trends as follows.

Solar radiation

For the reconstruction of diurnal trajectories of the solar radiation from the daily radiation sum, the sky was assumed to be clear. Then, the momentary radiation level is strongly related to the solar height. The solar height depends on the latitude of the location, the day of the year and time of the day according to the empirical relation

$$(B.2) \qquad \sin\beta(t) = \sin\lambda \, \sin\delta + \cos\lambda \, \cos\delta \, \cos\left(\frac{2\pi(t-12)}{24}\right),$$

where λ [radians] is the latitude of the location, δ [radians] is the declination of the sun and t is the local solar time expressed in hours. The solar declination varies throughout the year which according to Goudriaan (1982) is assumed to be constant during one day. The declination is calculated with

$$(B.3) \qquad \delta(\bar{t}) = -\frac{23.4\pi}{180} \cos\left(\frac{2\pi(\bar{t}+10)}{365}\right),$$

where $\bar{t}$ is the number of the day since January the 1st.

Due to the assumption of an unclouded sky, a proportional relationship between the daily radiation sum and the area under the curve in fig. B.2 can be derived

$$\text{(B.4)} \quad \int_{t_{sr}}^{t_{ss}} V_1 dt = \alpha \int_{t_{sr}}^{t_{ss}} \sin\beta(t) dt,$$

where V_1 [W m^{-2}] is the solar radiation, t_{sr}, t_{ss} represent the sun rise and sun set time respectively and α is a parameter to be defined yet.

Exploiting the symmetry property of equation (B.4) around solar noon, sun rise and sun set times are described by $t_{sr} = 12 - 0.5d$ and $t_{ss} = 12 + 0.5d$, with d the day length in hours. Then the integral on the right hand side of eqn. (B.4) is calculated as

$$\text{(B.5)} \quad \int_{t_{sr}}^{t_{ss}} \sin\beta(t) dt = \int_{12-0.5d}^{12+0.5d} \sin\lambda \sin\delta + \cos\lambda \cos\delta \cos\left(\frac{2\pi(t-12)}{24}\right) dt$$

$$= \int_{12-0.5d}^{12+0.5d} \sin\lambda \sin\delta \, dt + 2 \cos\lambda \cos\delta \int_{12-0.5d}^{12} \cos\left(\frac{2\pi(t-12)}{24}\right) dt$$

$$= \sin\lambda \sin\delta \, d + \cos\lambda \cos\delta \, \frac{24}{\pi} \sin(\frac{\pi d}{24}).$$

The day length d is calculated with eqn. (B.2) using the fact that at sun rise and sunset $\sin\beta = 0$. Substituting $t_{ss} = 12 + 0.5d$ and $\sin\beta = 0$ in eqn. (B.2) yields

$$\text{(B.6)} \quad 0 = \sin\lambda \sin\delta + \cos\lambda \cos\delta \cos(\frac{\pi d}{24}) \Leftrightarrow d = \frac{24}{\pi} \cos^{-1}(-\frac{\sin\lambda\sin\delta}{\cos\lambda\cos\delta}).$$

Eqns. (B.4), (B.5) and (B.6) together with the measured daily radiation sum, suffice to calculate parameter α. Then, assuming a proportional relation between the the solar radiation and the solar height, which yields the following result

$$\text{(B.7)} \quad V_1(t) = \alpha \, \sin\beta(t)$$

Outdoor temperature

The air temperature is known to follow a periodic trend throughout the day. Generally, a minimum is reached just before sunrise and the temperature has a maximum in the afternoon. Of course, distinct deviations from this diurnal pattern may occur, for instance during the passage of a frontal zone. Here the diurnal trend in the air temperature is described by the following equation

$$(B.8) \qquad V_t = V_{t,min} + (V_{t,max} - V_{t,min}) \sin(\frac{2\pi(t+14)}{24})$$

where $V_{t,min}$ [$^{\circ}$C] and $V_{t,max}$ [$^{\circ}$C] are the minimum and maximum day temperature. This trajectory has a minimum at 4 am and a maximum at 16 pm.

Wind speed

The wind speed may change rapidly and many times within one day. In the present analysis both high and low frequency fluctuations are neglected and the measured daily mean values are used as momentary values of the windspeed.

Relative humidity

Relative humidity changes during the day. Here, any diurnal trends are omitted and daily average values of the relative humidity are used in the calculations.

Carbon dioxide concentration

No historic data were available of the carbon dioxide concentration in the outside air. In the present research a carbon dioxide concentration of 350 ppm is assumed.

APPENDIX C. NECESSARY CONDITIONS FOR OPTIMALITY OF THE SLOW SUB-PROBLEM: ALLEVIATION OF THE CALCULATIONS

In a general form the singular perturbed control problem analyzed in this thesis is defined as to find

$$(C.1) \qquad u^* = \arg \max_u J(u) = \Phi(x(t_f), t_f) - \int_{t_b}^{t_f} L(x, z, u, v, t)dt,$$

subject to

$$(C.2a) \qquad \frac{dx}{dt} = f(x, z, u, v, t), \qquad x(t_b) = x_b,$$

$$(C.2b) \qquad \varepsilon\frac{dz}{dt} = g(x, z, u, v, t), \qquad z(t_b) = z_b,$$

and constraints on the control inputs and the states. With the Hamiltonian defined as

$$(C.3) \qquad \mathcal{H} = -L(x, z, u, v, t) + \lambda^T f(x, z, u, v, t) + \eta^T g(x, z, u, v, t)$$

the costate equations are

$$(C.4a) \qquad -\frac{d\lambda}{dt} = \frac{\partial\mathcal{H}}{\partial x} = -\frac{\partial L}{\partial x} + \left(\frac{\partial f}{\partial x}\right)^T \lambda + \left(\frac{\partial g}{\partial x}\right)^T \eta,$$

$$(C.4b) \qquad -\varepsilon\frac{d\eta}{dt} = \frac{\partial\mathcal{H}}{\partial z} = -\frac{\partial L}{\partial z} + \left(\frac{\partial f}{\partial z}\right)^T \lambda + \left(\frac{\partial g}{\partial z}\right)^T \eta,$$

with the terminal boundary conditions $\lambda(t_f) = \partial\Phi(x(t_f))/\partial x$ and $\eta(t_f) = 0$. According to the maximum principle, the maximizing control should satisfy

$$(C.5) \qquad \mathcal{H}(x^*, z^*, u, \lambda^*, \eta^*, v, t) \leq \mathcal{H}(x^*, z^*, u^*, \lambda^*, \eta^*, v, t).$$

In this thesis, a gradient algorithm is employed to solve the control problem. The gradient of the Hamiltonian with respect to the control is defined as

(C.6) $\dfrac{\partial \mathcal{H}}{\partial u} = - \dfrac{\partial L}{\partial u} + \left(\dfrac{\partial f}{\partial u}\right)^{\mathrm{T}} \lambda + \left(\dfrac{\partial g}{\partial u}\right)^{\mathrm{T}} \eta.$

In the zero-th order slow sub-problem, $\varepsilon = 0$ and we consider

(C.7) $\displaystyle \max_{\bar{u}_0} \; \bar{J}_0(\bar{u}_0) = \Phi(\bar{x}_0(t_f),t_f) - \int_{t_b}^{t_f} L(\bar{x}_0,\bar{z}_0,\bar{u}_0,v,t)dt$

subject to the reduced order system description

(C.8a) $\dfrac{d\bar{x}_0}{dt} = f(\bar{x}_0,\bar{z}_0,\bar{u}_0,v,t), \qquad \bar{x}_0(t_b) = x_b,$

(C.8b) $0 = g(\bar{x}_0,\bar{z}_0,\bar{u}_0,v,t).$

Assuming eqn. (C.8b) has at least one real solution

(C.9) $\bar{z}_0 = h(\bar{x}_0,\bar{u}_0,v,t),$

the reduced order optimal control problem can be rewritten as

(C.10) $\displaystyle \max_{\bar{u}_0} \; \bar{J}_0(\bar{u}_0) = \Phi(\bar{x}_0(t_f),t_f) - \int_{t_b}^{t_f} L(\bar{x}_0,h(\bar{x}_0,\bar{u}_0,v),\bar{u}_0,v,t)dt$

subject to

(C.11) $\dfrac{d\bar{x}_0}{dt} = f(\bar{x}_0,h(\bar{x}_0,\bar{u}_0,v),\bar{u}_0,v,t), \qquad \bar{x}_0(t_b) = x_b.$

For this problem the Hamiltonian is defined as

(C.12) $\bar{\mathcal{H}}_0 = -L(\bar{x}_0,h(\bar{x}_0,\bar{u}_0,v),\bar{u}_0,v,t) + \bar{\lambda}_0^{\mathrm{T}} f(\bar{x}_0,h(\bar{x}_0,\bar{u}_0,v),\bar{u}_0,v,t)$

which yields with $\bar{L}_0 = L(\bar{x}_0,h(\bar{x}_0,\bar{u}_0,v,t),\bar{u}_0,v,t),$ $\bar{f}_0 = f(\bar{x}_0,h(\bar{x}_0,\bar{u}_0,v,t),\bar{u}_0,v,t)$ and $\bar{h}_0 = h(\bar{x}_0,\bar{u}_0,v,t),$ the costate equation

$$
\text{(C.13)} \qquad -\frac{d\bar{\lambda}_0}{dt} = \frac{\partial\bar{\mathcal{H}}_0}{\partial\bar{x}_0} = -\frac{\partial\bar{L}_0}{\partial\bar{x}_0} - \frac{\partial\bar{L}_0}{\partial\bar{h}_0}\frac{\partial\bar{h}_0}{\partial\bar{x}_0} + \left[\frac{\partial\bar{f}_0}{\partial\bar{x}_0} + \frac{\partial\bar{f}_0}{\partial\bar{h}_0}\frac{\partial\bar{h}_0}{\partial\bar{x}_0}\right]^{\mathrm{T}}\bar{\lambda}_0,
$$

and necessary condition $\bar{\mathcal{H}}_0(\bar{x}_0^*,\bar{u}_0,\bar{\lambda}_0^*,v,t) \leq \bar{\mathcal{H}}_0(\bar{x}_0^*,\bar{u}_0^*,\bar{\lambda}_0^*,v,t)$. During actual computation of the optimizing control the gradient of the Hamiltonian with respect to the control will be employed. The gradient is defined as

$$
\text{(C.14)} \qquad \frac{\partial\bar{\mathcal{H}}_0}{\partial\bar{u}_0} = -\frac{\partial\bar{L}_0}{\partial\bar{u}_0} - \frac{\partial\bar{L}_0}{\partial\bar{h}_0}\frac{\partial\bar{h}_0}{\partial\bar{u}_0} + \left[\frac{\partial\bar{f}_0}{\partial\bar{u}_0} + \frac{\partial\bar{f}_0}{\partial\bar{h}_0}\frac{\partial\bar{h}_0}{\partial\bar{u}_0}\right]^{\mathrm{T}}\bar{\lambda}_0.
$$

From the point of view of computation and interpretation, this way of solving the zero-th order outer problem has some disadvantages. First of all, the analytic derivation of the partial derivatives $\partial\bar{h}_0/\partial\bar{x}_0$ and $\partial\bar{h}_0/\partial\bar{u}_0$ can be quite cumbersome if the system equation g is non-linear. Alternatively, if both $\bar{z}_0$ and the partial derivatives are calculated using numerical approximations, the errors in $\bar{z}_0$ will propagate in the approximations of the partial derivatives which may obstruct a successful solution of the control problem. Secondly, using the previously outlined approach, valuable information about the quasi-steady-state solution of the fast costates $\bar{\eta}_0$ is lost. Besides having an interesting interpretation, the evolution of both $\bar{z}_0$ and $\bar{\eta}_0$ are needed for the calculation of the zero-th order fast solution. Therefore, in this thesis a different approach has been employed in which the structure of the necessary conditions for optimality of the original singular perturbed problem is maintained.

The zero-th order slow solution of the system is described by eqns. (C.8a) and (C.8b). Again, a unique solution $\bar{z}_0 = h(\bar{x}_0,\bar{u}_0,v,t)$ is assumed. With the Hamiltonian defined as

$$
\text{(C.15)} \qquad \bar{\mathcal{H}}_0 = -L(\bar{x}_0,\bar{z}_0,\bar{u}_0,v,t)+\bar{\lambda}_0^{\mathrm{T}}f(\bar{x}_0,\bar{z}_0,\bar{u}_0,v,t)+\bar{\eta}_0^{\mathrm{T}}g(\bar{x}_0,\bar{z}_0,\bar{u}_0,v,t),
$$

the costate equations are

(C.16a) $- \dfrac{d\bar{\lambda}_0}{dt} = \dfrac{\partial \mathcal{H}}{\partial \bar{x}_0} = - \dfrac{\partial \bar{L}_0}{\partial \bar{x}_0} + \left(\dfrac{\partial \bar{f}_0}{\partial \bar{x}_0}\right)^{\mathrm{T}} \bar{\lambda}_0 + \left(\dfrac{\partial \bar{g}_0}{\partial \bar{x}_0}\right)^{\mathrm{T}} \bar{\eta}_0,$

(C.16b) $0 = \dfrac{\partial \mathcal{H}}{\partial \bar{z}_0} = - \dfrac{\partial \bar{L}_0}{\partial \bar{z}_0} + \left(\dfrac{\partial \bar{f}_0}{\partial \bar{z}_0}\right)^{\mathrm{T}} \bar{\lambda}_0 + \left(\dfrac{\partial \bar{g}_0}{\partial \bar{z}_0}\right)^{\mathrm{T}} \bar{\eta}_0,$

and the optimizing control strategy should satisfy $\bar{\mathcal{H}}_0(\bar{x}_0^*, \bar{z}_0^*, \bar{u}_0, \bar{\lambda}_0^*, \bar{\eta}_0^*, v) \leq \bar{\mathcal{H}}_0(\bar{x}_0^*, \bar{z}_0^*, \bar{u}_0^*, \bar{\lambda}_0^*, \bar{\eta}_0^*, v)$. The gradient of the Hamiltonian with respect to the control is given by

(C.17) $\dfrac{\partial \bar{\mathcal{H}}_0}{\partial \bar{u}_0} = - \dfrac{\partial \bar{L}_0}{\partial \bar{u}_0} + \left(\dfrac{\partial \bar{f}_0}{\partial \bar{u}_0}\right)^{\mathrm{T}} \bar{\lambda}_0 + \left(\dfrac{\partial \bar{g}_0}{\partial \bar{u}_0}\right)^{\mathrm{T}} \bar{\eta}_0.$

Eqn. (C.15) asserts that the quasi-steady-state of z described by $0 = g(\bar{x}_0, \bar{z}_0, \bar{u}_0, v)$ is a constraint which has to be satisfied by the optimal control strategies and $\bar{\eta}_0$ is the associated time varying constraint multiplier.

Due to the fact that eqn. (C.16b) is linear in the costates, it is easily rewritten as

(C.18) $\bar{\eta}_0 = \left(\left(\dfrac{\partial \bar{g}_0}{\partial \bar{z}_0}\right)^{\mathrm{T}}\right)^{-1} \left(\dfrac{\partial \bar{L}_0}{\partial \bar{z}_0} - \left(\dfrac{\partial \bar{f}_0}{\partial \bar{z}_0}\right)^{\mathrm{T}} \bar{\lambda}_0\right).$

Eqn. (C.18) can be substituted in (C.15), (C.16a) and (C.17).

If for the singular perturbed system the partial derivatives of the Hamiltonian with respect to the states and the control (eqns. (C.4) and (C.6)) are available, the previously demonstrated approach simplifies the computation of the zero-th order slow solution significantly. Equations (C.15), (C.16a) and (C.17) are exactly the same as (C.3), (C.4a) and (C.5), but with $\bar{x}$ substituted instead of x etc. Thus, for the computation of the costate dynamics and the gradient of the Hamiltonian with respect to the control in the zero-th order slow solution, the only remaining step is the solution of eqn. (C.8b), i.e. eqn. (C.9). The result obtained from eqn. (C.9) is then substituted into eqn. (C.18) and both are substituted into eqns.

(C.15), (C.16a) and (C.17).

This approach actually yields the same result as eqns. (C.11) to (C.14), which can be seen as follows. From eqn. (C.8b) the partial derivatives of $\bar{z}_0$ with respect to $\bar{x}_0$ and $\bar{u}_0$ are derived as

(C.19) $\quad \dfrac{\partial \bar{z}_0}{\partial \bar{u}_0} = \dfrac{\partial \bar{h}_0}{\partial \bar{u}_0} = - \left(\dfrac{\partial \bar{g}_0}{\partial \bar{z}_0} \right)^{-1} \dfrac{\partial \bar{g}_0}{\partial \bar{u}_0}, \quad \dfrac{\partial \bar{z}_0}{\partial \bar{x}_0} = \dfrac{\partial \bar{h}_0}{\partial \bar{x}_0} = - \left(\dfrac{\partial \bar{g}_0}{\partial \bar{z}_0} \right)^{-1} \dfrac{\partial \bar{g}_0}{\partial \bar{x}_0}$

Substitution of (C.19) into (C.13) and (C.14) yields the same result as the substitution of (C.18) into (C.17).

APPENDIX D. NOTATION

D.1. Chapters 2 and 5

Symbol	Short explanation	Def. in eqn.
x	(slow) state variable	2.1
z	(fast) state variable	5.72
f	(slow) system equation	2.1
g, G	(fast) system equation	5.74
u	control input	2.1
v	exogenous input	2.1
c	model parameter	2.1
J	performance criterion	2.4
Φ	gross income of product sold	2.4
L	operating cost of climate conditioning equipment	2.4
s, t, τ	time	2.1
t_b	initial time	2.1
t_f	final time	2.4
n	number of state variables	2.1
nx	number of slow state variables x	5.72
nz	number of fast state variables z	5.72
m	number of control variables	2.1
p	number of external inputs	2.1
q	number of model parameters	2.1
ε	small number	5.59
I_{xc}	index set containing the constrained states	2.3
n_{xc}	number of state constraints	5.43
$x_{i,min}$	lower bound on i-th state variable	2.3
$x_{i,max}$	upper bound on i-th state variable	2.3
$u_{i,min}$	lower bound on i-th control variable	2.2
$u_{i,max}$	upper bound on i-th control variable	2.2
$\dot{x}$, $\dot{z}$	time derivative of x and z	2.1
$\mathcal{H}$	Hamiltonian	5.18
λ, η	Lagrange multiplier, costate, adjoint variable	5.10

D.2. Chapters 3, 4, 6 and 7

State variables

Symbol	Short explanation	Units	Def. in eqn.
X_c, Z_c	carbon dioxide concentration in greenhouse	kg m^{-3}	3.3
X_d	total crop dry weight	kg m^{-2}	3.1
X_h, Z_h	absolute humidity of greenhouse air	kg m^{-3}	3.24
X_n	non-structural crop dry weight	kg m^{-2}	3.10
X_s	structural crop dry weight	kg m^{-2}	3.11
X_t, Z_t	greenhouse air temperature	$^{\circ}$C	3.4

Costate variables

Symbol	Short explanation	Units	Def. in eqn.
η_c	marginal value of carbon dioxide concentration in greenhouse	ct m kg^{-1}	6.8b
η_t	marginal value of greenhouse air temperature	ct m^{-2} $^{\circ}$C^{-1}	6.8c
η_h	marginal value of absolute greenhouse air humidity	ct m kg^{-1}	6.8d
λ_d	marginal value of total crop dry weight	ct kg^{-1}	6.8a
λ_n	marginal value of non-structural crop dry weight	ct kg^{-1}	–
λ_s	marginal value of structural crop dry weight	ct kg^{-1}	–

Control inputs

Symbol	Short explanation	Units	Def. in eqn.
U_c	carbon dioxide supply rate	kg m^{-2} s^{-1}	3.23
U_{ls}	aperture of lee side vents	%	3.28
U_q	energy supply by heating system	W m^{-2}	3.60
U_t	temperature of heating pipes	°C	3.25
U_v	ventilation rate	m s^{-1}	3.60
U_{ws}	aperture of windward side vents	%	3.28

External inputs

Symbol	Short explanation	Units	Def. in eqn.
V_i	solar irradiation	W m^{-2}	3.3
V_t	outdoor air temperature	°C	3.27
V_w	outdoor wind speed	m s^{-1}	3.28
V_c	outdoor carbon dioxide concentration	kg m^{-3}	3.30
V_v	outdoor humidity	kg m^{-3}	3.32

Model outputs

Symbol	Short explanation	Units	Def. in eqn.
Y_d	total crop dry weight	kg m^{-2}	3.21
Y_{fw}	crop fresh weight	kg m^{-2}	3.9
Y_{fwh}	fresh weight per head	g head^{-1}	4.2

Mass and energy flows

Symbol	Short explanation	Units	Def. in eqn.
$\phi_{c,al,pl}$	net carbon dioxide uptake by the canopy	kg m^{-2} s^{-1}	3.29
$\phi_{c,al,ou}$	carbon dioxide losses due to		
	ventilation	kg m^{-2} s^{-1}	3.30
$\phi_{h,pl,al}$	canopy transpiration rate	kg m^{-2} s^{-1}	3.32
$\phi_{h,al,ou}$	humidity losses to outside air due		
	to ventilation	kg m^{-2} s^{-1}	3.31
ϕ_{phot}	gross canopy photosyntesis rate	kg m^{-2} s^{-1}	3.2
$\phi_{phot,max}$	max. gross canopy photosyntesis rate		
	after canopy closure	kg m^{-2} s^{-1}	3.2
ϕ_{resp}	maintenance respiration rate	kg m^{-2} s^{-1}	3.8
ϕ_{vent}	ventilation rate	m s^{-1}	3.28
$Q_{pl,al}$	energy transfer from heating pipes to air	W m^{-2}	3.25
$Q_{al,ou}$	energy transfer from greenhouse air		
	to outside air	W m^{-2}	3.27
Q_{rad}	energy input from the sun	W m^{-2}	3.26

Variables

Symbol	Short explanation	Units	Def. in eqn.
ε	light use efficiency	kg J^{-1}	3.5
Γ	carbon dioxide compensation point	kg m^{-3}	3.4
pph	auction price per lettuce head	ct head^{-1}	4.2
r_{gr}	specific growth rate	s^{-1}	3.19
σ_{co2}	canopy conductance for CO$_2$ transport		
	in leaves	m s^{-1}	3.6
σ_{car}	carboxylation conductance	m s^{-1}	3.7

Constants

Symbol	Short explanation	Units	Def. in eqn.
c_α	conversion factor	–	3.1
$c_{\alpha\beta}$	yield factor	–	3.59
$c_{al,ou}$	energy transfer through greenhouse cover	$W\ m^{-2}\ ^\circ C^{-1}$	3.27
c_β	yield factor	–	3.1
c_{bnd}	boundary layer conductance	$m\ s^{-1}$	3.6
$c_{cap,al,p}$	heat capacity of the air at constant pressure	$J\ m^{-3}\ ^\circ C^{-1}$	–
$c_{cap,c}$	mass capacity of greenhouse air for carbon dioxide	m	3.23
$c_{cap,h}$	mass capacity of greenhouse air for humidity	m	3.24
$c_{cap,q}$	heat capacity of greenhouse air	$J\ m^{-2}\ ^\circ C^{-1}$	3.22
$c_{cap,q,v}$	heat capacity per volume unit of greenhouse air	$J\ m^{-3}\ ^\circ C^{-1}$	3.27
$c_{car,1}$	temperature effect on c_{car}	$m\ s^{-1}\ ^\circ C^{-2}$	3.7
$c_{car,2}$	temperature effect on c_{car}	$m\ s^{-1}\ ^\circ C^{-1}$	3.7
$c_{car,3}$	temperature effect on c_{car}	$m\ s^{-1}$	3.7
c_{co2}	unit price of carbon dioxide	$ct\ kg^{-1}$	4.4
$c_{co2,1}$	temperature effect on CO_2 diffusion in leaves	$m\ s^{-1}\ ^\circ C^{-2}$	3.59
$c_{co2,2}$	temperature effect on CO_2 diffusion in leaves	$m\ s^{-1}\ ^\circ C^{-1}$	3.59
$c_{co2,3}$	temperature effect on CO_2 diffusion in leaves	$m\ s^{-1}$	3.59
c_ε	light use efficiency at high CO_2 concentrations	$kg\ J^{-1}$	3.5
c_{fw}	ratio crop fresh weight to crop dry weight	–	3.9

Symbol	Short explanation	Units	Def. in eqn.
c_Γ	carbon dioxide compensation point at 20 $^{\circ}$C	kg m^{-3}	3.4
c_{gr}	specific growth rate	s^{-1}	3.63
$c_{h,pl,al}$	leaf transpiration coefficient	m s^{-1}	3.32
c_{H2O}	molecular mass of water	kg kmol^{-1}	3.32
c_l	light use efficiency	kg J^{-1}	3.59
c_k	extinction coefficient	-	3.2
$c_{lar,d}$	shoot leaf area ratio	m^{-2} kg^{-1}	3.2
$c_{lar,s}$	shoot leaf area ratio	m^2 kg^{-1}	3.12
$c_{ls,1}$	lee side ventilation rate parameter	-	3.28
$c_{ls,2}$	lee side ventilation rate parameter	-	3.28
c_{par}	fraction PAR of solar radiation	-	3.3
$c_{pl,al}$	heat transfer coefficient	W m^{-2} $^{\circ}$C^{-1}	3.25
c_{pl}	plant density	-	4.2
$c_{pl,d}$	effective canopy surface	m^2 kg^{-1}	3.59
$c_{pl,s}$	effective canopy surface	m^2 kg^{-1}	3.63
$c_{prl,1}$	basic price per head	ct head^{-1}	4.3
$c_{prl,2}$	additional price per unit head weight	ct g^{-1} head^{-1}	4.3
c_q	unit price of heating energy	ct J^{-1}	4.4
$c_{Q10,\Gamma}$	Q10-factor of carbon dioxide compensation point	-	3.4
$c_{Q10,gr}$	Q10-factor of growth	-	3.19
$c_{Q10,resp}$	Q10-factor maintenance respiration	-	3.8
c_{rad}	heat load coefficient due to solar radiation	-	3.26
$c_{rad,rf}$	transmission coefficient of roof for solar radiation	-	3.3

Symbol	Short explanation	Units	Def. in eqn.
$c_{resp,s}$	maintenance respiration rate of the shoot at 25 $^{\circ}$C	s^{-1}	3.8
$c_{resp,r}$	maintenance respiration rate of the root at 25 $^{\circ}$C	s^{-1}	3.8
$c_{resp,1}$	maintenance respiration rate	s^{-1}	3.59
$c_{resp,2}$	maintenance respiration rate	s^{-1}	3.60
$c_{resp,3}$	maintenance respiration rate	s^{-1}	3.63
$c_{resp,4}$	growth respiration rate	s^{-1}	3.65
$c_{r,gr,max}$	saturation growth rate at 20 $^{\circ}$C	s^{-1}	3.19
c_R	gas constant	$J\ K^{-1}\ kmol^{-1}$	3.32
$c_{\rho,al}$	density of the air	$kg\ m^{-3}$	–
c_{stm}	stomatal conductance	$m\ s^{-1}$	3.6
c_τ	ratio root weight to total crop dry weight	–	3.2
$c_{t,abs}$	absolute temperature	K	3.32
c_{window}	window aperture per square meter soil	$m\ s^{-1}$	3.28
$c_{v,1}$	saturation water vap. pressure parameter	$J\ m^{-3}$	3.32
$c_{v,2}$	saturation water vap. pressure parameter	–	3.32
$c_{v,3}$	saturation water vap. pressure parameter	$^{\circ}$C	3.32
$c_{ws,1}$	windward side ventilation rate parameter	–	3.28
$c_{ws,2}$	windward side ventilation rate parameter	–	3.28

SUMMARY

In this thesis a methodology is developed for the construction and analysis of an optimal greenhouse climate control system.

In chapter 1, the results of a literature survey are presented and the research objectives are defined. In the literature, optimal greenhouse climate management systems have been commonly presented and analysed as hierarchical systems. The main reasons were the inherent complexity of the system and existing differences in dynamic response times of the process variables involved. In general terms, the hierarchical control schemes contained two layers. An upper layer emphasizes control of the crop growth dynamics and a lower layer is concerned with control of the greenhouse climate. With respect to optimal greenhouse climate management it has not become completely clear from the literature how the hierarchical structure should be derived, how the relations between the different layers should be defined nor what kind of performance criterion should be used at each level. It is one of the objectives of this thesis to investigate the hierarchical decomposition of greenhouse climate management.

Until now, in research on optimal greenhouse climate management, the main emphasis was on control of the carbon dioxide concentration and temperature in the greenhouse. Since in horticultural practice as well as in research, the humidity level in the greenhouse is considered to be an important climate variable determining the quality and quantity of crop production, a second objective of this research is to explicitly include humidity control in the control system design.

For application of optimal control in horticultural practice, it is necessary to have a quantative model which describes the dynamic response of the greenhouse crop production process to the control and exogenous inputs with some accuracy. A third objective of this thesis is to analyse and validate dynamic models of the greenhouse crop production process.

In optimal greenhouse climate control, predictions of the auction price and the weather are important. A final objective of this thesis is to investigate briefly the predictability of auction prices and to develop a methodology for greenhouse climate control which deals with errors in the model and the predictions of both auction price and weather, while maintaining near optimal performance.

In this thesis the production of a lettuce crop is used as a vehicle for the illustration of the methodology developed.

In chapter 2 the optimal greenhouse climate control problem is defined. The objective of optimal greenhouse climate control during the production of a lettuce crop is defined as to control the greenhouse climate such that the net return is maximized. The net return is defined as the difference between the revenues of the harvested lettuce crop and the climate conditioning costs. In the control problem physical limitations of the control inputs are included. Also simple bound constraints are imposed on the state of the greenhouse climate. These constraints represent unmodelled effects of the greenhouse climate on the quality and quantity of crop production.

In chapter 3, dynamic models of crop growth and greenhouse climate are presented and analysed. With data collected in two lettuce growth experiments in a greenhouse, the models used in this research are calibrated and validated. It is shown that the models quite accurately describe the dynamics of the process variables considered in this research. Also it is illustrated that in the crop production process differences in response times do exist. The greenhouse climate responds rapidly to changes in control and external inputs, whereas crop growth responds comparatively slow to changes in the environmental conditions.

A methodology for a first-order sensitivity analysis of dynamic models is presented and one of the lettuce growth models is analysed. It is shown that in this model of lettuce growth, only a few parameters mainly determine crop growth. The solar radiation level and carbon dioxide concentration are important environmental conditions. The temperature is relatively less important in this model.

At the end of the chapter the models of lettuce growth and greenhouse climate are integrated to yield a model of the crop production process. This model is also validated.

In chapter 4, the performance criterion used in optimal greenhouse climate control is defined in more detail. It is shown that a linear relation between the harvest fresh weight of the crop and the auction price of lettuce exists. The time-varying parameters of this linear relation show distinct diurnal trends which offer an opportunity for predicting the auction price.

In chapter 5, the methodology for the solution and analysis of optimal control problems is presented. Necessary conditions for the existence of an optimal control trajectory are derived for a control problem with state and control constraints.

It is shown that, in optimal control, the necessary conditions

for optimality have a meaningful economic interpretation which can be used in the analysis of optimal greenhouse climate management.

Considerable attention is paid to the solution of control problems in which both slow and fast dynamics interact. Using the framework of singular perturbed systems, the control problem in which both slow and fast dynamics are included, is decomposed into two sub-problems. One sub-problem emphasizes efficient control of the slow dynamics, the other sub-problem emphasizes efficient control of the fast dynamics. It is shown that the performance criteria used in both sub-problems have a clear relationship with the main objective of the original control problem.

The methodology of a first-order sensitivity analysis of open-loop optimal control problems is derived.

An algorithm is presented which is used to solve the optimal control problem iteratively on a digital computer is described.

Finally, a feedback, feedforward control scheme based on the framework of optimal control is derived which is expected to yield near optimal performance in the presence of perturbations in the model and in the external inputs.

In chapter 6 the methodology derived in chapter 5 is applied to the optimal greenhouse climate control problem using the model defined in chapter 3 and the performance criterion defined in chapter 4. For the full control problem, in which both greenhouse climate dynamics and crop growth dynamics are included, the necessary conditions are derived. Also the equations of the slow sub-problem, aiming at economic optimal control of the crop growth dynamics, and of the fast sub-problem, emphasizing efficient control of the greenhouse climate dynamics, are explicitly stated. The equations are analysed to gain insight into the operation of optimal greenhouse climate control.

In chapter 7, optimal greenhouse climate control is investigated with simulations. Using the measured data obtained during one of the lettuce growth experiments in the greenhouse, optimal greenhouse climate control is compared with climate control supervised by the grower. The simulations show that using optimal control, greenhouse heating, carbon dioxide supply and ventilation are more efficiently used. Also, it is shown that the humidity level in the greenhouse largely determines the ventilation rate and strongly affects the performance of optimal greenhouse climate control.

The feedback, feedforward control scheme is evaluated in simulations. It is shown that using a short-term weather prediction, the control scheme is able to achieve near optimal performance in the presence of large perturbations of the state and the weather from

precalculated nominal trajectories. These results suggest that accurate long term weather predictions no longer limit the application of optimal greenhouse climate control in practice.

In simulations, the decomposition of the greenhouse climate control problem is successfully evaluated. The performance of both sub-problems closely approximates the performance of the full control problem in which both slow and fast dynamics are included. Also, the control trajectories resulting from the decomposition closely approximate the control trajectories calculated for the full problem. Another simulation shows the importance of using an explicit economic criterion for control of the greenhouse climate dynamics. The decomposition supplies valuable information on the form of the objective function appropriate for use in control of the greenhouse climate dynamics.

Finally, a sensitivity analysis supplies insight into the performance sensitivity of open-loop optimal greenhouse climate for perturbations in the model parameters and initial conditions.

Chapter 8 contains a synthesis of the results obtained in the previous chapters. Two concepts for the implementation of optimal greenhouse climate management in horticultural practice are presented. The concepts are compared and their operation is discussed. It is indicated that both control systems are able to deal with uncertainty in the weather and the auction prices. Also, practical aspects like the amount of CPU-time needed, the flexibility of the hierarchical structure, the role of the grower in greenhouse climate management as well as the contribution of optimal control to the improvement of the efficiency of greenhouse crop production are discussed. Finally, it is indicated how the methodology developed in this thesis can be applied to multiple harvest crops like tomatoes and cucumbers.

Chapter 9 contains concluding remarks as well as suggestions for further research.

SAMENVATTING

In dit proefschrift is een methodiek beschreven voor het ontwerp en de analyse van een economisch optimaal kasklimaatbesturingssysteem.

In hoofdstuk 1 worden de resultaten van een literatuurstudie gepresenteerd en de doelstelling van het onderzoek nader afgebakend. In de literatuur zijn optimale kasklimaatbesturingssystemen veelal voorgesteld en bestudeerd als hiërarchische structuur. Belangrijkste redenen hiervoor waren de complexiteit van het bestudeerde proces en de aanwezigheid van verschillen in responsietijd in het proces. In grove lijnen geschetst werd, in deze hiërarchische structuur, op één niveau aandacht besteed aan de optimale besturing van de gewasgroeiprocessen. Het daaronder liggende niveau richtte zich op de besturing van het kasklimaat. De literatuur heeft echter weinig duidelijkheid verschaft over de manier waarop in zijn algemeenheid genoemde hiërarchische structuur tot stand moet worden gebracht, noch welke doelfunkties op de verschillende niveaus moeten worden gehanteerd en wat hun onderlinge relatie is. Dit aspect wordt in dit proefschrift nader onderzocht.

Uit de literatuur blijkt dat in voorgaand onderzoek aan optimale kasklimaatbesturing de aandacht vooral werd gericht op sturing van de temperatuur en de koolzuurgasconcentratie in de kas. Aangezien in de tuinbouwpraktijk de luchtvochtigheid in de kas ook als een belangrijke klimaatgrootheid wordt gezien die de kwaliteit en kwantiteit van de gewasproduktie beïnvloedt, wordt de luchtvochtigheid in dit proefschrift expliciet in het ontwerp van de klimaatregeling opgenomen.

Voor de toepassing van optimale besturing in de tuinbouwpraktijk is het nodig een modelbeschrijving van het gewasproduktieproces te hebben. Dit model dient een redelijk nauwkeurige beschrijving te geven van de responsie van het gewasproduktieproces op manipuleerbare en niet-manipuleerbare ingangsgrootheden. In dit proefschrift wordt aandacht besteed aan de analyse en validatie van dynamische modellen van het gewasproduktieproces.

Bij optimale kasklimaatbesturing spelen voorspellingen van het weer en de veilingprijs een belangrijke rol. In dit proefschrift wordt de voorspelbaarheid van veilingprijzen summier onderzocht. Tevens wordt onderzocht hoe bij optimale kasklimaatbesturing omgegaan moet worden met fouten in de modellen en fouten in de voorspelling van het weer en de veilingprijzen.

De teelt van een slagewas wordt gebruikt als voorbeeld voor de illustratie van de ontwikkelde methoden.

In hoofdstuk 2 wordt het optimale kasklimaatbesturingsvraagstuk
gedefinieerd. Doelstelling van de optimale kasklimaatbesturing is om
gedurende een gehele teelt van sla het kasklimaat zodanig te regelen
dat het verschil tussen de inkomsten verkregen uit de verkoop van het
geoogste gewas op de veiling en de kosten verbonden aan de
klimatisering van de kas, wordt gemaximaliseerd. In het
besturingsvraagstuk worden fysieke begrenzingen van de sturingen
meegenomen alsmede begrenzingen op de temperatuur,
koolzuurgasconcentratie en luchtvochtigheid in de kas.

In hoofdstuk 3 worden dynamische modellen van het kasklimaat en
de gewasgroei van sla beschreven. Tijdens twee teelten van sla in een
experimenteerkas zijn gegevens verzameld voor de calibratie en
validatie van deze modellen. De validatie toont aan dat de modellen
met een redelijke nauwkeurigheid de gewasgroei alsmede het kasklimaat
beschrijven. De simulaties laten een verschil in responsiesnelheid
tussen het kasklimaat en de gewasgroei zien. Het kasklimaat reageert
snel op de ingangsgrootheden, vergeleken met de relatief trage
responsie van de gewasgroei. Dit gedrag wordt later in dit
proefschrift gebruikt voor een hiërarchische opsplitsing van het
regelsysteem.
Een methode voor de gevoeligheidsanalyse van dynamische modellen
wordt beschreven, en een gewasgroeimodel van sla wordt geanalyseerd.
De gevoeligheidsanalyse laat zien dat maar een klein aantal van de
parameters in het model een wezenlijke bijdrage levert aan de
gesimuleerde gewasgroei. De globale straling en de koolzuurgas-
concentratie in de kas blijken belangrijke ingangsgrootheden, de
temperatuur heeft in dit model een minder sterke invloed op de totale
drogestofproduktie.
Aan het eind van het hoofdstuk worden de modellen van de
gewasgroei en het kasklimaat geïntegreerd tot een model van het kas-
gewasproduktieproces. Validatie laat zien dat het resulterende model
goed in staat is de gemeten data te beschrijven.

In hoofdstuk 4 wordt de doelfunktie voor het regelaarontwerp
nader gedefinieerd. Op basis van een analyse van veilingprijzen wordt
een relatie beschreven tussen het versgewicht van sla en de
veilingprijs. De tijdvariante parameters vertonen een duidelijke
seizoensgebonden trend. Deze trend biedt een mogelijk aanknopingspunt
voor voorspelling van de veilingprijs.

In hoofdstuk 5 worden methodieken voor het oplossen en
analyseren van optimale besturingsvraagstukken beschreven.
Noodzakelijke voorwaarden waaraan een optimale sturing moet voldoen
worden afgeleid. Een economische interpretatie van de verkregen

vergelijkingen wordt gegeven.

De nodige aandacht wordt besteed aan optimale besturing van processen waarin verschillende responsiesnelheden voorkomen, zoals waargenomen in het gewasproduktieproces. Op basis van de theorie van singulier verstoorde systemen wordt een decompositie van het optimale besturingsvraagstuk in twee deelvraagstukken afgeleid. Eén deelvraagstuk richt zich op de optimale besturing van de trage dynamica. Het tweede deelvraagstuk richt zich op de efficiënte besturing van de snelle dynamica. Aangetoond wordt dat de doelfunkties in beide deelvraagstukken een duidelijke relatie hebben met de doelfunktie van het oorspronkelijke vraagstuk waarbij zowel de trage als de snelle dynamica tegelijk in beschouwing worden genomen.

Een numeriek algorithme wordt beschreven waarmee het optimale besturingsvraagstuk iteratief door een computer kan worden opgelost.

Een methode voor de gevoeligheidsanalyse van open-lus besturingsvraagstukken voor kleine variaties in de modelparameters en begincondities van de procestoestand wordt gepresenteerd.

Tenslotte wordt in dit hoofdstuk een regelschema afgeleid waarmee een bijna optimale regeling van het proces kan worden verkregen bij optredende fouten in het model en de voorspelling van de externe inputs. Dit regelschema bevat een terugkoppeling van de toestand van het gewasproduktieproces en een voorwaartskoppeling van het buitenklimaat.

In hoofdstuk 6 wordt de methodiek, afgeleid in hoofdstuk 5, toegepast op de modellen beschreven in hoofdstuk 3 en op de doelfunktie gedefinieerd in hoofdstuk 4. De vergelijkingen van de noodzakelijke voorwaarden van het volledige optimale besturingsvraagstuk, waarin zowel met de kasklimaatdynamica als met de gewasgroeidynamica rekening wordt gehouden, worden gegeven. Ook worden de vergelijkingen gepresenteerd van het trage deelvraagstuk, waarin alleen met de gewasgroeidynamica rekening wordt gehouden. Tenslotte worden de vergelijkingen van het snelle deelvraagstuk, waarin uitsluitend met de kasklimaatdynamica rekening wordt gehouden, gepresenteerd. Door middel van een analyse van de getoonde vergelijkingen wordt inzicht gegeven in de werking van optimale kasklimaatbesturing.

In hoofdstuk 7 wordt door middel van simulaties het optimale kasklimaatbesturingsvraagstuk nader bestudeerd. Gebruikmakend van de meetgevens verkregen tijdens één van de experimenten in de kas, wordt optimale kasklimaatbesturing vergeleken met kasklimaatbesturing onder supervisie van de tuinder. De simulaties geven aan dat optimale kasklimaatbesturing efficiënter gebruik maakt van de verwarming, efficiënter koolzuurgas doseert en efficiënter ventileert. De

luchtvochtigheid in de kas bepaalt in hoge mate de ventilatie en heeft als zodanig een grote invloed op de efficiëntie van de optimale kasklimaatbesturing.

In simulaties wordt het feedback-feedforward regelschema geëvalueerd. Aangetoond wordt dat met behulp van voorwaartskoppeling van een korte termijn weersvoorspelling en terugkoppeling van de toestand, een bijna optimale besturing van het gewasproduktieproces kan worden verkregen. Deze resultaten geven aan dat voor de toepassing van optimale kasklimaatbesturing in de praktijk, een nauwkeurige lange termijn weersvoorspelling niet langer een limiterende voorwaarde is.

Met behulp van simulaties wordt, met succes, de decompositie van het volledige optimale kasklimaatbesturingsvraagstuk in twee deelvraagstukken geëvalueerd. Getoond wordt dat de efficiëntie van de twee deelvraagstukken samen nagenoeg gelijk is aan de efficiëntie van het totale besturingsvraagstuk. Ook is de sturing, berekend met behulp van de decompositie, bijna identiek aan de besturing berekend door oplossing van het volledige vraagstuk waarbij de trage gewasgroeidynamica en de snelle kasklimaatdynamica tegelijk in beschouwing worden genomen. Tevens wordt met behulp van een simulatie aangetoond dat het ook daadwerkelijk aanbeveling verdient om de regeling van de kasklimaatdynamica te baseren op een economisch criterium. De decompositie levert waardevolle informatie over de vorm van het economische criterium dat daarvoor gebruikt moet worden.

Tenslotte wordt, met behulp van de gevoeligheidsanalyse, inzicht verkregen in de rol van modelparameters en beginvoorwaarden op de performance van het open-lus optimale kasklimaatbesturingsvraagstuk.

In hoofdstuk 8 vindt een synthese plaats van de resultaten verkregen in de voorgaande hoofdstukken. Twee concepten voor de implementatie van optimale kasklimaatbesturing in de praktijk worden beschreven. De twee concepten worden met elkaar vergeleken en aspecten als de wijze waarop in beide concepten met fouten in de weersvoorspelling en voorspelling van de veilingprijs kan worden omgegaan, alsmede rekentijd, flexibiliteit van de hiërarchische structuur en de rol van de tuinder bij optimale kasklimaatbesturing, worden besproken. De bijdrage van optimale besturing aan het verbeteren van de efficiëntie van overdekte teelten wordt bediscussieerd en de uitbreiding van de in dit proefschrift gepresenteerde technieken naar klimaatbesturing tijdens de produktie van een gewas met een meermalige oogst, zoals tomaat en komkommer, wordt beschreven.

In hoofdstuk 9 wordt dit onderzoek afgerond met conclusies en aanbevelingen voor toekomstig onderzoek.

DE BETEKENIS VAN DIT ONDERZOEK VOOR DE TUINBOUWPRAKTIJK

De kosten voor klimatisering van de kas behoren tot de belangrijkste kostenposten van de Nederlandse glastuinbouw. Efficiënter energiegebruik kan daarom bijdragen tot een beter bedrijfsresultaat en een effectiever gebruik van natuurlijke hulpbronnen. Dit kan niet alleen worden gerealiseerd met behulp van energiebesparende maatregelen zoals schermen. Efficiënter energiegebruik kan ook worden bereikt door de klimaatregeling in kassen te baseren op een afweging van de kosten voor de klimatisering van de kas en de baten verkregen uit de verkoop van het geoogste produkt. Dit is een typisch voorbeeld van een optimaal besturingsvraagstuk.

De basis voor optimale besturingstheorie is reeds in de beginjaren '60 gelegd. Toepassing van deze techniek bij kasklimaatregeling in de tuinbouwpraktijk is tot op heden echter uitgebleven. Dit proefschrift vormt een eerste stap op weg naar toepassing van optimale besturingstheorie in de tuinbouwpraktijk: het beschrijft en analyseert een efficiënt regelsysteem voor het kasklimaat.

Het klimaatregelsysteem is gebaseerd op een modelbeschrijving van het gewasproduktieproces. In dit onderzoek is de teelt van sla als voorbeeld gebruikt. Het model beschrijft hoe de luchttemperatuur, koolzuurgasconcentratie en luchtvochtigheid in de kas worden beïnvloed door de verwarming, de toediening van koolzuurgas uit een opslagtank en de luchtuitwisseling met de buitenlucht door de ventilatieramen. Tevens beschrijft het model de invloed van niet-manipuleerbare buitenklimaatgrootheden zoals de windsnelheid, temperatuur, luchtvochtigheid, koolzuurgasconcentratie en zonnestraling op de genoemde binnenklimaatgrootheden. Daarnaast beschrijft het model de gewichtsontwikkeling van sla onder invloed van de luchttemperatuur, koolzuurgasconcentratie en de stralingsintensiteit in de kas. Voor toepassing van het klimaatregelsysteem in de praktijk is het van belang dat het model een nauwkeurige beschrijving geeft van het slaproduktieproces. Dit aspect is onderzocht tijdens twee kasexperimenten. Daarbij werd het kasklimaat geregeld volgens de geldende maatstaven in de praktijk. Bij vergelijking van het model met meetgegevens van het kasklimaat en het gewas bleek het model goed in staat het slaproduktieproces tijdens deze twee teelten te beschrijven.

Het regelsysteem is er op gericht de netto-winst van de slaproduktie te maximaliseren. De netto-winst is in dit onderzoek gedefinieerd als het verschil tussen de inkomsten verkregen uit de verkoop van de geoogste sla op de veiling en de kosten verbonden aan de klimatisering van de kas. Om de winst te kunnen maximaliseren is

voorspelling van de veilingprijs noodzakelijk. In Nederland wordt sla geveild in klasseringen afhankelijk van het oogstgewicht. Onderzoek van veilingprijzen van sla heeft aangetoond dat er een linear verband bestaat tussen het oogstgewicht van een krop sla en de prijs. In de veilingprijs werden duidelijke seizoensafhankelijke trends waargenomen. Deze trends bieden een aanknopingspunt voor voorspelling van de veilingprijs. Voorspelling van de veilingprijs werd verder in dit onderzoek niet gebruikt.

In dit onderzoek zijn uitsluitend kosten in rekening gebracht voor de dosering van koolzuurgas en de verwarming van de kas. Arbeidskosten en kosten verbonden aan het gebruik van electriciteit, water, nutriënten en kosten voor ziekte- en plaagbestrijding zijn verondersteld onafhankelijk te zijn van de gekozen regeling en zijn daarom niet in beschouwing genomen.

In de praktijk wordt de maximale hoeveelheid warmte die aan een kas kan worden toegediend, begrensd door de verwarmingscapaciteit van de ketel. Ook de maximale hoeveelheid koolzuurgas die in een kas kan worden gedoseerd, wordt door de afmeting van het doseersysteem bepaald. Dit soort fysieke grenzen kunnen een grote invloed hebben op de werking van de klimaatregeling en zijn daarom expliciet meegenomen in het ontwerp van het regelsysteem.

Tenslotte zijn in het regelaarontwerp boven- en ondergrenzen opgelegd aan de luchttemperatuur, koolzuurgasconcentratie en relatieve luchtvochtigheid in de kas. Deze grenzen zijn gebruikt om te voorkomen dat de klimaatregeling resulteert in een klimaat dat ongunstig is voor de plant zoals hoge luchtvochtigheid, hoge koolzuurgasconcentraties en extreem lage temperaturen. Met deze omstandigheden is in het gewasproduktiemodel (nog) geen rekening gehouden.

In dit proefschrift zijn twee varianten uitgewerkt voor de toepassing van optimale kasklimaatregeling in de praktijk. In beide varianten bestaat het regelsysteem uit twee delen. Eén deel, een zogenaamde gewasgroeiregelaar, regelt de groei van het gewas op een efficiënte wijze. Het tweede deel, de klimaatregelaar, zorgt voor de regeling van het klimaat in de kas. Hoewel deze tweedeling van optimale kasklimaatbesturing in grove lijnen al enige tijd geleden in de literatuur is aangegeven, is de belangrijkste bijdrage van dit proefschrift gelegen in het feit dat dit idee nu in detail is uitgewerkt en geanalyseerd.

Bij de eerste variant geeft de tuinder aan het begin van de teelt aan hoe lang de teelt zal duren, hoe groot het plantgewicht is bij aanvang van de teelt, welke veilingprijs hij verwacht op het oogsttijdstip en welke waarden van de luchttemperatuur, luchtvochtigheid en koolzuurgasconcentratie niet door de klimaatregeling mogen worden overschreden of onderschreden.

Vervolgens berekent de gewasgroeiregelaar op basis van een lange termijn weersvoorspelling (bijvoorbeeld langjarige gemiddelden) een groeipad voor het gewas. Tevens wordt aan dat groeipad een economische waarde toegekend die uitdrukt hoeveel een eenheid gewasgroei op een bepaald moment bijdraagt aan de winst op het oogsttijdstip. Als in de loop van de teelt betere voorspellingen van het weer en de veilingprijs beschikbaar komen, kan een nieuw pad voor de gewasgroei en de economische waarde worden uitgerekend. Dit is ook noodzakelijk als de werkelijke gewasgroei zeer sterk afwijkt van het vooraf berekende groeipad. Deze herbereking zal hooguit wekelijks dienen te worden herhaald.

Zowel het groeipad van het gewas als de daaraan verbonden economische waarde worden gebruikt door de klimaatregelaar. De klimaatregelaar berekent direct economisch optimale instelwaarden voor de verwarming, de koolzuurgasdosering en de ventilatie. Daarbij wordt gebruik gemaakt van het gewasgroeipad, de daaraan verbonden economische waarde, een korte termijn weersvoorspelling en meetwaarden van het actuele weer. Om rekening te houden met optredende verschillen tussen het werkelijke weer en de weersvoorspelling en het werkelijke en berekende kasklimaat zal deze berekening elke minuut moeten worden herhaald.

De hiervoor geschetste eerste variant van het efficiënte klimaatregelsysteem wijkt sterk af van de huidige generatie klimaatregelaars toegepast in de tuinbouwpraktijk. Bij de klimaatregeling in de praktijk worden niet zozeer streefwaarden voor de gewasgroei ingesteld, maar geeft de tuinder streefwaarden, zogenaamde set-points, aan voor de luchttemperatuur, koolzuurgasconcentratie en luchtvochtigheid. In wezen is dit een gewasgroeiregeling maar dan onder supervisie van de tuinder. De klimaatstreefwaarden worden vervolgens door de klimaatregelaar gerealiseerd. In de praktijk zijn genoemde klimaat set-points echter niet gebaseerd op overwegingen ten aanzien van *efficiëntie*.

De tweede variant van de efficiënte kasklimaatregeling, beschreven en onderzocht in dit proefschrift, is meer in overeenstemming met de gangbare praktijk. Ook dit regelsysteem bestaat uit een gewasgroeiregelaar en een kasklimaatregelaar, alleen de werking is iets anders dan bij de eerste variant van het optimale regelsysteem. Eerst wordt, zoals eerder reeds beschreven, een groeipad voor het gewas met de daaraan verbonden economische waarde berekend. Gebruikmakend van dit groeipad en de economische waarde en een korte termijn weersvoorspelling, worden vervolgens economisch optimale streefwaarden voor de luchttemperatuur, luchtvochtigheid en koolzuurgasconcentratie bepaald. De klimaatregelaar dient er daarna voor te zorgen dat door middel van verwarming, koolzuurgasdosering en ventilatie, deze streefwaarden in de kas worden gerealiseerd. In dit

proefschrift is aangetoond dat vaste streefwaarden voor het kasklimaat economisch gezien niet het beste resultaat opleveren. Een beter resultaat wordt verkregen als de set-points regelmatig aan de gunstige of ongunstige buitenklimaatomstandigheden worden aangepast. Met behulp van de methode beschreven in dit proefschrift kan dit op een efficiënte wijze worden gerealiseerd.

Hoewel de tweede variant van het optimale kasklimaatregelsysteem door het gebruik van set-points voor het klimaat meer in overeenstemming is met de praktijk, heeft dit onderzoek uitgewezen dat toepassing van de eerste variant, waarbij direct optimale instellingen voor de verwarming, koolzuurgasdosering en ventilatie worden berekend, een verdere verbetering in efficiëntie kan opleveren. De reden is gelegen in het feit dat in de eerste variant ook bij de regeling van het kasklimaat efficiëntie wordt nagestreefd, terwijl dat bij de tweede variant, net als in de praktijk, niet het geval is.

In dit onderzoek is het optimale klimaatregelsysteem niet onder praktijkomstandigheden getest. Wel is door middel van computersimulaties inzicht verkregen in de werking en de mogelijke voordelen van deze wijze van klimaatregelen. Dit inzicht werd verkregen door optimale kasklimaatbesturing te vergelijken met klimaatregeling onder supervisie van de tuinder. Bij deze vergelijking werd volledige voorkennis verondersteld over het weer tijdens de gehele teelt en de veilingprijs op het oogsttijdstip. De vergelijking werd gebaseerd op meetgegevens van het weer en de klimaatregeling in de kas, verkregen tijdens een kasexperiment met sla in de winter van 1992. De simulaties toonden aan dat optimale kasklimaatbesturing efficiënter verwarmt, efficiënter koolzuurgas doseert en efficiënter ventileert. Zo reageerde bijvoorbeeld de koolzuurgasdosering efficiënter op de zonnestraling en de ventilatie, daarbij beter gebruikmakend van de mogelijkheden om de produktie van het gewas te verhogen onder gunstige weersomstandigheden. Net als in de praktijk werd bij optimale kasklimaatbesturing de kas voornamelijk geventileerd om een te hoge relatieve luchtvochtigheid te voorkomen. Gevonden werd dat regeling van de relatieve luchtvochtigheid een grote invloed heeft op de efficiëntie van de kasklimaatbesturing omdat de daarvoor noodzakelijke ventilatieuitwisseling met de buitenlucht, energie- en koolzuurgasverlies uit de kas tot gevolg heeft.

Modelfouten en grote afwijkingen tussen weersvoorspelling en de werkelijke weersomstandigheden kunnen de efficiëntie van de optimale regeling in de praktijk verminderen. Met behulp van simulaties is aangetoond dat de methoden ontwikkeld in dit proefschrift in staat zijn om te corrigeren voor modelfouten en fouten in de weersvoorspelling zonder een groot verlies aan winst.

In dit onderzoek is aangetoond dat optimale besturingstheorie bij kan dragen tot een efficiënter gebruik van energie in de glastuinbouw. De modelstudie beschreven in dit proefschrift suggereert een verbetering van de efficiëntie die in sommige omstandigheden kan oplopen tot 10% bij de teelt van sla. Experimenten in de praktijk zullen moeten uitwijzen of deze verbetering ook daadwerkelijk kan worden gerealiseerd. Dit onderzoek heeft echter een essentiële eigenschap van optimale besturingstheorie benadrukt, namelijk dat gedurende de gehele teelt continu de kosten van de klimatisering worden afgewogen tegen de baten van de gewasgroei en produktie. Dit is een kenmerk dat bij de huidige generatie kasklimaatcomputers ontbreekt.

CURRICULUM VITAE

Eldert Jan van Henten werd geboren op 1 maart 1963 te Tiel. In 1981 behaalde hij het VWO diploma aan de Gemeentelijke Scholengemeenschap te Doetinchem, en in 1987, met lof, het diploma van landbouwkundig ingenieur aan de Landbouwuniversiteit te Wageningen.

Van november 1987 tot en met augustus 1993 werkte hij in Wageningen bij het toenmalige Instituut voor Mechanisatie-, Arbeid- en Gebouwen, IMAG-DLO, als onderzoeksmedewerker. Gedurende de laatste 4 jaren van deze periode werkte hij aan dit proefschrift, als assistent in opleiding vanuit de Landbouwuniversiteit gedetacheerd bij het IMAG-DLO. In de periode november 1993 tot en met mei 1994 was hij in dienst van Silsoe Research Institute, Silsoe, Engeland, alwaar hij onderzoek verrichtte aan optimale regelwetten voor niet-lineare systemen. Sinds 1 november 1994 is hij als senior wetenschappelijk medewerker in dienst van het Instituut voor Milieu- en Agritechniek (IMAG-DLO) en draagt hij bij aan het meet- en regeltechnisch onderzoek gericht op de agrarische sector.

NOTES